THE UNIVERSITY OF SYDNEY

Thesis submission in fulfillment of the requirements for the degree of

Doctor of Philosophy, Faculty of Health and Medicine, The University of Sydney

Year of Award: 2022

Targeting Innate Immunity in Acute Kidney Injury

Dr Jennifer Li

MBBS, BE/BMedSci, FRACP, FASN

Centre for Transplant and Renal Research, Westmead Institute for Medical Research

Faculty of Health and Medicine, University of Sydney

SID: [REDACTION] | Jennifer.li1@sydney.edu.au

Candidature period: 03/2019 – 09/2022

Supervisors

A/Professor Natasha Rogers, MBBS, FRACP, FASN, PhD

Professor Stephen Alexander, MBBS, FRACP, MD, MPH

Professor Philip O'Connell, MBBS, BSc (Med), PhD, FRACP, FAHMS

The Westmead Institute FOR MEDICAL RESEARCH

THESIS OVERVIEW AND ABSTRACT

Acute kidney injury (AKI) is an umbrella term for various aetiological insults, disrupting the kidneys' capacity to carry out many of its essential physiological function. We focused on the ischemia reperfusion injury (IRI) model of AKI, which is applicable across native and transplant kidney AKI. The current standard of care for patients with acute kidney injury (AKI) is limited to optimising supportive care and renal replacement therapy.

Unfortunately, there are no disease modifying interventions available in clinical practice, which have significant implications to short- and long-term outcomes following AKI, including chronic kidney disease, cardiovascular and mortality risks. AKI in the immediate days following kidney transplantation (including delayed graft function, DGF) also portends poorer outcomes, with increased risk of acute rejection and worse overall graft- and patient-survival metrics.

This PhD aims to determine if modulation of the innate immune response can be harnessed to limit the acute injury and maladaptive immune response which accompanies acute kidney injury. (Fig 0.1)

- Chapter 1 presents an overview of the clinical and research landscape of acute kidney injury (AKI) and delayed graft function (DGF), includes general overview of clinical trials for AKI/DGF. This is followed by detailed description of pathophysiology and key immunological mechanisms in an ischemia reperfusion injury (IRI) model for AKI/DGF as background for the subsequent chapters.

- Chapter 2 focuses on the role of dendritic cells and whether cellular therapy with tolerogenic dendritic cells (tolDC) in mice can effectively limits the degree of renal injury, cell death and inflammation.

- Chapter 3 explores the role of pyroptosis in AKI. This is a highly immunogenic form of regulated cell death which occurs in both immune cells and renal tubular epithelial cells. Gasdermin D (GSDMD) proteins are the terminal effectors of pyroptosis and were targeted in attempts to avert severe AKI.

- Chapter 4 explores the Australian Chronic Allograft Dysfunction (AUSCAD) study cohort to determine if a molecular/transcriptomic profile can be matched with clinical and biopsy data to determine the patients most likely to benefit from early, effective intervention for AKI/DGF. The role of neutrophils was explored in a pilot study to determine feasibility of NETosis staining in archived biopsies.

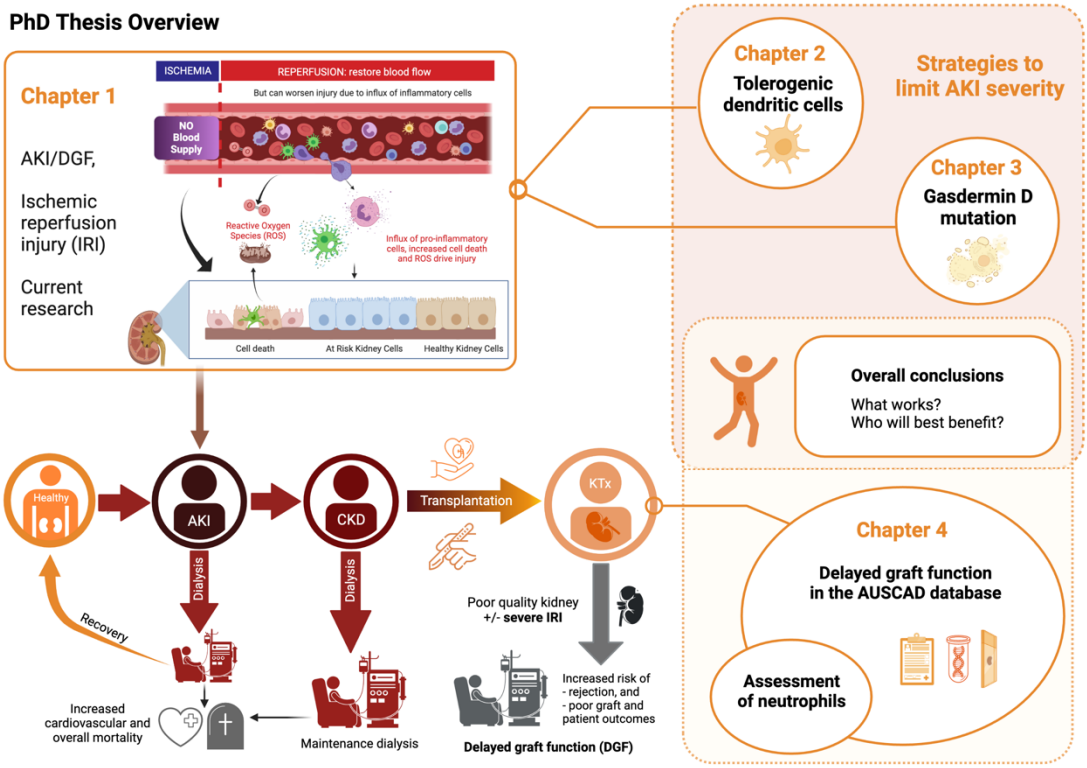

Figure 0.1: PhD overview and organisation. Image created using Biorender.com

The impact of COVID-19 during the candidature: Access to the laboratory and procurement of equipment were significantly delayed due to lockdown restrictions in NSW and global supply shortages during the COVID-19 pandemic – thus limiting the progress with planned experiments outlined from the start of this PhD. There were plans to perform experiments in mice kidney transplantation models of DGF to link the pre-clinical to clinical data but unfortunately due to change in personnel and travel restrictions, a specialist vet microsurgeon could not be involved. Further work on these topics will be performed during the post-doctoral research period.

Table of contents

Authorship attribution statement and declaration of originality

Chapter 1: Literature Review

Material from this chapter has been published as a book chapters and review article - I was first author and I performed extensive literature review, drafted the manuscript, and created accompanying figures. A/Prof Natasha Rogers, Professor Angus Thomson, Professor Wayne Hawthorne, Professor Germaine Wong, and Professor Jeremy Chapman assisted with revision/editing of the final submission files for the respective manuscripts as senior authors.

Chapter 2: Tolerogenic Dendritic Cell Therapy for AKI.

Material from this chapter has been submitted to Kidney International and is currently under revision. I co-designed the study experiments with my supervisor, performed animal and laboratory experiments, data collection, statistical and bioinformatic analysis, manuscript writing and revision experiments. A/Prof Natasha Rogers assisted with mice ischemia-reperfusion injury surgery. Professor Angus Thomson, Professor Philip O'Connell and Professor Stephen Alexander provided expert opinion during interim data review and manuscript stages. Dr Joey Lai assisted with library preparation and processing of TolDC bulk RNAseq samples, which were sequenced by the Australian Genome Research Facility and processing of the raw FASTQ files (for QC, alignment and mapping into BAM files and generation of the raw counts matrix was performed by Dr Brian Gloss from Westmead bioinformatics). I performed all downstream analysis after obtaining the raw count matrices, and Mr Harry Robertson and Dr Ellis Patrick from the Department of Mathematics (USyd) provided feedback during the interim analysis.

Our collaborators from the University of Queensland included Dr Andrew Mallett and Dr Quan Nguyen labs (including Mr Samuel Holland, Ms Arti Raghbur and Dr Nicholas Matigian) helped perform the 10x Visium spatial transcriptomic experiments, data acquisition, alignment, and mapping of raw output files from the frozen mouse kidney specimens. I performed all downstream analysis of the aligned/mapped files, including QC, filtering, differential expression, and pathway analysis.

Dr Min Hu and Elvira Jimenez-Vera assisted set up of flow cytometry experiments. Dr Katie Trinh and Mr Harry Robertson assisted with the review of the manuscript. I presented results of this project at: Transplantation Society of Australia and New Zealand Conference (2022), Australia New Zealand Society of Nephrology Conference (2021).

The following summarises which figures, and tables of Chapter 2 which were submitted to the journal

Figure	Submitted?	Figure	Submitted?	Table	Submitted?	Table	Submitted?
2.1	no	2.19	yes	2.1	no	2.13	yes
2.2	no	2.20	yes	2.2	no	2.14	yes
2.3	no	2.21	yes	2.3	no	2.15	yes
2.4	no	2.22	yes	2.4	yes	2.16	yes
2.5	no	2.23	yes	2.5	yes	2.17	yes
2.6	yes	2.24	yes	2.6	no	2.18	yes
2.7	yes	2.25	no	2.7	no	2.19	yes
2.8	yes	2.26	yes	2.8	no	2.20	yes
2.9	yes	2.27	yes	2.9	yes	2.21	yes
2.10	no	2.28	no	2.10	yes	2.22	yes
2.11	yes	2.29	yes	2.11	no	2.23	yes
2.12	yes	2.30	yes	2.12	yes	2.24	yes
2.13	yes	2.31	yes				
2.14	yes	2.32	yes				
2.15	yes	2.33	no				
2.16	yes	2.34	no				
2.17	yes	2.35	yes				
2.18	yes	2.36	yes				

Chapter 3: Pyroptosis and Gasdermin D mutation in AKI.

The initial concept was planned by A/Prof Natasha Rogers and Professor Stephen Alexander. A/Prof Natasha Rogers performed the original mice IRI surgeries and molecular profiling. Together, we performed chimeric mice model experiments. I was responsible for histology and imaging experiments, collection and analysis of data, and preparation of the draft manuscript.

Dr Daniel Meijles (St George's, University of London) assisted with measurement of reactive oxygen species and Dr Sohel Julovi, Dr Katie Trinh and Mr Aadhar Moudgil assisted with revision and editing of the manuscript for journal submission. This project has been presented at local and international conferences, including American Transplantation Congress (2020), The Transplant Society Conference (2020), NSW Has Scientific Talent Competition (2020) and Australia New Zealand Society of Nephrology Conference (2022)

Chapter 4: Delayed graft function gene transcriptomic signature

The Australian Chronic Allograft Dysfunction (AUSCAD) cohort is a study based at Westmead Hospital and the Westmead Institute for Medical Research. Professor Philip O'Connell is the principal investigator, the de-identified clinical database was managed by Dr Karen Keung (up to 2019) and Ms Patricia Anderson, and Ms Elvira Jimenez-Vera has been instrumental for collection and maintenance of the biobank specimens stored at the Westmead Institute for Medical Research. Professor Jeremy Chapman, Professor Germaine Wong and Dr Brian Nankivell from the Department of Renal Medicine (Westmead Hospital) assisted with kidney biopsy sampling for study patients during protocol biopsies. Dr Meena Shingde from the Department of Pathology (Westmead Hospital) provided expert advice and also independent re-scoring of 3- and 12-month biopsy samples. I expanded and updated patient and variables collected in the clinical database up to October 2020 with the assistance of Dr Sebastian Hultin (for donor variables) and Ms Haina Wang (for recipient variables). Dr Brian Gloss assisted in the quality control, alignment, and mapping of raw FASTQ files to generate BAM files and raw counts matrices.

I performed statistical analysis of the clinical data and bioinformatic analysis of these kidney biopsy bulk RNA-seq samples, with a focus on delayed graft function and outcomes. Mr Harry Robertson assisted with significant RNA data cleaning as both he and Dr Sebastian Hultin are also utilising this dataset from a fibrosis angle. The neutrophil component of this chapter was a collaboration between my supervisor Professor Philip O'Connell and the R&D team at CSL Ltd. (Melbourne, Australia) - to assess the role of neutrophils early in delayed graft function in kidney transplant recipients in the AUSCAD cohort. Analysis of the pilot sequencing data (first 88 samples from 2018) were performed by external bioinformaticians and interpreted by Dr Mark Biondo and Dr Christina Gamelli (all from CSL Ltd). My role was to quantify neutrophil infiltration in an attempt to validate their findings. I was responsible for testing and optimisation of neutrophil staining methods of available paraffin human kidney biopsy samples, image acquisition and data analysis. My Honours student (Miss Haina Wang) assisted in staining, cell counting and analysis of these results – which she presented as part of her honours thesis for Applied Medical Sciences (University of Sydney). Ms Naheela Lala (lab assistant) aided obtaining archived sections.

Attesting authorship attribution statement

As the primary supervisor for the candidature upon which this thesis is based, I can confirm that the authorship attribution statements above are correct.

Supervisor: **A/Prof Natasha Rogers**

Signature: Date: 4/9/22

As co-supervisors for the candidature upon which this thesis is based, I can confirm that the authorship attribution statements above are correct.

Supervisor: **Professor Philip O'Connell**

Signature: Date: 5th September 2022

Supervisor: **Professor Stephen Alexander**

Signature: Date: 4/9/22

Declaration of originality

This is to certify that to the best of my knowledge; the content of this thesis is my own work and all the assistance received in preparing this thesis and sources have been acknowledged.

Name: **Dr Jennifer Li** (ORCID: 0000-0003-0186-8613)

Signature: Date: 25/08/2022

Publications, presentations, and funding during candidature

Scholarships And Prizes

- University of Sydney Completion Scholarship (2022)
- TTS Scientific Travel Award (2022)
- TSANZ Early Career Researcher Awards (2019-2022)
- TSANZ President's Prize - Basic Science (2019)
- National Health and Medical Research Council Postgraduate Scholarship (GNT116877, 2019-2022)
- BJ Amos Travelling Scholarship, Westmead Hospital Association (2019)

Chapter 1: Reviews

- **Li, J.,** Wong, G., Chapman, J.R., Outcomes in Kidney Transplantation (*Comprehensive Clinical Nephrology*, edited by J Floege, accepted – awaiting final production, 2022)
- **Li, J.,** Rogers, N.M., Thomson, A., Myeloid and Mesenchymal Stem Cell Therapies for Solid Organ Transplant Tolerance. *Transplantation. 2021;*105(12): e303-e321.PMID:33756544.
- **Li, J.,** Rogers, N.M., Hawthorne, W., Ischemia Reperfusion Injury, *Organ Repair and Regeneration: preserving organs in the regenerative medicine era* (Orlando, 1st edn Jan 2021)

No additional permissions were required from Elsevier or Wolters Kluwer as I was the first author

Chapter 2: Tolerogenic Dendritic Cells In Acute Kidney Injury

Manuscript: submitted, *revisions in progress* (***KI-05-22-0916***)

Conference presentation and abstracts:

- The Transplantation Society Congress 2022 mini oral presentation
- Transplantation Society of Australia and New Zealand president's prize session 2021 & 2022
- Australia New Zealand Society of Nephrology ASM 2021 young investigator session.

Chapter 3: Gasdermin D And Pyroptosis In Acute Kidney Injury

Manuscript: Gasdermin D mutation protects against acute kidney injury (*being submitted*)

Conference presentations and abstracts:

- Transplantation Society of Australia and New Zealand (2020)
- The Transplantation Society Congress (2020)
- American Transplantation Society (AST) Congress (2020)

Other Publications Related To AKI and/or Transplantation

- ***A20 Mutation*** **In Acute Kidney Injury**

  Manuscript: Rogers, N.M, …, **Li, J.,** et al The impact of TNFAIP3 gene variation on NF-KB activation in acute kidney injury (*revision under review* ***KI-08-21-1453***)

  Conference presentation and abstract: TSANZ 2019 president's prize session

- **Li, J.,** Raghubar, A., (co-first author), et al, The Utility of Spatial Transcriptomics for Solid Organ Transplantation. (*Revisions requested*, ***TPA-2022-0861***)

- Hu, M., Rogers, N., **Li, J.,** et al. Antigen Specific Regulatory T cells in Kidney Transplantation and other Tolerance Settings. *Front. Immunol*. 2021; 12:717594. PMID: 34512640

- Robertson, H., **Li, J**., et al Transcriptomic analysis identifies a tolerogenic dendritic cell signature. *Front Immunology, 2021;*12:733231. PMID: 34745103.

- El-Rashid, M., … **Li, J**., et al. Repurposing of metformin and colchicine reveals differential modulation of acute and chronic kidney injury. *Scientific Reports*, 2020;10,21968. PMID: 33319836.

Acknowledgements

This PhD candidature, when not under COVID lockdown restrictions, was spent at the Centre for Transplant and Renal Research of The Westmead Institute for Medical Research. I am grateful for the immense support provided by my supervisors A/Prof Natasha Rogers, Professor Stephen Alexander, and Professor Philip O'Connell. They have guided me along this winding research path and imparted important life advice for the road ahead as I work towards being an independent clinician-scientist. This candidature was made possible through financial support provided by the National Health and Medical Research Council's Postgraduate Scholarship, Westmead Association's BJ Amos Grant and USyd Completion Scholarship.

I also have to thank the support provided by Dr Brian Nankivell, Ms Kathy Kable, Professor Jeremy Chapman, Professor Gopi Rangan and Professor Germaine Wong, who have always had time for a coffee or a chat whenever I sought their counsel. The recent PhD graduates Dr Karen Keung, Dr Katrina Chau, Dr Ankit Sharma, Dr Titi Chen, Dr Eric Au and Dr Jennifer Zhang had offered plenty of condolences throughout the last few years for when experiments needed further "optimisation" and Dr Sarah So for providing supportive care when required. The current Rogers group members Dr Sohel Julovi, Dr Katie Trinh, Ms Atharva Kale and Mr Harry Robertson (and formerly Dr Kedar Ghimire) have provided immense support and sanity checks. Dr Min Hu, Ms Elvira Jimenez-Vera, Ms Patricia Anderson, Dr Sebastian Hultin and Ms Haina Wang have been amazing friends and a special thanks to Elvira and Trish for their tireless work with the AUSCAD samples and Min for her mastery of flow cytometry. I thank our collaborators from the University of Queensland, Professor Andrew Mallett, Dr Nicholas Matigian, Dr Quan Nguyen, Ms Arti Raghubar and Mr Samuel Holland for their collaboration for spatial transcriptomic experiments.

A special thanks must go to Dr Meena Shingde for her involvement with re-scoring histopathology samples and Dr Brian Gloss' assistance processing the large repository of FASTQ files for the AUSCAD study. Finally, I must thank my family for tolerating my foray into PhD land, the house master – Tofu the cavoodle, and my nieces for providing endless entertainment with all their antics.

Common abbreviations

AMBR	antibody mediated rejection
AKI	acute kidney injury
ALR	absent in melanoma (AIM2)-like receptors
ATI	acute tubular injury
ATN	acute tubular necrosis
AUSCAD	Australian Chronic Allograft Dysfunction Study
BMDC	bone marrow-derived dendritic cell
CASP	caspase
CCL	chemokine ligand
CCR	C-C chemokine receptor
CD	cluster of differentiation
CKD	chronic kidney disease
CXCL	C-x-C motif ligand
DAMP	danger associated molecular patterns
DBD	donation after brain death
DC	dendritic cell
DCD	donation after cardiac death
DEG	differential expressed gene
DGF	delayed graft function
ECD	extended criteria donor
FOXP3	forkhead box p3
GSDMD	gasdermin D
GPX4	glutathione perioxidase 4
HR	hazards ratio
IL	interleukin (eg IL-10 = interleukin 10)
IRI	ischemia reperfusion injury
KDPI	kidney donor profile index
KO	knock out
LFC	log2-fold change
LPS	lipopolysaccharide
MHC	major histocompatibility complex
Mreg	regulatory macrophages
NFkB	nuclear factor kappa B
NK	natural killer
NLR	NOD-like receptors
NLRP3	NACHT- LRR- and pyrin domain-containing protein 3
OR	odds ratio
PBS	phosphate buffered saline
PAMP	pathogen associated molecular pattern
PRR	pattern recognition receptors
RNAseq	RNA sequencing
RTEC	renal tubular epithelial cell
scRNAseq	single cell RNAseq
TCMR	T-cell mediated rejection
TCR	T-cell receptor
TGF	transforming growth factor
TGFBR	TGF-beta receptor
TLR	toll-like receptor
TolDC	tolerogenic DC
Treg	regulatory T-cell
VitD3	Vitamin D3 (or 1,25-dihydroxy Vitamin D)

Gene names can be found on www.genecards.org

List of figures

List of Tables

THE UNIVERSITY OF SYDNEY

The Westmead Institute FOR MEDICAL RESEARCH

1 Chapter 1

Literature review of acute kidney injury and ischemia reperfusion injury

1.1 Acute kidney injury: clinical definition and implications

Acute kidney injury (AKI) is characterised by an abrupt reduction of kidney function leading to impaired fluid, electrolyte and acid-base handling, accumulation of uremic toxins and a persistent, systemic inflammatory state[1]. AKI is associated with significant nephron loss and survivors of AKI are at higher risk of developing CKD and kidney failure[1-4]. Limiting AKI severity may limit nephron loss and potentially reduce CKD and other morbidities. Despite this, there are no proven therapies that modify or treat AKI outside current strategies of prevention and supportive care through optimisation of fluid status ± renal replacement therapy (peritoneal dialysis or haemodialysis). It is crucial to continue to explore mechanisms which underpin the pathophysiology of ischemia reperfusion injury (IRI), an important cause of AKI, to focus efforts on translating research leading to clinically meaningful applications.

It is estimated that 1 in 5 hospital admissions in developed countries is complicated by AKI[5], with over 130,000 cases of AKI hospitalisations and 10% in-hospital mortality in 2012-2012[6]. All incident AKI diagnosis confers increased hospital stay[6], worse short- and long-term morbidity and mortality risks and poorer quality of life. Regardless of the cause, these risks are amplified in patients with severe AKI or needing renal replacement therapy during the admission[1-9]. There is an increased mortality risk for those who are dialysis dependent, for example, a 60-year-old male on dialysis has approximately 10-fold mortality compared to the general population (the younger the patient, the more dramatic the mortality difference the between the dialysis to general population).[9,10]

Studies into AKI have added complexity from heterogenous diagnostic criteria. The three most commonly cited criteria are KDIGO (Kidney Disease: Improving Global Outcomes, RIFLE (Risk, Injury, Failure, Loss of kidney function and End-stage kidney disease) and AKIN (Acute Kidney Injury Network) criteria[1,7,11,12] (Table 1.1). The Kidney Disease: Improving Global Outcomes (KDIGO) criteria is most commonly used in clinical practice but current criteria do not incorporate biomarkers of kidney damage (such as *NGAL*, *KIM-1* or *IL-18*) suggested by the acute disease quality initiative (ADQI) workgroup[13] and lack the ability to detect subclinical AKI (biochemical or histological evidence of tissue injury without creatinine or urine changes to meet criteria of AKI). Antecedent clinical trials have been based on these definitions, but in recent

years has seen a shift towards the use of the term acute kidney disease (AKD) to describe the spectrum of kidney injury within the first 90 days since onset and reserving "AKI" for the first 7 days of injury which fit the KDIGO criteria[14]. This was reflected in the 2020 KDIGO consensus conference classification of AKD to better predict mortality, prognosticate incident CKD risk and harmonise terms used for AKD care and future clinical research[14]. (Fig 1.1)

Table 1.1: ***Clinical definitions for acute kidney injury*** *(AKI) from the KDIGO guidelines, AKIN and RIFLE criteria*

	Serum Creatinine (SCr) increase from baseline	**Urine Output (UO)**
KDIGO	**Stage 1**: ↑ SCr ≥ 26.5 µmol/L or 1.5-1.9x **Stage 2**: ↑ SCr > 2 – 2.9x **Stage 3**: ↑ SCr > 3x, or SCr ≥354 µmol/L, or eGFR < 35ml/min/1.73m^2 in age < 18, or needing dialysis	<0.5 mL/kg for 6-12 hours <0.5 mL/kg for > 12 hours
AKIN	**Stage 1**: ↑ SCr ≥ 26.5 µmol/L or 1.5-1.9x **Stage 2**: ↑ SCr > 2 – 2.9x **Stage 3:** ↑ SCr > 3x, or SCr ≥354 µmol/L, or needing dialysis	<0.5 mL/kg for > 6 hours <0.5 mL/kg for > 12 hours Anuric
RIFLE	**Risk**: ↑ SCr 1.5-1.9x or GFR decrease > 25% **Injury**: ↑ SCr 2x or GFR decrease > 50% **Failure**: ↑ SCr 3x or GFR decrease > 75% or SCr ≥354 µmol/L **Loss**: persisting complete loss renal function > 4 weeks **ESRD**: more than 3 months	<0.5 mL/kg for > 6 hours <0.5 mL/kg for > 12 hours <0.3ml/kg for 24 hours or Anuric for ≥ 12 hours

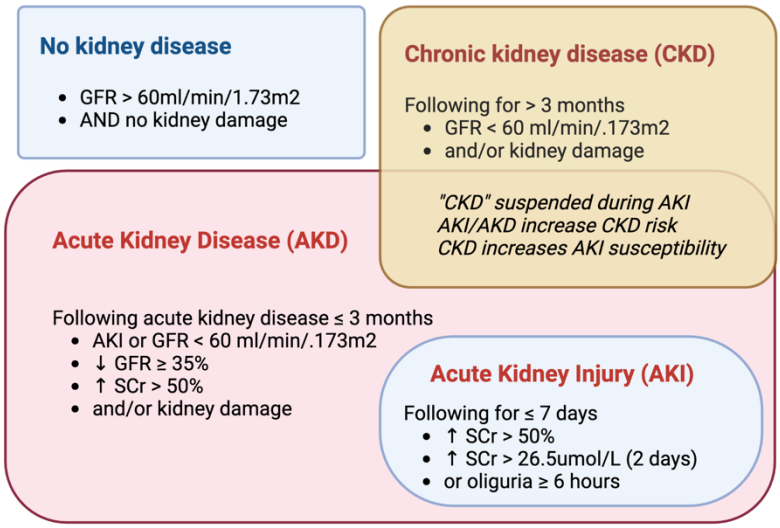

Figure 1.1: ***Updated KDIGO classification of acute kidney injury*** *(AKI), acute kidney disease (AKD) and chronic kidney disease (CKD) based on the 2020 consensus conference. Created using BioRender.com*

1.2 Delayed graft function: AKI in early kidney transplantation

For those patients with CKD who progress to kidney failure the treatment options are limited to renal supportive care, dialysis, and kidney transplantation. Overall, kidney transplantation offers the best survival advantage for the ESKD patient compared to other renal replacement modalities.[15] The significant mismatch between the kidney donors versus the growing population of people with kidney failure being wait-listed for transplantation has driven the utilisation of less 'ideal' organs to meet demands.

In 2017, there were 1109 new kidney transplants and 964 patients active on the transplant wait-list for 3056 incident ESRD patients, 2929 incident + 10,624 prevalent dialysis patients in Australia[16-19]. While the overall survival for highly selected patients on the wait list was favourable (with 1- and 3- year survival 98.9 and 93.6% respectively), there were 10 deaths over the year while waiting for a kidney transplant.[18] Further expansion of the donor pool is inevitable and this includes utilisation of marginal donors (aged > 70 years; or younger donors with risk factors including hypertension, diabetes mellitus or significant cardiovascular disease), extended criteria donors (ECD if meeting ≥ 2 of the following: age > 65 years, pre-existing hypertension or diabetes, or terminal creatinine > 132 μmol/L) and after circulatory compromise (donation after circulatory death, DCD). Approximately half of all deceased kidney transplants in 2017 were from DCD or ECD grafts[20], which are less 'ideal' compared to organs from standard criteria donation (or donation after brain death, DBD)[21-25] – due to heighted sensitivities to AKI and unfavourable long term outcomes[26-29]. The risks associated with AKI are also greater when considering the allografts with higher kidney donor profile index (KDPI), a surrogate measure which correlates with the risk of graft failure after deceased donor kidney transplantation[30-32].

Development of delayed graft function (DGF), a form of severe AKI in the early post-transplant period, is associated with poorer long-term sequelae[15,27,33]. AKI in the kidney allograft overlaps with regards to risks and precipitants[29,34-36] (Fig 1.2) as native kidney AKI but is complicated by the universal exposure to ischemia reperfusion injury (IRI) in the peri-operative period. This is in addition to the alloimmune response, potential toxicities of anti-rejection medications and pre-donation AKI insults[37].

DGF can occur in approximately 20-25% of DBD and 50% in DCD kidneys[15,26], but this is highly centre, transplant era and definition dependent. The heterogeneity of criteria used to define DGF[27,35] is significant, but the most common definition (also used by the FDA) is the need for dialysis (haemodialysis or peritoneal dialysis) in the first 7 days post transplantation[27,38-40].

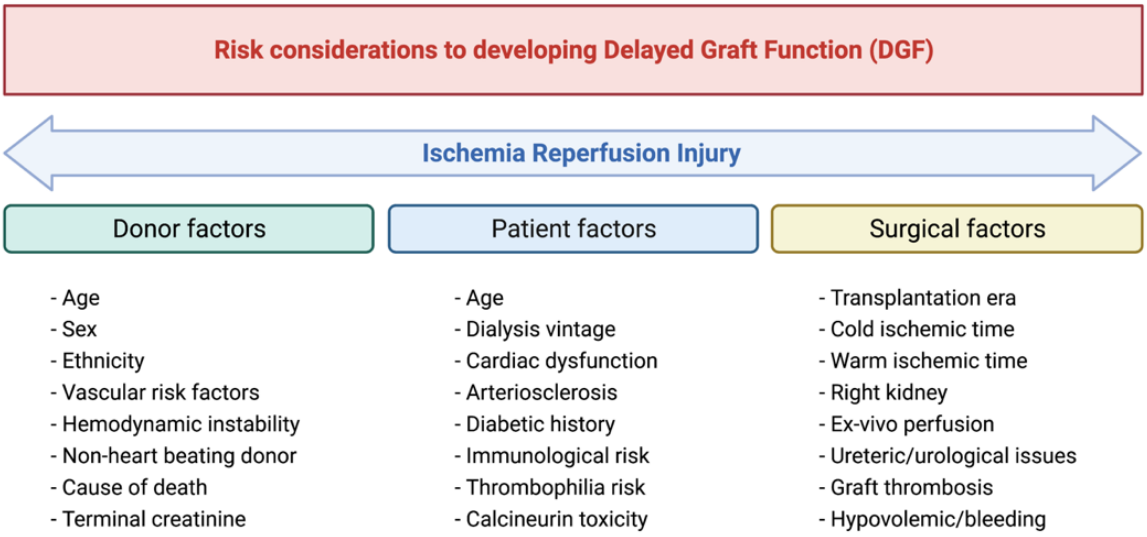

Figure 1.2: ***Donor, surgery, and patient related risk factors*** *in addition to ischemia reperfusion injury which influence the risk of developing delayed graft function*

The categorical delineation of DGF does not incorporate subclinical injury (slow graft function) or stratify severity of injury correlating with DGF. Data from the Australia and New Zealand Dialysis and Transplant Registry (ANZDATA) has shown that DGF ≥ 14 days increases the risk of death and death-censored graft loss[26] and increases risk of graft rejection[41]. Similarly, a German single centre study[42] found similar results, as DGF ≥ 14 days was associated with significantly reduced graft survival if KDPI was below 85%, whereas any DGF for kidneys with KDPI ≥ 85% portended worse outcomes. Pair-kidney analysis of recipients of grafts from the same donor showed that the recipient with DGF was at higher risk of death-censored graft loss[25].

1.3 Clinical studies targeting ischemic AKI and DGF

Human studies targeting AKI and DGF have unfortunately failed to translate earlier pre-clinical targets into practice and remains an unmet need in clinical nephrology. Selected key studies are summarised in Table 1.2. Clinical trials targeting AKI in critically ill patients have failed to show benefit so far. The ATHOS-3 trial[43] reported better overall and dialysis-free survival with the administration of angiotensin II for patients with vasodilatory shock, but the control group included patients with severe liver disease (by significantly higher MELD scores), which is a significant confounder to baseline renal function. Recombinant alkaline phosphatase was used in the multinational STOP-AKI trial as an anti-inflammatory agent to reduce renal IRI in patients with septic shock but disappointingly did not reach statistical significance for the primary end point of improving creatinine-clearance within the first 7-days.[44] Neither N-acetylcysteine or deferoxamine[45] improve the renal outcomes in hemodynamically compromised patients. The use of remote ischemic conditioning (RECO sepsis[46]) and calcifediol (ACTIVATE-AKI[47]) were still ongoing at the time of this review.

Similarly, there have been a dearth of positive results in surgery-related AKI and transplantation-related DGF. Studies that have attempted to limit renal IRI with donor-interventions prior to retrieval have been disappointing[48-54] and limited to regional (or national) legislation to what can or cannot be administered to deceased donors. Machine perfusion technologies (including regional perfusion, hypothermic versus normothermic machine perfusion) promise to alleviate the burden and morbidity associated with clinical DGF[55-57], with the additional opportunity to administer therapies while on circuit but available data so far have failed to support any significant impact. Furthermore, machine perfusion is limited to deceased donor kidney transplantation. Remote ischemic preconditioning for the prevention of DGF in kidney transplantation recipients have not worked and the magnitude of effect in other studies of peri-operative setting and myocardial infarction have been limited.[58-60] Therapies which modulate the complement, cytokine, adhesion molecules, anti- and pro-apoptotic factors have either been negative, do not have available data or were terminated on the grounds of adverse profiles or recruitment struggles[58-82]. Using Belatacept in place of calcineurin inhibitors (tacrolimus and cyclosporine) to minimise the vasoconstriction and haemodynamic side effects has been limited by an excess of biopsy proven rejection[74,75,83-86] and using

a vasodilatory agent such as verapamil[87] has not prevented DGF. Augmentation of oxygen carrying capacity with erythropoietin[88-90], heme arginate[70] and perioperative bovine haemoglobin[91] has no evidence to support its use. Eplenerone[92], a mineralocorticoid antagonist is being investigated as a preventative agent for DGF due to its proposed anti-oxidant and anti-inflammatory effect. Hepatocyte growth factor mimetic (BB3)[93], which may promote tubular cell regeneration and implicated in the late stages of IRI is currently under investigation.

The potential barriers to successful clinical translation may be many-fold, ranging from the choice of pre-clinical model to clinical trial design issues[94,95]. Murine models have been extremely useful in the study of kidney disease but the ability to control the timing of injury (and intervention) is not always possible, nor is severe injury requiring dialysis feasible (given the high animal mortality associated). The use of sex- and age- limited mice is often controlled for reproducibility in the laboratory environment but limit translatability to human clinical use. Furthermore, clinical studies are limited by heterogeneous definitions for AKI and DGF as previously described likely increased the difficulty to conduct clinical studies across different clinical sites, ethical jurisdictions, clinical protocols, aetiology of AKI, patient comorbidities and limitations of funding, patient withdrawal and statistical power considerations. Arbitrary thresholds, for example, creatinine increase by of 26μmol/L versus 1.5x rise from baseline for mild AKI are difficult to reconcile with predictive outcomes due to limited evidence. Incorporating biomarkers into AKI definitions may improve this in the future but modelling of optimal thresholds against long-term surrogate markers or hard endpoints are needed improve the diagnostic criteria and its predictive capabilities.

Table 1.2: ***Summary human clinical trials*** *for either DGF (transplantation); or AKI in high-risk, non-transplant patients.*

Study type	N	Study variable	Intervention	Effect	Comments	Reference
DGF in transplantation - donor related interventions						
Meta-analysis	1068 *11 trials*	Corticosteroid	Given to brain-dead donors before retrieval	NS	Significant heterogeneity	D'Aragon[48]
RCT	24	AVP (arginine vasopressin)	Given to brain-dead donors before retrieval	NS		Pennefather[51]
RCT	97	Desmopressin	Given to brain-dead donors before retrieval	NS		Guesde[49]
RCT	160	NAC (N-acetylcysteine)	Infused in donor pre- cerebral angiography and organ retrieval	NS		Orban[50]
RCT	487	Dopamine	Given to brain-dead donors before retrieval	NS		Schnuelle[53,54]

RCT	455	Methylprednisolone	Administered before organ retrieval	NS		Reindl-scwaighofer[52]
DGF in transplantation – ex vivo machine perfusion						
Meta-analysis	2266 *16 trials*	Hypothermic machine perfusion	Compared to static cold storage for all types of deceased kidney donors	↓DGF RR 0.75 (DCD donors)	Only 1 study for normothermic perfusion	Tingle[55]
Meta-analysis	2374 vs 8716 *(7 trials)*	Hypothermic machine perfusion	Compared to cold storage for expanded criteria kidney transplant donors	↓DGF OR 0.59		Jiao[56]
Observational study	339	Hypothermic machine perfusion	Compared to cold storage	DGF in 4.4% and slow graft function in 12.1%	Lower DGF than expected	Ciancio[57]
DGF in transplantation - procurement and interventions during ex-vivo perfusion						
RCT	59	YSPSL (recombinant P-selectin glycoprotein ligand IgG fusion protein)	Ex-vivo flush prior to organ perfusion	NS		Osama Gaber[96]
RCT	19	Alteplase (Tissue plasminogen activator)	Machine perfusion post organ procurement	NS		Woodside[97]
Single arm trial	60	Oxygen carrier (HEMO2life)	Ex vivo (perfusion fluid)	Single arm only	American Transplant society abstract	NCT02652520[98]
RCT	U	Mirococept (EMPIRIKAL)	Ex vivo perfusion of kidneys prior to transplantation		In progress	Kassimatis[99]
RCT	U	Renaparin	Ex-vivo machine perfusion prior to transplantation		In progress	NCT03773211[100]
RCT	U	Curcumin	Perfusion fluid prior to kidney implantation		In progress	NCT01285375[101]
RCT	U	Custodiol-N solution	Perfusion fluid		In progress	NCT03627013[102]
RCT	92	Etanercept (anti-TNFα)	Machine perfusion		In progress	NCT01731457[103]
DGF in transplantation - recipient related interventions						
Remote ischemia reconditioning						
RCT	60	Remote ischemic post-conditioning	Immediately post re-perfusion	NS		Kim[58]
RCT	80	Remote ischemic pre-conditioning	Intra operative for living donor transplant	NS		Nicholson[60]
RCT	225	Remote ischemic pre-conditioning (CONTEXT)	Intra operative for deceased donor transplant	NS		Krogstrup[59]
Immunomodulation						
RCT	50	Anti-thymocyte globulin	Prior to reperfusion	NS		Ritschi 2018
RCT	U	Anti-thymocyte globulin versus basiliximab (PREDICT-DGF)	Not specified	NS	Terminated, Recruitment issues	NCT02056938[63]
RCT	57	Eculizumab	Paediatric patients administered pre-operatively at induction	NS	Graft loss secondary to adenovirus post eculizumab	Kaabak[80]
RCT	288	Eculizumab (PROTECT)	Induction and 18 hours post operatively	NS	Terminated	NCT02145182[62]
RCT	70	Berinert (C1 esterase inhibitor)	Day of transplant	NS	Fewer dialysis sessions weeks 2 – 4	Jordan[104]

Pilot study	7	GSK1070806 (anti-IL-18 monoclonal antibody)	Intraoperative prior to reperfusion	NS	Terminated, high rate adverse events	NCT02723786[61]
RCT	252	Tomaralimab (OPN-305, anti-TLR-2 monoclonal antibody)	Intraoperative	No results posted	No published results	NCT01794663[64]
RCT	80	Reparixin (CXCL8 inhibitor)	Not specified	No results posted	No published results	NCT00248040[67]
RCT	278	Basiliximab versus thymoglobulin	1st dose intra operatively pre-reperfusion	NS		Brennan[79]
RCT	262	Enlimomab (anti-ICAM-1, EARTS trial)	1st dose pre-transplantation, part of induction therapy	NS		Salmela[81]
RCT	56	FTY720 (sphingosine-1-phosphate receptor agonist, fingolimod)	Immunosuppression for patients at risk of DGF (fingolimod + everolimus and steroids only)	NS	Terminated, Excessive biopsy proven rejection	Tedesco-silva[82]
RCT	668	FTY720 (sphingosine-1-phosphate receptor agonist, fingolimod)	FTY720 versus mycophenolate for maintenance immunosuppression	No results posted	Results not yet published	NCT00239863[68]
RCT	58	Diannexin (recombinant annexin V protein)	Intravenous infusion, timing not specified	No results posted	Subsequent phase II/III trial terminated	NCT00615966[66]
RCT	U	Allogenic umbilical cord derived mesenchymal stem cells	Pre-operative infusion of MSC		In progress	Sun[105]
RCT	374	I5NP (siRNA p53)	For DCD, ECD or SCD with CIT > 24hr		In progress	NCT00802347[65]
RCT	594	QPI-1002 (siRNA p53)	Timing not specified. Brain-dead donors aged > 45 years old		In progress	NCT02610296[71]
RCT	U	Infliximab (anti-TNFα, CTOT-19)	Infliximab at induction with thymoglobulin, steroid, MPA, CNI		In progress	NCT02495077[72]
Calcineurin adjustment/minimisation						
Meta-analysis	1209 *2 trials*	Belatacept	Conversion CNI to belatacept	NS		Masson[86]
RCT	686	Belatacept (BENEFIT)	Belatacept versus cyclosporine	NS	Not specifically for DGF	Vincenti[85]
RCT	69	Belatacept	Either Beletacept or tacrolimus in addition to mycophenolate maintenance therapy	NS	Excess risk for biopsy proven rejection	NCT01856257[74] Newell[84]
RCT	U	Belatacept	Conversion CNI to belatacept on day 7		In progress	NCT01837043[75]
RCT	U	Cyclosporine (Cis-A-rein)	Prior to reperfusion		In progress	Orban[106]
RCT	U	Conversion CNI therapy to Sirolimus	Switch on day 7		In progress	NCT00931255[77]
RCT	U	Envarsus	In place of tacrolimus to reduce delays in recovery from DGF		In progress	NCT03864926[69]
Other agents for DGF						
Cohort study	348	Verapamil	Intraoperatively immediately following reperfusion	NS		Gupta[87]
Observational study	986	Hydroxyethyl Starch	Not specified	Higher risk DGF		Patel[107]
RCT	60	Sanguinate (purified bovine haemoglobin)	Perioperative infusion	No results posted	With-drawn	NCT02658162[91]

RCT	72	Epoetin-alpha	Intraoperatively.	NS		Sureshkumar[90]
RCT	108	Epoeitin-beta (PROTECT)	Pre-operative	NS		Martinez[88]
RCT	40	Heme arginase (HOT trial)	First dose pre-operatively	NS	Thesis online, unpublished	NCT01430156[76]
RCT	U	Frusemide infusion	Post-operative	No results posted	Withdrawn	NCT02312115[73]
RCT	U	Eplerenone (EPURE)	First dose just prior to transplantation		In progress	NCT02490904[92]
RCT	U	Heme Arginate	Pre and 20-28hours post transplantation		In progress	NCT03646344[70]
RCT	U	Dexmedetomidine	During transplant surgery		In progress	NCT03327389[108]
RCT	U	Estrogen (PERT)	Estrogen (Premarin) intra-operatively		In progress	NCT03663543[78]
RCT	U	BB3 (hepatocyte growth factor mimetic)	Within 24 hours of transplantation		In progress	NCT02474667[93]
Native kidney AKI – surgery related AKI						
RCT	16	Ischemic preconditioning and ketorolac	Intra-operatively for partial nephrectomy	Reduced AKI	Small numbers, nephrectomy amount not reported	Kil[109]
RCT	240	ABT-719 (alpha-melanocyte stimulating hormone analogue)	Prevention of AKI in patients undergoing high risk cardiac surgery	NS	Terminated	McCullough 2016
RCT	156	Allogeneic bone marrow derived mesenchymal stem cells (ACT-AKI)	Infused for cardiac surgery patients at high risk of AKI	NS	Terminated	NCT01602328[110]
RCT	U	Pneumoperitoneum pre-conditioning	prior to laparoscopic partial nephrectomy		Not yet recruiting	NCT03822338[111]
RCT	U	Remote ischemic pre-conditioning	Partial nephrectomy		In progress	NCT03068689[112]
RCT	U	Non-milk derived protein (UNICORN)	Post-cardiac surgery		In progress	NCT03715868[113]
RCT	U	Inhaled nitric oxide	Prevention of AKI in patients with endothelial dysfunction post cardiopulmonary bypass		In progress	NCT02836899[114]
RCT	U	QPI-1002 (siRNA of p53)	AKI prevention for cardiac surgery		In progress	NCT03510897[115]
Critically ill/septic patients						
RCT	100	Early nephrologist involvement	Referral for elevated biomarker (TIMP2xIGFBP7)	No results posted	Results not published	NCT02730637[116]
RCT	321	Angiotensin AII (ATHOS-3)	Vasodilatory shock	Better survival and dialysis-free at day 7	Control group had worse liver disease	Tumlin[43]
RCT	80	N-acetylcysteine plus deferoxamine	Critically ill patients with new incidence of hypotension	NS		Fraga[45]
RCT	301	Recombinant alkaline phosphatase (STOP-AKI)	Patients with sepsis associated AKI	NS		Pickkers[44]
RCT	U	Remote ischemic conditioning (RECO sepsis)	Septic shock, within 24 hours of study inclusion		In progress	NCT03201575[117] Cour[46]
RCT	U	Calcifediol or calcitriol (ACTIVATE-AKI)	Critically ill patients intensive care		In progress	NCT02962102[47]

The treatment effect was denoted with NS (or "not significant") if it did not prevent DGF. If insufficient data was publicly available, it was denoted as "U" (unknown). DGF: delayed graft function; AKI: acute kidney injury; CNI: calcineurin inhibitor; CIT; cold ischemia time.

1.3.1 Pre-clinical studies targeting renal IRI

Pre-clinical studies are the foundation from which druggable targets are often identified for clinical testing, but these have well known limitations. For one, the immune pathways in animals (particularly in mice) can vary between strains and species and impedes direct translation to human pathophysiology. Mice are housed in tightly regulated environments and usually lack the same comorbidities seen in patients, which may or may not interact with the targeted treatment. Determining therapeutic dosing of an experimental drug is also a major undertaking, with different therapeutic/toxicity thresholds, acceptable off target side effects in addition to potential pharmacological and pharmacokinetic interactions with other medications (eg immunosuppressive agents). The target/mechanisms listed in table 1.3 are yet to be tested in human subjects.

*Table 1.3: **pre-clinical studies** focusing on ischemia-reperfusion injury in animal models.*

Host	AKI model	Target/mechanism	Effect	Reference
Targeting inflammasome, caspases and cell death pathways				
129/SvJ	Unilateral or bilateral IRI	Cathepsin $G^{-/-}$	Cathepsin $G^{-/-}$ mice had fewer neutrophils and less tubular injury	Shimoda[118]
C57BL/6J	1-hour cold storage of kidney graft	Q-VD-OPh (pan-caspase inhibitor) in perfusion fluid during cold ischemic phase	Q-VD-OPh reduced caspase-3 (but not caspase-1) activation and with less tubular injury.	Nydam[119]
C57BL/6J	Bilateral IRI	Necrostatin-1 administered post IRI injury, compared to zVAD (pan-caspase inhibitor)	Necrostatin-1 reduced IRI but there was no protection with the pan-caspase inhibitor	Linkermann[120]
Wistar rats	Bilateral IRI	Saline, vehicle and inhibition of Casp-1: Ac-DEVD-CHO Casp-3: Ac-YVAD-CMK Pan-casp: Boc-D-FMK	Casp-1 inhibition protected from severe renal injury. Casp-1 and Casp-3 reduced oxidative and nitrosative stress. Pan-caspase inhibition was ineffective.	Chatterjee[121]
C57BL/6J BALB/c	Bilateral nephrectomy with kidney transplant	Caspase-8 shRNA (short hairpin RNA) prior to allogenic kidney transplant	Caspase-8 silencing in recipient mice had lower renal allograft survival, increased necroptosis and HMGB-1 release. RIPK3 knockout mice had less IRI injury, fibrosis, necrotic cells and HMGB1 protein expression in the nephrectomy/IRI.	Lau[122]
	Left IRI, right nephrectomy for AKI model and transplant	RIPK3 knockout mice for assessment of IRI	Donor kidney from RIPK3 knockout model was associated with less inflammation, HMGB1 and increased graft survival.	Lau[122]
C57BL/6N	Cold ischemia with kidney transplant	Caspase-$1^{-/-}$ KO mice	Casp-1 KO mice did not protect mice from AKI with 30 minutes cold ischemia prior to kidney transplantation	Jain[123]
B6/129-jF2	Bilateral IRI	Caspase-$1^{-/-}$ KO mice	Casp-1 KO mice were protected against severe AKI, with less neutrophil infiltration.	Melnikov[124]
C57BL/6J	Bilateral IRI	Caspase$1^{-/-}$, $ASC^{-/-}$, $NLRP3^{-/-}$, IL-$1R^{-/-}$, IL-$18^{-/-}$ KO mice or anakinra (IL-1R antagonist)	$NLRP3^{-/-}$ (and caspase-$1^{-/-}$, $asc^{-/-}$) mice had less tubular injury. IL-1R inhibition with anakinra did not protect from IRI.	Shigeoka[125]
C57BL/6J	Bilateral IRI	Caspase$1^{-/-}$, $ASC^{-/-}$, $NLRP3^{-/-}$ $NLRC4^{-/-}$ KO mice	$NLRP3^{-/-}$ and $ASC^{-/-}$ mice had less tubular injury	Iyer,[126]
C57BL/6J	Bilateral IRI and cisplatin	$NLPR3^{-/-}$ KO mice	$NLPR3^{-/-}$ protected against severe IRI	Kim[127]
C57BL/6J	Bilateral IRI and cisplatin	Casp$11^{-/-}$ and GSDMD $^{-/-}$ KO mice	GSDMD KO was not protective against ischemic AKI but increased casp-11 and GSDMD increased after IRI	Miao[128]

C57BL/6J	Bilateral IRI and cisplatin	GSDMD$^{-/-}$ GSDME$^{-/-}$ KO mice	GSDMD and GSDME KO sensitizes *DOI:10.21203/rs.3.rs-1719338/v1*	Tonnus *Pre-print*
Rats: Lewis & Fisher344	Kidney transplant ± cold ischemia (12, 16hr)	MCC950 (NLRP3 inhibitor) added to UW solution and administered to mice after transplantation	MCC950 reduced tubular injury if kidneys exposed to 12 or 16hr cold ischemic time. Less CD3 and CD68 infiltration after 7 days in the allogenic model with MCC950 treatment.	Zou[129]
C57BL/6J	In vivo bilateral IRI model	Hydroxychloroquine (suppresses cathepsin and NLRP3 inflammasome)	Hydroxychloroquine treatment resulted in less tubular injury	Tang[130]
C57BL/6J	Right nephrectomy, left IRI	Beta-hydroxybutyrate modulates the FOXO3/pyroptosis pathway	Beta-hydroxybutyrate treatment partially protected against IRI	Tajima[131]
Sprague Dawley rats	Right nephrectomy, left kidney IRI	FGF-10 (regulation of autophagy and inflammatory signalling)	FGF-10 reduced SCr, anti-TNF levels and had less tubular injury. FGF-10 effects were mitigated by rapamycin	Tan[132]
Sprague Dawley rats	Left nephrectomy, Right IRI	Rapamycin (mTOR inhibitor) given day -3 until experiment end	Rapamycin inhibited proliferation and delayed recovery from ischemic injury.	Lieberthal[133]
C57BL/6J	Bilateral IRI	ATG5$^{-/-}$ (autophagy protein)	More severe tubular injury, accumulation of p62 and LC3-1 (marker of oxidative stress) in ATG5 knockout mice	Liu[134]
Targeting complement, signalling and adhesion molecules				
Sprague Dawley rats	Bilateral IRI	Thombospondin-1 (TSP-1)$^{-/-}$	TSP-1 null mice had less tubular injury	Thakar[135]
C57BL/6J	Bilateral IRI, kidney transplant with 4 hours cold ischemia	Reduced CD47 activity (KO mice, siRNA or CD47 antibody) in IRI and transplant model	Mice with reduced CD47 activity were protected from IRI (native kidney and transplant model). This was associated with increased c-myc, proliferation and resistance to exogenous TSP-1 (induced by HIF-2a)	Rogers[136]
C57BL/6J	Bilateral IRI	HIF1a and HIF2a$^{-/-}$ KO mice	HIF1a or HIF2a deficiency mice both had more severe IRI compared to wild type controls	Hill[137]
C57BL/6J	Bilateral IRI	ICAM-1$^{-/-}$ KO mice	ICAM-1$^{-/-}$ mice had less tubular injury	Kelly[138]
FVB mice	Bilateral IRI	Diannexin (annexin V analogue) prior to surgery	Diannexin reduced tubular injury and expression of KIM-1 and NGAL	Wever[139]
C57BL/6J	Bilateral IRI	C5aR$^{-/-}$ KO mice	C5aR knockout mice had less tubular injury, pro-inflammatory cytokines and fibrosis	Peng[140]
C57BL/6J	Kidney transplant with 4 hours cold ischemia	C3, ReIB and Fas siRNA (silencing RNA) perfusion of donor kidney (in vivo) prior to transplantation	siRNA treated mice had less tubular injury and improved graft survival	Zheng[141]
C57BL/6J BALB/c	Bilateral IRI Or kidney Tx with 1-hour cold ischemia	Bβ(15-42) – breakdown product of fibrin at time of procedure	Treated mice had less IRI, reduced ICAM-1, VCAM-1 and E-selection expression and subsequently fewer inflammatory infiltrates	Sorensen[142]
Wistar rats	Bilateral IRI	Bone morphogenic protein-7 (osteogenic protein-1)	BMP-7 given prior to IRI procedure reduced renal tubular injury	Vukivevic[143]
C57BL/6J	Bilateral IRI	Sphingosine-1 phosphate$^{-/-}$ (S1P) KO mice	Deletion of S1P resulted in upregulation of endothelial adhesion molecules and worse IRI/tubular injury	Perry[144]
C57BL/6J	Bilateral IRI	Shingosine-1-phosphate receptor-3$^{-/-}$ DC	SIPR3 deficient DC protected mice from IRI tubular injury	Bawja[145]
C57BL/6J	Bilateral IRI	FTY720 (sphingosine-1 analogue, fingolimod)	FTY720 were partially protected against IRI	Kaudel[146]
C57BL/6J	Bilateral IRI	Curcumin liposomes	Reduced IRI via NFKB pathway	Rogers[147]
C57BL/6J BALB/c	Bilateral IRI. Kidney Tx, 1hr cold ischemia	AQGV (EA-230) – synthetic oligopeptide derived from beta-human chorionic gonadotropin	EA-230 reduced IRI injury in the AKI model and improved allograft survival compared to non-treated mice if given 1-hr pre or 24-hrs post transplantation in the DGF model	Gueler[148]
Fischer rats	Left IRI, right nephrectomy	A20 via adenovirus vector	A20 expression reduced tubular injury and transcript levels of NF-kB and endothelial activation	Lutz[149]
C57BL/6J	Bilateral IRI	IL-18$^{-/-}$ KO mice	IL-18 deficiency mice had less tubular injury	Wu[150]

C57BL/6J	Bilateral IRI	Recombinant mouse IL-33	Pre-treatment with IL-33 protected against renal IRI and increased CD45+CD127+GATA3+CD3-CD19-CD11b-CD11c-CD56- cells (IC2 cells) and M2 macrophage phenotype	Cao[151]
C57BL/6J	Bilateral IRI	IL-10$^{-/-}$ KO mice with or without anti- IL-6 antibody	IL-10 mice had less tubular injury IL6-blockade= no significant difference	Sakai[152]
C57BL/6J	Bilateral IRI	Tissue factor$^{-/-}$ KO mice Protease-activated receptor 1$^{-/-}$	TF or PAR deficiency had less tubular injury	Sevastos[153]
Targeting cellular immunity				
C57BL/6J	Bilateral IRI	Macrophage depletion by liposomal clodronate	Macrophage deficient mice had less tubular injury	Day[154]
Rabbit	Renal artery occlusion	Neutrophil depletion by nitrogen mustard treatment	Neutropenia did not protect against IRI	Paller[155]
C57BL/6J	Bilateral IRI	Clopidogrel or DNase I	DNase I treatment pre-IRI reduced biochemical but not histological evidence of IRI. Clopidogrel led to reduced NETosis and tissue inflammation.	Jansen[156]
C57BL/6J	Bilateral IRI	CD11c^{+} F4/80^{+} DC depletion by liposomal clodronate	Depletion of CD11c^{+} cells lead to prolonged inflammation and less anti-inflammatory DC phenotype and IL-10 levels at day 7.	Kim[157]
C57BL/6J	Bilateral IRI	Thymectomy and antibody mediated T-cell depletion	Partial, but not complete reduction in tubular injury	Yokota[158]
C57BL/6J	Bilateral IRI	RAG-1$^{-/-}$ KO mice	RAG knockout mice were not protected from IRI compared to wild type controls	Park[159]
C57BL/6J	Bilateral IRI	Enhanced T-cell specific Nrf2 in Keap1$^{-/-}$ KO mice	Nrf2 augmented (keap-1 deletion) mice were found to have increased basal T-reg population and partially protected from IRI compared to wild type controls	Noel[160]
C57BL/6J	Bilateral IRI	B cell deficient mice μMT (Igh-6^{tm1Cgn})	B-cell deficiency reduced severity of IRI injury	Burne-Taney[161]
Wistar rats	Right IRI and left nephrectomy	Cyclosporin vs Tacrolimus vs Rapamycin vs Mycophenolate	Rapamycin reduced caspase-3 activity; and levels of pro-IL-1b, pro-caspase-1 but not the active subunits. Other agents did not have significant effect.	Yang[162]
Sprague-Dawley rats	Nephrectomy, contralateral IRI	Blockade of CXCR3 and CCL5 (TAK antagonist) to modulate NKT and T-cells	Blockade was associated with less tubular injury	Tsutahara[163]
C57BL/6J	Bilateral IRI	NKT cell blockade by CD1d monoclonal antibody or Jα18$^{-/-}$ KO mice	Depletion of NKT cells by either method protected against IRI, with less tubular injury	Li[164]
C57BL/6J	Bilateral IRI	Talin (L325R) mutation	Impaired beta-2 integrin to neutrophil function resulted in less tubular injury	Yago[165]
Targeting the reactive oxygen species pathway				
Swiss Mice	Unilateral IRI, contralateral nephrectomy	Apotransferrin	Did not affect IRI induced renal apoptosis but reduced neutrophil infiltration, renal superoxide formation.	De Vries[166]
Sprague-Dawley Rat	Left IRI with Right Nephrectomy	Resveratrol (2,5,4'-trihydroxystilbene phenol antioxidant)	Resveratol reduced cell death, TLR-4, MyD88, NK-kB, caspase-3	Li[167]
C57BL/6J	Left IRI with right nephrectomy	PrC-210 (Aminothiol reactive oxygen species scavenger)	PrC-210 reduced IRI induced injury and caspase-3 activity	Bath[168]

IRI: ischemia reperfusion injury, casp: caspase, KO: knock out, HMGB: high motility group box1, RIPK: receptor interacting protein kinase, NLRP: NOD-, LRR- and pyrin domain-containing protein 3), GSDM: gasdermin, siRNA: silencing RNA, TSP: thrombospondin, ATG – autophagy related, HIF: hypoxia inducible factor, ICAM: intercellular adhesion molecule 1, VCAM: vascular cell adhesion protein 1, KIM: kidney injury molecule, NGAL: neutrophil gelatinase-associated lipocalin, SIRP: signal regulatory protein, RAG: recombination activating gene, Nrf2: nuclear respiratory factor2.

1.4 Acute kidney injury studied through ischemia reperfusion injury

Renal ischemia reperfusion injury (IRI) is a common experimental model to investigate AKI. In essence, restricted blood supply results in a mismatch between oxygen and nutrient delivery to meet cellular demand to form the ischemic phase. Reliance on anaerobic metabolism and impaired aerobic metabolism impairs the ability to generate sufficient energy rich phosphates to support essential cellular processes. The switch to glycolysis also leads to the accumulation of waste products, including lactate (leading to acidotic environment) and hypoxanthine (substrate for reactive oxygen species formation), which further compounds the insult of ischemia. The inability to support energy-dependent mechanisms of cellular homeostasis leads to cellular dysfunction and/or death. Reperfusion can halt further ischemia mediated insult by restoring oxygen and nutrient delivery to save viable ischemic tissue, but paradoxically, can further exacerbate injury through generation of reactive oxygen species and an intensified immune response and inflammation.[169] (Fig 1.3) Areas of irreversible damage may be accompanied by viable tissue which is 'stunned', a phenotype characterised by persistent period of dysfunction post reperfusion.[170] These viable cells then can enter a hibernation phase following prolonged ischemia, characterised by an adaptive metabolic phenotype favouring glycolysis or anaerobic metabolism as their adenosine 5'-triphosphate (ATP) energy source.[171,172]

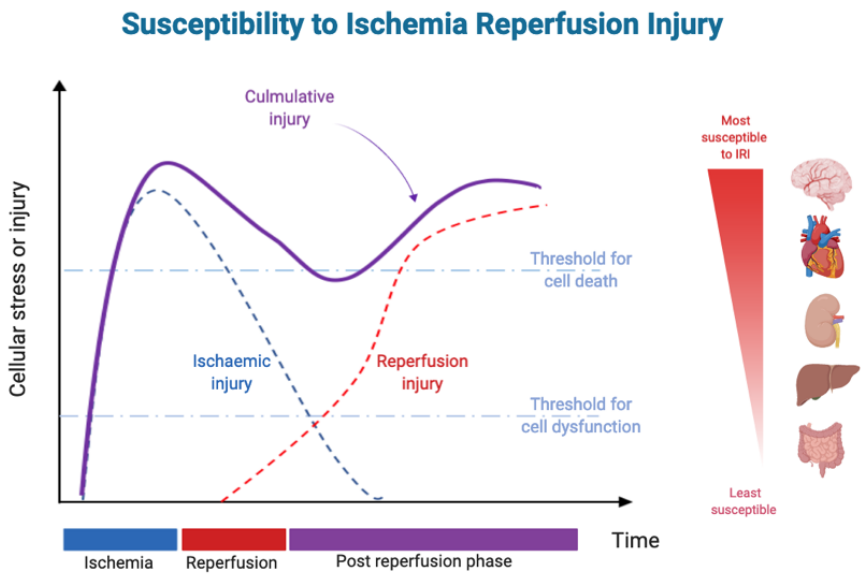

Figure 1.3: ***Biphasic phases of ischemia-reperfusion injury****. The damage sustained during the ischemic phase can be exacerbated during the reperfusion phase due to the generation of reactive oxygen species and inflammation. The sensitivity or susceptibility of organs to IRI is variable and related to their metabolically activity* (image created with BioRender).

Ischemia reperfusion injury (IRI) can affect all cell types but there are organ-specific differences with respect to sensitivity, severity, and reversibility of IRI. The kidney is a complex organ with highly metabolically active cells, including proximal renal tubular epithelial cells, and is susceptible to IRI/hypoperfusion states such as arterial emboli, severe atherosclerotic disease, renal vein thrombosis, shock states (cardiogenic, septic, hypovolemic or vasodilatory causes). Renal IRI occurs in all kidney transplantation procedures, with varying severity dependant on live-donor versus deceased-donor operations and the degree of warm ± cold ischemic insults. IRI is an important cause of acute kidney injury (AKI) for both native and transplant kidneys and logically the chosen pre-clinical model for this thesis.

1.4.1 The murine renal ischemia reperfusion model: animal and surgical considerations

Animals used in the pre-clinical studies of IRI have changed over time, with mice being the favoured study subject in the past 20 years due to the ability to control both phenotype and genotype, selection of stable generations of in-bred strains with or without mutations, predictable life cycle, size, housing, and up-scaling study numbers compared to larger animals such as rabbits, dogs, and non-human primates. Despite the obvious differences, humans and mice have comparable genetic homology and are overall suitable models to study human health and disease in the correctly selected murine model.[173-175] There are known variations in genetic susceptibility in mice strains to ischemia reperfusion injury, age, and gender. Typically, for renal ischemia injury studies, male C57Bl/6 and BALB/c mice are most commonly used and selected for similar ages (young mice 8 to 12-weeks of age are more likely to tolerate the IRI procedure and AKI better than aged mice, who may not survive appropriately for the study).

Warm ischemia is the most commonly studied mechanism of renal IRI, using atraumatic microvascular clips to temporarily clamp one or both renal pedicles controlling for mode of anaesthesia, surgical approach (lateral versus midline laparotomy), occlusion time, core body temperature and whether the surgery is accompanied by unilateral nephrectomy. The outcomes following renal IRI surgery can be variable if these factors are not defined in a standardised protocol across for all mice and treatment groups. Furthermore, it is desirable to maintain consistent operator(s) to minimise the inter-operator variability. Visual inspection of

the kidney confirmation for hyperaemic pink or pink-red colour following reperfusion, as there is risk of venous thrombosis following prolonged clamping and bleeding from incorrect clip placement. (Fig 1.4)

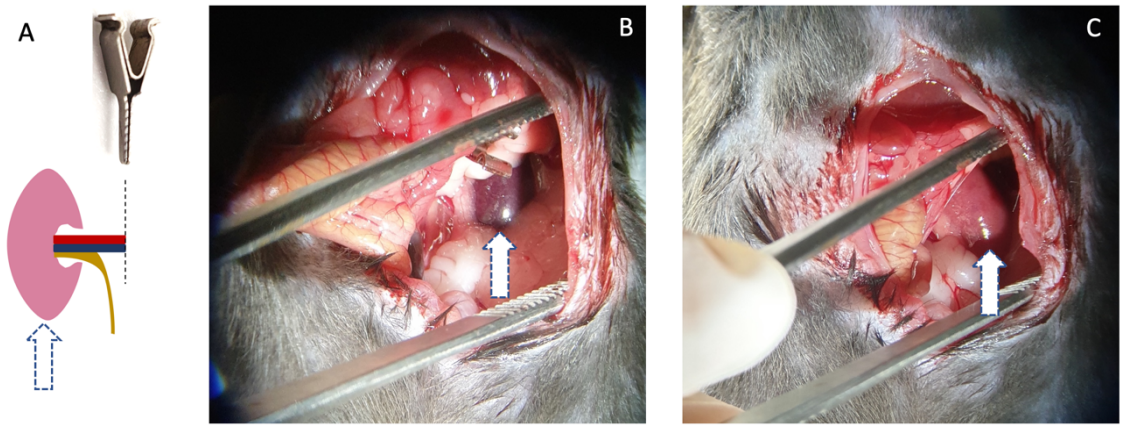

*Figure 1.4: **Mouse ischemia reperfusion injury model**. (a) application of a microvascular, atraumatic clamp to the renal pedicles to occlude blood supply to and from the kidney for a defined time period; (b) left ischemic kidney (white arrow in B) during clamping; and (c) reperfusion visualised (white arrow in C) after removal of the ischemic clamps.*

Mice are recovered and monitored over the subsequent days for signs of pain, distress, and significant weight loss (weight loss > 10-15% may signify an unwell mouse, either from surgery or severe AKI). Animals were euthanised typically between 24 to 72-hours post renal IRI surgery to collect blood/samples for AKI studies.

1.4.2 Acute tubular injury: limitations of histological scoring systems

The characteristics of acute tubular injury (ATI, also known as acute tubular necrosis/ATN) include tubular dilatation, interstitial oedema, epithelial vacuolisation, brush border integrity and intraluminal slough and cast formation. There is no validated scoring system for ATI severity, which is a significant source of heterogeneity for research in this area. We used arbitrary, categorical scores to quantify tubular injury in our mice models, similar to earlier publications[136]: score 0 for minimal or absent injury, 1 for <10%, 2 for 10 – 24%, 3 for 25 – 50% and 5 for > 50% of the area involved. Pieters et al[176] proposed a system to score ATI severity in a retrospective cohort of kidney transplant patients, and demonstrated a correlation between ATI severity and long term estimated glomerular filtration rate, although allograft rejection and 12-month kidney biopsy Banff scores[177] were not included (Table1.4).

Table 1.4: summary of histological criteria for renal tubular injury used in literature.

Scoring	**0**	**1**	**2**	**3**	**4**
Banff criteria: Gold standard for assessing the human renal allograft in rejection *(selected components)*[177]					
Tubulitis (t)	nil	<25%	26-50%	>50%	-
Interstitial inflammation (i)	<10%	10-25%	26-50%	>50%	-
Interstitial fibrosis (ci)	<5%	5-26%	26-50%	>50%	-
Tubular atrophy (ct)	nil	<25%	26-50%	>50%	-
Total inflammation (ti)	<10%	10-25%	26-50%	>50%	-
Inflammation in IFTA (iIFTA)	<10%	10-25%	26-50%	>50%	-
Pieters criteria for scoring acute tubular injury in the human renal allograft[176]					
Dilatation	0-1%	>1-10%	>10-25%	>24-50%	>50%
Vacuolisation	0-1%	>1-10%	>10-25%	>24-50%	>50%
Casts	0-1%	>1-10%	>10-25%	>24-50%	>50%
Interstitial oedema	0-1%	>1-10%	>10-25%	>24-50%	>50%
Mouse criteria for histological scoring in renal acute tubular injury[152]					
Tubular epithelial injury (‘tubulitis’)	0%	1-25%	26-50%	51-75%	>75%
Loss of brush border	0%	1-25%	26-50%	51-75%	>75%
Cast formation	0%	1-25%	26-50%	51-75%	>75%
Tubular dilatation	0%	1-25%	26-50%	51-75%	>75%

IFTA: interstitial fibrosis and tubular atrophy

1.5 Pathophysiology of ischemia reperfusion injury

The pathophysiology of ischemia reperfusion injury is complex and can involve alterations in kidney tubular structure, function, and metabolism, abnormal repair, disruptions to the microvascular and altered immune response[178-181]. The subsequent section of this chapter will focus on the key immune-related aspects of IRI.

1.5.1 Cellular inflammation

Regardless of organ, IRI affects the microvasculature and leads to endothelial damage and increased vascular permeability from alterations of the glycocalyx and cytoskeletal elements of cell-cell interactions and facilitates transmigration of leukocytes through upregulation of P-selectin (initiates cell rolling), intercellular adhesion molecule 1 (ICAM-1, for cell adhesion) and platelet and endothelial cell adhesion molecule (PECAM-1, for diapedesis)[182]. (Fig 1.5) The following section describes the key immune cells in IRI – dendritic cells, monocytes/macrophages, neutrophils, NK-T cells, T- and B- cell lymphocytes.

Dendritic cells (DC) have a critical role in both injury and reparative phases following IRI and can be from derived from the circulating (bone marrow derived and seen in the first 3 hours post IRI) or tissue-derived (tissue-resident) pool of dendritic cells. They are important sentinels and are the most effective antigen presenting cells (APC) to provide a link between the innate and adaptive immune response[183]. DCs respond to danger associated molecular patterns (DAMP), such as high motility group box (HMGB) and heat shock protein (HSP) via toll-like receptors (TLR), or antigens (self-antigen in native IRI, or foreign peptides in the setting of IRI or alloimmune response in solid organ transplantation) processed to form the MHC complexes to present to the T-cell receptor.

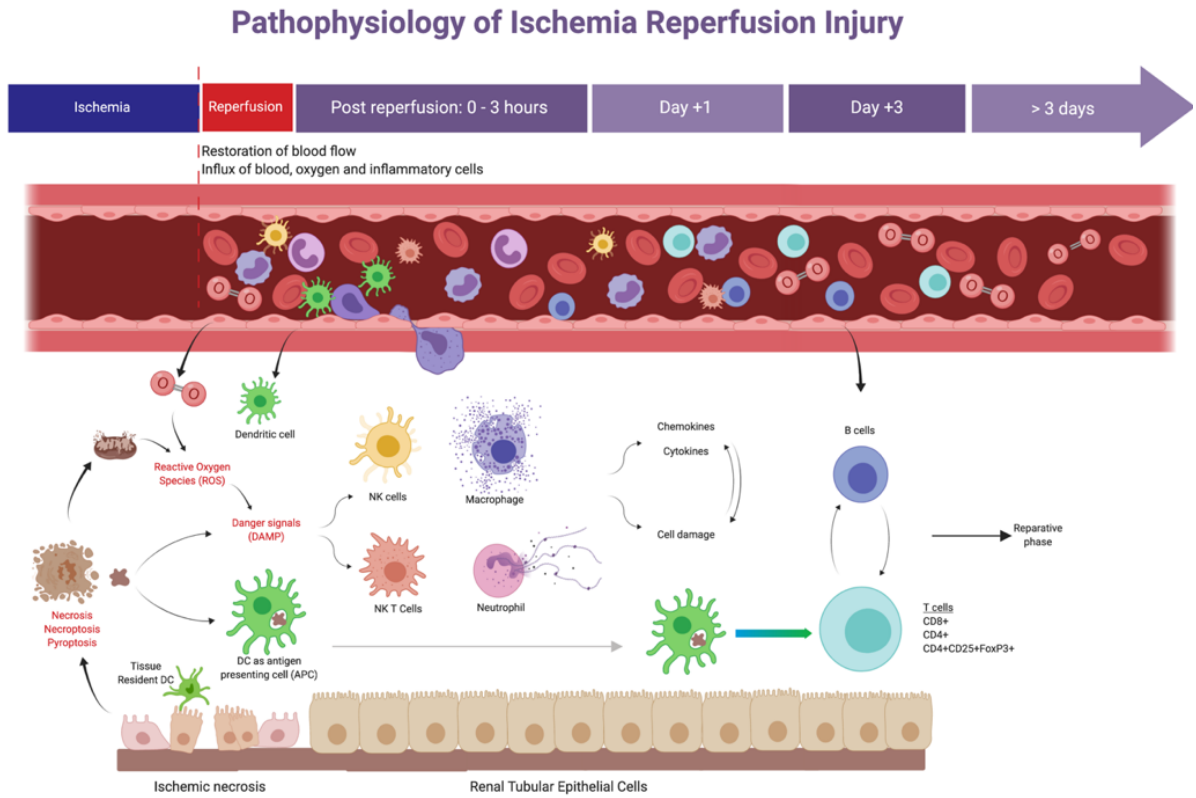

*Figure 1.5: **Summary of inflammation in ischemia reperfusion injury**. Severe ischemia results in cellular necrosis and release of DAMP signals, self-peptides and reactive oxygen species. This is followed by cellular adhesion, migration, and transmigration from the microcirculation to the site of injury. These innate cells further promote the inflammatory cascade through release of various chemokines and cytokines. Dendritic cells are the most important antigen presenting cells (either derived from tissue resident or circulating populations) which link the innate and adaptive immune system. (Created with BioRender).*

Stimulated DCs have an increased co-stimulatory capacity through maturation and upregulation of co-stimulatory molecules (MHCII, CD40, CD80 and CD86) and can also promote local inflammation by production of NF-kB related cytokines following activation of the TLR-MyD88 pathways. Previous studies have shown depletion of DCs in transgenic mice (via CD11c-diptheria toxin) demonstrating less biochemical

or histological injury following renal IRI.[184] Dendritic cells can also display an immunomodulatory (also known as tolerogenic or regulatory) phenotype in the reparative phase via production of anti-inflammatory cytokines (IL-10) and induction of regulatory T-cells.[136,185]

Monocytes/macrophages are also present in the early stages of IRI and have similar ontogeny, phenotype, and function to dendritic cells. Macrophages are also able to present antigen, have a role in both injury and reparative phases and in particular and are important in phagocytosis and processing of cellular debris in the setting of sterile inflammation. Macrophages have been segregated into M1 (classically activated) and M2 (alternatively activated) phenotype, but delineation is likely a representation of different activation stages of macrophages, similar to mature versus tolerogenic dendritic cells[186]. The M1 macrophage phenotype which are activated by various stimuli, including pattern recognition receptor (PRR) and DAMP signalling, reactive oxygen species, chemokines and IFN-γ released by T-helper and NKT cells[187], as opposed to the alternate M2 macrophage, which has wound healing and immunoregulatory capacity.

Neutrophils along with DCs and macrophages are the earliest responders to IRI but the role of neutrophils in IRI is yet to be definitely delineated. As studies have shown neutropenia to be protective in cardiac[188], hepatic[189], pulmonary[190] and intestinal[191] IRI and the targeting neutrophil recruitment molecules (such as CD44[192], ICAM-1[138] and cathepsin G[118]) also confers a degree of renoprotection, but neutrophil-depleted animals were not protected from IRI[155,193]. No doubt, neutrophils can contribute to the early inflammation, and DAMP such as HMGB1 can induce neutrophil NETosis, or release of its chromatin granular contents (including proteinases and cationic peptides), reactive oxygen species, and chemokines and cytokines to exacerbate and perpetuate tissue injury.

Natural killer-T (NK-T) cells are also early primary responders in IRI. NKT cells are a unique subset of the T-cell population, which express both CD161 (NK1.1 as the murine homolog) and a T-cell receptor but do not recognise peptides associated with antigen presenting cell and major histocompatibility complex (MHC) molecules. Instead, they respond to glycolipid presented by CD1d[194,195], produce substantial pro-inflammatory Th-1 type (IFN-γ, TNF-α) and Th2 (IL-4, IL-13) cytokines and can modulate both dendritic

and T-cell[196]. DCs can also activate NK-T cells through sphingosine-1-phosphate (S1P) IRI[145] and while S1P-receptor-3 (S1P3) knock out mice were protected from renal IRI[145], clinical studies using fingolimod (S1P inhibitor) did not translate to protection[68,82]. Adenosine 2A receptor tolerised dendritic cells loaded with NK-T cell antigens were able to limit NK-T activation and protect against acute kidney injury[197]. Natural killer (NK) cells are also seen early in the inflammatory process[198] and have direct cytotoxic capacity[199] but their role in IRI is uncertain. CD137+ NK cells can stimulate renal tubular epithelial cells to express CD137-ligand and CXCR2 to induce neutrophil migration and tubular epithelial cells themselves can produce CCR5 that is required for NK cell chemotaxis, but further research is required to elucidate their role[200].

T-cell lymphocytes including effector ($CD4^+$ and $CD8^+$) and regulatory ($CD4^+CD25^+FoxP3^+$) T cells are important in the pathogenesis and recovery following IRI. Effector T-cells can remain in the kidney following IRI, function as memory T-cells[201] and further influence the development of chronic kidney disease and future adaptive immunological response to solid organ transplantation. Early in the IRI injury, $CD4^+$ T-cells are the first to be recruited and have been shown to influence the severity of IRI, with less hepatic injury in $CD4^+$ T-cell deficient mice.[202] They also influence neutrophil recruitment following hepatic IRI.[203] Both Th1 and Th2 $CD4^+$ T-cell subsets are seen in renal parenchyma following IRI and has been shown to be dependent on IL16[204] CD28-B7-1 (T-cell to endothelial cell) expression.[205] Regulatory T-cells (Tregs) derived from either natural tolerance (self-tolerance to peripherally sampled antigens) or induced (exposure to antigens primed in the context of co-stimulation) are important in IRI. Worse renal IRI is seen following anti-CD25 antibody mediated depletion of Tregs[206], while adoptive transfer of third party Tregs up to 24hrs post injury has shown benefit in animal models.[207]

B lymphocytes are the latest to join in the inflammatory milieu and have been shown to have varying effects in renal IRI, ranging from protective[161,202,208] to impairing repair processes.[209] Depletion of both T- and B-cell confer no protection against renal IRI in mice[161] but B-cell deficiency has been shown to be protective against IRI[210] and more recent studies have suggested their increasingly important role in IRI, maladaptive repair and link between IRI and long term chronic renal disease[209,211,212].

1.5.2 Reactive oxygen and nitrogen species

Reactive oxygen species (ROS) are critical in the pathophysiology of IRI. The primary ROS moieties released in IRI are superoxide and hydrogen peroxide (enzymatically dismutated superoxide) which interact with various lipids and proteins to cause oxidative stress.[213] Superoxide will also interact with bioavailable *nitric oxide* (NO) to form reactive nitrogen species (RNS) such as peroxynitrite. ROS and RNS both can contribute to cellular dysfunction, impaired vascular tone, tissue damage and can also act as DAMP signals to further promote the inflammatory cascade[214]. In addition to peroxynitrite, other important and biologically active ROS moieties includes malondialdehyde, conjugated dienes, hydroxynonenol and oxidised glutathione. Inducible nitric oxide synthase (iNOS) is activated by inflammation and the endothelial (eNOS) isoform is important for the regulation of vascular muscle tone and generation of superoxide when uncoupled in the absence of essential co-factors. iNOS is found in all inflammatory cells and produces large amounts of NO to generate peroxynitrite.[215,216]

Major sources of superoxide include NADPH oxidase (NOX – expressed in phagocytic cells such as macrophages and neutrophils) and mitochondrial cytochrome P450 peroxidases (mcP450). NOX knockout mice suffer less injury following IRI in the kidneys[217,218], but also this effect is seen in the myocardium[219], lung[220] and liver[221]. Superoxide is readily converted into hydrogen peroxide by superoxide dismutase (SOD-2), localised in the outer mitochondrial membrane[222,223] and mcP450 further metabolises hydrogen peroxide into highly pro-inflammatory hypobromous and hypochlorous acid[224], uncoupled endothelial nitric oxide synthase and xanthine oxidase. Excess ROS in IRI can lead to the accumulation of dynamin 1 like protein (DRP1) in the mitochondrial membrane, further exacerbating mitochondrial fragmentation, release of mitochondrial DNA resulting in both mitophagy and cell death.[222,225,226] (Table 1.5) Other important ROS pathways include xanthine oxidase (for purine metabolism) and heme oxygenase (degradation of heme to bilirubin to release iron and carbon monoxide[227]. Inhibition of xanthine oxidase[228] and expression of heme oxygenase in the renal parenchyma[229] or infiltrating myeloid cells[230] have all shown beneficial protection in the setting of renal IRI. Interventions that enhance ROS scavenging are universally protective against IRI[168,231,232]. However, no ROS-mediating agents have performed sufficiently effectively in clinical trials to reach clinical use[233-236].

Table 1.5: ***Sources of superoxide and reactive oxygen species***

Sources	Source	Comments
NADPH oxidases (NOX)	Macrophages and neutrophils	Membrane bound amalgamated subunits such as NOX1-5, Duox1 & 2. These generate superoxide and modulate damage by conversion of xanthine oxidase and uncoupling of endothelial nitric oxide synthase
Cytochrome P450 enzymes	Liver predominant	CYP450 enzymes use oxygen or NADPH to alter the redox status of lipids, steroids and vitamins. They are also found as eosinophil peroxidase and neutrophil myeloperoxidase that produce hypobromous and hypochlorous acid
Mitochondrial oxidative phosphorylation	Mitochondria	Electron leak from Complexes I and III from the mitochondrial electron transport chain causes reduction of oxygen to superoxide. Superoxide dismutase (SOD) and monoamide oxidases are also found in the mitochondrial membrane and produce hydrogen peroxide, oxidizes cytochrome C
Nitric oxide synthase (NOS)	Neuronal NOS Inducible NOS Endothelial NOS	nNOS is constitutively expressed, iNOS is induced with inflammation and eNOS is critical in the regulation of vascular tone. These enzymes require the cofactor tetrahydrobiopterin to oxidise L-arginine to L-citrulline and produce nitric oxide (NO). Excess NO can combine with superoxide to generate peroxynitrite, which further mediates ROS damage.
Xanthine oxidase (XO)	Variable, highest in endothelium	Xanthine dehydrogenase (XDH) undergoes translation in the setting of inflammation into xanthine oxidase (XO) and can generate superoxide and hydrogen peroxide
Heme oxygenase (HO)	Variable	Heme oxygenase is usually undetectable at basal levels but upregulated in response to IRI and is critical for cytoprotection – anti-oxidant, anti-inflammatory and anti-apoptotic capacity

1.5.3 Danger signals linking sterile inflammation to cell death

Under physiological conditions, danger-associated molecular patterns (DAMP) are normally sequestered within the cell and not visible to the immune system but are released into the extracellular environment following cellular injury. Studies have indicated exogenous administration of DAMPs can exacerbate IRI injury, whereas inhibition of DAMPs can reduce severity of injury[237]. DAMPs are a key link between sterile injury (i.e. following IRI and transplant rejection) and an amplified immune response. Examples of endogenous DAMPs which bind to intracellular or cytosolic receptors such as NOD-like receptors (NLR) or AIM2-like receptors (ALR) include ATP, cathepsin, mitochondrial ROS and lactic acid. DAMPS which engage extracellular pattern recognition receptors (PRR), such as toll-like receptor (TLR), include high-motility group box-1 (HMGB-1), S100 proteins, heat-shock proteins (HSP), cytosolic DNA, neutrophil-derived alarmins, fibrinogen and Tamm-Horsfall glycoproteins[238], elastin-derived peptides which act via integrins and adenosine via P2X and P2Y receptors[239,240].

DAMP-TLR interactions seem to have organ specific effects, as global knockout of TLR2 and TLR4 are protective against renal[241,242] and myocardial[243] IRI but were associated with decreased survival with lung IRI[238]. In addition to TLR binding, DAMPs also require varying co-receptor and adaptor molecules, such as CD14, MD-2, NLRP3 for effective downstream signal transduction[237]. Subsequent downstream signal transduction involves 5 important adaptor molecules, including: *myeloid differentiation factor 88* (MyD88), *MyD88-adaptor like* (Mal), *TIR domain-containing adaptor inducing IFN-beta* (TRIF), *TRIF-related adaptor molecule* (TRAM) and *sterile alpha and HEAT-armadillo motifs* (SARM)[244]. The MyD88-dependent pathway is activated by all TLR molecules (except TLR3) and requires *IL-1R-associated kinases* (IRAK-1, -4), *TNF receptor-associated factor 6* (TRAF-6) and *mitogen activated kinases* (MAPK) to eventually activate the NFκB transcription factor to drive inflammation. MyD88-independent pathways (via TRIF) can also be activated via both TLR3 or TLR4 and the *interferon regulatory factor* (IRF) family of transcription factors.

1.5.4 Regulated cell death: apoptosis, autophagy and parthanatos

The mode of cell death influences the release of intracellular contents in response to injury during IRI influences its pro-inflammatory potential[245-247]. (Fig 1.6) The following section will describe these briefly necrosis and regulated necrosis (necroptosis, pyroptosis and ferroptosis) all contribute to the hyperacute inflammation of renal IRI – these pathways are likely share common features although the detailed mechanisms are still under investigation.

Apoptosis, qualitatively distinct and less common than necrosis following IRI, generates a more immunologically tolerant environment. It is characterised by cell shrinkage, chromatin condensation, plasma membrane blebbing and apoptotic bodies.[248] Exposure of phosphatidylserine on the cell surface is one of the important signals to promote efferocytosis and clearance of inflammatory debris by macrophages.[249,250] Initiation of apoptosis can be via the intrinsic or extrinsic pathways in IRI. The extrinsic pathway involves activation of death factors of the TNF-family ligands (TNF-α, *TNF-related apoptosis-inducing ligand* or TRAIL, and *Fas-ligands* or Fas-L) and cell surface receptors (TNF-R1, TRAIL-R1, TRAIL-R2 and Fas)[251,252] with activation of initiator and executioner caspases[253]. This leads to oligomerisation of the

cytoplasmic regions of death receptors including *Fas-associated death domain* (FADD), procaspase-8 and *cellular FADD-like ICE* (c-FLIP).

The intrinsic pathways of apoptosis in response to mitochondrial stress leads to damage of its outer membrane and release of cytochrome C, which combines with *apoptotic protease activating factor* (*Apaf-1*) to initiate apoptosome complex formation, procaspase-9 recruitment, autolytic cleavage, and activation. Apoptosis is regulated primarily by *B-cell lymphoma 2* (*Bcl-2*) family, which is either pro- or anti-apoptotic based on the homology domains (BH) and can be divided into 3 main subsets: *pro-apoptotic members* (*Bim*, *Bid Bad* and *Puma*), p*ro-apoptotic effector* molecules (*Bax* and *Bak*) and *anti-apoptotic proteins* (Bcl-2, *Bcl-xl*, *Bcl-G*).[254] These subsets are also regulated by p53, an important tumour suppressor gene involved in apoptosis. Trials using QPI-1002 to silence p53 is currently in progress for both DGF following transplantation and AKI following major cardiac surgery.

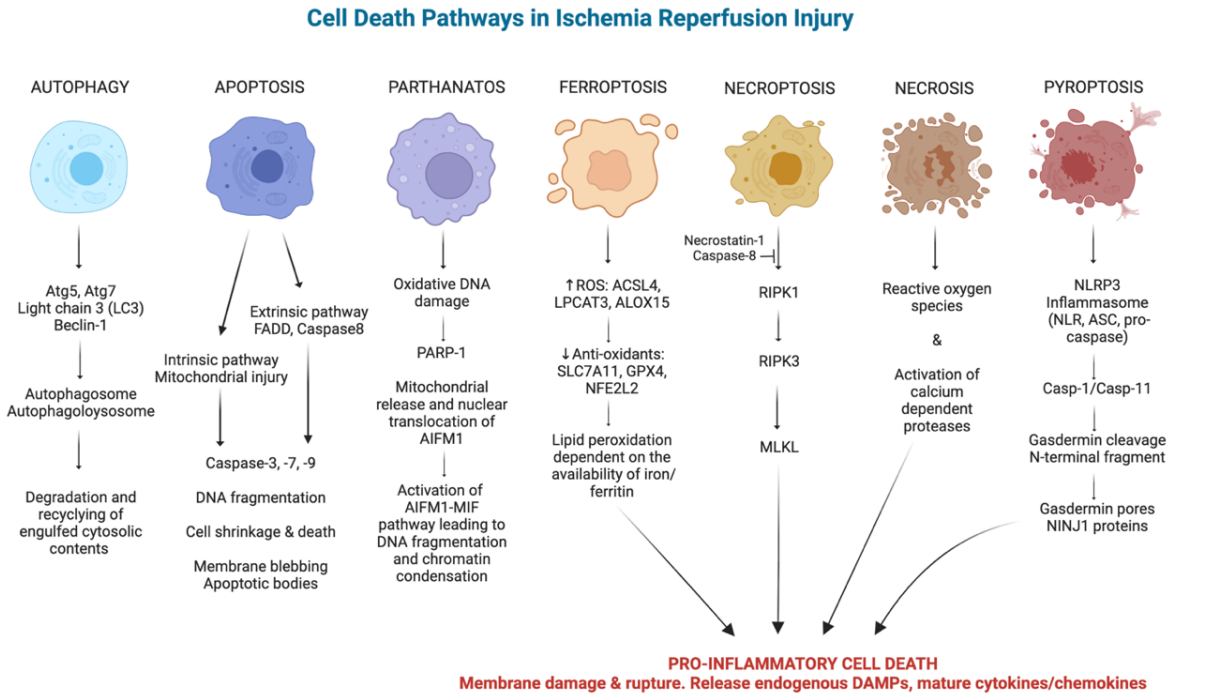

Figure 1.6: ***Key cell death pathways*** *in ischemia reperfusion injury. Abbreviations: autophagy related gene (Atg), Fas-ligand associated death domain (FADD), poly(ADP) polymerase-1 (PARP-1), reactive oxygen species (ROS), acyl-CoA synthetase long chain family member (ACSL4), lysophospholipid acyltransferase 5 (LPCAT3), arachidonate 5-lipoxygenase (ALOX5), solute carrier family 7 member 11 (SLC7A11), glutathione peroxidase 4 (GPX4), nuclear factor receptor-2 (NFE2L2), receptor interacting protein kinase (RIPK), mixed linage kinase domain like (MLKL), NACHT- LRR- and pyrin domain-containing protein 3 (NLRP3), Apoptosis-associated speck-like protein containing a CARD (ASC), ninjuri-1 (NINJ1). (Created with BioRender).*

Autophagy (or "self-eating") is initiated in response to external stimuli, such as the hypoxia and nutrient deprivation of IRI and is essential to prevent the formation of damaging, cytotoxic protein aggregates or damaged cellular components[255]. There are currently 3 recognised forms of autophagy: macroautophagy (commonly referred to as autophagy), microautophagy (engulfment of cytoplasmic contents directly by lysosomes via invagination) and chaperone-mediated autophagy (where proteins are targeted by HSP70 and transported to the lysosome). The process of autophagy follows the following 5 steps, including: (1) nucleation of the double membrane phagophore; (2) expansion of the phagophore to engulf intracellular components; (3) maturation of the phagophore into an autophagosome; (4) fusion of autophagosome with lysosome to form autolysosomes; and (5) lysosomal degradation of engulfed cytosolic elements with end-products, such as amino acids and fatty acids recycled in de novo protein synthesis or energy production via Krebs cycle and gluconeogenesis.[256] Autophagy is rapidly induced in IRI to protect cells from injury and death[257,258], and is highly regulated by the *autophagy-related genes* (*Atg*)[259]. Pharmacological inhibition of autophagy (hydroxychloroquine, or 3-methyladenine) has shown mixed results with exacerbation of renal IRI[260] and protection from IRI[130] - likely due to the degree of inhibition and the risk of excess accumulation of damaged mitochondria and ubiquitin-positive protein aggregates[261]. Suppression of ATG5 by doxycycline[134], or induction by FGF-10[132] or rapamycin (mTOR inhibitor)[133] were associated with worse outcomes post mouse renal IRI, which suggest possible ATG-specific roles. The effects of autophagy on other tissues are no clearer, as studies of this pathway in hepatic IRI[134,262-265] and myocardial IRI[266] also showing differing results. Although autophagy is crucial for cardiac development (embryonic loss of Atg5, Atg7 or Beclin-1 leads to structural abnormalities)[267], preconditioning of cardiomyocytes with rapamycin (mTOR inhibitor) induces autophagy and confers protection from IRI[268] but downregulation of autophagy can prevent cellular death and promote cardiac repair[269]. Clearly, autophagy is important in IRI, but further research is needed to clarify the specific roles and potential as therapeutic targets in the future.

Parthanatos has been increasingly recognised in IRI and other forms of kidney injury[253,270]. The key enzyme, poly(adenosine diphosphate ribose) polymerase-1 (PARP-1) is involved with nuclear DNA repair but with excessive oxidative stress induced DNA damage, hyperactivation of PARP-1 leads to depletion of ATP (ineffective glycolysis), NAD+ (PARylation) and release of apoptosis-inducing factor, mitochondrion-associated-1 (AIFM-1). AIFM-1 may or may not work in combination with macrophage inhibitory factor

(MIF) in parthanatos. Early studies to limit IRI/AKI via PARP-1 inhibition[271,272] and restoration of NAD+/nicotinamide[273,274] have been promising thus far.

1.5.5 Inflammatory cell death: necrosis, necroptosis, ferroptosis and pyroptosis

Necrosis is the major pathway of cell death in IRI in response to ischemia, depletion of ATP stores, ROS exceeding the cell's antioxidant capacity, and activation of calcium dependent proteases due to increased intracellular calcium levels from both reduced uptake in the endoplasmic reticulum and disruption of the inner mitochondrial membrane. Both ROS and calcium dependent proteases lead to damage and breakdown of lysosomal and plasma membranes – leading to cellular and organelle swelling, uncontrolled release intracellular contents and danger-associated molecular pathogens (DAMPs) to drive a robust inflammatory response[169,275-278]. While necrosis is passive and uncontrolled, necroptosis is a regulated form of necrosis which progresses independently of caspases.

Necroptosis results in plasma membrane destruction and release of DAMP signals but retains a morphologically intact nucleus. Necroptosis can be initiated in IRI engagement of TNF superfamily receptors, toll-like receptors (particularly TLR 3 and TLR4) and interferon receptors. In the absence of caspases (especially caspase-8), the multimerisation of *Fas-associated protein with death domain* (FADD) will preferentially recruit *receptor interacting serine/threonine kinase* (RIPK1 and RIPK3) to initiate necroptosis via the *substrate - mixed lineage kinase domain-like protein* (MLKL).[279] These mechanisms are supported by animal studies which demonstrated increased necroptosis following IRI. Transplantation in caspase-8 deficient mice and RIPK3 knockout mice exhibited less IRI, necrosis, fibrosis and HMGB1 levels[122]. Necrostatin-1 (RIPK1 inhibitor) has also been shown to limit necroptosis in pre-clinical studies including for cerebral and myocardial IRI[280] but have had varying results in renal IRI.[120,281] Current phase 2 clinical trials are underway for necrostatin in ulcerative colitis[282] and there is a limited therapeutic opportunity in the setting of IRI given the rapid progression of the necroptosome signalling cascade – but necrostatin potentially could be used if IRI injury is anticipated, such as major cardiac surgery or solid organ transplantation.

Ferroptosis is another form of pro-inflammatory cell death following IRI[283-287] due to lipid peroxidation of polyunsaturated fatty acid components of membranes by lipooxygenases[288]. Studies have shown vitamin E[289], ferrostatin-1 and liproxstatin-1 can be used as lipophilic radical traps to limit ferroptosis[253,290,291] as can iron chelators deferoxamine[288] and desferasirox[292]. Essentially, ferroptosis is dependent on (1) the balance between reactive oxygen stress to antioxidant capacity and (2) iron metabolism. Iron is usually stored intracellularly as ferritin (composed of ferritin heavy chain (FTH1) and light chain (FTL)) and degraded by nuclear receptor coactivator 4 (NCOA4). Accumulation of excess free iron in the ferrous form (Fe^{2+}) catalyses the production of reactive oxygen species through the Fenton reaction to facilitate lipid peroxidation and ferroptosis[293]. GPX4 is a glutathione-dependent enzyme, central to protection against excess lipid peroxidation, and can be inactivated by either depletion of glutathione, inhibition of the Xc^- transulfuration pathway (which includes SLC3A2 and SLC7A11) by erastin, sulfasalazine or sorafenib[253], or direct binding to compounds such as RSL3[253]. GPX4 stabilisation or upregulation by irisin[294] and quercetin[295] have shown promise in limiting AKI following IRI. Nuclear respiratory factor-2 (NRF2, NFE2L2), which can activate SLC7A11 and haem-oxygenase (HO-1, Hmox1), has been identified as a protective factor against ferroptosis[296,297]. Hmox1 can both exacerbate and protect against ferroptosis and may be dependent on the context and cell type. Members of heat shock protein family, including HSPB-1 (or HSP27) and HSP family A member 5 (HSPA5 or GRP78)), which can also bind and stabilise GPX4 to inhibit ferroptosis.

Pyroptosis is one of the most pro-inflammatory forms of cell death and crucial to control bacterial infections[298], HIV-induced cell death[299] and tumour surveillance[300] but recent evidence has elucidate the importance of this pathway in AKI. During this candidature, Miao et al.,[128] published data to support the role of caspase-11, non-canonical activation of pyroptosis in acute kidney injury from IRI or cisplatin[128], similar to our work. The key steps in pyroptosis include activation, inflammasome assembly, activation of caspases, gasdermin cleavage and oligo-dimerisation, insertion into lipid membranes to form pores to initiate cell death and release of pro-inflammatory cytokines. Inflammasome activation requires a priming signal with molecules (such as lipopolysaccharide, CpG oligonucleotides, α-synuclein, adenosine diphosphate (ADP), sphingosine-1-phosphate, TNF-α and type I interferon); and sensor signal with agents such as ADP,

adenosine triphosphate, various danger- and pathogen-associated molecular patterns (DAMP and PAMPs), uric acid and cholesterol crystals, calcium, potassium efflux, nigericin or viruses to trigger inflammasome assembly[301]. Ultimately, these diverse priming signals upregulates NF-κB and JAK/STAT related products, and post-translational modification of inflammasome components, and signal 2 (sensor) completes the inflammasome activation process.

Inflammasome assembly of the sensor NOD-like receptors (NLR), ASC (adaptor apoptosis-associated speck-like protein containing a caspase recruitment domain (CARD)) and pro-caspase-1 is key to the canonical pathway. Of the NLR sensors, NLRP3 is the most well researched and relevant to our kidney injury model and expressed in both immune cells and renal tubular epithelial cells. NLRP3 (or NACHT-LRR- and pyrin domain-containing protein 3) can sense various particles, including DAMPS, PAMPS, crystalline substances, nucleic acids, ATP and can also be directly activated by RIPK3 (linking pyroptosis and necroptosis). As a result, activated caspase-1 (Casp-1) is released and able to increase cleavage of pro-IL-1β, pro-IL-18 and gasdermin proteins to release their active subunits to form membrane pores and release pro-inflammatory cytokines. Alternatively, pyroptosis can be activated by the non-canonical pathway through direct binding to TLR-4 agonists such as LPS to the N-terminal CARD to release active caspase-11 (mice) or caspase-4 or 5 (human), which in turn acts on gasdermin and secondary activation of the NLRP3/canonical pathway as described earlier. Inhibition of caspase-1[121,123,302,303] and caspase-11[119,128,304-307] have both been shown as important contributors to the pathophysiology and severity of acute kidney injury. Studies in caspase-1, NLRP3, ASC and IL-18 deficient mice demonstrated protection against renal injury[124-126,308,309] but pharmacological agents have shown mixed results – hydroxychloroquine (downregulates cathepsin leading to suppression of NLRP3)[130] was protective, while anakinra (antibody blockade of the downstream IL-1 receptor) did not achieve significant effects[125]. The use of pan-caspase inhibitors such as Q-VD-OPh[119] and zVAD-FMK[120] however has not been as promising in acute kidney injury, possibly due to unintended dysregulation of other cell death pathways with pan-inhibition[245]. This section will describe upstream mechanisms, while chapter 3 will contain the detailed discussion of caspase-1 vs caspase-11 gasdermin D processing to the execution of pyroptosis[310].

1.6 Tolerogenic dendritic cells and their therapeutic potential

As described earlier, DC are early responders in the immune process following AKI and a prime target to modulate AKI severity[186]. Of particular interest is the use of tolerogenic DC therapy (tolDC). To date, there are no clinical studies testing tolDC as therapy for AKI[311]. There are a handful of early pre-clinical studies which have tested adenosine-2A receptor agonist[197], sphingosine-1-phosphate agonist[145,312] or rapamycin[313] conditioned tolDC in murine AKI models.

TolDC can be generated either (1) in-vivo, utilising nanoparticles to deliver tolerising agents to autologous immature dendritic cells in vivo[314,315], or (2) ex-vivo by culturing peripheral blood $CD14^+$ monocytes (or bone marrow in mice models) with low dose GM-CSF ± IL-4 (to direct differentiation towards the DC lineage) plus subsequent exposure to a tolerising agent, commonly 1,25-dihydroxy-vitamin D (vitamin D3), interleukin-10[316] and/or dexamethasone. Agents which have been shown to induce DC tolerance[317-320] are summarised in Fig 1.7. The advantage of using ex-vivo tolDC is the ability to phenotype cell products prior to infusion and timing of infusion can be altered depending on the protocol and availability of banked cells. Thus, ex-vivo therapy is more attractive for time-dependent scenarios of surgery, transplantation, or acute kidney injury, as opposed to chronic inflammation in most autoimmune diseases.

Vitamin D3 is the most widely used agent to tolerise DC[321-325] and some protocols add additional agents such as dexamethasone or IL-10 to achieve stable tolDC phenotype[325-327]. Vitamin D3 binds with its nuclear vitamin D receptor (VDR) and heterodimeries with retinoic-X receptor (RXR) before binding with vitamin D response elements (VDRE) in promoter regions at multiple gene loci, thus acts as a transcription factor to control expression of various metabolism, inflammation, and calcium homeostasis related genes[328-330]. In dendritic cells, this process decreases expression of MHCII and co-stimulatory molecules, suppresses NF-κB and upregulates IL-10 transcription[331,332]. Recent evidence also supports vitamin D engaging with methylcytosine dioxygenase ten-eleven translocation (TET2) enzyme to control DNA demethylation, chromatin remodelling[332] and can activate the JAK2/STAT3 pathway, which may be synergistic to the known effects of IL-10 on this pathway also[333]. Ex-vivo derived tolDCs characteristically display maturation resistance (with low expression of MHC and co-stimulatory molecules), secrete anti-inflammatory cytokines

(in particular IL-10)[334,335], induce T-cell anergy/hypo-responsiveness and have the ability to induce Treg[325] despite exposure to TLR2/TLR4 agonist (such as LPS or monophosphoryl lipid A) or pattern recognition receptor (PRR) ligands[336,337].

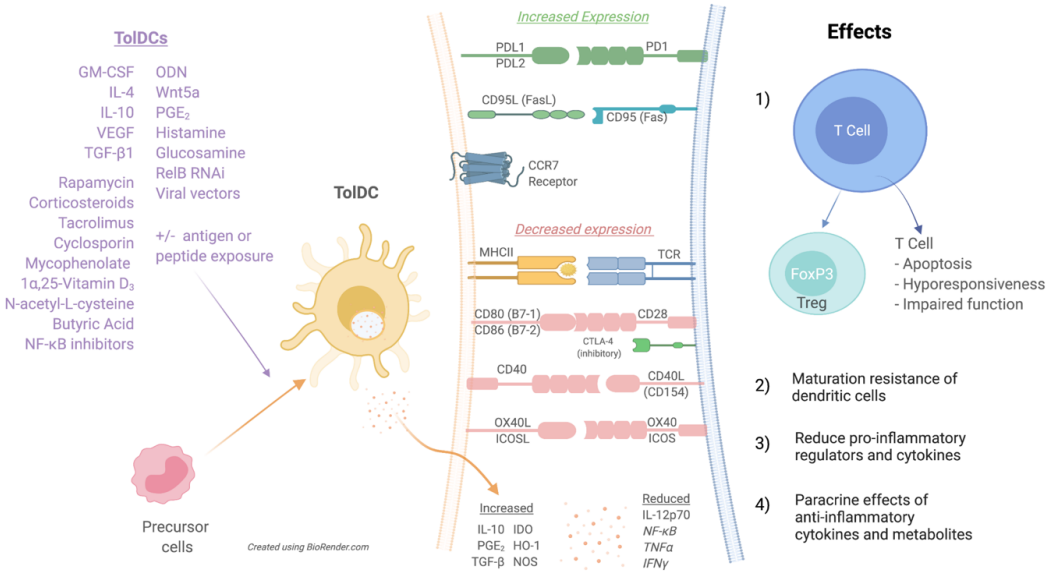

Figure 1.7: ***Overview of mechanisms how tolerogenic dendritic cells (TolDC) achieve tolerance*** *through direct cell-cell contact with altered expression of co-stimulatory and co-inhibitory molecules. These cells can also influence the cells in the immediate microenvironment through altered cytokine, chemokine and/or enzyme release to influence downstream cell survival, differentiation, and function. See abbreviations list for cytokine, chemokine, and enzyme details. Regulatory T cells (Treg), Forkhead box p3 (Foxp3), antigen presenting cells (APC).*

TolDC exhibit flow, functional or transcriptomic phenotype[338-340] on a spectrum which is less than classical activated DCs but more 'activated' than naïve, immature DC alone – thus they can also be described as semi-mature or 'alternatively-activated' dendritic cells (AADC). AADC retain the ability to hone into inflamed tissue via CXCR3 and CCR7 recptors.[341-344] The anti-inflammatory (or peripheral tolerance in the setting of transplantation) actions of tolDC are multifactorial. Inhibition of T-cell proliferation and tolDC mediated T cell anergy/apoptosis can occur through several mechanisms, including: reduced antigen presentation, downregulation of co-stimulatory molecules CD40, CD80 and CD86, upregulate inhibitory PDL1[345,346] and CTLA-4[85,347], and prevention of extracellular ATP activation of the purinergic P2X7-TLR-MyD88 signalling pathway[348-351]. Tolerogenic DC can also promote de novo expansion of peripheral $CD4^+CD25^+Foxp3^+$-Treg[352-354], or functionally-suppressive $CD4^+CD25^-Foxp3^+$ T-regulatory-1 cells (Tr1), and $CD8^+$ Tregs through modulation of cytokines expression such as IL-10, TGF-β or indoleamine 2,3-

dioxygenase (IDO).[355-358] In allogenic transplant models, cross-dressing or uptake of donor DC-derived apoptotic cell components and exosomes can also promote tolerance[359-363].

Regulatory or tolerogenic cell therapies have gathered value evidence from early clinical trials for solid organ transplant tolerance and autoimmune diseases[317,318,364,365]. Summary of the current human clinical studies for tolDC therapy for auto-immune and transplant application is shown in Table 1.6. Autologous tolDC are attractive in that they are avoid the risk of sensitisation, but they have variable efficacy, achieving tolerance in murine heart transplant models[359,360,366] but are less effective compared to allogeneic tolDC in NHP models.[367,368] Ex-vivo generated autologous tolDCs are not antigen specific (donor-derived tolDC have additional cross-presentation mechanisms[369]) and are more effective when pulsed with target antigens, such as citrullinated peptides or synovial derived antigens used in phase I rheumatoid arthritis studies[370,371].

The ONE Study[372] is the seminal study for cellular therapy in clinical transplantation tolerance. It was a phase I/II pilot study to test the safety and feasibility of tolerogenic dendritic cells, regulatory macrophages (Mreg) and regulatory T-cells (Treg) in low immunological risk, living-donor kidney transplantation across institutions in the United Kingdom, Germany, and United States of America. In the DC arm, un-pulsed (non-antigen specific) autologous tolerogenic DCs (ATDC) were generated by exposing peripheral $CD14^+$ monocytes to low dose GM-CSF. Compared to the reference group, who received standard of care immunosuppression based on the ELITE-Symphony[373] protocol, patients did not experience additional rejection or adverse events and pooled cell therapy group. A similar phase I/II clinical trial is currently underway run by the University of Pittsburgh for living donor kidney or liver transplantation. In this study, donor derived, peripheral monocytes are exposed to both vitamin D3 and IL-10 to induce tolerance and cells are assessed by flow cytometry and cytokine expression before infusion into the donor pre-transplantation. Both these studies pre-treat the transplant recipient (1 day prior in the ONE trial for ATDC and 7 days prior in the Pittsburgh trials) to induce tolerance before exposure to the allograft/allo-antigens, in line with murine and non-human primate pre-clinical studies[319,367,368,374-377].

Table 1.6: ***Human clinical studies using GMP-grade tolDC cell therapy***

Trial	Immunoregulatory cell details and Reported Quality Assurance (QA)	Immunosuppression comments & outcomes	Reference
***TRANSPLANTATION: The ONE Study* (multi-centre, UK, USA, and Germany)**			
Phase I/ II clinical trial Living donor Kidney Transplant N = 11 enrolled N = 8 treated	**ATDC** study arm (autologous tolerogenic DCs): ▪ un-pulsed, peripheral blood monocytes cultured in low dose GM-CSF for 6-days **Dose:** $1x10^6$ cells/kg cells infused day -1 (prior) to transplantation **QA:** Immature phenotype ▪ HLA-DR^{lo} $CD80^{lo}$ $CD86^{lo}$ $CD83^{lo}$ $CD40^{l}$ ▪ Maintained immature state when stimulated with either LPS or LPS + IFN-γ. T-cell hypo-proliferation in mixed lymphocyte reaction.	Followed up for 60 weeks. Prednisolone tapered by week 15. Tacrolimus target levels specified in keeping with ELITE-Symphony. Consider mycophenolate weaning if no suspicion of rejection on the 9-month biopsy. Pooled data for cell therapy group (CTG) of ATDC, regulatory macrophages and regulatory T-cells reported by The One Study. Overall, the CTG group showed no evidence of increased rejection, with less viral infections compared to reference trial group (standard of care immunosuppression)	NCT02252055 Sawitzki[372] Geissler[378] Marin[379]
***TRANSPLANTATION*: Allogeneic regulatory dendritic cells in (1) kidney and (2) liver transplantation (University of Pittsburgh)**			
Phase I/II clinical trial Living donor 1) kidney transplantation 2) liver transplantation Recruiting phase	Donor derived CD14+ peripheral blood monocytes. **TolDC:** monocytes supplemented with vitamin D, IL10 **Dose:** 1) Kidney: $0.5\text{-}10x10^6$ cells/kg infused 7 days prior to transplantation 2) Liver: $2.5\text{-}10x10^6$ cells/kg infused 7 days prior to transplantation ***QA:*** Recovered monocytes used to generate DC-regs must have <1% $CD3^+$ T cells, >70% viability, >95% purity ▪ Tolerogenic phenotype: HLA-DR^- $CD11c^+$ $CD14^+$ $CD40^{lo}$ $CD80l^o$ $CD86^{lo}$ PD-$L1^{hi}$ $CCR7^+$ $CD83^{lo}$ ▪ PDL1:CD86 ratio >3.5 ▪ Cytokines: high IL-10, low/absent IL-12p70 & TNF-α	Preconditioning with half dose mycophenolate and donor derived, tolerogenic DC infusion 7 days prior to surgery. Maintenance immunosuppression: (1) kidney: standard triple immunosuppression; (2) liver: standard immunosuppression first 6 months, then protocolised wean stratified on liver biopsy results to wean off MPA and subsequently tacrolimus No published results yet – trial in progress	NCT03726307 NCT 03164265 Thomson[380-382]
Rheumatoid arthritis			
Phase 1 pilot study **AutoDECRA** N = 13	Autologous, peripheral monocyte cultured with vitamin D & dexamethasone. Pulsed with synovial autoantigens ***QA***: Similar to above, tested for MHCII, CD40, CD80, CD83, CD86 and TLR-2 expression to test maturation resistance using monophosphyoryl lipid A (MPLA)	Direct injection of $1\text{-}10x10^6$ tolDC arthroscopically into knee synovial space of patients with active inflammation, with no concerns regarding safety/adverse reaction	NCT01352858 Harry[383] Bell[371]
Phase 1 pilot study **Rheumavax** N = 34	Autologous, monocyte derived DC treated with Bay11-7082 and pulsed with 4x citrullinated peptide antigens ***QA***: Similar to above, tested for maturation markers and suppression in a mixed lymphocyte reaction	$1\text{-}5x10^6$ cells administered intradermally Safe with no disease flares	Benham[370]
Type 1 diabetes			
Phase 1 pilot study N = 10	Autologous, monocytes tolerized with anti-sense phosphonothioate-modified OGN against CD40/CD80/CD86 ***QA***: Similar to above, tested for maturation markers and suppression in a mixed lymphocyte reaction	$10x10^6$ tolDC injected intradermally every 2 weeks for 4x doses tolDC tolerated without any adverse events	NCT00445913 Giannoukakis[384]
Multiple sclerosis			
Phase 1 pilot **TOLERVIT-MS**	Autologous DC treated with Vitamin D, loaded with myelin peptides	In progress	NCT02903537
Phase 1b trial	Autologous monocytes cultured with GM-CSF, IL-4, X-VIVO-15, dexamethasone and 2% autologous serum ***QA***: Similar to above. Peptide specific by exposure to myelin basic protein, proteolipid protein, myelin oligodendrocyte glycoprotein + aquaporin4	Dose escalation administration to patients with multiple sclerosis and neuromyelitis optica. Increase in Tr1 regulatory T cell and IL-10 production. Safe after 12-weeks observation.	NCT02283671 Zubizarreta[385]
Ulcerative colitis			
Phase 1 pilot study N = 9	Autologous monocytes exposed to vitamin A + dexamethasone. $2\text{-}10x10^6$ cells injected intraperitoneally ***QA***: Maturation resistance checked against cytokine cocktail of IL-1β, IL-6, TFN-α and PGE2	3 patients withdrew due to worsening UC symptoms. Appeared to be safe in the remaining 6 patients with no significant change to disease activity/quality of life scores.	Jauregui-amezaga[386]

1.7 Conclusion

Limiting AKI severity is important for renal and overall health of our patients. Effective clinical interventions to do this are lacking and this PhD aims to uncover new targets in the immune pathways which are critical to AKI pathophysiology.

In Chapter 2, we test whether tolerogenic dendritic cells, which exerts its anti-inflammatory effects via multiple mechanisms, can limit renal ischemia reperfusion injury. This particularly attractive, as future clinical trials can leverage the platform built by groups already conducting phase I/IIa clinical trials for solid organ transplant tolerance. Current studies administer cell therapies approximately 1-week prior to transplantation, limiting the applicability to deceased donor transplantation. Our approach was to administer tolerogenic dendritic cells the day prior or during animal surgery (thus a providing a pre-operative window of therapy) for scenarios of surgery related AKI (for example with major cardiac surgery) or transplantation (delayed graft function). We performed detailed flow, molecular and transcriptomic profiling of both the tolerogenic cells and kidney post infusion/IRI to support their beneficial effects for limiting AKI. In Chapter 3, we also test whether limiting pyroptosis, a pro-inflammatory form of cell death could limit AKI severity. Mutant mice with the *I105N* mutation in gasdermin D (GSDMD) were used and these produce hypofunctional GSDMD pores, limiting pyroptosis and in theory limit cell death and injury following IRI surgery. We also test via chimeric mice models, whether mutations in the parenchymal or blood/immune cell compartment and the administration of a GSDMD inhibitor influenced outcomes.

In Chapter 4, we extend our analysis to human clinical and transcriptomic data collected in the Australian Chronic Allograft Dysfunction (AUSCAD) study at Westmead Hospital. In particular, there was a focus on whether the preimplantation biopsy could be used to select patients who were more likely to have severe DGF and/or poor long-term (12-months) outcomes. The rationale was to determine whether select transcripts from the pre-implantation biopsy could be used as biomarkers to enrich patient selection for future translational trials.

1.8 REFERENCES

1. Kellum JA, Romagnani P, Ashuntantang G, Ronco C, Zarbock A, Anders H-J. Acute kidney injury. *Nature Reviews Disease Primers*. 2021/07/15 2021;7(1):52. doi:10.1038/s41572-021-00284-z
2. Gallagher M, Cass A, Bellomo R, et al. Long-Term Survival and Dialysis Dependency Following Acute Kidney Injury in Intensive Care: Extended Follow-up of a Randomized Controlled Trial. *PLOS Medicine*. 2014;11(2):e1001601. doi:10.1371/journal.pmed.1001601
3. Chawla LS, Bellomo R, Bihorac A, et al. Acute kidney disease and renal recovery: consensus report of the Acute Disease Quality Initiative (ADQI) 16 Workgroup. *Nature Reviews Nephrology*. 02/27/online 2017;13:241. doi:10.1038/nrneph.2017.2
4. Ricci Z, Cruz D, Ronco C. The RIFLE criteria and mortality in acute kidney injury: A systematic review. *Kidney International*. 2008/03/01/ 2008;73(5):538-546. doi:https://doi.org/10.1038/sj.ki.5002743
5. Rewa O, Bagshaw SM. Acute kidney injury—epidemiology, outcomes and economics. Review Article. *Nature Reviews Nephrology*. 01/21/online 2014;10:193. doi:10.1038/nrneph.2013.282
6. Health AIo, Welfare. *Australia's welfare 2013*. 2013. https://www.aihw.gov.au/reports/australias-welfare/australias-welfare-2013
7. Thomas ME, Blaine C, Dawnay A, et al. The definition of acute kidney injury and its use in practice. *Kidney International*. 2015/01/01/ 2015;87(1):62-73. doi:https://doi.org/10.1038/ki.2014.328
8. Murugan R, Kellum JA. Acute kidney injury: what's the prognosis? *Nature reviews Nephrology*. 2011;7(4):209-217. doi:10.1038/nrneph.2011.13
9. Wang AY, Bellomo R, Cass A, et al. Health-related quality of life in survivors of acute kidney injury: The Prolonged Outcomes Study of the Randomized Evaluation of Normal versus Augmented Level Replacement Therapy study outcomes. *Nephrology*. 2015/07/01 2015;20(7):492-498. doi:10.1111/nep.12488
10. ANZDATA Registry. 41st Report, Chapter 3: Mortality in End Stage Kidney Disease. Australia and New Zealand Dialysis and Transplant Registry, Adelaide, Australia. 2018. Available at: http://www.anzdata.org.au
11. KDIGO AKI Practice guidelines. *Kidney International*. 2012;
12. Lopes JA, Jorge S. The RIFLE and AKIN classifications for acute kidney injury: a critical and comprehensive review. *Clinical Kidney Journal*. 2012;6(1):8-14. doi:10.1093/ckj/sfs160
13. Ostermann M, Zarbock A, Goldstein S, et al. Recommendations on Acute Kidney Injury Biomarkers From the Acute Disease Quality Initiative Consensus Conference: A Consensus Statement. *JAMA Network Open*. 2020;3(10):e2019209-e2019209. doi:10.1001/jamanetworkopen.2020.19209
14. Lameire NH, Levin A, Kellum JA, et al. Harmonizing acute and chronic kidney disease definition and classification: report of a Kidney Disease: Improving Global Outcomes (KDIGO) Consensus Conference. *Kidney International*. 2021;100(3):516-526. doi:10.1016/j.kint.2021.06.028
15. Hariharan S, Israni AK, Danovitch G. Long-Term Survival after Kidney Transplantation. *New England Journal of Medicine*. 2021;385(8):729-743. doi:10.1056/NEJMra2014530
16. ANZDATA Registry. 41st Report, Chapter 1: Incidence of End Stage Kidney Disease. Australia and New Zealand Dialysis and Transplant Registry, Adelaide, Australia. 2018. Available at: http://www.anzdata.
17. ANZDATA Registry. 41st Report, Chapter 4: Haemodialysis. Australia and New Zealand Dialysis and Transplant Registry, Adelaide, Australia. 2018. Available at: http://www.anzdata.org.au.
18. ANZDATA Registry. 41st Report, Chapter 6: Australian Transplant Waiting List. Australia and New Zealand Dialysis and Transplant Registry, Adelaide, Australia. 2019. Available at: http://www.anzdata.org.au
19. ANZDATA Registry. 41st Report, Chapter 7: Kidney Transplantation. Australia and New Zealand Dialysis and Transplant Registry, Adelaide, Australia. 2018. Available at: http://www.anzdata.org.au.
20. ANZDATA Registry. 41st Report, Chapter 8: Kidney Donation. Australia and New Zealand Dialysis and Transplant Registry, Adelaide, Australia. 2018. Available at: http://www.anzdata.org.au.
21. Rao PS, Ojo A. The Alphabet Soup of Kidney Transplantation: SCD, DCD, ECD—Fundamentals for the Practicing Nephrologist. *Clinical Journal of the American Society of Nephrology*. 2009;4(11):1827. doi:10.2215/CJN.02270409
22. Aubert O, Kamar N, Vernerey D, et al. Long term outcomes of transplantation using kidneys from expanded criteria donors: prospective, population based cohort study. *BMJ : British Medical Journal*. 2015;351:h3557. doi:10.1136/bmj.h3557
23. Schold JD, Meier-Kriesche H-U. Which Renal Transplant Candidates Should Accept Marginal Kidneys in Exchange for a Shorter Waiting Time on Dialysis? *Clinical Journal of the American Society of Nephrology*. 2006;1(3):532-538. doi:10.2215/cjn.01130905
24. Ponticelli CE. The impact of cold ischemia time on renal transplant outcome. *Kidney International*. 2015;87(2):272-275. doi:10.1038/ki.2014.359
25. Lim WH, McDonald SP, Russ GR, et al. Association Between Delayed Graft Function and Graft Loss in Donation After Cardiac Death Kidney Transplants—A Paired Kidney Registry Analysis. *Transplantation*. 2017;101(6):1139-1143. doi:10.1097/tp.0000000000001323
26. Lim WH, Johnson DW, Teixeira-Pinto A, Wong G. Association Between Duration of Delayed Graft Function, Acute Rejection, and Allograft Outcome After Deceased Donor Kidney Transplantation. *Transplantation*. 2019;103(2):412-419. doi:10.1097/tp.0000000000002275
27. Yarlagadda SG, Coca SG, Formica RN, Jr., Poggio ED, Parikh CR. Association between delayed graft function and allograft and patient survival: a systematic review and meta-analysis. *Nephrology Dialysis Transplantation*. 2008;24(3):1039-1047. doi:10.1093/ndt/gfn667
28. Podesta MA, Cucchiari D, Ponticelli C. The diverging roles of dendritic cells in kidney allotransplantation. *Transplantation reviews (Orlando, Fla)*. Jul 2015;29(3):114-20. doi:10.1016/j.trre.2015.04.001
29. Siedlecki A, Irish W, Brennan DC. Delayed Graft Function in the Kidney Transplant. *American Journal of Transplantation*. 09/19 2011;11(11):2279-2296. doi:10.1111/j.1600-6143.2011.03754.x
30. Clayton PA, Dansie K, Sypek MP, et al. External validation of the US and UK kidney donor risk indices for deceased donor kidney transplant survival in the Australian and New Zealand population. *Nephrol Dial Transplant*. Dec 1 2019;34(12):2127-2131. doi:10.1093/ndt/gfz090
31. Helanterä I, Ibrahim HN, Lempinen M, Finne P. Donor Age, Cold Ischemia Time, and Delayed Graft Function. *Clinical Journal of the American Society of Nephrology*. 2020;15(6):813. doi:10.2215/CJN.13711119
32. Arias-Cabrales CE, Pérez-Sáez MJ, Redondo-Pachón D, et al. Relevance of KDPI value and acute rejection on kidney transplant outcomes in recipients with delayed graft function – a retrospective study. https://doi.org/10.1111/tri.13654. *Transplant International*. 2020/09/01 2020;33(9):1071-1077. doi:https://doi.org/10.1111/tri.13654
33. Perico N, Cattaneo D, Sayegh MH, Remuzzi G. Delayed graft function in kidney transplantation. *The Lancet*. 2004/11/13/ 2004;364(9447):1814-1827. doi:https://doi.org/10.1016/S0140-6736(04)17406-0
34. Ojo AO, Wolfe RA, Held PJ, Port FK, Schmouder RL. DELAYED GRAFT FUNCTION: RISK FACTORS AND IMPLICATIONS FOR RENAL ALLOGRAFT SURVIVAL1. *Transplantation*. 1997;63(7)

35. Mannon RB. Delayed Graft Function: The AKI of Kidney Transplantation. *Nephron*. 2018;140(2):94-98. doi:10.1159/000491558
36. Wu WK, Famure O, Li Y, Kim SJ. Delayed graft function and the risk of acute rejection in the modern era of kidney transplantation. *Kidney International*. 2015;88(4):851-858. doi:10.1038/ki.2015.190
37. Boffa C, Leemkolk F, Curnow E, et al. Transplantation of Kidneys From Donors With Acute Kidney Injury: Friend or Foe? *American Journal of Transplantation*. 2017/02/01 2016;17(2):411-419. doi:10.1111/ajt.13966
38. (FDA) FaDA. Delayed Graft Function in Kidney Transplantation: Developing Drugs for Prevention Guidance for Industry. *Guidance for Industry*. 2019;
39. Singh RP, Farney AC, Rogers J, et al. Kidney transplantation from donation after cardiac death donors: lack of impact of delayed graft function on post-transplant outcomes. *Clin Transplant*. Mar-Apr 2011;25(2):255-64. doi:10.1111/j.1399-0012.2010.01241.x
40. Mallon DH, Summers DM, Bradley JA, Pettigrew GJ. Defining delayed graft function after renal transplantation: simplest is best. *Transplantation*. Nov 27 2013;96(10):885-9. doi:10.1097/TP.0b013e3182a19348
41. Mogulla MR, Bhattacharjya S, Clayton PA. Risk factors for and outcomes of delayed graft function in live donor kidney transplantation – a retrospective study. *Transplant International*. 2019/06/17 2019;0(0)doi:10.1111/tri.13472
42. Schrezenmeier E, Müller M, Friedersdorff F, et al. Evaluation of severity of delayed graft function in kidney transplant recipients. *Nephrology Dialysis Transplantation*. 2022;37(5):973-981. doi:10.1093/ndt/gfab304
43. Tumlin JA, Murugan R, Deane AM, et al. Outcomes in Patients with Vasodilatory Shock and Renal Replacement Therapy Treated with Intravenous Angiotensin II. *Critical care medicine*. 2018;46(6):949-957. doi:10.1097/CCM.0000000000003092
44. Pickkers P, Mehta RL, Murray PT, et al. Effect of Human Recombinant Alkaline Phosphatase on 7-Day Creatinine Clearance in Patients With Sepsis-Associated Acute Kidney Injury: A Randomized Clinical TrialEffect of Human Recombinant Alkaline Phosphatase on Kidney Function in Sepsis-Associated AKIEffect of Human Recombinant Alkaline Phosphatase on Kidney Function in Sepsis-Associated AKI. *JAMA*. 2018;320(19):1998-2009. doi:10.1001/jama.2018.14283
45. Fraga CM, Tomasi CD, Damasio DdC, Vuolo F, Ritter C, Dal-Pizzol F. N-acetylcysteine plus deferoxamine for patients with prolonged hypotension does not decrease acute kidney injury incidence: a double blind, randomized, placebo-controlled trial. *Critical Care*. 2016/10/17 2016;20(1):331. doi:10.1186/s13054-016-1504-1
46. Cour M, Buisson M, Klouche K, et al. Remote ischemic conditioning in septic shock (RECO-Sepsis): study protocol for a randomized controlled trial. *Trials*. 2019;20(1):281-281. doi:10.1186/s13063-019-3406-4
47. Activated Vitamin D for the Prevention and Treatment of Acute Kidney Injury.
48. D'Aragon F, Belley-Cote E, Agarwal A, et al. Effect of corticosteroid administration on neurologically deceased organ donors and transplant recipients: a systematic review and meta-analysis. *BMJ Open*. 2017;7(6):e014436-e014436. doi:10.1136/bmjopen-2016-014436
49. Guesde R, Barrou B, Leblanc I, et al. Administration of desmopressin in brain-dead donors and renal function in kidney recipients. *The Lancet*. 1998/10/10/ 1998;352(9135):1178-1181. doi:https://doi.org/10.1016/S0140-6736(98)05456-7
50. Orban J-C, Quintard H, Cassuto E, Jambou P, Samat-Long C, Ichai C. Effect of N-acetylcysteine pretreatment of deceased organ donors on renal allograft function: a randomized controlled trial. *Transplantation*. 2015;99(4):746-753. doi:10.1097/TP.0000000000000395
51. Pennefather H, Stephen et al. . USE OF LOW DOSE ARGININE VASOPRESSIN TO SUPPORT BRAIN-DEAD ORGAN DONORS. *Transplantation*. 1995;
52. Reindl-Schwaighofer R, Kainz A, Jelencsics K, et al. Steroid pretreatment of organ donors does not impact on early rejection and long-term kidney allograft survival: Results from a multicenter randomized, controlled trial. *Am J Transplant*. 2019;19(6):1770-1776. doi:10.1111/ajt.15252
53. Schnuelle P, Drüschler K, Schmitt WH, et al. Donor organ intervention before kidney transplantation: Head-to-head comparison of therapeutic hypothermia, machine perfusion, and donor dopamine pretreatment. What is the evidence? *American Journal of Transplantation*. 2019/04/01 2019;19(4):975-983. doi:10.1111/ajt.15317
54. Schnuelle P, Schmitt WH, Weiss C, et al. Effects of Dopamine Donor Pretreatment on Graft Survival after Kidney Transplantation: A Randomized Trial. *Clinical journal of the American Society of Nephrology : CJASN*. 2017;12(3):493-501. doi:10.2215/CJN.07600716
55. Tingle SJ, Figueiredo RS, Moir JA, Goodfellow M, Talbot D, Wilson CH. Machine perfusion preservation versus static cold storage for deceased donor kidney transplantation. *Cochrane Database Syst Rev*. Mar 15 2019;3(3):Cd011671. doi:10.1002/14651858.CD011671.pub2
56. Jiao B, Liu S, Liu H, Cheng D, Cheng Y, Liu Y. Hypothermic machine perfusion reduces delayed graft function and improves one-year graft survival of kidneys from expanded criteria donors: a meta-analysis. *PloS one*. 2013;8(12):e81826. doi:10.1371/journal.pone.0081826
57. Ciancio G, Gaynor JJ, Sageshima J, et al. Favorable Outcomes With Machine Perfusion and Longer Pump Times in Kidney Transplantation: A Single-Center, Observational Study. *Transplantation*. 2010;90(8)
58. Kim WH, Lee J-H, Kim GS, Sim HY, Kim SJ. The Effect of Remote Ischemic Postconditioning on Graft Function in Patients Undergoing Living Donor Kidney Transplantation. *Transplantation*. 2014;98(5):529-536. doi:10.1097/tp.0000000000000098
59. Krogstrup NV, Oltean M, Nieuwenhuijs-Moeke GJ, et al. Remote Ischemic Conditioning on Recipients of Deceased Renal Transplants Does Not Improve Early Graft Function: A Multicenter Randomized, Controlled Clinical Trial. *American Journal of Transplantation*. 2017/04/01 2017;17(4):1042-1049. doi:10.1111/ajt.14075
60. Nicholson ML, Pattenden CJ, Barlow AD, Hunter JP, Lee G, Hosgood SA. A Double Blind Randomized Clinical Trial of Remote Ischemic Conditioning in Live Donor Renal Transplantation. *Medicine (Baltimore)*. 2015;94(31):e1316-e1316. doi:10.1097/MD.0000000000001316
61. Efficacy, Safety, Tolerability and Pharmacokinetic (PK) Study of GSK1070806 for the Prevention of Delayed Graft Function (DGF) in Adult Subjects After Renal Transplantation.
62. Prevention of Delayed Graft Function Using Eculizumab Therapy (PROTECT Study).
63. ATG Versus Basiliximab in Kidney Transplant Displaying Low Immunological Risk But High Susceptibility to DGF.
64. Placebo-Controlled Study to Evaluate the Safety and Efficacy of OPN-305 in Preventing Delayed Renal Graft Function.
65. I5NP for Prophylaxis of Delayed Graft Function in Kidney Transplantation.
66. Phase 2 Study of the Safety of Diannexin in Kidney Transplant Recipients.
67. Reparixin in Prevention of Delayed Graft Dysfunction After Kidney Transplantation.
68. Efficacy and Safety of FTY720 Versus Mycophenolate Mofetil (MMF, Roche Brand) in de Novo Adult Renal Transplant Recipients.
69. Envarsus in Delayed Graft Function (E-DGF).
70. Heme Arginate in Transplantation Study.
71. QPI-1002 for Prevention of Delayed Graft Function in Recipients of an Older Donor Kidney Transplant.
72. Effects of Inhibiting Early Inflammation in Kidney Transplant Patients.
73. Delayed Renal Allograft Function and Furosemide Treatment.
74. Open-Label Phase 2 Trial of a Steroid-Free, CNI-Free, Belatacept-Based Immunosuppressive Regimen.

75. Early Conversion From CNI to Belatacept in Renal Transplant Recipients With Delayed and Slow Graft Function.
76. Induction of HO-1; a Therapeutic Approach to Reduce Ischaemia Reperfusion Injury (IRI) Following Deceased Donor Renal Transplantation.
77. Tacrolimus to Sirolimus Conversion for Delayed Graft Function.
78. Estrogen in Kidney Study.
79. Brennan DC, Daller JA, Lake KD, Cibrik D, Del Castillo D. Rabbit Antithymocyte Globulin versus Basiliximab in Renal Transplantation. *New England Journal of Medicine*. 2006/11/09 2006;355(19):1967-1977. doi:10.1056/NEJMoa060068
80. Kaabak M, Babenko N, Shapiro R, Zokoyev A, Dymova O, Kim E. A prospective randomized, controlled trial of eculizumab to prevent ischemia-reperfusion injury in pediatric kidney transplantation. *Pediatric Transplantation*. 2018/03/01 2018;22(2):e13129. doi:10.1111/petr.13129
81. Salmela K, Wramner L, Ekberg H, et al. A RANDOMIZED MULTICENTER TRIAL OF THE ANTI-ICAM-1 MONOCLONAL ANTIBODY (ENLIMOMAB) FOR THE PREVENTION OF ACUTE REJECTION AND DELAYED ONSET OF GRAFT FUNCTION IN CADAVERIC RENAL TRANSPLANTATION: A Report Of The European Anti-ICAM-1 Renal Transplant Study Group. *Transplantation*. 1999;67(5):729-736.
82. Tedesco-Silva H, Lorber MI, Foster CE, et al. FTY720 and everolimus in de novo renal transplant patients at risk for delayed graft function: results of an exploratory one-yr multicenter study. *Clinical Transplantation*. 2009/09/01 2009;23(5):589-599. doi:10.1111/j.1399-0012.2009.01070.x
83. Newell KA, Asare A, Sanz I, et al. Longitudinal Studies of a B Cell–Derived Signature of Tolerance in Renal Transplant Recipients. *American Journal of Transplantation*. 2015/11/01 2015;15(11):2908-2920. doi:10.1111/ajt.13480
84. Newell KA, Mehta AK, Larsen CP, et al. Lessons Learned: Early Termination of a Randomized Trial of Calcineurin Inhibitor and Corticosteroid Avoidance Using Belatacept. *Am J Transplant*. 2017;17(10):2712-2719. doi:10.1111/ajt.14377
85. Vincenti F, Charpentier B, Vanrenterghem Y, et al. A Phase III Study of Belatacept-based Immunosuppression Regimens versus Cyclosporine in Renal Transplant Recipients (BENEFIT Study). *American Journal of Transplantation*. 2010/03/01 2010;10(3):535-546. doi:10.1111/j.1600-6143.2009.03005.x
86. Masson P HL, Chapman JR, Craig JC, Webster AC. Belatacept for kidney transplant recipients. *Cochrane Database of Systematic Reviews*. 2014;Issue 11. Art. No.: CD010699
87. Gupta N, Caldas M, Sharma N, et al. Does Intra-Operative Verapamil administration in Kidney Transplantation Improve Graft Function. *Clinical Transplantation*. 2019/06/17 2019;0(ja):e13635. doi:10.1111/ctr.13635
88. Martinez F, Kamar N, Pallet N, et al. High Dose Epoetin Beta in the First Weeks Following Renal Transplantation and Delayed Graft Function: Results of the Neo-PDGF Study. *American Journal of Transplantation*. 2010/07/01 2010;10(7):1695-1700. doi:10.1111/j.1600-6143.2010.03142.x
89. Nemoto T, Yokota N, Keane WF, Rabb H. Recombinant erythropoietin rapidly treats anemia in ischemic acute renal failure. *Kidney Int*. Jan 2001;59(1):246-51. doi:10.1046/j.1523-1755.2001.00485.x
90. Sureshkumar KK, Hussain SM, Ko TY, Thai NL, Marcus RJ. Effect of High-Dose Erythropoietin on Graft Function after Kidney Transplantation: A Randomized, Double-Blind Clinical Trial. *Clinical Journal of the American Society of Nephrology*. 2012;7(9):1498. doi:10.2215/CJN.01360212
91. A Study on SANGUINATE™ for the Reduction of Delayed Graft Function in Kidney Transplant Patients.
92. Eplerenone in Patients Undergoing REnal Transplant (EPURE TRANSPLANT). https://ClinicalTrials.gov/show/NCT02490904.
93. Reduce the Severity of DGF in Recipients of a Deceased Donor Kidney.
94. Liu KD, Humphreys BD, Endre ZH. The ten barriers for translation of animal data on AKI to the clinical setting. *Intensive Care Med*. Jun 2017;43(6):898-900. doi:10.1007/s00134-017-4810-4
95. Hukriede NA, Soranno DE, Sander V, et al. Experimental models of acute kidney injury for translational research. *Nature Reviews Nephrology*. 2022/05/01 2022;18(5):277-293. doi:10.1038/s41581-022-00539-2
96. Osama Gaber A, Mulgaonkar S, Kahan BD, et al. YSPSL (rPSGL-Ig) for improvement of early renal allograft function: a double-blind, placebo-controlled, multi-center Phase IIa study1,2,3. *Clinical Transplantation*. 2011/07/01 2011;25(4):523-533. doi:10.1111/j.1399-0012.2010.01295.x
97. Woodside KJ, Goldfarb DA, Rabets JC, et al. Enhancing kidney function with thrombolytic therapy following donation after cardiac death: a multicenter quasi-blinded prospective randomized trial. *Clinical Transplantation*. 2015/12/01 2015;29(12):1173-1180. doi:10.1111/ctr.12647
98. Evaluation of a Marine OXYgen Carrier: HEMO2Life® for hypOthermic Kidney Graft Preservation, Before Transplantation (OXYOP).
99. Kassimatis T, Qasem A, Douiri A, et al. A double-blind randomised controlled investigation into the efficacy of Mirococept (APT070) for preventing ischaemia reperfusion injury in the kidney allograft (EMPIRIKAL): study protocol for a randomised controlled trial. *Trials*. 2017;18(1):255-255. doi:10.1186/s13063-017-1972-x
100. Renaparin® in Kidney Transplantation.
101. Safety and Preliminary Efficacy of the Treatment of Kidney Allografts With Curcumin-containing Preservation Solution.
102. Custodiol-N Solution Compared With Custodiol Solution in Organ Transplantation (Kidney, Liver and Pancreas).
103. Limitation of Ischemic Injury of a Kidney Stored in Machine Perfusion in Hypothermia - Evaluation of the Impact on Kidney Allograft Function.
104. Jordan SC, Choi J, Aubert O, et al. A phase I/II, double-blind, placebo-controlled study assessing safety and efficacy of C1 esterase inhibitor for prevention of delayed graft function in deceased donor kidney transplant recipients. *American Journal of Transplantation*. 2018/12/01 2018;18(12):2955-2964. doi:10.1111/ajt.14767
105. Sun Q, Hong L, Huang Z, et al. Allogeneic mesenchymal stem cell as induction therapy to prevent both delayed graft function and acute rejection in deceased donor renal transplantation: study protocol for a randomized controlled trial. *Trials*. 2017;18(1):545-545. doi:10.1186/s13063-017-2291-y
106. Orban J-C, Fontaine E, Cassuto E, et al. Effects of cyclosporine A pretreatment of deceased organ donors on kidney graft function (Cis-A-rein): study protocol for a randomized controlled trial. *Trials*. 2018;19(1):231-231. doi:10.1186/s13063-018-2597-4
107. Patel MS, Niemann CU, Sally MB, et al. The Impact of Hydroxyethyl Starch Use in Deceased Organ Donors on the Development of Delayed Graft Function in Kidney Transplant Recipients: A Propensity-Adjusted Analysis. *American Journal of Transplantation*. 2015/08/01 2015;15(8):2152-2158. doi:10.1111/ajt.13263
108. Effect of Dexmedetomidine on Renal Function and Delayed Graft Function After Kidney Transplantation.
109. Kil HK, Kim JY, Choi YD, Lee HS, Kim TK, Kim JE. Effect of Combined Treatment of Ketorolac and Remote Ischemic Preconditioning on Renal Ischemia-Reperfusion Injury in Patients Undergoing Partial Nephrectomy: Pilot Study. *J Clin Med*. 2018;7(12):470. doi:10.3390/jcm7120470
110. A Study to Evaluate the Safety and Efficacy of AC607 for the Treatment of Kidney Injury in Cardiac Surgery Subjects.

111. Pneumoperitoneum Preconditioning for the Prevention of Renal Function After Laparoscopic Partial Nephrectomy.
112. Remote Ischaemic PreConditioning (RIPC) in Partial Nephrectomy for the Prevention of Ischemia/Reperfusion Injury.
113. Pre-operative Short-term Administration of a Formula Diet Containing a Non-milk-derived Protein Source for Prevention of Acute Kidney Injury After Cardiac Surgery.
114. Effect of Nitric Oxide in Cardiac Surgery Patients With Endothelial Dysfunction.
115. QPI-1002 Phase 3 for Prevention of Major Adverse Kidney Events (MAKE) in Subjects at High Risk for AKI Following Cardiac Surgery.
116. Prevention of Acute Kidney Injury Through Biomarker-guided Nephrological Intervention.
117. REmote Ischemic COnditioning in Septic Shock.
118. Shimoda N, Fukazawa N, Nonomura K, Fairchild RL. Cathepsin g is required for sustained inflammation and tissue injury after reperfusion of ischemic kidneys. *Am J Pathol*. 2007;170(3):930-940. doi:10.2353/ajpath.2007.060486
119. Nydam TL, Plenter R, Jain S, Lucia S, Jani A. Caspase Inhibition During Cold Storage Improves Graft Function and Histology in a Murine Kidney Transplant Model. *Transplantation*. 2018;102(9):1487-1495. doi:10.1097/tp.0000000000002218
120. Linkermann A, Brasen JH, Himmerkus N, et al. Rip1 (receptor-interacting protein kinase 1) mediates necroptosis and contributes to renal ischemia/reperfusion injury. *Kidney Int*. Apr 2012;81(8):751-61. doi:10.1038/ki.2011.450
121. Chatterjee PK, Todorovic Z, Sivarajah A, et al. Differential effects of caspase inhibitors on the renal dysfunction and injury caused by ischemia-reperfusion of the rat kidney. *Eur J Pharmacol*. Oct 25 2004;503(1-3):173-83. doi:10.1016/j.ejphar.2004.09.025
122. Lau A, Wang S, Jiang J, et al. RIPK3-Mediated Necroptosis Promotes Donor Kidney Inflammatory Injury and Reduces Allograft Survival. *American Journal of Transplantation*. 2013/11/01 2013;13(11):2805-2818. doi:10.1111/ajt.12447
123. Jain S, Plenter R, Jeremy R, Nydam T, Gill RG, Jani A. The impact of Caspase-1 deletion on apoptosis and acute kidney injury in a murine transplant model. *Cell Signal*. Sep 2021;85:110039. doi:10.1016/j.cellsig.2021.110039
124. Melnikov VY, Ecder T, Fantuzzi G, et al. Impaired IL-18 processing protects caspase-1-deficient mice from ischemic acute renal failure. *J Clin Invest*. May 2001;107(9):1145-52. doi:10.1172/JCI12089
125. Shigeoka AA, Mueller JL, Kambo A, et al. An inflammasome-independent role for epithelial-expressed Nlrp3 in renal ischemia-reperfusion injury. *Journal of immunology (Baltimore, Md : 1950)*. 2010;185(10):6277-6285. doi:10.4049/jimmunol.1002330
126. Iyer SS, Pulskens WP, Sadler JJ, et al. Necrotic cells trigger a sterile inflammatory response through the Nlrp3 inflammasome. *Proc Natl Acad Sci U S A*. Dec 1 2009;106(48):20388-93. doi:10.1073/pnas.0908698106
127. Kim H-J, Lee DW, Ravichandran K, et al. NLRP3 Inflammasome Knockout Mice Are Protected against Ischemic but Not Cisplatin-Induced Acute Kidney Injury. *Journal of Pharmacology and Experimental Therapeutics*. 2013;346(3):465. doi:10.1124/jpet.113.205732
128. Miao N, Yin F, Xie H, et al. The cleavage of gasdermin D by caspase-11 promotes tubular epithelial cell pyroptosis and urinary IL-18 excretion in acute kidney injury. *Kidney International*. 2019;96(5):1105-1120. doi:10.1016/j.kint.2019.04.035
129. Zou X-f, Gu J-h, Duan J-h, Hu Z-d, Cui Z-l. The NLRP3 inhibitor Mcc950 attenuates acute allograft damage in rat kidney transplants. *Transplant immunology*. 2020/08/01/ 2020;61:101293. doi:https://doi.org/10.1016/j.trim.2020.101293
130. Tang T-T, Lv L-L, Pan M-M, et al. Hydroxychloroquine attenuates renal ischemia/reperfusion injury by inhibiting cathepsin mediated NLRP3 inflammasome activation. *Cell Death & Disease*. 2018/03/02 2018;9(3):351. doi:10.1038/s41419-018-0378-3
131. Tajima T, Yoshifuji A, Matsui A, et al. β-hydroxybutyrate attenuates renal ischemia-reperfusion injury through its anti-pyroptotic effects. *Kidney International*. 2019;95(5):1120-1137. doi:10.1016/j.kint.2018.11.034
132. Tan X, Zhu H, Tao Q, et al. FGF10 Protects Against Renal Ischemia/Reperfusion Injury by Regulating Autophagy and Inflammatory Signaling. Original Research. *Frontiers in Genetics*. 2018-November-23 2018;9(556)doi:10.3389/fgene.2018.00556
133. Lieberthal W, Fuhro R, Andry C, Patel V, Levine JS. Rapamycin Delays But Does Not Prevent Recovery from Acute Renal Failure: Role of Acquired Tubular Resistance. *Transplantation*. 2006;82(1):17-22. doi:10.1097/01.tp.0000225772.22757.5e
134. Liu S, Hartleben B, Kretz O, et al. Autophagy plays a critical role in kidney tubule maintenance, aging and ischemia-reperfusion injury. *Autophagy*. 2012/05/13 2012;8(5):826-837. doi:10.4161/auto.19419
135. Thakar CV, Zahedi K, Revelo MP, et al. Identification of thrombospondin 1 (TSP-1) as a novel mediator of cell injury in kidney ischemia. *J Clin Invest*. 2005;115(12):3451-3459. doi:10.1172/JCI25461
136. Rogers NM, Zhang ZJ, Wang J-J, Thomson AW, Isenberg JS. CD47 regulates renal tubular epithelial cell self-renewal and proliferation following renal ischemia reperfusion. *Kidney International*. 2016;90(2):334-347. doi:10.1016/j.kint.2016.03.034
137. Hill P, Shukla D, Tran MGB, et al. Inhibition of hypoxia inducible factor hydroxylases protects against renal ischemia-reperfusion injury. *Journal of the American Society of Nephrology : JASN*. 2008;19(1):39-46. doi:10.1681/ASN.2006090998
138. Kelly KJ, Williams WW, Jr., Colvin RB, et al. Intercellular adhesion molecule-1-deficient mice are protected against ischemic renal injury. *J Clin Invest*. Feb 15 1996;97(4):1056-63. doi:10.1172/JCI118498
139. Wever KE, Wagener FADTG, Frielink C, et al. Diannexin protects against renal ischemia reperfusion injury and targets phosphatidylserines in ischemic tissue. *PloS one*. 2011;6(8):e24276-e24276. doi:10.1371/journal.pone.0024276
140. Peng Q, Wu W, Wu K-Y, et al. The C5a/C5aR1 axis promotes progression of renal tubulointerstitial fibrosis in a mouse model of renal ischemia/reperfusion injury. *Kidney International*. 2019;96(1):117-128. doi:10.1016/j.kint.2019.01.039
141. Zheng X, Zang G, Jiang J, et al. Attenuating Ischemia-Reperfusion Injury in Kidney Transplantation by Perfusing Donor Organs With siRNA Cocktail Solution. *Transplantation*. 2016;100(4):743-752. doi:10.1097/tp.0000000000000960
142. Sörensen I, Rong S, Susnik N, et al. Bβ(15-42) attenuates the effect of ischemia-reperfusion injury in renal transplantation. *Journal of the American Society of Nephrology : JASN*. 2011;22(10):1887-1896. doi:10.1681/ASN.2011010031
143. Vukicevic S, Basic V, Rogic D, et al. Osteogenic protein-1 (bone morphogenetic protein-7) reduces severity of injury after ischemic acute renal failure in rat. *J Clin Invest*. 1998;102(1):202-214. doi:10.1172/JCI2237
144. Perry HM, Huang L, Ye H, et al. Endothelial Sphingosine 1-Phosphate Receptor-1 Mediates Protection and Recovery from Acute Kidney Injury. *Journal of the American Society of Nephrology*. 2016;27(11):3383. doi:10.1681/ASN.2015080922
145. Bajwa A, Huang L, Kurmaeva E, et al. Sphingosine 1-Phosphate Receptor 3–Deficient Dendritic Cells Modulate Splenic Responses to Ischemia-Reperfusion Injury. *Journal of the American Society of Nephrology*. 2016;27(4):1076. doi:10.1681/ASN.2015010095
146. Kaudel CP, Schmiddem U, Frink M, et al. FTY720 for Treatment of Ischemia-Reperfusion Injury Following Complete Renal Ischemia in C57/BL6 Mice. *Transplantation Proceedings*. 2006/04/01/ 2006;38(3):679-681. doi:https://doi.org/10.1016/j.transproceed.2006.01.033
147. Rogers NM, Stephenson MD, Kitching AR, Horowitz JD, Coates PTH. Amelioration of renal ischaemia–reperfusion injury by liposomal delivery of curcumin to renal tubular epithelial and antigen-presenting cells. *British Journal of Pharmacology*. 2012/05/01 2012;166(1):194-209. doi:10.1111/j.1476-5381.2011.01590.x
148. Gueler F, Shushakova N, Mengel M, et al. A novel therapy to attenuate acute kidney injury and ischemic allograft damage after allogenic kidney transplantation in mice. *PloS one*. 2015;10(1):e0115709-e0115709. doi:10.1371/journal.pone.0115709

149. Lutz J, Luong LA, Strobl M, et al. The A20 gene protects kidneys from ischaemia/reperfusion injury by suppressing pro-inflammatory activation. *Journal of Molecular Medicine*. 2008/12/01 2008;86(12):1329-1339. doi:10.1007/s00109-008-0405-4
150. Wu H, Craft ML, Wang P, et al. IL-18 contributes to renal damage after ischemia-reperfusion. *Journal of the American Society of Nephrology : JASN*. 2008;19(12):2331-2341. doi:10.1681/ASN.2008020170
151. Cao Q, Wang Y, Niu Z, et al. Potentiating Tissue-Resident Type 2 Innate Lymphoid Cells by IL-33 to Prevent Renal Ischemia-Reperfusion Injury. *Journal of the American Society of Nephrology*. 2018;29(3):961. doi:10.1681/ASN.2017070774
152. Sakai K, Nozaki Y, Murao Y, et al. Protective effect and mechanism of IL-10 on renal ischemia–reperfusion injury. *Laboratory Investigation*. 2019/05/01 2019;99(5):671-683. doi:10.1038/s41374-018-0162-0
153. Sevastos J, Kennedy SE, Davis DR, et al. Tissue factor deficiency and PAR-1 deficiency are protective against renal ischemia reperfusion injury. *Blood*. 2007;109(2):577. doi:10.1182/blood-2006-03-008870
154. Day YJ, Huang L, Ye H, Linden J, Okusa MD. Renal ischemia-reperfusion injury and adenosine 2A receptor-mediated tissue protection: role of macrophages. *Am J Physiol Renal Physiol*. Apr 2005;288(4):F722-31. doi:10.1152/ajprenal.00378.2004
155. Paller MS. Effect of neutrophil depletion on ischemic renal injury in the rat. *The Journal of Laboratory and Clinical Medicine*. 1989;113(3):379-386. doi:10.5555/uri:pii:0022214389901017
156. Jansen MPB, Emal D, Teske GJD, Dessing MC, Florquin S, Roelofs JJTH. Release of extracellular DNA influences renal ischemia reperfusion injury by platelet activation and formation of neutrophil extracellular traps. *Kidney International*. 2017;91(2):352-364. doi:10.1016/j.kint.2016.08.006
157. Kim M-G, Su Boo C, Sook Ko Y, et al. Depletion of kidney CD11c+ F4/80+ cells impairs the recovery process in ischaemia/reperfusion-induced acute kidney injury. *Nephrology Dialysis Transplantation*. 2010;25(9):2908-2921. doi:10.1093/ndt/gfq183
158. Yokota N, Daniels F, Crosson J, Rabb H. Protective effect of T cell depletion in murine renal ischemia-reperfusion injury. *Transplantation*. 2002;74(6):759-763.
159. Park P, Haas M, Cunningham PN, Bao L, Alexander JJ, Quigg RJ. Injury in renal ischemia-reperfusion is independent from immunoglobulins and T lymphocytes. *American Journal of Physiology-Renal Physiology*. 2002/02/01 2002;282(2):F352-F357. doi:10.1152/ajprenal.00160.2001
160. Noel S, Martina MN, Bandapalle S, et al. T Lymphocyte–Specific Activation of Nrf2 Protects from AKI. *Journal of the American Society of Nephrology*. 2015;26(12):2989. doi:10.1681/ASN.2014100978
161. Burne-Taney MJ, Yokota-Ikeda N, Rabb H. Effects of Combined T- and B-Cell Deficiency on Murine Ischemia Reperfusion Injury. *American Journal of Transplantation*. 2005/06/01 2005;5(6):1186-1193. doi:10.1111/j.1600-6143.2005.00815.x
162. Yang BIN, Jain S, Pawluczyk IZA, et al. Inflammation and caspase activation in long-term renal ischemia/reperfusion injury and immunosuppression in rats. *Kidney International*. 2005;68(5):2050-2067. doi:10.1111/j.1523-1755.2005.00662.x
163. Tsutahara K, Okumi M, Kakuta Y, et al. The Blocking of CXCR3 and CCR5 Suppresses the Infiltration of T Lymphocytes in Rat Renal Ischemia Reperfusion: 812. *Transplantation*. 2012;94(10S):1138.
164. Li L, Huang L, Sung S-sJ, et al. NKT Cell Activation Mediates Neutrophil IFN-γ Production and Renal Ischemia-Reperfusion Injury. *The Journal of Immunology*. 2007;178(9):5899. doi:10.4049/jimmunol.178.9.5899
165. Yago T, Liu Z, Ahamed J, McEver RP. Cooperative PSGL-1 and CXCR2 signaling in neutrophils promotes deep vein thrombosis in mice. *Blood*. 2018;132(13):1426. doi:10.1182/blood-2018-05-850859
166. de Vries B, Walter SJ, von Bonsdorff L, et al. Reduction of circulating redox-active iron by apotransferrin protects against renal ischemia-reperfusion injury1. *Transplantation*. 2004;77(5):669-675. doi:10.1097/01.Tp.0000115002.28575.E7
167. Li J, Li L, Wang S, et al. Resveratrol Alleviates Inflammatory Responses and Oxidative Stress in Rat Kidney Ischemia-Reperfusion Injury and H₂O₂-Induced NRK-52E Cells via the Nrf2/TLR4/NF-κB Pathway. *Cellular Physiology and Biochemistry*. 2018;45(4):1677-1689. doi:10.1159/000487735
168. Bath NM, Fahl WE, Redfield RRI. Significant Reduction of Murine Renal Ischemia-Reperfusion Cell Death Using the Immediate-Acting PrC-210 Reactive Oxygen Species Scavenger. *Transplantation Direct*. 2019;5(7):e469. doi:10.1097/txd.0000000000000909
169. Kalogeris T, Baines CP, Krenz M, Korthuis RJ. Cell biology of ischemia/reperfusion injury. *Int Rev Cell Mol Biol*. 2012;298:229-317. doi:10.1016/B978-0-12-394309-5.00006-7
170. Bolli R, Marban E. Molecular and cellular mechanisms of myocardial stunning. *Physiol Rev*. Apr 1999;79(2):609-34. doi:10.1152/physrev.1999.79.2.609
171. Depre C, Vatner SF. Mechanisms of cell survival in myocardial hibernation. *Trends Cardiovasc Med*. Apr 2005;15(3):101-10. doi:10.1016/j.tcm.2005.04.006
172. Depre C, Wang L, Sui X, et al. H11 kinase prevents myocardial infarction by preemptive preconditioning of the heart. *Circ Res*. Feb 3 2006;98(2):280-8. doi:10.1161/01.RES.0000201284.45482.e8
173. Perlman RL. Mouse models of human disease: An evolutionary perspective. *Evol Med Public Health*. 2016;2016(1):170-176. doi:10.1093/emph/eow014
174. Ramesh G. RP. Mouse Models and Methods for Studying Human Disease, Acute Kidney Injury (AKI). *Mouse Genetics Methods in Molecular Biology (Methods and Protocols)*. 2014;1194
175. Wei Q, Dong Z. Mouse model of ischemic acute kidney injury: technical notes and tricks. *Am J Physiol Renal Physiol*. 2012;303(11):F1487-F1494. doi:10.1152/ajprenal.00352.2012
176. Pieters TT, Falke LL, Nguyen TQ, et al. Histological characteristics of Acute Tubular Injury during Delayed Graft Function predict renal function after renal transplantation. *Physiological Reports*. 2019;7(5):e14000. e14000. doi:doi:10.14814/phy2.14000
177. Roufosse C, Simmonds N, Clahsen-van Groningen M, et al. A 2018 Reference Guide to the Banff Classification of Renal Allograft Pathology. *Transplantation*. 2018;102(11):1795-1814. doi:10.1097/tp.0000000000002366
178. Devarajan P. Update on Mechanisms of Ischemic Acute Kidney Injury. *Journal of the American Society of Nephrology*. 2006;17(6):1503. doi:10.1681/ASN.2006010017
179. Basile DP, Anderson MD, Sutton TA. Pathophysiology of acute kidney injury. *Compr Physiol*. Apr 2012;2(2):1303-53. doi:10.1002/cphy.c110041
180. Bonventre JV, Yang L. Cellular pathophysiology of ischemic acute kidney injury. *J Clin Invest*. Nov 2011;121(11):4210-21. doi:10.1172/jci45161
181. Zuk A, Bonventre JV. Acute Kidney Injury. *Annu Rev Med*. 2016;67:293-307. doi:10.1146/annurev-med-050214-013407
182. Takada M, Nadeau KC, Shaw GD, Tilney NL. Early cellular and molecular changes in ischemia/reperfusion injury: inhibition by a selectin antagonist, P-selectin glycoprotein ligand-1. *Transplant Proc*. Feb-Mar 1997;29(1-2):1324-5. doi:10.1016/s0041-1345(96)00577-5
183. Banchereau J, Steinman RM. Dendritic cells and the control of immunity. *Nature*. 1998/03/01 1998;392(6673):245-252. doi:10.1038/32588
184. Li L, Okusa MD. Macrophages, dendritic cells, and kidney ischemia-reperfusion injury. *Semin Nephrol*. 2010;30(3):268-277. doi:10.1016/j.semnephrol.2010.03.005

185. Agrawal A, Agrawal S, Gupta S. Role of Dendritic Cells in Inflammation and Loss of Tolerance in the Elderly. Review. *Front Immunol*. 2017-July-26 2017;8(896)doi:10.3389/fimmu.2017.00896
186. Rogers NM, Ferenbach DA, Isenberg JS, Thomson AW, Hughes J. Dendritic cells and macrophages in the kidney: a spectrum of good and evil. *Nature reviews Nephrology*. 09/30 2014;10(11):625-643. doi:10.1038/nrneph.2014.170
187. Huen SC, Cantley LG. Macrophage-mediated injury and repair after ischemic kidney injury. *Pediatric nephrology (Berlin, Germany)*. Feb 2015;30(2):199-209. doi:10.1007/s00467-013-2726-y
188. Litt MR, Jeremy RW, Weisman HF, Winkelstein JA, Becker LC. Neutrophil depletion limited to reperfusion reduces myocardial infarct size after 90 minutes of ischemia. Evidence for neutrophil-mediated reperfusion injury. *Circulation*. Dec 1989;80(6):1816-27. doi:10.1161/01.cir.80.6.1816
189. Langdale LA, Flaherty LC, Liggitt HD, Harlan JM, Rice CL, Winn RK. Neutrophils contribute to hepatic ischemia-reperfusion injury by a CD18-independent mechanism. *J Leukoc Biol*. May 1993;53(5):511-7. doi:10.1002/jlb.53.5.511
190. Eppinger MJ, Jones ML, Deeb GM, Bolling SF, Ward PA. Pattern of injury and the role of neutrophils in reperfusion injury of rat lung. *J Surg Res*. Jun 1995;58(6):713-8. doi:10.1006/jsre.1995.1112
191. Simpson R, Alon R, Kobzik L, Valeri CR, Shepro D, Hechtman HB. Neutrophil and nonneutrophil-mediated injury in intestinal ischemia-reperfusion. *Ann Surg*. Oct 1993;218(4):444-53; discussion 453-4. doi:10.1097/00000658-199310000-00005
192. Rouschop KMA, Roelofs JJTH, Claessen N, et al. Protection against Renal Ischemia Reperfusion Injury by CD44 Disruption. *Journal of the American Society of Nephrology*. 2005;16(7):2034. doi:10.1681/ASN.2005010054
193. Melnikov VY, Faubel S, Siegmund B, Lucia MS, Ljubanovic D, Edelstein CL. Neutrophil-independent mechanisms of caspase-1- and IL-18-mediated ischemic acute tubular necrosis in mice. *J Clin Invest*. Oct 2002;110(8):1083-91. doi:10.1172/JCI15623
194. Godfrey DI, Kronenberg M. Going both ways: immune regulation via CD1d-dependent NKT cells. *J Clin Invest*. Nov 2004;114(10):1379-88. doi:10.1172/JCI23594
195. Godfrey DI, MacDonald HR, Kronenberg M, Smyth MJ, Van Kaer L. NKT cells: what's in a name? *Nat Rev Immunol*. Mar 2004;4(3):231-7. doi:10.1038/nri1309
196. Bendelac A, Savage PB, Teyton L. The biology of NKT cells. *Annu Rev Immunol*. 2007;25:297-336. doi:10.1146/annurev.immunol.25.022106.141711
197. Li L, Huang L, Ye H, et al. Dendritic cells tolerized with adenosine A_2AR agonist attenuate acute kidney injury. *J Clin Invest*. Nov 2012;122(11):3931-42. doi:10.1172/jci63170
198. Kim HJ, Lee JS, Kim A, et al. TLR2 signaling in tubular epithelial cells regulates NK cell recruitment in kidney ischemia-reperfusion injury. *Journal of immunology (Baltimore, Md : 1950)*. Sep 1 2013;191(5):2657-64. doi:10.4049/jimmunol.1300358
199. Zhang ZX, Wang S, Huang X, et al. NK cells induce apoptosis in tubular epithelial cells and contribute to renal ischemia-reperfusion injury. *Journal of immunology (Baltimore, Md : 1950)*. Dec 1 2008;181(11):7489-98. doi:10.4049/jimmunol.181.11.7489
200. Kim HJ, Lee JS, Kim JD, et al. Reverse signaling through the costimulatory ligand CD137L in epithelial cells is essential for natural killer cell-mediated acute tissue inflammation. *Proc Natl Acad Sci U S A*. Jan 3 2012;109(1):E13-22. doi:10.1073/pnas.1112256109
201. Ascon M, Ascon DB, Liu M, et al. Renal ischemia-reperfusion leads to long term infiltration of activated and effector-memory T lymphocytes. *Kidney Int*. Mar 2009;75(5):526-35. doi:10.1038/ki.2008.602
202. Burne MJ, Daniels F, El Ghandour A, et al. Identification of the CD4(+) T cell as a major pathogenic factor in ischemic acute renal failure. *J Clin Invest*. Nov 2001;108(9):1283-90. doi:10.1172/JCI12080
203. Caldwell CC, Okaya T, Martignoni A, Husted T, Schuster R, Lentsch AB. Divergent functions of CD4+ T lymphocytes in acute liver inflammation and injury after ischemia-reperfusion. *Am J Physiol Gastrointest Liver Physiol*. Nov 2005;289(5):G969-76. doi:10.1152/ajpgi.00223.2005
204. Wang S, Diao H, Guan Q, et al. Decreased renal ischemia-reperfusion injury by IL-16 inactivation. *Kidney Int*. Feb 2008;73(3):318-26. doi:10.1038/sj.ki.5002692
205. De Greef KE, Ysebaert DK, Dauwe S, et al. Anti-B7-1 blocks mononuclear cell adherence in vasa recta after ischemia. *Kidney Int*. Oct 2001;60(4):1415-27. doi:10.1046/j.1523-1755.2001.00944.x
206. Kinsey GR, Sharma R, Huang L, et al. Regulatory T cells suppress innate immunity in kidney ischemia-reperfusion injury. *J Am Soc Nephrol*. Aug 2009;20(8):1744-53. doi:10.1681/ASN.2008111160
207. Gandolfo MT, Jang HR, Bagnasco SM, et al. Foxp3+ regulatory T cells participate in repair of ischemic acute kidney injury. *Kidney Int*. Oct 2009;76(7):717-29. doi:10.1038/ki.2009.259
208. Burne-Taney MJ, Ascon DB, Daniels F, Racusen L, Baldwin W, Rabb H. B cell deficiency confers protection from renal ischemia reperfusion injury. *Journal of immunology (Baltimore, Md : 1950)*. Sep 15 2003;171(6):3210-5. doi:10.4049/jimmunol.171.6.3210
209. Jang HR, Gandolfo MT, Ko GJ, Satpute SR, Racusen L, Rabb H. B cells limit repair after ischemic acute kidney injury. *J Am Soc Nephrol*. Apr 2010;21(4):654-65. doi:10.1681/ASN.2009020182
210. Burne-Taney MJ, Ascon DB, Daniels F, Racusen L, Baldwin W, Rabb H. B Cell Deficiency Confers Protection from Renal Ischemia Reperfusion Injury. *The Journal of Immunology*. 2003;171(6):3210. doi:10.4049/jimmunol.171.6.3210
211. Kreimann K, Jang M-S, Rong S, et al. Ischemia Reperfusion Injury Triggers CXCL13 Release and B-Cell Recruitment After Allogenic Kidney Transplantation. Original Research. *Front Immunol*. 2020-August-06 2020;11doi:10.3389/fimmu.2020.01204
212. Cippà PE, Liu J, Sun B, Kumar S, Naesens M, McMahon AP. A late B lymphocyte action in dysfunctional tissue repair following kidney injury and transplantation. *Nature Communications*. 2019/03/11 2019;10(1):1157. doi:10.1038/s41467-019-09092-2
213. Griendling KK, Touyz RM, Zweier JL, et al. Measurement of Reactive Oxygen Species, Reactive Nitrogen Species, and Redox-Dependent Signaling in the Cardiovascular System: A Scientific Statement From the American Heart Association. *Circulation research*. 2016;119(5):e39-e75. doi:10.1161/RES.0000000000000110
214. Kvietys PR, Granger DN. Role of reactive oxygen and nitrogen species in the vascular responses to inflammation. *Free Radic Biol Med*. Feb 1 2012;52(3):556-592. doi:10.1016/j.freeradbiomed.2011.11.002
215. Forstermann U, Closs EI, Pollock JS, et al. Nitric oxide synthase isozymes. Characterization, purification, molecular cloning, and functions. *Hypertension*. Jun 1994;23(6 Pt 2):1121-31. doi:10.1161/01.hyp.23.6.1121
216. Forstermann U, Sessa WC. Nitric oxide synthases: regulation and function. *Eur Heart J*. Apr 2012;33(7):829-37, 837a-837d. doi:10.1093/eurheartj/ehr304
217. Simone S, Rascio F, Castellano G, et al. Complement-dependent NADPH oxidase enzyme activation in renal ischemia/reperfusion injury. *Free Radic Biol Med*. Sep 2014;74:263-73. doi:10.1016/j.freeradbiomed.2014.07.003
218. Kleikers PW, Wingler K, Hermans JJ, et al. NADPH oxidases as a source of oxidative stress and molecular target in ischemia/reperfusion injury. *J Mol Med (Berl)*. Dec 2012;90(12):1391-406. doi:10.1007/s00109-012-0963-3
219. Looi YH, Grieve DJ, Siva A, et al. Involvement of Nox2 NADPH oxidase in adverse cardiac remodeling after myocardial infarction. *Hypertension*. Feb 2008;51(2):319-25. doi:10.1161/HYPERTENSIONAHA.107.101980
220. Fisher AB, Al-Mehdi AB, Muzykantov V. Activation of endothelial NADPH oxidase as the source of a reactive oxygen species in lung ischemia. *Chest*. Jul 1999;116(1 Suppl):25S-26S. doi:10.1378/chest.116.suppl_1.25s

221. Harada H, Hines IN, Flores S, et al. Role of NADPH oxidase-derived superoxide in reduced size liver ischemia and reperfusion injury. *Arch Biochem Biophys*. Mar 1 2004;423(1):103-8. doi:10.1016/j.abb.2003.08.035
222. Bhargava P, Schnellmann RG. Mitochondrial energetics in the kidney. *Nature reviews Nephrology*. 2017;13(10):629-646. doi:10.1038/nrneph.2017.107
223. Di Lisa F, Kaludercic N, Carpi A, Menabo R, Giorgio M. Mitochondria and vascular pathology. *Pharmacol Rep*. Jan-Feb 2009;61(1):123-30.
224. Davies MJ, Hawkins CL, Pattison DI, Rees MD. Mammalian heme peroxidases: from molecular mechanisms to health implications. *Antioxid Redox Signal*. Jul 2008;10(7):1199-234. doi:10.1089/ars.2007.1927
225. Granger DN, Kvietys PR. Reperfusion injury and reactive oxygen species: The evolution of a concept. *Redox Biology*. 2015/12/01/ 2015;6:524-551. doi:https://doi.org/10.1016/j.redox.2015.08.020
226. Sedeek M, Nasrallah R, Touyz RM, Hébert RL. NADPH oxidases, reactive oxygen species, and the kidney: friend and foe. *Journal of the American Society of Nephrology : JASN*. 2013;24(10):1512-1518. doi:10.1681/ASN.2012111112
227. Ryter SW, Morse D, Choi AM. Carbon monoxide and bilirubin: potential therapies for pulmonary/vascular injury and disease. *Am J Respir Cell Mol Biol*. Feb 2007;36(2):175-82. doi:10.1165/rcmb.2006-0333TR
228. Tsuda H, Kawada N, Kaimori JY, et al. Febuxostat suppressed renal ischemia-reperfusion injury via reduced oxidative stress. *Biochem Biophys Res Commun*. Oct 19 2012;427(2):266-72. doi:10.1016/j.bbrc.2012.09.032
229. Chen HH, Lu PJ, Chen BR, Hsiao M, Ho WY, Tseng CJ. Heme oxygenase-1 ameliorates kidney ischemia-reperfusion injury in mice through extracellular signal-regulated kinase 1/2-enhanced tubular epithelium proliferation. *Biochim Biophys Acta*. Oct 2015;1852(10 Pt A):2195-201. doi:10.1016/j.bbadis.2015.07.018
230. Rossi M, Thierry A, Delbauve S, et al. Specific expression of heme oxygenase-1 by myeloid cells modulates renal ischemia-reperfusion injury. *Sci Rep*. Mar 15 2017;7(1):197. doi:10.1038/s41598-017-00220-w
231. Moens AL, Champion HC, Claeys MJ, et al. High-dose folic acid pretreatment blunts cardiac dysfunction during ischemia coupled to maintenance of high-energy phosphates and reduces postreperfusion injury. *Circulation*. Apr 8 2008;117(14):1810-9. doi:10.1161/CIRCULATIONAHA.107.725481
232. Pleiner J, Schaller G, Mittermayer F, et al. Intra-arterial vitamin C prevents endothelial dysfunction caused by ischemia-reperfusion. *Atherosclerosis*. Mar 2008;197(1):383-91. doi:10.1016/j.atherosclerosis.2007.06.011
233. Bjelakovic G, Gluud C. Surviving antioxidant supplements. *J Natl Cancer Inst*. May 16 2007;99(10):742-3. doi:10.1093/jnci/djk211
234. Bjelakovic G, Nikolova D, Gluud LL, Simonetti RG, Gluud C. Mortality in randomized trials of antioxidant supplements for primary and secondary prevention: systematic review and meta-analysis. *JAMA*. Feb 28 2007;297(8):842-57. doi:10.1001/jama.297.8.842
235. Flaherty JT, Pitt B, Gruber JW, et al. Recombinant human superoxide dismutase (h-SOD) fails to improve recovery of ventricular function in patients undergoing coronary angioplasty for acute myocardial infarction. *Circulation*. May 1994;89(5):1982-91. doi:10.1161/01.cir.89.5.1982
236. Rapola JM, Virtamo J, Ripatti S, et al. Randomised trial of alpha-tocopherol and beta-carotene supplements on incidence of major coronary events in men with previous myocardial infarction. *Lancet*. Jun 14 1997;349(9067):1715-20. doi:10.1016/S0140-6736(97)01234-8
237. Piccinini AM, Midwood KS. DAMPening inflammation by modulating TLR signalling. *Mediators of inflammation*. 2010;2010doi:10.1155/2010/672395
238. Jiang D, Liang J, Fan J, et al. Regulation of lung injury and repair by Toll-like receptors and hyaluronan. *Nat Med*. Nov 2005;11(11):1173-9. doi:10.1038/nm1315
239. Rosin DL, Okusa MD. Dangers within: DAMP responses to damage and cell death in kidney disease. *J Am Soc Nephrol*. Mar 2011;22(3):416-25. doi:10.1681/asn.2010040430
240. Xu Q, Zhao B, Ye Y, et al. Relevant mediators involved in and therapies targeting the inflammatory response induced by activation of the NLRP3 inflammasome in ischemic stroke. *Journal of Neuroinflammation*. 2021/05/31 2021;18(1):123. doi:10.1186/s12974-021-02137-8
241. Leemans JC, Stokman G, Claessen N, et al. Renal-associated TLR2 mediates ischemia/reperfusion injury in the kidney. *J Clin Invest*. Oct 2005;115(10):2894-903. doi:10.1172/JCI22832
242. Wu H, Chen G, Wyburn KR, et al. TLR4 activation mediates kidney ischemia/reperfusion injury. *J Clin Invest*. 2007;117(10):2847-2859. doi:10.1172/JCI31008
243. Arslan F, Keogh B, McGuirk P, Parker AE. TLR2 and TLR4 in ischemia reperfusion injury. *Mediators of inflammation*. 2010;2010:704202. doi:10.1155/2010/704202
244. Kenny EF, O'Neill LA. Signalling adaptors used by Toll-like receptors: an update. *Cytokine*. Sep 2008;43(3):342-9. doi:10.1016/j.cyto.2008.07.010
245. Linkermann A, Chen G, Dong G, Kunzendorf U, Krautwald S, Dong Z. Regulated cell death in AKI. *Journal of the American Society of Nephrology : JASN*. 2014;25(12):2689-2701. doi:10.1681/ASN.2014030262
246. Krautwald S, Linkermann A. The fire within: pyroptosis in the kidney. *American Journal of Physiology-Renal Physiology*. 2014/01/15 2014;306(2):F168-F169. doi:10.1152/ajprenal.00552.2013
247. Hutton HL, Ooi JD, Holdsworth SR, Kitching AR. The NLRP3 inflammasome in kidney disease and autoimmunity. https://doi.org/10.1111/nep.12785. *Nephrology*. 2016/09/01 2016;21(9):736-744. doi:https://doi.org/10.1111/nep.12785
248. Kerr JF, Wyllie AH, Currie AR. Apoptosis: a basic biological phenomenon with wide-ranging implications in tissue kinetics. *Br J Cancer*. Aug 1972;26(4):239-57. doi:10.1038/bjc.1972.33
249. Doran AC, Yurdagul A, Tabas I. Efferocytosis in health and disease. *Nature Reviews Immunology*. 2020/04/01 2020;20(4):254-267. doi:10.1038/s41577-019-0240-6
250. Elliott MR, Koster KM, Murphy PS. Efferocytosis Signaling in the Regulation of Macrophage Inflammatory Responses. *Journal of immunology (Baltimore, Md : 1950)*. Feb 15 2017;198(4):1387-1394. doi:10.4049/jimmunol.1601520
251. Walczak H, Bouchon A, Stahl H, Krammer PH. Tumor necrosis factor-related apoptosis-inducing ligand retains its apoptosis-inducing capacity on Bcl-2- or Bcl-xL-overexpressing chemotherapy-resistant tumor cells. *Cancer research*. Jun 1 2000;60(11):3051-7.
252. Walczak H, Krammer PH. The CD95 (APO-1/Fas) and the TRAIL (APO-2L) apoptosis systems. *Exp Cell Res*. Apr 10 2000;256(1):58-66. doi:10.1006/excr.2000.4840
253. Tang D, Kang R, Berghe TV, Vandenabeele P, Kroemer G. The molecular machinery of regulated cell death. *Cell Research*. 2019/05/01 2019;29(5):347-364. doi:10.1038/s41422-019-0164-5
254. Tait SW, Green DR. Mitochondria and cell death: outer membrane permeabilization and beyond. *Nat Rev Mol Cell Biol*. Sep 2010;11(9):621-32. doi:10.1038/nrm2952
255. Levine B, Klionsky DJ. Development by self-digestion: molecular mechanisms and biological functions of autophagy. *Dev Cell*. Apr 2004;6(4):463-77.

256. Glick D, Barth S, Macleod KF. Autophagy: cellular and molecular mechanisms. *J Pathol*. May 2010;221(1):3-12. doi:10.1002/path.2697
257. Chien CT, Shyue SK, Lai MK. Bcl-xL augmentation potentially reduces ischemia/reperfusion induced proximal and distal tubular apoptosis and autophagy. *Transplantation*. Nov 15 2007;84(9):1183-90. doi:10.1097/01.tp.0000287334.38933.e3
258. Suzuki C, Isaka Y, Takabatake Y, et al. Participation of autophagy in renal ischemia/reperfusion injury. *Biochem Biophys Res Commun*. Mar 28 2008;368(1):100-6. doi:10.1016/j.bbrc.2008.01.059
259. Mizushima N. Autophagy: process and function. *Genes Dev*. Nov 15 2007;21(22):2861-73. doi:10.1101/gad.1599207
260. Jiang M, Wei Q, Dong G, Komatsu M, Su Y, Dong Z. Autophagy in proximal tubules protects against acute kidney injury. *Kidney international*. 2012;82(12):1271-1283. doi:10.1038/ki.2012.261
261. Isaka Y, Kimura T, Takabatake Y. The protective role of autophagy against aging and acute ischemic injury in kidney proximal tubular cells. *Autophagy*. Sep 2011;7(9):1085-7. doi:10.4161/auto.7.9.16465
262. Cursio R, Colosetti P, Codogno P, Cuervo AM, Shen HM. The role of autophagy in liver diseases: mechanisms and potential therapeutic targets. *BioMed research international*. 2015;2015:480508. doi:10.1155/2015/480508
263. Cursio R, Colosetti P, Gugenheim J. Autophagy and liver ischemia-reperfusion injury. *BioMed research international*. 2015;2015:417590. doi:10.1155/2015/417590
264. Evankovich J, Zhang R, Cardinal JS, et al. Calcium/calmodulin-dependent protein kinase IV limits organ damage in hepatic ischemia-reperfusion injury through induction of autophagy. *Am J Physiol Gastrointest Liver Physiol*. Jul 15 2012;303(2):G189-98. doi:10.1152/ajpgi.00051.2012
265. Kim JS, Nitta T, Mohuczy D, et al. Impaired autophagy: A mechanism of mitochondrial dysfunction in anoxic rat hepatocytes. *Hepatology*. May 2008;47(5):1725-36. doi:10.1002/hep.22187
266. Aghaei M, Motallebnezhad M, Ghorghanlu S, et al. Targeting autophagy in cardiac ischemia/reperfusion injury: A novel therapeutic strategy. *J Cell Physiol*. Aug 2019;234(10):16768-16778. doi:10.1002/jcp.28345
267. Lee E, Koo Y, Ng A, et al. Autophagy is essential for cardiac morphogenesis during vertebrate development. *Autophagy*. Apr 2014;10(4):572-87. doi:10.4161/auto.27649
268. Khan S, Salloum F, Das A, Xi L, Vetrovec GW, Kukreja RC. Rapamycin confers preconditioning-like protection against ischemia-reperfusion injury in isolated mouse heart and cardiomyocytes. *J Mol Cell Cardiol*. Aug 2006;41(2):256-64. doi:10.1016/j.yjmcc.2006.04.014
269. Huang Z, Han Z, Ye B, et al. Berberine alleviates cardiac ischemia/reperfusion injury by inhibiting excessive autophagy in cardiomyocytes. *Eur J Pharmacol*. Sep 5 2015;762:1-10. doi:10.1016/j.ejphar.2015.05.028
270. Kers J, Leemans JC, Linkermann A. An Overview of Pathways of Regulated Necrosis in Acute Kidney Injury. *Semin Nephrol*. May 2016;36(3):139-52. doi:10.1016/j.semnephrol.2016.03.002
271. Zheng J, Devalaraja-Narashimha K, Singaravelu K, Padanilam BJ. Poly(ADP-ribose) polymerase-1 gene ablation protects mice from ischemic renal injury. *American Journal of Physiology-Renal Physiology*. 2005/02/01 2005;288(2):F387-F398. doi:10.1152/ajprenal.00436.2003
272. Martin DR, Lewington AJ, Hammerman MR, Padanilam BJ. Inhibition of poly(ADP-ribose) polymerase attenuates ischemic renal injury in rats. *Am J Physiol Regul Integr Comp Physiol*. Nov 2000;279(5):R1834-40. doi:10.1152/ajpregu.2000.279.5.R1834
273. Poyan Mehr A, Tran MT, Ralto KM, et al. De novo NAD+ biosynthetic impairment in acute kidney injury in humans. *Nature Medicine*. 2018/09/01 2018;24(9):1351-1359. doi:10.1038/s41591-018-0138-z
274. Tran MT, Zsengeller ZK, Berg AH, et al. PGC1α drives NAD biosynthesis linking oxidative metabolism to renal protection. *Nature*. 2016/03/01 2016;531(7595):528-532. doi:10.1038/nature17184
275. Bonventre JV, Yang L. Cellular pathophysiology of ischemic acute kidney injury. *J Clin Invest*. 2011;121(11):4210-4221. doi:10.1172/JCI45161
276. Eltzschig HK, Collard CD. Vascular ischaemia and reperfusion injury. *British Medical Bulletin*. 2004;70(1):71-86. doi:10.1093/bmb/ldh025
277. Festjens N, Vanden Berghe T, Vandenabeele P. Necrosis, a well-orchestrated form of cell demise: signalling cascades, important mediators and concomitant immune response. *Biochim Biophys Acta*. Sep-Oct 2006;1757(9-10):1371-87. doi:10.1016/j.bbabio.2006.06.014
278. Majno G, Joris I. Apoptosis, oncosis, and necrosis. An overview of cell death. *Am J Pathol*. Jan 1995;146(1):3-15.
279. Vanden Berghe T, Linkermann A, Jouan-Lanhouet S, Walczak H, Vandenabeele P. Regulated necrosis: the expanding network of non-apoptotic cell death pathways. *Nat Rev Mol Cell Biol*. Feb 2014;15(2):135-47. doi:10.1038/nrm3737
280. Oerlemans MI, Liu J, Arslan F, et al. Inhibition of RIP1-dependent necrosis prevents adverse cardiac remodeling after myocardial ischemia-reperfusion in vivo. *Basic Res Cardiol*. Jul 2012;107(4):270. doi:10.1007/s00395-012-0270-8
281. Pefanis A, Ierino FL, Murphy JM, Cowan PJ. Regulated necrosis in kidney ischemia-reperfusion injury. *Kidney International*. 2019;96(2):291-301. doi:10.1016/j.kint.2019.02.009
282. GSK2982772 Study in Subjects With Ulcerative Colitis. https://ClinicalTrials.gov/show/NCT02903966.
283. Choi N, Whitlock R, Klassen J, et al. Early intraoperative iron-binding proteins are associated with acute kidney injury after cardiac surgery. *The Journal of Thoracic and Cardiovascular Surgery*. 2019/01/01/ 2019;157(1):287-297.e2. doi:https://doi.org/10.1016/j.jtcvs.2018.06.091
284. Linkermann A, Bräsen Jan H, Darding M, et al. Two independent pathways of regulated necrosis mediate ischemia–reperfusion injury. *Proceedings of the National Academy of Sciences*. 2013/07/16 2013;110(29):12024-12029. doi:10.1073/pnas.1305538110
285. Su L, Jiang X, Yang C, et al. Pannexin 1 mediates ferroptosis that contributes to renal ischemia/reperfusion injury. *Journal of Biological Chemistry*. 2019;294(50):19395-19404. doi:10.1074/jbc.RA119.010949
286. Ni L, Yuan C, Wu X. Targeting ferroptosis in acute kidney injury. *Cell Death & Disease*. 2022/02/24 2022;13(2):182. doi:10.1038/s41419-022-04628-9
287. Sui M, Xu D, Zhao W, et al. CIRBP promotes ferroptosis by interacting with ELAVL1 and activating ferritinophagy during renal ischaemia-reperfusion injury. https://doi.org/10.1111/jcmm.16567. *J Cell Mol Med*. 2021/07/01 2021;25(13):6203-6216. doi:https://doi.org/10.1111/jcmm.16567
288. Dixon Scott J, Lemberg Kathryn M, Lamprecht Michael R, et al. Ferroptosis: An Iron-Dependent Form of Nonapoptotic Cell Death. *Cell*. 2012/05/25/ 2012;149(5):1060-1072. doi:https://doi.org/10.1016/j.cell.2012.03.042
289. Avunduk MC, Yurdakul T, Erdemli E, Yavuz A. Prevention of renal damage by alpha tocopherol in ischemia and reperfusion models of rats. *Urological Research*. 2003/08/01 2003;31(4):280-285. doi:10.1007/s00240-003-0329-y
290. Tonnus W, Meyer C, Steinebach C, et al. Dysfunction of the key ferroptosis-surveilling systems hypersensitizes mice to tubular necrosis during acute kidney injury. *Nature Communications*. 2021/07/20 2021;12(1):4402. doi:10.1038/s41467-021-24712-6
291. Linkermann A, Skouta R, Himmerkus N, et al. Synchronized renal tubular cell death involves ferroptosis. *Proceedings of the National Academy of Sciences*. 2014/11/25 2014;111(47):16836-16841. doi:10.1073/pnas.1415518111
292. Imoto S, Kono M, Suzuki T, et al. Haemin-induced cell death in human monocytic cells is consistent with ferroptosis. *Transfusion and Apheresis Science*. 2018/08/01/ 2018;57(4):524-531. doi:https://doi.org/10.1016/j.transci.2018.05.028

293. Zhang S, Xin W, Anderson GJ, et al. Double-edge sword roles of iron in driving energy production versus instigating ferroptosis. *Cell Death & Disease*. 2022/01/10 2022;13(1):40. doi:10.1038/s41419-021-04490-1
294. Zhang J, Bi J, Ren Y, et al. Involvement of GPX4 in irisin's protection against ischemia reperfusion-induced acute kidney injury. https://doi.org/10.1002/jcp.29903. *Journal of Cellular Physiology*. 2021/02/01 2021;236(2):931-945. doi:https://doi.org/10.1002/jcp.29903
295. Wang Y, Quan F, Cao Q, et al. Quercetin alleviates acute kidney injury by inhibiting ferroptosis. *Journal of Advanced Research*. 2021/02/01/ 2021;28:231-243. doi:https://doi.org/10.1016/j.jare.2020.07.007
296. Sun X, Ou Z, Chen R, et al. Activation of the p62-Keap1-NRF2 pathway protects against ferroptosis in hepatocellular carcinoma cells. https://doi.org/10.1002/hep.28251. *Hepatology*. 2016/01/01 2016;63(1):173-184. doi:https://doi.org/10.1002/hep.28251
297. Sun X, Niu X, Chen R, et al. Metallothionein-1G facilitates sorafenib resistance through inhibition of ferroptosis. https://doi.org/10.1002/hep.28574. *Hepatology*. 2016/08/01 2016;64(2):488-500. doi:https://doi.org/10.1002/hep.28574
298. Miao EA, Leaf IA, Treuting PM, et al. Caspase-1-induced pyroptosis is an innate immune effector mechanism against intracellular bacteria. *Nat Immunol*. Dec 2010;11(12):1136-42. doi:10.1038/ni.1960
299. Doitsh G, Galloway NL, Geng X, et al. Cell death by pyroptosis drives CD4 T-cell depletion in HIV-1 infection. *Nature*. Jan 23 2014;505(7484):509-14. doi:10.1038/nature12940
300. Yu P, Zhang X, Liu N, Tang L, Peng C, Chen X. Pyroptosis: mechanisms and diseases. *Signal Transduction and Targeted Therapy*. 2021/03/29 2021;6(1):128. doi:10.1038/s41392-021-00507-5
301. Paik S, Kim JK, Silwal P, Sasakawa C, Jo E-K. An update on the regulatory mechanisms of NLRP3 inflammasome activation. *Cellular & molecular immunology*. 2021/05/01 2021;18(5):1141-1160. doi:10.1038/s41423-021-00670-3
302. Yang BIN, Jain S, Pawluczyk IZA, et al. Inflammation and caspase activation in long-term renal ischemia/reperfusion injury and immunosuppression in rats. *Kidney International*. 2005;68(5):2050-2067. doi:10.1111/j.1523-1755.2005.00662.x
303. Melnikov VY, Ecder T, Fantuzzi G, et al. Impaired IL-18 processing protects caspase-1–deficient mice from ischemic acute renal failure. *J Clin Invest*. 05/01/ 2001;107(9):1145-1152. doi:10.1172/JCI12089
304. Aglietti Robin A, Estevez A, Gupta A, et al. GsdmD p30 elicited by caspase-11 during pyroptosis forms pores in membranes. *Proceedings of the National Academy of Sciences*. 2016/07/12 2016;113(28):7858-7863. doi:10.1073/pnas.1607769113
305. Kayagaki N, Stowe IB, Lee BL, et al. Caspase-11 cleaves gasdermin D for non-canonical inflammasome signalling. *Nature*. 2015/10/01 2015;526(7575):666-671. doi:10.1038/nature15541
306. Zhang Z, Shao X, Jiang N, et al. Caspase-11-mediated tubular epithelial pyroptosis underlies contrast-induced acute kidney injury. *Cell Death & Disease*. 2018/09/24 2018;9(10):983. doi:10.1038/s41419-018-1023-x
307. Yang J-R, Yao F-H, Zhang J-G, et al. Ischemia-reperfusion induces renal tubule pyroptosis via the CHOP-caspase-11 pathway. *American Journal of Physiology-Renal Physiology*. 2014/01/01 2013;306(1):F75-F84. doi:10.1152/ajprenal.00117.2013
308. Bakker PJ, Butter LM, Claessen N, et al. A tissue-specific role for Nlrp3 in tubular epithelial repair after renal ischemia/reperfusion. *Am J Pathol*. Jul 2014;184(7):2013-22. doi:10.1016/j.ajpath.2014.04.005
309. Bakker PJ, Butter LM, Kors L, et al. Nlrp3 is a key modulator of diet-induced nephropathy and renal cholesterol accumulation. *Kidney Int*. May 2014;85(5):1112-22. doi:10.1038/ki.2013.503
310. Cookson BT, Brennan MA. Pro-inflammatory programmed cell death. *Trends Microbiol*. Mar 2001;9(3):113-4.
311. Morante-Palacios O, Fondelli F, Ballestar E, Martínez-Cáceres EM. Tolerogenic Dendritic Cells in Autoimmunity and Inflammatory Diseases. *Trends in Immunology*. 2021;42(1):59-75. doi:10.1016/j.it.2020.11.001
312. Rousselle TV, Kuscu C, Kuscu C, et al. FTY720 Regulates Mitochondria Biogenesis in Dendritic Cells to Prevent Kidney Ischemic Reperfusion Injury. Original Research. *Front Immunol*. 2020-June-23 2020;11doi:10.3389/fimmu.2020.01278
313. Namwanje M, Bisunke B, Rousselle TV, et al. Rapamycin Alternatively Modifies Mitochondrial Dynamics in Dendritic Cells to Reduce Kidney Ischemic Reperfusion Injury. *Int J Mol Sci*. May 20 2021;22(10)doi:10.3390/ijms22105386
314. Cifuentes-Rius A, Desai A, Yuen D, Johnston APR, Voelcker NH. Inducing immune tolerance with dendritic cell-targeting nanomedicines. *Nature Nanotechnology*. 2021/01/01 2021;16(1):37-46. doi:10.1038/s41565-020-00810-2
315. Phillips BE, Garciafigueroa Y, Engman C, Trucco M, Giannoukakis N. Tolerogenic Dendritic Cells and T-Regulatory Cells at the Clinical Trials Crossroad for the Treatment of Autoimmune Disease; Emphasis on Type 1 Diabetes Therapy. *Front Immunol*. 2019;10:148-148. doi:10.3389/fimmu.2019.00148
316. Buelens C, Verhasselt V, De Groote D, Thielemans K, Goldman M, Willems F. Interleukin-10 prevents the generation of dendritic cells from human peripheral blood mononuclear cells cultured with interleukin-4 and granulocyte/ macrophage-colony-stimulating factor. https://doi.org/10.1002/eji.1830270326. *European journal of immunology*. 1997/03/01 1997;27(3):756-762. doi:https://doi.org/10.1002/eji.1830270326
317. Morelli AE, Thomson AW. Tolerogenic dendritic cells and the quest for transplant tolerance. Review Article. *Nature Reviews Immunology*. 07/13/online 2007;7:610. doi:10.1038/nri2132
318. Li J, Thomson AW, Rogers NM. Myeloid and Mesenchymal Stem Cell Therapies for Solid Organ Transplant Tolerance. *Transplantation*. Dec 1 2021;105(12):e303-e321. doi:10.1097/tp.0000000000003765
319. Moreau A, Varey E, Bouchet-Delbos L, Cuturi M-C. Cell therapy using tolerogenic dendritic cells in transplantation. *Transplantation research*. 2012/09/28 2012;1(1):13. doi:10.1186/2047-1440-1-13
320. Divito SJ, Morelli AE. Method of Generating Tolerogenic Maturation-Resistant Dendritic Cells and Testing for Their Immune-Regulatory Functions In Vivo in the Context of Transplantation. In: Boyd AS, ed. *Immunological Tolerance: Methods and Protocols*. Springer New York; 2019:181-193.
321. Canning MO, Grotenhuis K, de Wit H, Ruwhof C, Drexhage HA. 1-alpha,25-Dihydroxyvitamin D3 (1,25(OH)(2)D(3)) hampers the maturation of fully active immature dendritic cells from monocytes. *Eur J Endocrinol*. Sep 2001;145(3):351-7. doi:10.1530/eje.0.1450351
322. Penna G, Adorini L. 1 Alpha,25-dihydroxyvitamin D3 inhibits differentiation, maturation, activation, and survival of dendritic cells leading to impaired alloreactive T cell activation. *Journal of immunology (Baltimore, Md : 1950)*. Mar 1 2000;164(5):2405-11. doi:10.4049/jimmunol.164.5.2405
323. Piemonti L, Monti P, Sironi M, et al. Vitamin D3 affects differentiation, maturation, and function of human monocyte-derived dendritic cells. *Journal of immunology (Baltimore, Md : 1950)*. May 1 2000;164(9):4443-51. doi:10.4049/jimmunol.164.9.4443
324. Schlitzer A, McGovern N, Ginhoux F. Dendritic cells and monocyte-derived cells: Two complementary and integrated functional systems. *Semin Cell Dev Biol*. May 2015;41:9-22. doi:10.1016/j.semcdb.2015.03.011
325. Unger WW, Laban S, Kleijwegt FS, van der Slik AR, Roep BO. Induction of Treg by monocyte-derived DC modulated by vitamin D3 or dexamethasone: differential role for PD-L1. *European journal of immunology*. Nov 2009;39(11):3147-59. doi:10.1002/eji.200839103
326. Anderson AE, Sayers BL, Haniffa MA, et al. Differential regulation of naïve and memory CD4+ T cells by alternatively activated dendritic cells. *J Leukoc Biol*. Jul 2008;84(1):124-33. doi:10.1189/jlb.1107744
327. Ferreira LMR, Muller YD, Bluestone JA, Tang Q. Next-generation regulatory T cell therapy. *Nature Reviews Drug Discovery*. 2019/10/01 2019;18(10):749-769. doi:10.1038/s41573-019-0041-4
328. Barragan M, Good M, Kolls JK. Regulation of Dendritic Cell Function by Vitamin D. *Nutrients*. 2015;7(9)doi:10.3390/nu7095383

329. Carlberg C. Vitamin D Signaling in the Context of Innate Immunity: Focus on Human Monocytes. Mini Review. *Front Immunol*. 2019-September-13 2019;10doi:10.3389/fimmu.2019.02211
330. Ferreira Gabriela B, Vanherwegen A-S, Eelen G, et al. Vitamin D3 Induces Tolerance in Human Dendritic Cells by Activation of Intracellular Metabolic Pathways. *Cell Reports*. 2015/02/10/ 2015;10(5):711-725. doi:https://doi.org/10.1016/j.celrep.2015.01.013
331. Mora JR, Iwata M, von Andrian UH. Vitamin effects on the immune system: vitamins A and D take centre stage. *Nature Reviews Immunology*. 2008/09/01 2008;8(9):685-698. doi:10.1038/nri2378
332. Català-Moll F, Ferreté-Bonastre AG, Godoy-Tena G, et al. Vitamin D receptor, STAT3, and TET2 cooperate to establish tolerogenesis. *Cell Reports*. 2022/01/18/ 2022;38(3):110244. doi:https://doi.org/10.1016/j.celrep.2021.110244
333. Riley JK, Takeda K, Akira S, Schreiber RD. Interleukin-10 Receptor Signaling through the JAK-STAT Pathway: REQUIREMENT FOR TWO DISTINCT RECEPTOR-DERIVED SIGNALS FOR ANTI-INFLAMMATORY ACTION*. *Journal of Biological Chemistry*. 1999/06/04/ 1999;274(23):16513-16521. doi:https://doi.org/10.1074/jbc.274.23.16513
334. Hutchinson JA, Geissler EK. Now or never? The case for cell-based immunosuppression in kidney transplantation. *Kidney Int*. Jun 2015;87(6):1116-24. doi:10.1038/ki.2015.50
335. Moreau A, Alliot-Licht B, Cuturi M-C, Blancho G. Tolerogenic dendritic cell therapy in organ transplantation. *Transplant International*. 2017/08/01 2017;30(8):754-764. doi:10.1111/tri.12889
336. Naranjo-Gómez M, Raïch-Regué D, Oñate C, et al. Comparative study of clinical grade human tolerogenic dendritic cells. *Journal of translational medicine*. 2011;9:89-89. doi:10.1186/1479-5876-9-89
337. Chamorro S, García-Vallejo JJ, Unger WWJ, et al. TLR Triggering on Tolerogenic Dendritic Cells Results in TLR2 Up-Regulation and a Reduced Proinflammatory Immune Program. *The Journal of Immunology*. 2009;183(5):2984. doi:10.4049/jimmunol.0801155
338. Navarro-Barriuso J, Mansilla MJ, Naranjo-Gómez M, et al. Comparative transcriptomic profile of tolerogenic dendritic cells differentiated with vitamin D3, dexamethasone and rapamycin. *Sci Rep*. 2018/10/08 2018;8(1):14985. doi:10.1038/s41598-018-33248-7
339. Navarro-Barriuso J, Mansilla MJ, Quirant-Sánchez B, Teniente-Serra A, Ramo-Tello C, Martínez-Cáceres EM. Vitamin D3-Induced Tolerogenic Dendritic Cells Modulate the Transcriptomic Profile of T CD4+ Cells Towards a Functional Hyporesponsiveness. Original Research. *Front Immunol*. 2021-January-20 2021;11doi:10.3389/fimmu.2020.599623
340. Robertson H, Li J, Kim HJ, et al. Transcriptomic Analysis Identifies A Tolerogenic Dendritic Cell Signature. Original Research. *Front Immunol*. 2021-October-20 2021;12doi:10.3389/fimmu.2021.733231
341. Sánchez-Sánchez N, Riol-Blanco L, de la Rosa G, et al. Chemokine receptor CCR7 induces intracellular signaling that inhibits apoptosis of mature dendritic cells. *Blood*. 2004;104(3):619-625. doi:10.1182/blood-2003-11-3943
342. Sánchez-Sánchez N, Riol-Blanco L, Rodríguez-Fernández JL. The Multiple Personalities of the Chemokine Receptor CCR7 in Dendritic Cells. *The Journal of Immunology*. 2006;176(9):5153. doi:10.4049/jimmunol.176.9.5153
343. Wadwa M, Klopfleisch R, Adamczyk A, et al. IL-10 downregulates CXCR3 expression on Th1 cells and interferes with their migration to intestinal inflammatory sites. *Mucosal Immunology*. 2016/09/01 2016;9(5):1263-1277. doi:10.1038/mi.2015.132
344. Maldonado RA, von Andrian UH. How tolerogenic dendritic cells induce regulatory T cells. *Advances in immunology*. 2010;108:111-165. doi:10.1016/B978-0-12-380995-7.00004-5
345. Bakdash G, Sittig SP, van Dijk T, Figdor CG, de Vries IJ. The nature of activatory and tolerogenic dendritic cell-derived signal II. *Front Immunol*. 2013;4:53. doi:10.3389/fimmu.2013.00053
346. Chemnitz JM, Parry RV, Nichols KE, June CH, Riley JL. SHP-1 and SHP-2 associate with immunoreceptor tyrosine-based switch motif of programmed death 1 upon primary human T cell stimulation, but only receptor ligation prevents T cell activation. *Journal of immunology (Baltimore, Md : 1950)*. Jul 15 2004;173(2):945-54. doi:10.4049/jimmunol.173.2.945
347. Azuma H, Chandraker A, Nadeau K, et al. Blockade of T-cell costimulation prevents development of experimental chronic renal allograft rejection. *Proc Natl Acad Sci U S A*. Oct 29 1996;93(22):12439-44. doi:10.1073/pnas.93.22.12439
348. Crikis S, Lu B, Murray-Segal LM, et al. Transgenic overexpression of CD39 protects against renal ischemia-reperfusion and transplant vascular injury. *Am J Transplant*. 2010;10(12):2586-2595. doi:10.1111/j.1600-6143.2010.03257.x
349. Rajakumar S, Roberts V, Lu B, et al. CD39 Over-Expression Protects Against Ischemic-Induced AKI through Adenosine2-Receptor Mechanisms, but Promotes Renal Fibrosis: 1417. *Transplantation*. 2012;94(10S)
350. Yoshida O, Kimura S, Jackson EK, et al. CD39 expression by hepatic myeloid dendritic cells attenuates inflammation in liver transplant ischemia-reperfusion injury in mice. *Hepatology (Baltimore, Md)*. 2013;58(6):2163-2175. doi:10.1002/hep.26593
351. Zhao R, Qiao J, Zhang X, et al. Toll-Like Receptor-Mediated Activation of CD39 Internalization in BMDCs Leads to Extracellular ATP Accumulation and Facilitates P2X7 Receptor Activation. *Front Immunol*. 2019;10:2524-2524. doi:10.3389/fimmu.2019.02524
352. Steinman RM, Hawiger D, Nussenzweig MC. Tolerogenic Dendritic Cells. *Annual Review of Immunology*. 2003;21(1):685-711. doi:10.1146/annurev.immunol.21.120601.141040
353. Hill M, Cuturi MC. Negative vaccination by tolerogenic dendritic cells in organ transplantation. *Current opinion in organ transplantation*. Dec 2010;15(6):738-43. doi:10.1097/MOT.0b013e32833f7114
354. Li H, Shi B. Tolerogenic dendritic cells and their applications in transplantation. *Cellular & molecular immunology*. Jan 2015;12(1):24-30. doi:10.1038/cmi.2014.52
355. Audiger C, Rahman MJ, Yun TJ, Tarbell KV, Lesage S. The Importance of Dendritic Cells in Maintaining Immune Tolerance. *Journal of immunology (Baltimore, Md : 1950)*. 2017;198(6):2223-2231. doi:10.4049/jimmunol.1601629
356. Kohli K, Janssen A, Förster R. Plasmacytoid dendritic cells induce tolerance predominantly by cargoing antigen to lymph nodes. *European journal of immunology*. 2016;46(11):2659-2668. doi:10.1002/eji.201646359
357. Levings MK, Gregori S, Tresoldi E, Cazzaniga S, Bonini C, Roncarolo MG. Differentiation of Tr1 cells by immature dendritic cells requires IL-10 but not CD25+CD4+ Tr cells. *Blood*. 2005;105(3):1162-1169. doi:10.1182/blood-2004-03-1211
358. Idoyaga J, Fiorese C, Zbytnuik L, et al. Specialized role of migratory dendritic cells in peripheral tolerance induction. *J Clin Invest*. 02/01/ 2013;123(2):844-854. doi:10.1172/JCI65260
359. Pêche H, Renaudin K, Beriou G, Merieau E, Amigorena S, Cuturi MC. Induction of tolerance by exosomes and short-term immunosuppression in a fully MHC-mismatched rat cardiac allograft model. *Am J Transplant*. Jul 2006;6(7):1541-50. doi:10.1111/j.1600-6143.2006.01344.x
360. Pêche H, Trinité B, Martinet B, Cuturi MC. Prolongation of heart allograft survival by immature dendritic cells generated from recipient type bone marrow progenitors. *Am J Transplant*. Feb 2005;5(2):255-67. doi:10.1111/j.1600-6143.2004.00683.x
361. Robbins PD, Morelli AE. Regulation of immune responses by extracellular vesicles. *Nat Rev Immunol*. Mar 2014;14(3):195-208. doi:10.1038/nri3622
362. Morelli AE. The Immune Regulatory Effect of Apoptotic Cells and Exosomes on Dendritic Cells: Its Impact on Transplantation. https://doi.org/10.1111/j.1600-6143.2005.01197.x. *American Journal of Transplantation*. 2006/02/01 2006;6(2):254-261. doi:https://doi.org/10.1111/j.1600-6143.2005.01197.x

363. Ono Y, Perez-Gutierrez A, Nakao T, et al. Graft-infiltrating PD-L1hi cross-dressed dendritic cells regulate antidonor T cell responses in mouse liver transplant tolerance. https://doi.org/10.1002/hep.29529. *Hepatology*. 2018/04/01 2018;67(4):1499-1515. doi:https://doi.org/10.1002/hep.29529
364. Hu M, Rogers NM, Li J, et al. Antigen Specific Regulatory T Cells in Kidney Transplantation and Other Tolerance Settings. *Front Immunol*. 2021;12:717594. doi:10.3389/fimmu.2021.717594
365. Bottomley MJ, Brook MO, Shankar S, Hester J, Issa F. Towards regulatory cellular therapies in solid organ transplantation. *Trends in Immunology*. 2022/01/01/ 2022;43(1):8-21. doi:https://doi.org/10.1016/j.it.2021.11.001
366. Bériou G, Pêche H, Guillonneau C, Merieau E, Cuturi MC. Donor-specific allograft tolerance by administration of recipient-derived immature dendritic cells and suboptimal immunosuppression. *Transplantation*. Apr 27 2005;79(8):969-72. doi:10.1097/01.tp.0000158277.50073.35
367. Ezzelarab MB, Lu L, Shufesky WF, Morelli AE, Thomson AW. Donor-Derived Regulatory Dendritic Cell Infusion Maintains Donor-Reactive CD4(+)CTLA4(hi) T Cells in Non-Human Primate Renal Allograft Recipients Treated with CD28 Co-Stimulation Blockade. *Front Immunol*. 2018;9:250-250. doi:10.3389/fimmu.2018.00250
368. Ezzelarab MB, Raich-Regue D, Lu L, et al. Renal Allograft Survival in Nonhuman Primates Infused With Donor Antigen-Pulsed Autologous Regulatory Dendritic Cells. *Am J Transplant*. Jun 2017;17(6):1476-1489. doi:10.1111/ajt.14182
369. Morelli AE, Thomson AW. The Secret Behind Non-Antigen-Pulsed Autologous Dendritic Cell Therapy in Transplantation. https://doi.org/10.1111/ajt.12705. *American Journal of Transplantation*. 2014/05/01 2014;14(5):989-990. doi:https://doi.org/10.1111/ajt.12705
370. Benham H, Nel HJ, Law SC, et al. Citrullinated peptide dendritic cell immunotherapy in HLA risk genotype–positive rheumatoid arthritis patients. *Science Translational Medicine*. 2015;7(290):290ra87. doi:10.1126/scitranslmed.aaa9301
371. Bell GM, Anderson AE, Diboll J, et al. Autologous tolerogenic dendritic cells for rheumatoid and inflammatory arthritis. *Annals of the Rheumatic Diseases*. 2017;76(1):227. doi:10.1136/annrheumdis-2015-208456
372. Sawitzki B, Harden PN, Reinke P, et al. Regulatory cell therapy in kidney transplantation (The ONE Study): a harmonised design and analysis of seven non-randomised, single-arm, phase 1/2A trials. *The Lancet*. 2020;395(10237):1627-1639. doi:10.1016/S0140-6736(20)30167-7
373. Ekberg H, Tedesco-Silva H, Demirbas A, et al. Reduced Exposure to Calcineurin Inhibitors in Renal Transplantation. *New England Journal of Medicine*. 2007/12/20 2007;357(25):2562-2575. doi:10.1056/NEJMoa067411
374. Ezzelarab MB, Lu L, Guo H, et al. Eomesodermin(lo) CTLA4(hi) Alloreactive CD8+ Memory T Cells Are Associated With Prolonged Renal Transplant Survival Induced by Regulatory Dendritic Cell Infusion in CTLA4 Immunoglobulin-Treated Nonhuman Primates. *Transplantation*. Jan 2016;100(1):91-102.
375. Ezzelarab MB, Zahorchak AF, Lu L, et al. Regulatory dendritic cell infusion prolongs kidney allograft survival in nonhuman primates. *Am J Transplant*. Aug 2013;13(8):1989-2005. doi:10.1111/ajt.12310
376. Raich-Regue D, Glancy M, Thomson AW. Regulatory dendritic cell therapy: from rodents to clinical application. *Immunology letters*. Oct 2014;161(2):216-21. doi:10.1016/j.imlet.2013.11.016
377. Zahorchak AF, Macedo C, Hamm DE, Butterfield LH, Metes DM, Thomson AW. High PD-L1/CD86 MFI ratio and IL-10 secretion characterize human regulatory dendritic cells generated for clinical testing in organ transplantation. *Cell Immunol*. 2018;323:9-18. doi:10.1016/j.cellimm.2017.08.008
378. Geissler EK. The ONE Study compares cell therapy products in organ transplantation: introduction to a review series on suppressive monocyte-derived cells. *Transplantation research*. 2012;1(1):11-11. doi:10.1186/2047-1440-1-11
379. Marin E, Bouchet-Delbos L, Renoult O, et al. Human Tolerogenic Dendritic Cells Regulate Immune Responses through Lactate Synthesis. *Cell Metabolism*. 2019;30(6):1075-1090.e8. doi:10.1016/j.cmet.2019.11.011
380. Thomson AW, Humar A, Lakkis FG, Metes DM. Regulatory dendritic cells for promotion of liver transplant operational tolerance: Rationale for a clinical trial and accompanying mechanistic studies. *Human immunology*. May 2018;79(5):314-321. doi:10.1016/j.humimm.2017.10.017
381. Thomson AW, Tevar AD. Kidney transplantation: a safe step forward for regulatory immune cell therapy. *The Lancet*. 2020/05/23/ 2020;395(10237):1589-1591. doi:https://doi.org/10.1016/S0140-6736(20)30803-5
382. Thomson AW, Vionnet J, Sanchez-Fueyo A. Understanding, predicting and achieving liver transplant tolerance: from bench to bedside. *Nature Reviews Gastroenterology & Hepatology*. 2020/08/05 2020;doi:10.1038/s41575-020-0334-4
383. Harry RA, Anderson AE, Isaacs JD, Hilkens CMU. Generation and characterisation of therapeutic tolerogenic dendritic cells for rheumatoid arthritis. *Annals of the Rheumatic Diseases*. 2010;69(11):2042. doi:10.1136/ard.2009.126383
384. Giannoukakis N, Phillips B, Finegold D, Harnaha J, Trucco M. Phase I (safety) study of autologous tolerogenic dendritic cells in type 1 diabetic patients. *Diabetes Care*. Sep 2011;34(9):2026-32. doi:10.2337/dc11-0472
385. Zubizarreta I, Flórez-Grau G, Vila G, et al. Immune tolerance in multiple sclerosis and neuromyelitis optica with peptide-loaded tolerogenic dendritic cells in a phase 1b trial. *Proceedings of the National Academy of Sciences*. 2019/04/23 2019;116(17):8463-8470. doi:10.1073/pnas.1820039116
386. Jauregui-Amezaga A, Cabezón R, Ramírez-Morros A, et al. Intraperitoneal Administration of Autologous Tolerogenic Dendritic Cells for Refractory Crohn's Disease: A Phase I Study. *Journal of Crohn's and Colitis*. 2015;9(12):1071-1078. doi:10.1093/ecco-jcc/jjv144

2 Chapter 2

Tolerogenic Dendritic Cells protect against Acute Kidney Injury

Overview

Hypothesis	▪ Tolerogenic dendritic cells can protect against acute kidney injury
Aims	▪ Perform detailed functional and transcriptional phenotyping on tolDCs ▪ Ascertain if adoptive transfer of tolDC can protect against severe renal IRI. ▪ Characterise the kidney inflammatory and molecular profile following IRI
Main findings	▪ This chapter establishes the protective the role of tolerogenic dendritic cells in preventing severe acute kidney injury following ischemia reperfusion injury. ▪ The protection is not critically dependent on the recipient's own myeloid cells, and we show in depth molecular profiling of both tolerogenic dendritic cells and post injury kidney.
Data/code	▪ Supplementary digital files/code: https://github.com/jenli3/PhD2022. ▪ Tolerogenic DC bulk RNA-seq: GSE205322 (release after KI revisions) ▪ Spatial transcriptomics data upload: in progress (by QIMB bioinformatician)
Manuscript status	Material from this chapter has been reviewed by Kidney International and additional experiments requested for revised submission are currently in progress. This chapter includes original material not included in the KI submission (4000-word limit).

Tolerogenic dendritic cells protect against acute kidney injury

Jennifer S.Y. Li[1,2], MBBS, BE/BMedSci, FRACP
Harry Robertson[1,3] BSc
Katie Trinh[1] BMedSci, MBBS, FRACP
Arti M. Raghubar[4], BAppSci, MMolBio
Quan Nguyen[4] PhD
Nicholas Matigian[5] PhD
Ellis Patrick [1,3] PhD
Angus W. Thomson[6], PhD, DSc, FRCPath
Andrew J. Mallett[4,7,8], MBBS, FRACP, PhD
Natasha M. Rogers[1,2,9] MBBS, FRACP, PhD

[1]Centre for Transplant and Renal Research, Westmead Institute for Medical Research, Australia
[2]Sydney Medical School, Faculty of Health and Medicine, University of Sydney, Australia
[3] School of Mathematics and Statistics, University of Sydney, Australia
[4] Institute for Molecular Bioscience, The University of Queensland, Australia
[5] Queensland Cyber Infrastructure Foundation Bioinformatics, Brisbane, Australia
[6] Starzl Transplantation Institute, University of Pittsburgh School of Medicine, Pennsylvania, USA
[7] Department of Renal Medicine, Townsville University Hospital, Townsville, Australia
[8] College of Medicine and Dentistry, James Cook University, Australia
[9]Department of Renal Medicine, Westmead Hospital, Australia

2.1 Abstract

Effective interventions to treat or limit acute kidney injury (AKI) are lacking and here, we demonstrate that tolerogenic dendritic cells (tolDC) can provide renoprotection in an ischemia reperfusion injury (IRI) model of disease. Bone marrow-derived syngeneic or allogeneic DCs were tolerised with Vit-D3/IL-10. Syngeneic LPS-tolDC and Allo-tolDC were characterised by high PD-L1:CD86 expression, elevated IL-10 and restricted IL-12p70 secretion and suppressed transcriptomic inflammatory profile following exposure to lipopolysaccharide (LPS). When infused systemically, these cells successfully abrogated AKI without modifying infiltrating inflammatory cell populations. Allo-tolDC provided protection against IRI in mice pre-treated with liposomal clodronate therapy, suggesting the process was regulated by live, rather than reprocessed cells. Co-culture experiments and spatial transcriptomic analysis confirmed renoprotection was through reduced renal tubular epithelial cell death. These data provide strong evidence that tolDC have the ability to protect against AKI and warrants further exploration as a therapeutic option.

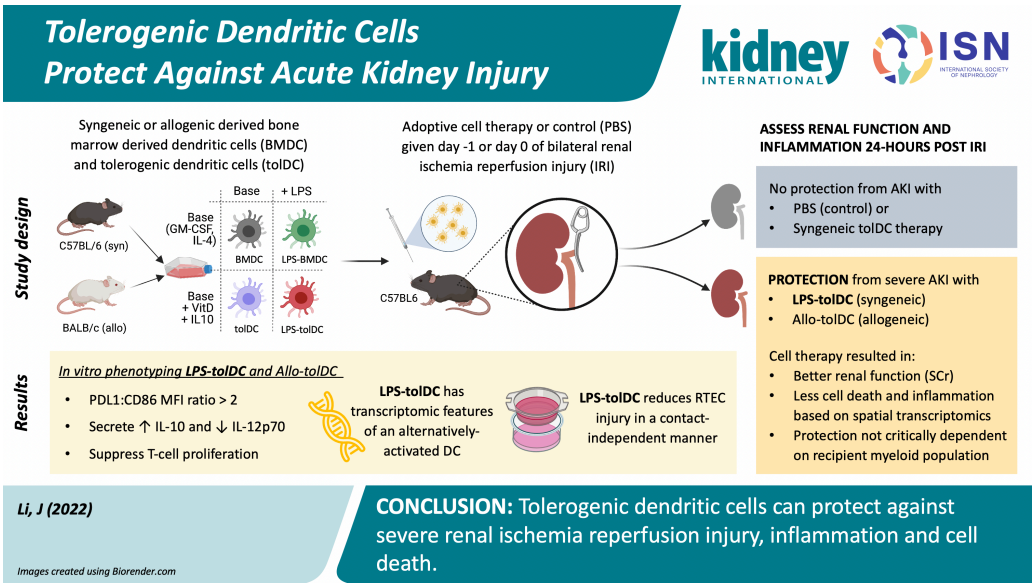

TRANSLATIONAL STATEMENT: Despite the ability to predict and identify AKI, clinicians can only offer supportive care and dialysis when the problem arises. Herein we demonstrate the potential use of tolerogenic dendritic cells (tolDC), demonstrating these cells can alter the early immunopathology and severity of AKI. There is an impetus to further explore the mechanistic role of tolDC in AKI and repair, but evidence from phase I/II clinical trials for solid-organ transplant tolerance suggest tolDC are safe. This provides tolDC with an immediate clinical advantage for bench-to-bedside translation of research to impact patient outcomes.

2.2 Introduction

Acute kidney injury (AKI) is a global disorder[1] which occurs in both community and acute hospital settings and epidemiological evidence clearly establishes that AKI is neither benign or self-limited, and survivors are confronted with an increased risk of chronic kidney disease[2], infection[3], cardiovascular morbidity[4] and mortality[5-7]. Despite known precipitants, improved biomarkers, and diagnostic classification[8-10], only supportive management is possible for AKI despite decades of research[11-13]. There is clearly an unmet need to improve the outcomes following AKI and a potential approach to modulate disease severity is by targeting the immunopathological component in AKI.[14] Dendritic cells (DC) are potent antigen processing presenting cells and injured/dying renal tubular epithelial cells (RTEC) release pro-inflammatory cytokines to recruit immune cells[15] and danger-associated molecular patterns (DAMPs) to activate DC. Mature DC generate effector T-cell responses in the tubulointerstitium[16], but the evidence for a direct effect of DC on RTEC independent T-cell subset or function is lacking, as is a comprehensive understanding of parenchymal molecular pathways changed in response to DC fluxes that occur in AKI. DC can be pharmacologically or genetically manipulated *in vitro* into a tolerogenic, or semi-mature (alternatively-activated) phenotype[17].

These tolerogenic DC (tolDC) display low-level co-stimulatory molecule expression, enhanced anti-inflammatory cytokine secretion and are capable of subverting effector T-cell responses and inducing regulatory T-cells. Renewed interest in cellular therapies has facilitated translation of pre-clinical studies to phase I/II clinical trials in transplantation tolerance[18-27] and autoimmune disease[28-34], with promising feasibility and safety data so far[26,33,35-38]. The attractiveness of tolDC-based therapy stems from the premise of antigen-specific immunosuppression, although realistically both autoimmunity and alloreactivity in transplantation are characterised by responsiveness to a broad range of antigens due to epitope spreading. The application of tolDC to clinical diseases lacking clear identification of antigenic specificity may still be beneficial given their anti-inflammatory mechanism of action. This represents a potential therapy for AKI and in this pre-clinical study, we investigate whether tolDC could limit RTEC damage in AKI, interrogate their mechanism of action, and provided essential phenotype and transcriptional information to guide an understanding of both tolDC biology and AKI.

2.3 Materials and methods

2.3.1 Animals

C57BL/6 and BALB/c mice obtained from Australian Bio-Resources (Garvan, Sydney, Australia) were housed in our animal facility (Westmead Institute for Medical Research), with 12-hour light/dark cycle, standard chow, and water *ad libitum*, approved under #4305 ethics protocol (Western Sydney Local Health District). Studies were performed in accordance with the Australian code for the care and use of animals for scientific purposes developed by the National Health and Medical Research Council of Australia.

2.3.2 Ex-vivo bone marrow derived dendritic cells (BMDC) and tolDC

Aseptic mice bone marrow was passed through 70μm cell filter and treated with red cell lysis buffer (eBioscience, Waltham, MA). Cells were then resuspended in DC media. DC media composed of RPMI 1640 media supplemented with 10% (v/v) heat-inactivated foetal calf serum, 1% (v/v) penicillin-streptomycin, 1% (v/v) L-glutamine, 1% (v/v) sodium pyruvate, 1% (v/v) non-essential amino acid, 10mM HEPES (4-(2-hydroxyethyl)-1-piperazineethanesulfonic acid (all Gibco, Waltham MA) along with 1000 IU/ml GM-CSF and 500 IU/ml interleukin-4 (Miltenyi Biotec, Germany)). Tolerogenic DC were generated with the addition of 20nM 1α,25-dihydroxyvitamin D3 (VitD3, Sigma, St Louis, MO) and 10ng/ml recombinant murine interleukin-10 (IL-10, Peprotech, Cranbury, NJ) to DC media, beginning on day 2 of culture. Medium, cytokines and vitD3/IL-10 were renewed every other day. To test maturation resistance, the TLR-4 agonist, lipopolysaccharide (LPS, InvivoGen, San Diego, CA) was used at 100pg/ml in select flasks on day 6, prior to cell collection on day 7. Magnetic beads were used to enrich for $live^{+}CD11c^{+}$ cells prior to in vivo studies using MACS Dead Cell Removal Kit and CD11c microbeads (Miltenyi Biotec).

2.3.3 Functional assessment of ex-vivo generated DCs

Cell surface marker profile of DCs were measured by flow cytometry. Single cell suspensions were washed in flow-wash buffer (PBS, 2% FCS), incubated with Fc block (anti-mouse CD16/32, BD Biosciences, Franklin Lakes, NJ) and then with fluorescent antibody cocktails (Table 2.1). Samples were analysed using the LSR Fortessa flow cytometer (BD Biosciences) with appropriate bead- and cell-based compensation

controls and data analysis was performed in FlowJo (v10.8.1 BD Bioscience). Reagents included in Table 2.1. To assess secretory functions, both IL-10 and IL12-p70 from the culture supernatant were quantified by enzyme-linked immunosorbent assay (ELISA). (ThermoFisher, Waltham, MA). To assess tolDC ability to suppress T-cell proliferation, they were used in a mixed lymphocyte reaction (MLR). C56BL/6 derived tolDC (or LPS-tolDC) and γ-irradiated, LPS-stimulated BMDC (irLPS-BMDC) were assigned as suppressor and stimulator cells respectively. BALB/c splenocytes labelled with CellTraceViolet (ThermoFisher) were used as responder cells. The MLR was set up for co-culture of stimulator + responder ± suppressor cells for 4 days before flow analysis. Positive controls were splenocytes exposed to 10ng/ml PMA and 1μg/ml ionomycin (Sigma Aldrich).

Table 2.1: ***Conjugated antibodies and reagents*** *used for cell surface phenotyping by flow cytometry*

Flow marker	Clone/ITEM description	Company
Dead cell marker	4',6-diamidino-2-phenylindole (DAPI)	Roche, Basel, Switzerland
CD3 - FITC	145-2c11	BD biosciences
NK1.1 - FITC	PK136	BD biosciences
B220 - FITC	RA36R2	BD biosciences
CD11c - APC	HL3	BD biosciences
CD11b – V500	HL3	BD biosciences
MHCII 1A/1E – BV711	14-4-4s	BD biosciences
CD40 – BV786	3/23	BD biosciences
CD80 - PE	16-10a1	BD biosciences
CD86 – PECy7	GL1	BD biosciences
PDL1 - PE	M1H5	BD biosciences

2.3.4 Transcriptomic profile of ex-vivo generated DCs

Bulk RNA-sequencing was performed on cultured, C57BL/6 derived DCs with conditions including naïve BMDC, LPS-BMDC, tolDC or LPS-TolDC groups, with 3 biological replicates for each group. Cells harvested on day 7 were enriched using live+ CD11c+ magnetic bead strategy and represents pure populations and thus, averting the need for single cell sequencing to delineate the identity in mixed samples. RNA was extracted from cultured cells using the ISOLATE II RNA Mini Kit (Bioline, London, UK) and RNA integrity number (RIN) determined by electrophoresis (Agilent 4200 Tapestation system, Santa Clara, CA).

All samples met minimum RIN ≥ 7.0 and cDNA libraries generated using the Stranded mRNA Prep Ligation Kit (Illumina, San Diego, CA) were sequenced using the NovaSeq 6000 platform (Illumina) with 100bp

single-end read length. These 12 samples were performed on same run. Raw data for trimming, quality control and alignment (STAR aligner to GRCm38-mm10 mouse reference genome) was performed by our in-house bioinformatician (Dr Brian Gloss), using Sydney University's high performance computing cluster.

Using R/R-studio (v4.1.2). *EdgeR*/*Limma* packages[1-3] were used for downstream analysis on the count matrix generated in pre-processing described above. Batch correction was not required as biological replicates in each treatment group were prepared, culture, and harvest/enrichment and RNA extraction were performed on the same dates, procedure and sequence run. Low counts (<10) were removed using the *filterByExpr* function and then normalised using *calcNormFactors*, using the trimmed mean of M-values (TMM) method[39], and takes a weighted average of gene-wise log-fold changes (M) and absolute expression levels (A). G* represent genes with valid M and A values. Observed counts (Y_{gk} or Y_{gr}) were retained if non-zero. Gene (g) for *k* and *r* (sample or condition):

$$M_g = log_2\left(\frac{Y_{gk}/N_k}{Y_{gk\prime}/N_{k\prime}}\right) \text{ and } A = \frac{1}{2}log_2\left(\left(Y_{gk}/N_k\right).\left(Y_{gk\prime}/N_{k\prime}\right)\right)$$

$$log_2(TMM_k^r) = \frac{\sum_{g\epsilon G*} w_{gk}^r . M_{gk}^r}{\sum_{g\epsilon G*} w_{gk}^r} \text{ where } M_{gk}^r = \frac{log_2\left(\frac{Y_{gk}}{N_k}\right)}{log_2\left(\frac{Y_{gr}}{N_r}\right)} \text{ and } w_{gk}^r = \frac{N_k - Y_{gk}}{N_k . Y_{gk}} + \frac{N_r - Y_{gr}}{N_r . Y_{gr}}$$

A contrast matrix was constructed to allow pair-wise comparison of all groups (BMDC, LPS-BMDC, tolDC and LPS-tolDC). (Table 2.2)

Table 2.2: ***Contrast matrix*** *of conditional comparisons for DC bulk RNA-seq with EdgeR and limma*

Comparison	Label	LPS-BMDC	LPS-tolDC	BMDC	tolDC
LPS-BMDC vs BMDC	lps.nil	1	0	-1	0
tolDC vs BMDC	tol.nil	0	0	-1	1
tolDC vs LPS-BMDC	tol.lps	-1	0	0	1
LPS-tolDC vs BMDC	lpstol.nil	0	1	-1	0
LPS-tolDC vs LPS-BMDC	lpstol.lps	-1	1	0	0
LPS-tolDC vs tolDC	lpstol.tol	0	1	0	-1

Differential gene expression was determined by the generalised linear model function *glmQLFTest*[4]. This generates gene-wise dispersion coefficients to represent the variability of each gene between biological conditions based on negative binomial modelling but using the quasi-likelihood (QL) method (utilising the F-test statistic) to minimise the higher false discovery rate (FDR) compared to standard likelihood ratio tests used otherwise[40,41]. The FDR threshold was set at 0.05 using the Benjamini-Hochberg method to correct for multiple hypothesis testing. Similarly, *limma* was used to compute the t-statistic for the dataset. The precision

weights of the mean-variance relationship, based on the log-counts per million (log-CPM) of RNA-seq data were determined using *voom*, followed by linear modelling and the empirical Bayes moderated t-statistic[5] was calculated using *lmfit* and *eBayes* respectively for DEG between groups. The t-statistic for each comparison was converted into Z-scores to by applying the quartile function (Q) to each row[6,7]. (Fig 2.1)

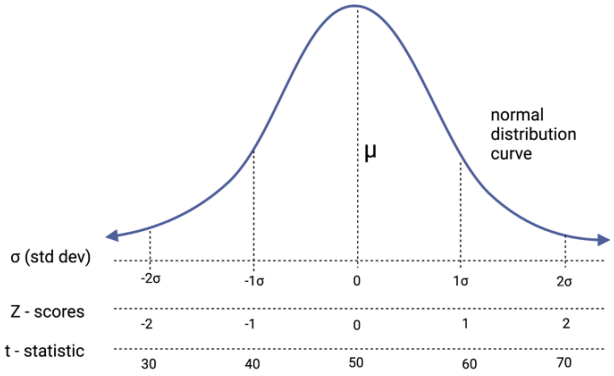

$$t.statistic = \frac{(\overline{mean} - hypothesized\ mean)}{std\ deviation/\sqrt{sample\ size}} \quad \text{and} \quad Z_{gene} = Q\left(\frac{rank(t.statistic)}{DGE\ length+1}\right)$$

Figure 2.1: ***Conversion of t-statistic and Z-scores*** *for differentially expressed genes in the DC dataset*

This Z-score allows for approximation of the standard deviation from the mean and assigns magnitude and direction of differentially expressed genes when comparing across multiple conditions (for example of a dataset with conditions A, B and C, significant Z-scores of common DEG for condition A when simultaneously comparing A|B and A|C). Pathway enrichment analysis was then performed to interpret the biological significance of DEG lists for specific conditions.

Gene set enrichment analysis[8] (GSEA) using the Gene Ontology (GO) database[9] was performed using *clusterProfiler*[10]. The adjusted P <0.05 (Benjamini-Hochberg method) was used as the minimum threshold for significance[11]. GSEA was chosen instead of over representation analysis as it leverages both magnitude and direction to determine genes at either the top or bottom ends of the input DEG gene vector are found in *a priori* defined gene sets are significantly different between two conditions. Over-representation analysis is useful to determine whether a list of genes (up- and down-regulated genes are analysed separately) is disproportionately contained within an *a priori* gene set, especially when magnitude is not known.

2.3.5 Renal tubular cell (RTEC) isolation and co-culture with DCs

Primary C57BL/6 RTEC were isolated as described previously[42]. Kidneys were digested using multi-tissue dissociation kit and GentleMacs (Miltenyi), incubated with CD326 microbeads (Miltenyi) and passed through LS columns. The positive cell fraction was suspended in defined RTEC K1 medium (see supplementary methods) and cultured on collagen-coated dishes (BD Biosciences). Cell passages 2-3 were seeded onto 6-well culture plates, and Transwell polyester inserts (0.4um pore, Corning, Corning, NY) were added to the RTEC wells with either (1) DC media alone or (2) LPS-tolDC + DC media and allowed to equilibrate for 24 hours. LPS (100ng/ml) was added to the RTEC chamber and RTEC collected at 0, 2, 4, 6 and 24-hours post-stimulation. RTEC KI media was made using base DMEM/F12 media supplemented with 25 ng/ml epidermal growth factor (Sigma Aldrich, St Louis, MO), 1 ng/ml prostaglandin E_1 (Cayman Chemicals, Ann Arbor, MI), 5×10^{-11} M triiodothyronine (Sigma Aldrich), 5×10^{-8} M hydrocortisone (Sigma-Aldrich), insulin–transferrin–sodium selenite supplement (Sigma Aldrich), 1% penicillin/streptomycin, 25mM HEPES and 5% FCS (ThermoFisher Scientific, Waltham, MA).

2.3.6 Bilateral renal ischemia reperfusion injury

Ten-to-twelve-week-old male C57BL/6 mice were anaesthetized using isoflurane/oxygen titrated to effect, with body temperature maintained at 36°C for bilateral ischemia-reperfusion injury (IRI). A mid-line abdominal incision allowed access to occlude the renal pedicles using microaneurysm clamps for 20 minutes before releasing and abdominal closure with 5/0 monofilament. For adoptive cell transfer experiments, mice received PBS alone (control), syngeneic tolDC, LPS-tolDC or allogeneic-tolDC ($1x10^6$, live/$CD11c^+$ cells in 150µl PBS) via a retro-orbital approach on the day prior (d-1) or day-of (d0) surgery.

In additional experiments**,** C56BL/6 mice received 0.1ml/10g body weight of liposome containing either control PBS or clodronate (Liposoma, Amsterdam, Holland) by intraperitoneal injection, followed by adoptive cell therapy and bilateral renal IRI 4 days later. All mice were euthanised after 24-hours reperfusion, with collection of blood by cardiac puncture and kidney tissue either snap frozen, embedded in optimal cutting temperature (OCT) compound or fixed in 10% neutral-buffered formalin.

2.3.7 Assessment of renal function, histology, and cell death

Renal function was determined by measurement of serum creatinine using Atellica CH enzymatic creatinine assay (ECre2, Siemens) by a centralised lab (Westmead Hospital ICPMR). Kidneys embedded in paraffin were sectioned at 4μm and stained with haematoxylin and eosin by standard methods.[42]

Brightfield images were acquired using the NanoZoomer HT and images viewed using NDP.scan (Hamamatsu, Shizuoka, Japan). Sections were scored by two blinded, independent observers for features of injury in five randomly selected areas in corticomedullary area. Markers of acute tubular damage (tubular dilatation, cell necrosis, infarction, and cast formation) were scored by semi-quantitative calculation of percentage of the corticomedullary junction involved: 0 (no features), 1-10%), 2 (11-25%), 3 (26-50%), 4 (51-75%) and 5 (>75%).

Kidneys preserved in OCT were sectioned at 5μm thickness and stained with the TMR-red TUNEL in situ cell death detection kit (Roche, Basel, Switzerland). Images were acquired using the Olympus FV1000 confocal laser scanning microscope (Olympus) and images reviewed using FV-10-ASW (v4.2, Olympus). The number of TUNEL positive cells in a 20x field over 5 different regions were averaged.

2.3.8 Kidney immune cell tracking and profiling

Single cell suspensions from collagenase/DNase-digested kidneys were incubated with Fc block prior to staining with conjugated antibodies (Table 2.3). Absolute cell counts (using BD TruCount, BD Bioscience) and relative proportions of live $CD45^+$ cells were assessed using the LSR Fortessa flow cytometer.

Cell tracking was performed using tolDC or LPS-tolDC labelled with CellTrace Violet prior to adoptive transfer of $2x10^6$ cells/mice on the day of IRI surgery. Kidneys were retrieved at 24-hours later, processed into a single cell suspension, and stained with Live/Dead fixable near IR stain (L34976, ThermoFisher) and CD45 antibody to analysis.

*Table 2.3: **Antibodies** used for kidney immune profiling by flow cytometry post IRI*

Flow marker	Clone/ITEM description	Company
Dead cell marker	4',6-diamidino-2-phenylindole (DAPI)	Roche, Basel, Switzerland
Dead cell marker	Live/Dead fixable near infra-red	ThermoFischer
CD3 - FITC	145-2c11	BD biosciences
NK1.1 - FITC	PK136	BD biosciences
B220 - FITC	RA36R2	BD biosciences
CD11c - APC	HL3	BD biosciences
CD11b – V500	HL3	BD biosciences
MHCII 1A/1E – BV711	14-4-4s	BD biosciences
CD40 – BV786	3/23	BD biosciences
CD80 - PE	16-10a1	BD biosciences
CD86 – PECy7	GL1	BD biosciences
PDL1 - PE	M1H5	BD biosciences
CD45 – BUV395	104	BD biosciences
F4/80 – V421	T45-2342	BD biosciences
Ly6G - PE	AL-21	BD biosciences
Ly6C – PECy7	1A8	BD biosciences
CD4 – PECy7	RM4-5	BD biosciences
CD8 – APCy7	53-6.7	BD biosciences
CD25 - APC	PC61	BD biosciences
CellTrack	CellTrack Red CMTPX	ThermoFisher
CellTrace	CellTrace Violet Cell Proliferation Kit	ThermoFisher

2.3.9 RTEC and Kidney PCR

RNA was extracted from either tissue or cell lysate using Isolate II RNA Mini Kit (Bioline) as per manufacturer's instructions. RNA was quantified using a Nanodrop (BioTek, Winooski, VT), and reverse-transcribed using a SensiFAST cDNA synthesis kit (Bioline). cDNA was amplified in triplicate with gene-specific primers (Invitrogen) using a CFX384 real-time PCR machine (Bio-Rad) using SensiFAST No-ROX (Bioline) and targeted TaqMan primers (ThermoFischer).

Primers include: Lipocalin-2 (Mm01324470_m1), HAVCR-1 (Mm00506686_m1), TNF-α (Mm00443258_m1), IL-1β (Mm00434228_m1), CXCR2 (Mm00436450_m1), CCL2 (Mm00441242_m1), IL-10 (Mm01288386_m1), IDO-1 (Mm00524210_m1), IDO-2 (Mm00524210_m1), iNos (Mm00440502_m1), NOX4 (Mm00479246_m1), SOD1 (Mm0700393_g1), SOD3 (Mm00448831_s1), 18S (Mm03928990_m1). Data was analysed using the ΔΔCT method with expression normalised to the house keeping gene and PBS-treated animals as the referent control.

2.3.10 Spatial transcriptomics

Spatial transcriptomics was performed on 6 fresh-frozen, kidney samples (n = 2 per group treated with PBS, tolDC or LPS-tolDC cells from C57BL/6 origin) using Visium slides (10x Genomics). Frozen samples in OCT were sent to the University of Queensland and the following section with sample handling, library preparation, sequencing, quality control, alignment and mapping were performed by Mr Samuel Holland and Ms Arti Raghubar under the supervision Prof Andrew Mallett and Prof Quan Nguyen. Detailed description of optimised methods[43] is summarised in the following section. OCT-embedded kidneys were processed according to the Visium Spatial Gene Expression Reagent Kits User Guide (CG000239Rev.C, 10x Genomics, Pleasanton, CA).

In brief, 8µm kidney cryosections were placed onto the active surface of pre-chilled slides (10x Genomics), dried at 37°c for 1 min, fixed in pre-chilled 100% methanol at -20°C for 30 min and then stained in Mayer's Hematoxylin for 5 min and Eosin for 2 min (H&E)[12]. Brightfield images were acquired (Axio Z1 slide scanner, Zeiss) and slides were processed for cDNA synthesis and library preparation with the following changes from the recommended protocol: amplified cDNA SPRIselect at 0.6x, fragmentation for 1 minute and all double sided SPRIselect at 0.55x and 0.7x. The final libraries were pooled and sequenced with NextSeq High Output 150 cycle kit (Illumina) loaded at 1.8pM on a NextSeq500 (Illumina) at Institute for Molecular Bioscience Sequencing Facility (University of Queensland). The following sequencing configuration was used: Read1 - 28bp, Index1 - 10bp, Index2 - 10bp, Read2 - 120bp. The generated ST libraries were first converted from raw base call files to FASTQ files using bcl2fastq/2.17, then trimmed of poly-A sequences on the 3' end and template switch oligo sequences on the 5' end. Cleaned FASTQ files were then mapped to the mouse reference genome (GRCm38-mm10) using Space Ranger V1.0 (10x Genomics) and mapped genes were aligned to the previous H&E image based on fiducial markings. All subsequent bioinformatic analysis was my work, with feedback from Prof Andrew Mallett and Dr Nicholas Matigian (bioinformatician).

STUtility[13] and *Seurat*[14] (v4) were used for downstream analysis in R programming environment. Spots with unique genes < 200, total counts < 100 and mitochondrial percentage > 30% were removed and then

normalisation by regularized negative binomial regression was performed using *SCTransform*[15] - with mitochondrial percentage and each sample set as variables to regress out of the *SCTransform* residuals. *CorSpatialGenes* was used to rank spatial patterns of gene expression, where neighbouring spots were identified if within 150µm distance and a 'spatial lag' for each gene was assigned as the summed expression of the gene across the neighbouring spots. The overall spatial correlation was then determined using Pearson correlation between the spatial lag and normalised count vector.[13]

Principal component analysis (PCA) was performed, and clusters determined using *FindNeighbors* and *FindClusters* functions. Briefly, the Euclidean distance in PCA space was used to construct a k-nearest neighbour graph and subsequently a shared nearest neighbour (SNN) graph, which models the similarity of two nodes relative to their connectivity or overlap in local neighbourhoods in high dimensional space based on the Jaccard distance[16] (Fig 2.2). Clustering was completed via the Louvain method for modularity optimisation and community aggregation[17] and the optimal resolution for *FindClusters* was 0.3 based on testing by SC3 stability[18] indices for 10 resolutions ranging between 0.1 to 1.6 using the *clustree* package[19].

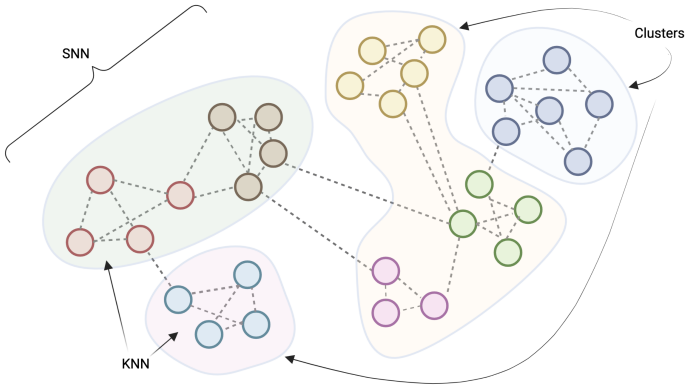

*Figure 2.2: **Unsupervised clustering**. Schematic representation of k nearest neighbour (KNN) and shared nearest neighbour (SNN) graphs then clustered based on Louvain modularity scores. Image created using BioRender.com*

Next, non-linear dimensionality reduction was performed using *RunTSNE* and *RunUMAP*; and differential gene expression between each 55µm spot was determined by Wilcoxon rank sum test using *FindMarkers* (between cluster pairs; spots vs neighbours; or between the spots found within the same cluster but on different sample groups (LPS-tolDC vs PBS or LPS-tolDC vs tolDC kidney samples)) or *FindAllMarkers* (between a cluster and the rest of the tissue) functions. $Wilcoxin.test.statistic = \sum_{i=1}^{Sample\ size}[sign(x_{2,i} - x_{1,i}).Rank_{,i}]$

where x is the corresponding ranked pairs from two distributions. Differential gene lists were filtered for a minimum fold-change (FC) ≥ 1.1 and adjusted-$P \leq 0.05$ thresholds and GSEA analysis performed using *clusterProfiler*.[10,20] Trimming was performed for display higher level GO annotations based on AmiGO2 and QuickGO slim.[21,22]

Cell composition was determined by regression-based spot deconvolution. The reference single cell RNA-seq reference was processed into *SingleCellExperiment*[23] for variance modelling followed by marker genes identification using *scoreMarkers*[24], a wrapper function to estimates effect size of differentially expressed genes. An area under the curve > 0.8 was used as the as the threshold metric, and the dataset was down-sampled to use 100 cells/cell type for regression-based deconvolution using *SPOTlight*. *SPOTlight* utilises seeded, non-negative matrix factorisation (NMF) and non-negative least squares (NNLS) regression to calculate the coefficients matrix[25,26] for our 10x Visium data to determine the cell mixture for each spot. The SPOTlight algorithm is based on the following:

$V \sim W \times H$	$G_i = G\ (cell\ marker\ genes) \cap G'(all\ genes\ from\ spatial\ data)$
	$W = matrix\ of\ G_i \times no\#cell\ types\ (or\ topics)$
$V' \sim W \times H'$	$H = (matrix\ of\ no\#cell\ types \times scRNAseq\ ref)$
	$H' = (matrix\ of\ no\#cell\ types \times capture\ spots\ in\ spatial\ data)$
$H' \sim Q \times P$	*Where the weights of cell types are computed to best fit H' to minimise the residuals by NNLS regression, Q, P are matrices of cell topic profiles and weights per spot*

Cell co-localisation was determined by the Jaccard similarly score, which compares the similarly and diversity of the sample set based on the number of observations in both sets compared to the total number in both sets: $J(A|B) = |A \cap B|/|A \cup B|$. To see if LPS-tolDC can be identified in the spatial data, Nebulosa[44] was used to derive gene-weighted kernel density estimation.

2.3.11 Statistical analysis

Data was analysed with using Prism (v9, GraphPad) unless otherwise stated. Data is represented as mean +/- standard deviation unless otherwise stated. Comparative tests used included t-test (parametric variables), Mann-Whitney U test (non-parametric variables) for means between two groups, or ANOVA between multiple groups (Dunnett's method for comparing every mean to the control, or Sídák method when multiple comparisons were performed). A $P < 0.05$ was deemed significant.

2.4 Results

2.4.1 Establishing optimal culture conditions to generate ex-vivo tolerogenic dendritic cells

Early optimisation steps for tolerogenic dendritic cell induction were required to determine a stable induction protocol to produce tolerogenic DCs which could resist full maturation in presence of LPS. Vitamin D3 (doses of 10, 20 and 40nM) or IL-10 (doses of 10, 15 and 20 ng/ml) alone were insufficient to induce tolerance. These results did not differ whether C57BL/6 mice imported from Australian BioResources (Garvan) or the Animal Resource Centre (Perth) were sourced to derive bone marrow from. The combination of VitD3 (20nM) and IL-10 (10ng/ml) was required to induce tolDC in our experiments, where tolDC were able to show limited upregulation of MHCII, CD40, CD80, CD86 in response to LPS compared to non-tolerogenic cells (Fig 2.3a). The CD11c cell fraction significantly improved from 68 to 95% of total cells following live^{+}CD11c^{+} microbead sorting (Fig 2.3b).

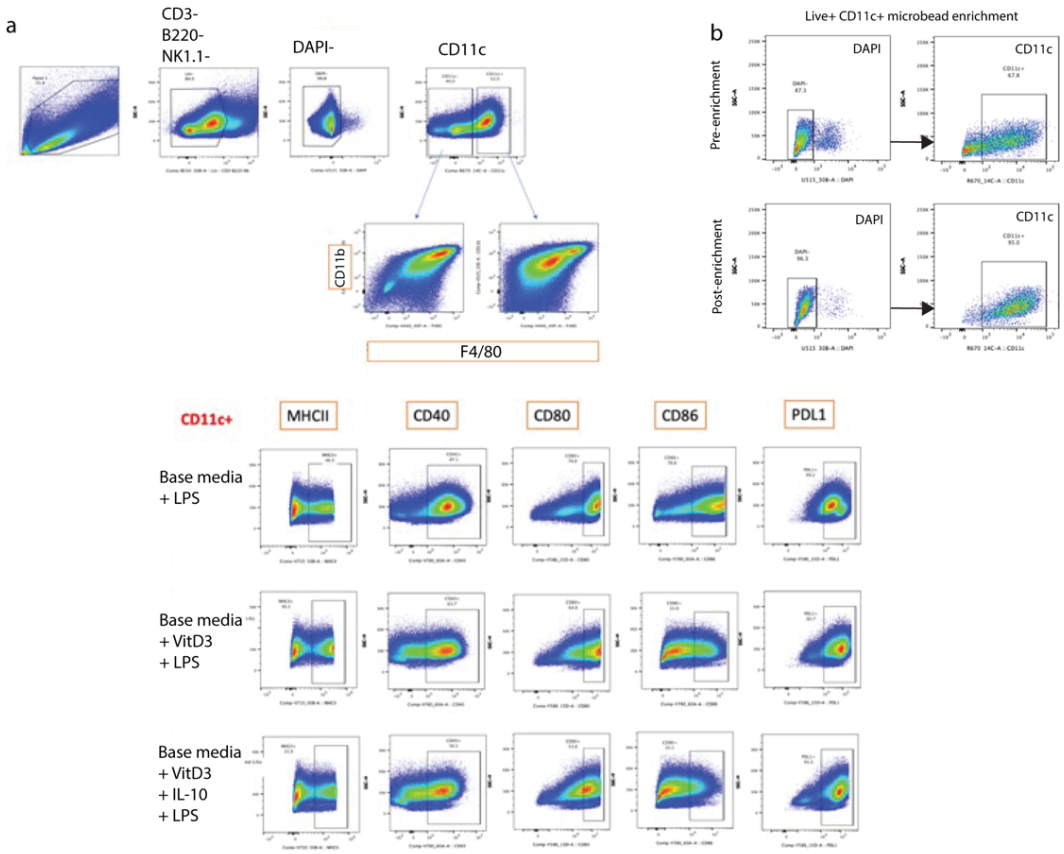

Figure 2.3: ***Representative flow cytometry of VitD3 + IL10 DC optimisation.*** *a) Gating for live+CD3- B220- NK1.1- CD11c+ cells for assessment of surface markers of activation (MHCII, CD40, CD80, CD86, PDL1) following LPS exposure for bone marrow cultures in base media only, base media + vitamin D3 and base media with combination vitamin D3 + IL-10. B) shows the proportion of live+ CD11c+ cells pre- and post- magnetic bead sorting.*

2.4.2 Tolerogenic dendritic cells (tolDC) display a restricted maturation response to LPS.

DCs (live^{+} CD3^{-} B220^{-} NK1.1^{-} CD11c^{+}) were assessed surface markers of activation by MHCII^{+}, CD40^{+}, CD80^{+}, CD86^{+} and PD-L1^{+}. PD-L1^{+} expression for both C57BL6 (Fig 2.4) and BALB/C (Fig 2.5) origin. Expression of MHCII^{+}, CD40^{+}, CD86^{+} and PD-L1^{+} were similar between naïve BMDC (grey, tinted) and tolDC (dotted line) regardless of mouse genotype.

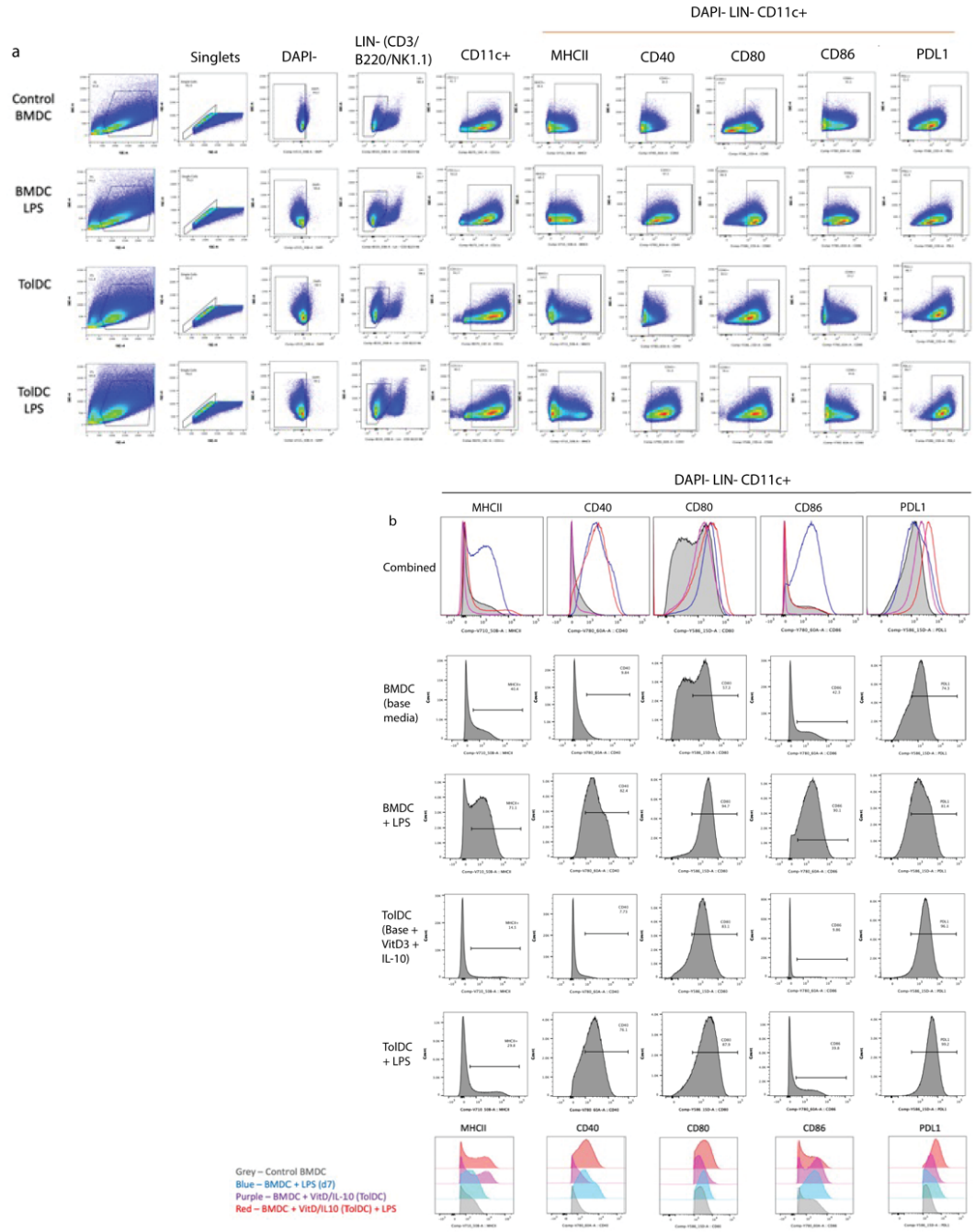

Figure 2.4: ***DC flow characterisation*** *a) for C57BL/6 derived cells, b) focusing on surface markers of activation in the DAPI- LIN- CD11c+ population, MHCII, CD40, CD80, CD86 and PDL1 for the different groups: BMDC (grey, solid tint), tolDC (black, dotted line), LPS-BMDC (blue line) and LPS-tolDC (red line).*

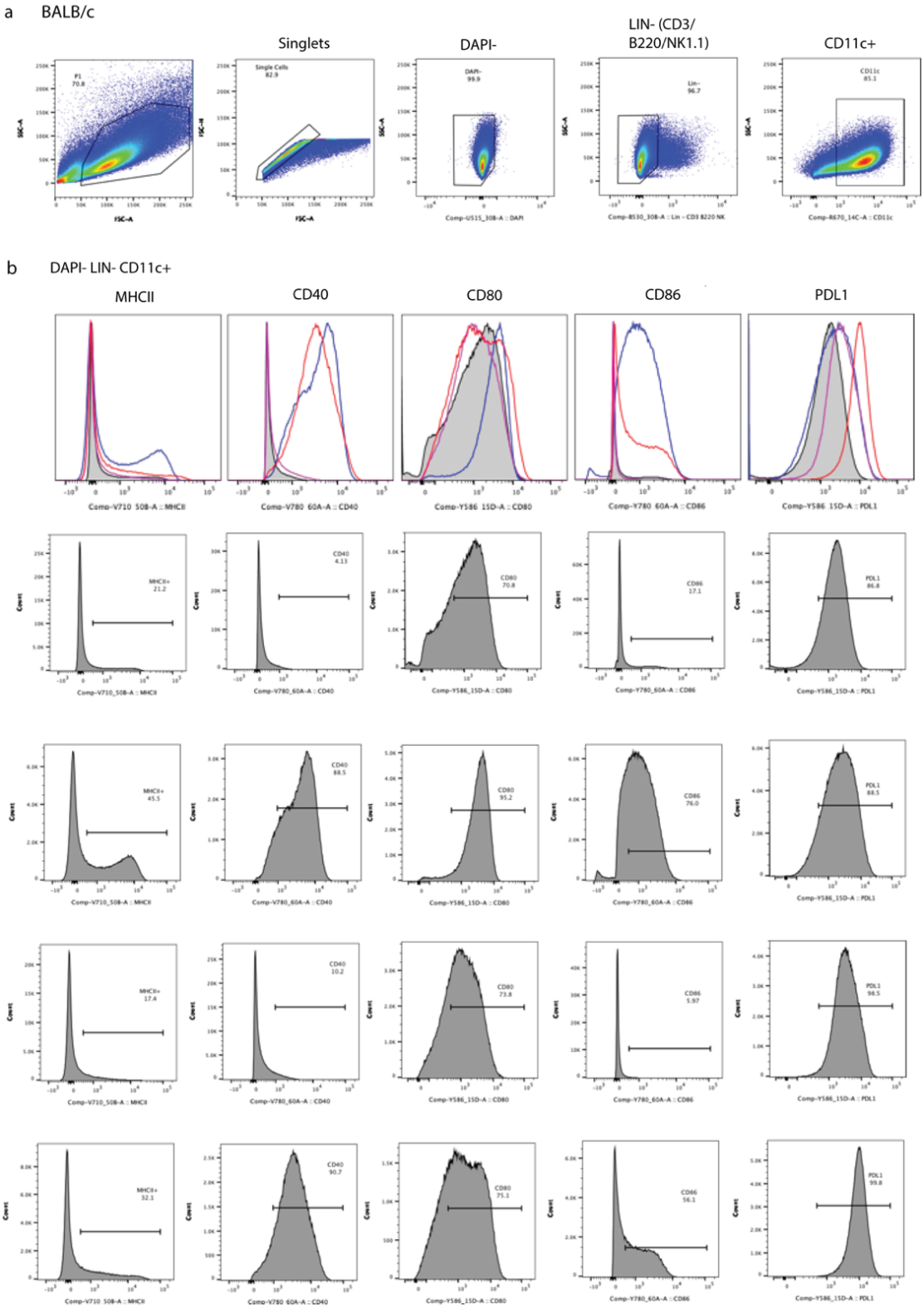

*Figure 2.5:**DC flow characterisation** for a) BALB/c derived cells, b) focusing on surface markers of activation in the DAPI- LIN- CD11c+ population, MHCII, CD40, CD80, CD86 and PDL1 for the different group. Top row is combined plots with BMDC (grey, solid tint), tolDC (black, dotted line), LPS-BMDC (blue line) and LPS-tolDC (red line), 2nd row is BMDC, 3rd row is LPS-BMDC, 4th row is TolDC and 5th (bottom row) is LPS-tolDC.*

These markers were upregulated following LPS stimulation of either BMDC (LPS-BMDC) and tolDC (LPS-tolDC), but MHCII^{+} and CD86^{+} expression was limited in LPS-tolDC compared to LPS-BMDC. Considering the PD-L1:CD86 MFI ratio, a marker of tolerogenicity, was >2.0 for C57BL/6-derived LPS-tolDC and both tolDC groups from BALB/c. (Fig 2.6 and *Supplementary table 2.12*)

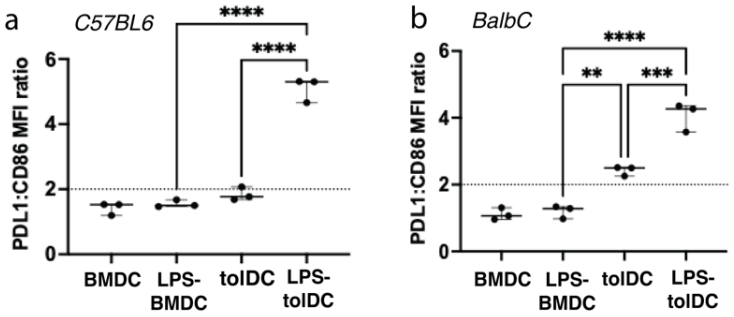

*Figure 2.6: **DC PDL1:CD86 MFI ratio** for a) C57BL6 and b) BALB/c derived cells. Values represented as mean +/- SD and *P < 0.05, **P < 0.01, ***P < 0.001, ****P < 0.0001.*

2.4.3 Both tolDC and LPS-tolDC display anti-inflammatory cytokine profiles

ELISA-based quantification of cell culture supernatant revealed increased anti-inflammatory IL-10 and suppressed pro-inflammatory IL-12p70 by both tolDC groups compared to non-tolerised BMDC despite LPS exposure. (Fig 2.7, *Supplementary table 2.13*) This trend was similar regardless of species background, but it was interesting to note absolute IL-10 and IL-12p70 concentration was markedly higher in BALB/c mice.

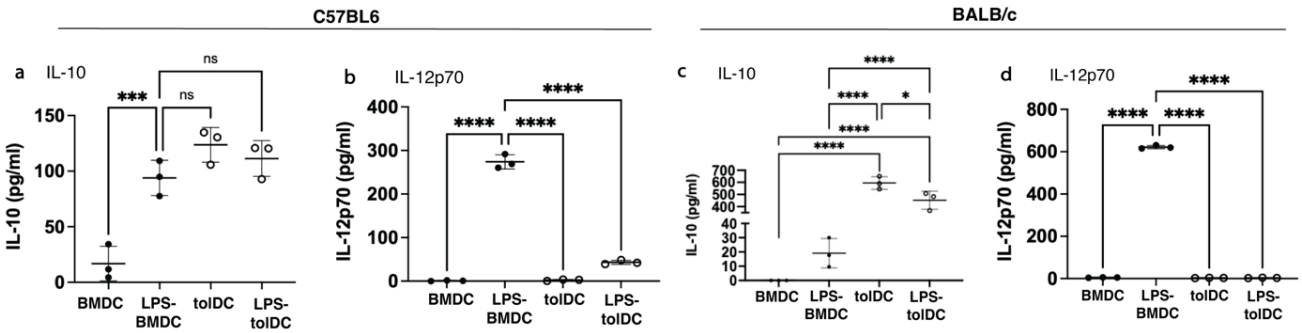

*Figure 2.7: **DC cytokines**. Supernatant from a) C57BL/6 and b) BALB/c derived DC were assessed for IL-10 and IL-12p70 secretion following LPS stimulation. Supernatants were collected on day 8 (with media change to IL-10 free media on day 7 to remove potential contamination from the original TolDC media). Values represented as mean +/- SD and *P < 0.05, **P < 0.01, ***P < 0.001, ****P < 0.0001.*

2.4.4 TolDC and LPS-tolDC limit T-cell proliferation in the mixed lymphocyte reaction

Robust T-cell proliferation was achieved in the presence of T-cell PMA/ionomycin or irradiated-LPS-BMDC (irLPS-BMDC). This response was abrogated with the addition of either tolDC or LPS-tolDC in a 1:1:1 ratio. This suppressive effect was lost when the tolDC to irLPS-BMDC cell ratio was decreased to 1:10, or when only tolDC culture supernatant was added to the mixed lymphocyte reaction. (Fig 2.8)

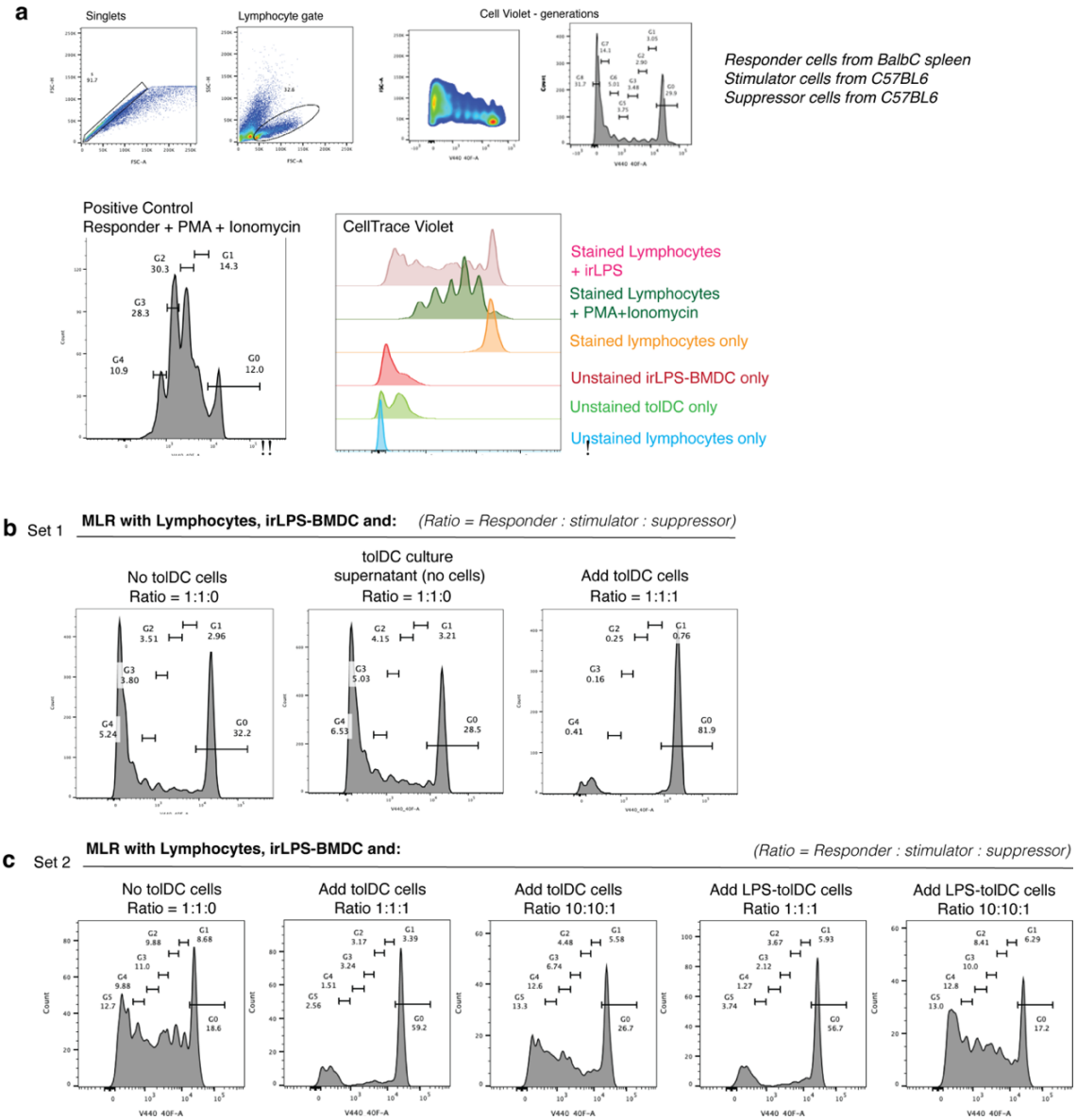

Figure 2.8: ***Representative TolDC MLR.*** *a) gating for mixed lymphocyte reaction testing of tolerogenic DCs and representative flow cytometry profiles of positive controls (lymphocytes (from spleen) incubated with PMA and ionomycin after 4 days), and negative controls and unstained responder (allogeneic lymphocyte), stimulator (irradiated LPS-BMD, irLPS-BMDC) and suppressor (tolDC) cells. B) the first MLR set up demonstrated when splenocytes, irLPS-BMDC were either incubated with control/no addition (left), tolDC culture supernatant (middle) or tolDC cells (right) – where only MLR set up with tolDC suppressors showed reduce proliferative generations.* ***C)*** *the second MLR set up tested with control/no addition (1st panel); tolDC number equal to irLPS-BMDC (2nd panel), tolDC number one-tenth of irLPS-BMDC (3rd panel); and similarly, LPS-tolDC at equal (4th panel) and one-tenth of irLPS-BMDC (5th panel).*

2.4.5 LPS-tolDC limits RTEC inflammation in a contact-independent manner

In vitro experiments showed LPS-tolDC could suppress RTEC inflammation in a contact-independent system following LPS exposure (Fig 2.9a). The kinetics determined over several time points in the first 24-hours shows differences between TNF-α, LCN-2 and KIM-1 expression from cultured renal epithelial cells. The expression of TNFα peaked 2-hours post-LPS exposure, but this rise was suppressed in presence of LPS-tolDC. Kidney injury molecule-1 (KIM-1) peaked at 6-hours and lipocalin-2 (LCN-2) peaked at 24-hours and post LPS but again, their mRNA transcript expression was limited in the presence of LPS-tolDC. (Fig 2.9b-c) Co-culture of RTEC with LPS-tolDC did not change RTEC expression of anti-inflammatory IL-10, TGF-β, IDO-1 and IDO-2 over the 24-hour period. (*Supplementary table 2.14*)

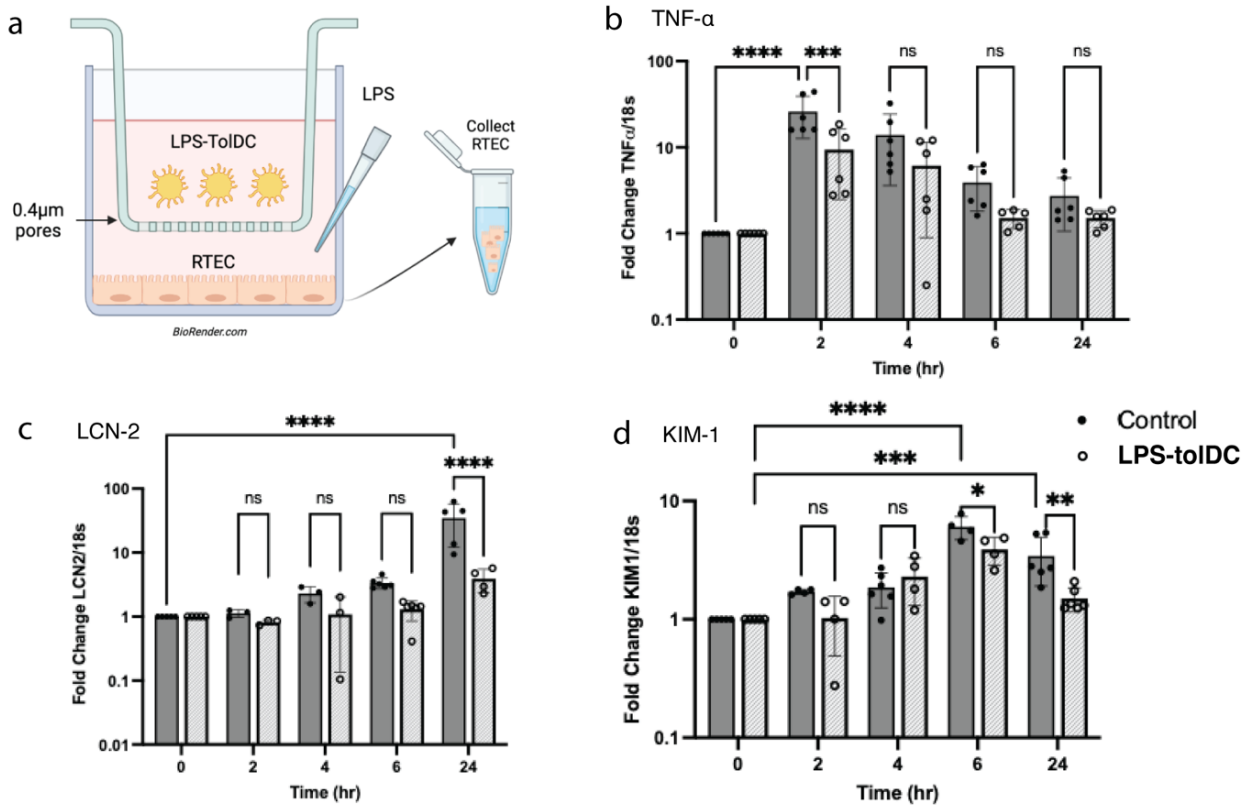

*Figure 2.9: **Contact independent RTEC protection**. a) LPS-tolDC was then co-cultured with renal tubular epithelial cells (RTEC) with the addition of LPS to the RTEC chamber. RTEC cell qPCR results are shown in dark grey data for control (media) versus light grey (LPS-tolDC) content in the insert well. The presence of LPS-tolDC blunted the degree of **b)** TNF-α, **c)** LCN-2 and **d)** KIM-1 increase in RTEC following LPS-exposure, supporting the presence of cell contact-independent mechanism by which LPS-tolDC can protect RTEC from injury. Values represented as mean +/- SD and *P < 0.05, **P < 0.01, ***P < 0.001, ****P < 0.0001.*

2.4.6 Transcriptomics profile of ex-vivo DCs

2.4.6.1 Common DEG for LPS-tolDC compared to other DCs

To determine potential genomic signature(s) that characterise murine TolDC, we performed bulk RNA-sequencing on live^{+}CD11c^{+} enriched BMDC, LPS-BMDC, TolDC, LPS-TolDC cells. Principal component analysis (PCA) showed clear separation of the groups within the first 2 principal components. (Fig 2.10a) Over 4000 differentially expressed genes (DEG) between the groups were identified (Table 2.4), but this was abbreviated to a common set of 69 up- and 121 down-regulated genes found for LPS-TolDC when compared all other groups (Fig 2.10b) which were at least absolute $\log_2$-fold change (LFC) ≥ 1.5. Volcano plots of differentially expressed genes for pairwise analysis is shown in Fig 2.10c.

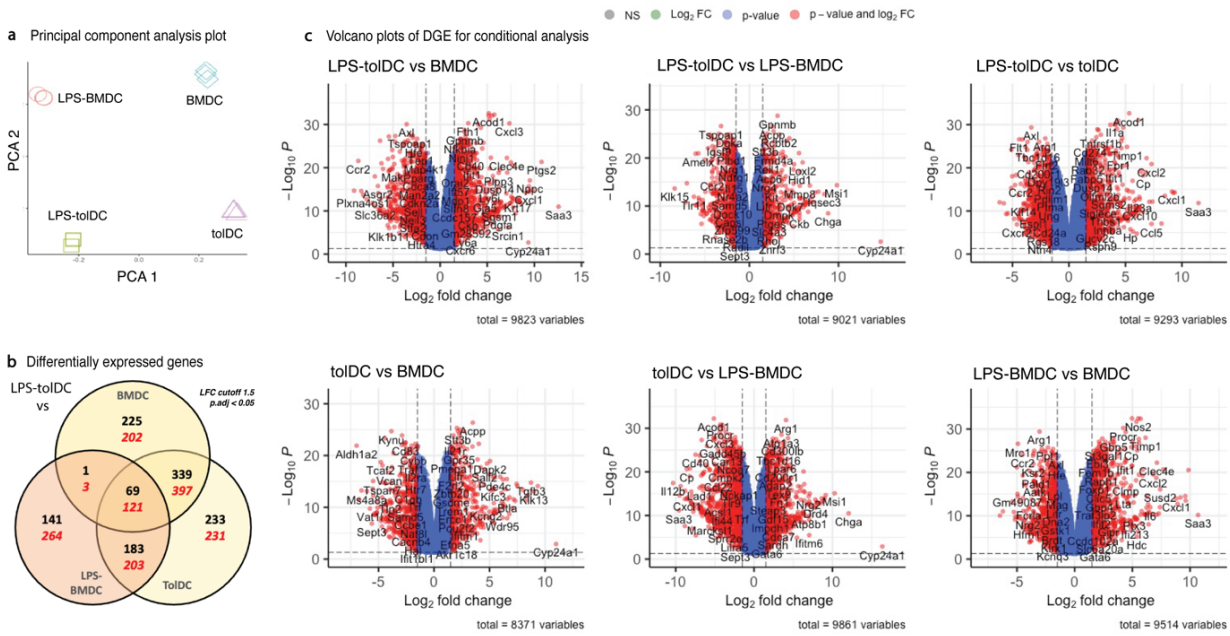

*Figure 2.10: **Bulk RNAseq DC analysis**. a) principal component analysis plot, b) Venn diagram of common differential gene expression (DEG) for LPS-tolDC versus other conditions, and c) volcano plots of DEG for pairwise conditional analysis of live+ CD11c+ DCs.*

*Table 2.4: **Number of differentially expressed genes** stratified by $\log_2$-fold change for adjusted P < 0.05*

	LPS-tolDC vs tolDC	LPS-tolDC vs LPS-BMDC	LPS-tolDC vs BMDC	tolDC vs LPS-BMDC	tolDC vs BMDC	LPS-BMDC vs BMDC
LFC > 0	4551	4553	5005	5083	4281	4745
LFC < 0	4742	4468	4818	4778	4090	4769
LFC > 1.5	634	394	824	878	406	708
LFC < -1.5	723	591	952	1012	500	679
LFC > 2	421	259	537	559	255	436
LFC > -2	458	346	653	688	299	361

2.4.6.2 Genes related to tolerance or vitD3 exposure

Vit D3 induction of tolDC is known to suppressed Muc1 and elevated Map7 expression, which is consistent with our data[45-47]. Both tolDC and LPS-tolDC had elevated *Cyp24a1* (which transcribes 24-hydroxylase to metabolise 1,25-dihydroxyvitamin D3 into the inactive form) and lower *Cyp27a1* expression (which transcribes 25-hydroxylase) in keeping with consistent with a negative feedback response to VitD3 exposure. Surprisingly, *IL-10* was not identified as a DEG in our RNAseq pairwise comparisons nor in published studies into tolDC microarray signatures[45,48], despite elevated IL-10 levels detected in the supernatant.

Ido1, which transcribes indolamine-pyrrole 2,3-dioxygenase was upregulated in LPS-tolDC vs unstimulated tolDC and this acts synergistically within the kynurenine pathway with downregulated *Kmo* (transcribes kynurenine-3-monooxygenase) and *Kynu* (kynureninase) to support tolerance. Furthermore, arginase (*Arg1)*, TGF-β (*Tgfb1*, *Tgfb3)* and haem-oxygenase *(Hmox1)* were all upregulated in both tolDC and LPS-tolDC when compared their respective non tolerogenic counterpart (BMDC and LPS-BMDC respectively), and also when naive tolDC was compared to LPS-tolDC. Both *IL-12a* and *IL-12b* were upregulated in LPS-tolDC (vs tolDC), but downregulated relative to LPS-BMDC. (Table 2.5)

Table 2.5: ***Log$_2$-fold change of select genes relevant to inflammatory or tolerance induction*** *with adj P < 0.05*

	LPS-tolDC vs tolDC		**LPS-tolDC vs LPS-BMDC**		**LPS-tolDC vs BMDC**		**tolDC vs BMDC**	
	LFC	**P adj**	**LFC**	**P adj**	**LFC**	**P adj**	**LFC**	**P adj**
Tgfb1	-0.37	8.36E-9	0.722	1.03E-12	0.13	8.49E-3	0.50	2.35E-10
Tgfb2	1.66	1.00E-4	-0.99	3.11E-4	0.88	6.24E-3	-	>0.05
Tgfb3	-2.83	7.23E-20	6.30	4.51E-12	5.91	9.02E-13	8.74	1.74E-15
Arg1	-2.10	1.58E-27	1.98	9.19E-26	-1.07	5.03E-22	1.02	3.00E-21
Arg2	3.24	3.47E-17	0.95	9.78E-11	3.78	6.51E-18	0.52	0.001
Ido1	1.78	1.24E-05	-	> 0.05	-0.88	8.29E-04	-2.66	3.17E-08
Kmo	-3.40	1.28E-16	-4.18	6.24E-17	-5.34	1.09E-19	-1.93	4.1E-15
Kynu	-0.95	6.94E-11	-4.29	1.86E-21	-4.79	3.68E-23	-3.84	2.91E-21
Hmox1	2.13	1.91E-22	1.35	4.83E-19	3.30	1.55E-25	1.17	3.58E-17
Mucl1	1.19	2.52E-02	-7.02	1.83E-15	-5.56	7.17E-14	-6.76	2.84E-12
Map7	0.36	2.76E-11	2.64	1.66E-11	2.00	5.15E-11	2.17	2.80E-11
Cyp27a1	-1.63	1.42E-04	14.73	2.62E-03	9.36	2.07E-03	10.99	1.22E-03
Cyp24a1	-1.98	2.19E-08	-1.59	1.12E-06	-3.01	4.90E-12	-1.03	2.73E-06
IL12a	5.13	1.35E-15	-0.51	8.70E-08	8.40	4.62E-13	3.28	3.62E-06
IL12b	5.93	2.03E-13	-4.41	1.56E-25	3.28	2.28E-14	-2.65	4.89E-07

2.4.6.3 Unique differentially expressed genes of LPS-tolDC vs all other groups

Dusp14, a member of the dual specificity phosphatases (also known as mitogen-activated protein (MAP) kinase phosphatase, MKP6), syndecan-1 (also known as CD138, *Sdc1*) and TGF-βRIII (*Tgfbr3*) were all commonly upregulated in the LPS-tolDCs compared to all other groups, and these genes have potential immunomodulatory roles. Conversely, *Ccr2, Ccr5, Kmo, Kynu,* and complement related genes *C1qb, C1qc* were downregulated in LPS-tolDC compared to other conditions. (Table 2.6) A select list of immune related differentially expressed genes for LPS-tolDC versus the other DCs is shown in *Supplementary table 2.15.*

Table 2.6: ***Common DEG identified for LPS-tolDC*** *vs BMDC, LPS-BMDC, tolDC (absolute LFC > 1.5 adj P < 0.05)*

Up-regulated			**Down-regulated**				
Cxcl3	Ugt1a10	Iglon5	Axl	Plxna4os1	Ppef2	L1cam	2510009E07Rik
Serpinb2	Zfp469	Shisa2	Flt1	Gm28884	Slc9a3r2	Jaml	Popdc2
Acpp	Slc4a3	Cnksr2	Plet1	Cyp27a1	Cdkl5	Cldn1	Smco3
Blnk	Mt2	Sprr2e	Igsf9	Trim72	Gm5833	Brca1	Klk15
Mmp13	Ltbp2	Dtx1	Tspoap1	Slc4a11	C1qb	Frmd4b	Klk1b27
Pdzk1ip1	Lamc3	R3hcc1	Galnt7	Enpp6	Ms4a3	Kntc1	Col6a3
Loxl2	Slc35g2	Arhgef19	Hs3st3b1	Rnase2b	Lrrc39	Mak	Plppr3
Sdc1	Srcin1	4930539E08Rik	Cass4	Etl4	Fgd2	Siglecf	Gm47507
Nppc	Ednrb	Ptges	Ccr5	Cxcr2	Rrm2	Clec10a	Flt4
Plpp3	Hpcal4	Btn1a1	Ccdc80	Ska1	Hes2	Ptprs	Gm38161
Zfat	Havcr1	Krt17	Rnase6	Nanos1	Kctd12b	Anln	Dmd
Lat	Vegfc	Dok7	Cbfa2t3	Cenpp	Tg	Zfp467	Gm44756
Dusp14	Gm28592	Ccdc155	Dck	Gm33103	Pkd1l2	Sh2d1b1	Hcar1
Rhov	Armcx1	Aebp1	Rasgrp3	Fbxo48	Ogdhl	Abcg3	Slc36a2
Nrg4	Gm26902	Bcr	Clec4b2	C1qc	Rs1	Cracr2b	Scn2b
Armcx4	Cavin3	Foxf2	Pros1	Iigp1	Bex6	Kif14	Lrrc14b
Pdgfb	Rsph9	Cnksr1	Cd300c	Myl10	Trib2	Ppef1	Gm13544
1700012B09Rik	Obsl1	Ntrk1	Ccr2	Gm19510	Clec4b1	Prr5l	Cacnb4
Sytl3	Igfbp7	Uchl1	Cysltr1	Dnase1l3	Bub1	Nlrp10	Ntn4
Gipr	Saa3	Inha	Naaa	Lmo1	Snai3	Gprc5c	Mir9-3hg
Gm15056	Rab33a	Tgfbr3	Tnfaip8l3	4933408N05Rik		Asgr2	Irf6
Gata6	Ugt1a9	Hephl1	Kmo	Gm26588	Gm10384	Phf11a	Elane
Col5a3	Gsta2	Rtn4r	Jup	Ctnnal1	Klk1b11	Tlr11	Plekhg6
			Heg1	Itpka	Ttc39a	B3gnt7	Cend1
			Klk1b11	Gm10384	Ttc39a	Kif4	Ldhc

2.4.6.4 Conserved tolerogenic genes of both LPS-tolDC and tolDC vs LPS-BMDC

To assess conserved genes from tolerogenic induction, DEG lists for LPS-TolDC and TolDC vs LPS-BMDC were used to find genes which were more expressed in TolDC and remained elevated despite LPS exposure (LPS-TolDC) when compared to LPS-BMDC. If a DEG was simultaneously in the same direction in both LPS-TolDC and TolDC compared to the reference LPS-BMDC, it was considered as a conserved tolerogenic DC gene despite changes in expression intensity in response to a TLR4-agonist. The top 100 up and down-regulated DGEs shown in Table 2.7 and heatmap in Fig 2.11. Of interest, both *Arg1* and *Tgfb1* are again upregulated, along with *Trem2* and *Havcr2* (also known as *Tim3*). *Kynu*, fatty acid binding protein 5 (*Fabp5*)

and activation markers *CD40, CD80, CD83* and *CD86* were all downregulated in the common tolDC set. Although MHCII related genes were upregulated (*H2-Aa, H2-Ab1, H2-DMa,* and *H2-DMb1*), these were coupled with reduced expression of other antigen presentation related genes, including basic leucine zipper transcription factor ATF-like 3 (*Batf3*) and adhesion G protein-coupled receptor E5 (*Adgre5*, or CD97).

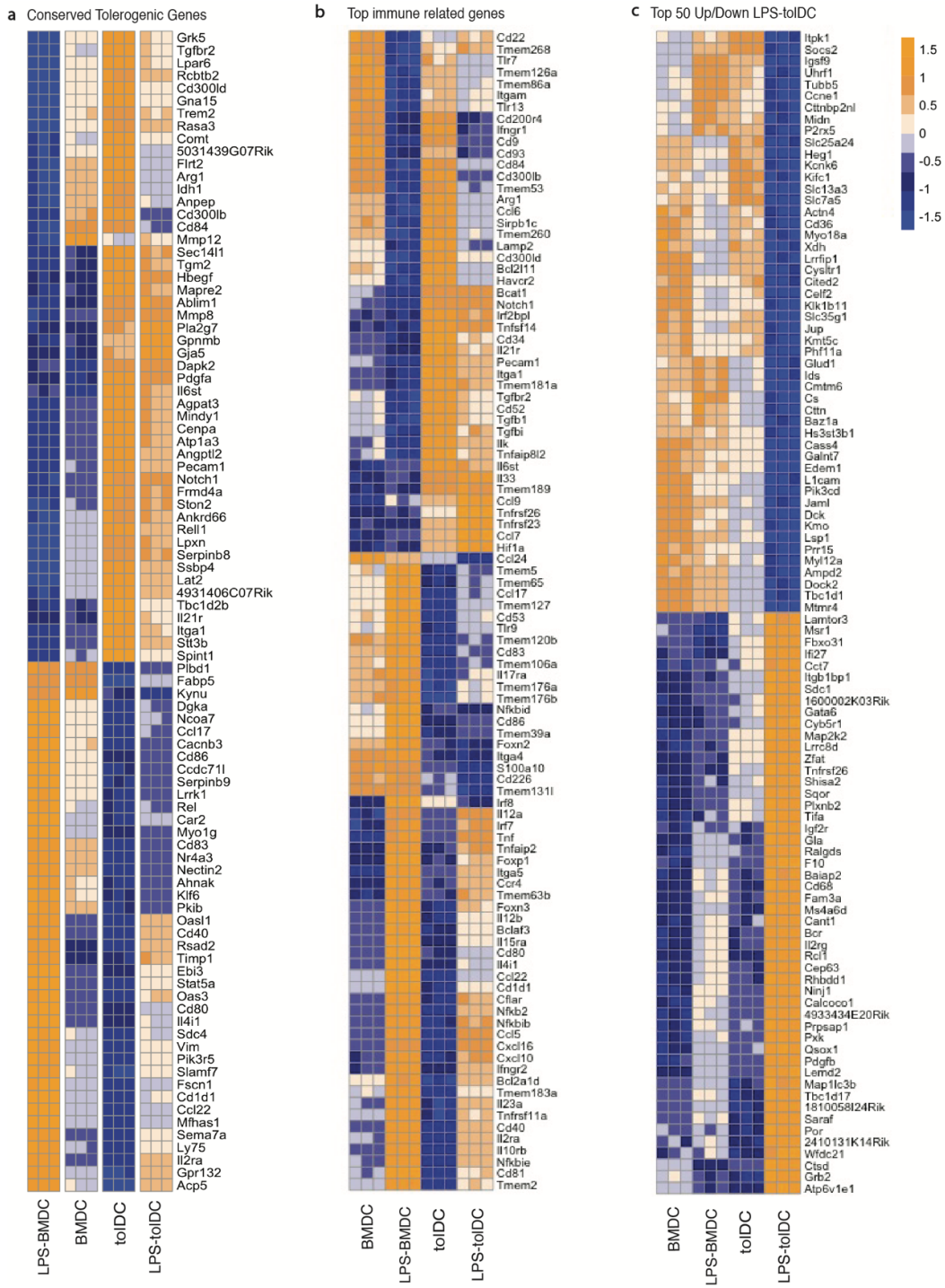

Figure 2.11: ***Heatmap of Z-scores for the different DC groups****. a) Conserved tolerogenic genes of both tolDC and LPS-tolDC compared to LPS-BMDC. b) top immune related genes conserved in both tolDC groups in direction of differential expression compared to LPS-BMDC and c) top 50 upregulated and downregulated genes of LPS-tolDC compared to all other groups.*

GSEA analysis of differentially expressed genes revealed that TolDC of any state (with/without LPS stimulation) showed significantly suppressed inflammatory pathways compared to LPS-BMDC. in particular, this involved the NF-κB and IL-12 signalling pathways for innate immunity and adaptor/lymphocyte mediated immunity given tolDCs can induce T-cell hypo-responsiveness, anergy and induce the development of peripheral Tregs (Fig 2.12)

Table 2.7: **Top 100 conserved tolDC genes** (LPS-tolDC AND tolDC vs LPS-BMDC, *adj P* < 0.05)

LPS-tolDC and **tolDC > LPS-BMDC**				**LPS-tolDC** and **tolDC < LPS-BMDC**			
Hebp1	Ssbp4	Cisd1	Havcr2	Ezr	Fscn1	Gpr132	Plbd1
Gpnmb	Cd84	Smox	Rps12	Cnn3	Pik3r5	Usp22	Cacnb3
Atp1a3	Gdf15	Pecam1	Tgfb1	Fchsd2	Lrrk1	Cdkn2b	Arhgef40
Arg1	Sec14l1	Dapk2	Fblim1	Ttc39c	Ebi3	Glipr2	Ramp3
Rcbtb2	Flrt2	Ms4a7	Zadh2	Trim30d	Adgre5	Cst3	Cytip
Tgm2	Rasa3	Agpat3	Aldh2	Rassf4	Ncoa7	Fabp5	Ahnak
Pla2g7	Angptl2	Spint1	Zranb3	Dennd5a	Cd80	Ccr4	Myo1g
4931406C07Rik	Tbc1d2b	Il6st	Dglucy	Cdkn1a	Slc52a3	Mthfr	Dgka
Stt3b	5031439G07Rik	Serpinb8	Relt	Cmpk2	Slamf7	Lif	Lgals1
Ablim1	Cd300ld	Mindy1	Vwf	Adora2a	Serpinb6b	Rel	Vim
Hbegf	Itsn1	Tmem189	Emilin2	Ankrd33b	Il4i1	Cd1d1	Cp
Mmp8	Grk5	Idh1	Cd34	Rasgrp1	Ccl17	Pop4	Nr4a3
Gja5	Ckb	Gna15	Rps8	Id2	Klf6	Pik3r1	Pmaip1
Trem2	Cd300lb	Ankrd66	Rpl12	Bahd1	Ifi203	Nrg1	Oasl1
Notch1	Btla	Rell1	Pdxk	E2f5	Acp5	Batf3	Nectin2
Tgfbr2	Mapre2	Lpar6	Gtf2i	Rftn1	Car2	Htr7	Cd86
Naip2	Cenpa	Il21r	Nrp1	Mllt6	Mfhas1	Sdc4	Sema7a
Ston2	Rpl32	Lpxn	Dnase2a	Il15ra	Timp1	Oas3	Aldh1a2
Frmd4a	Itgam	Itga1	Pfdn1	Malt1	Ccdc71l	Il2ra	Serpinb9
Nppc	B430306N03Rik	Anpep	Fam43a	Slamf1	Mob3a	Stk39	Stat5a
Comt	Mdh1	Adap2	Tbxas1	Kif21b	Gm13546	Alpk2	Cd40
Mmp12	Mt3	Acss2	Scamp1	Mknk2	Pkib	Ly75	Kynu
Lat2	Atp6v0d2	C77080	Speg	Cpeb2	H2-M2	Ikzf4	Cd83
P4hb	Dnmbp	Pdgfa	Ercc6	Herc6	Rsad2	Ccl22	Serpine1

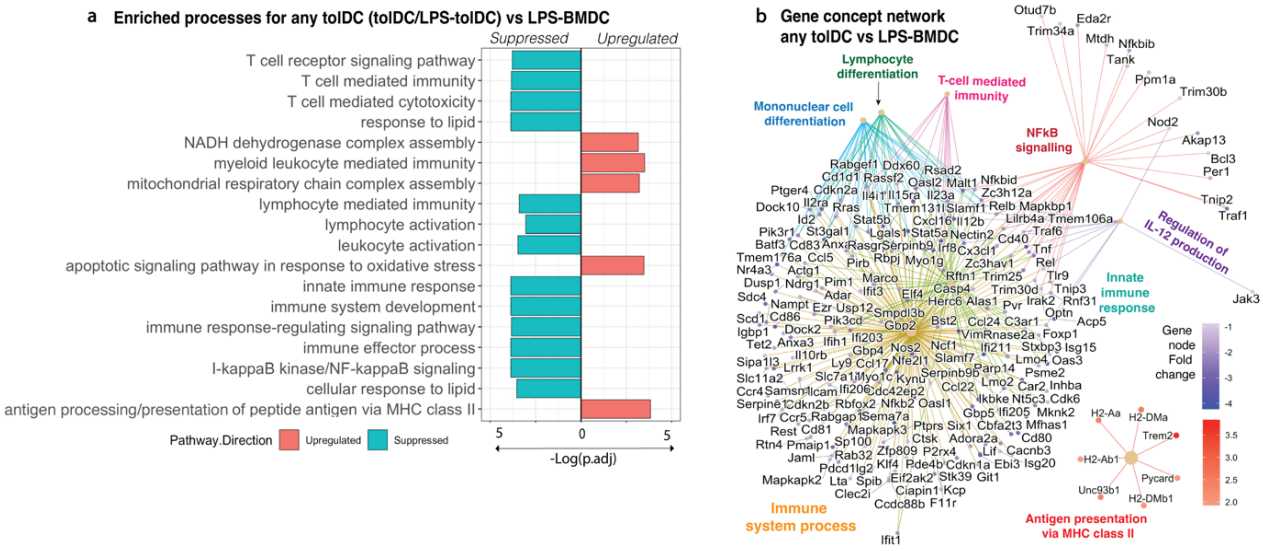

Figure 2.12: ***Conserved tolerogenic genes*** *by extracting common DEGs for tolDC and LPS-tolDC versus LPS-BMDC. a) GSEA enrichment shows suppressed pathways with common DEGs, and b) this was emphasised in the gene concept map for downregulated genes (purple) and upregulated genes (red) in relation to the main immune pathways of common DEGs.*

2.4.6.5 Effect of TLR4 activation on tolDC signatures

Specific comparison of LPS-TolDC vs LPS-BMDC and naïve TolDC vs BMDC revealed many suppressed genes, including *CCL5, CCL12, CCL17, CCL22, CCL24, CX3CL1, Kynu, TLR9, Vim, S100a8, S100a9, CD1d1, CD40, NLRP1b, IL-12b, IL-18, IL-23, Marco and C1qa, C1qb, C1qc,* and shared enriched negative pathway of '*innate immune response'* demonstrating both TolDC and LPS-TolDC involve less innate immune activation compared to their non-tolerogenic counterparts. (Fig 2.13).

Next, LPS-tolDC versus tolDC was performed to determine the features which differentiate these tolerogenic conditions. LPS-tolDC was associated with upregulation innate and adaptive immune related pathways (Fig 2.14a), in particular with TLR signalling due to LPS stimulation, increased NF-κB, immune cell chemotaxis and signalling to T-cell related pathways. Considering this in light of the relative down-regulation of immune pathways seen of LPS-tolDC compared to LPS-BMDC in the previous section, the degree of immune activation was less than that expected from non-tolerogenic DC, our LPS-tolDC has transcriptomic features of an 'alternatively-activated DC' phenotype.

Unique candidate genes which differentiate LPS-tolDC vs tolDC (excluding common DEG LPS-tolDC vs non-tolerogenic candidates) included *Ido1, Clec4a, Stfa3, Ms4a4a, Idi2, Tnf150, Slc28a3, Vcam1, Slc25a29, Dscaml1, Mycl, Fkbp9, Jam2, Fabp5* and *Cd101*. Other genes of interest which differentiated LPS-tolDC to tolDC included upregulation of *Ccr2, Ccr5, Ccr7*, *Cxcr2*, *Cd274* (PDL-1), *TNFAIP3* (A20) and select C-type Lectin-type receptors (*Clec4a, Clec4d, Clec4e*).

Comparing these candidate genes to a recent 39-gene signature for meta-analysis of human alternatively-activated, monocyte-derived tolDC[48] revealed overlap of 27 out of 39 candidate genes to for LPS-tolDC vs tolDC. Further analysis showed 26 of these 27 overlap genes were also found in the LPS-BMDC vs BMDC DEG list and only *Ifi27* (which encodes interferon-α inducible protein 27) remaining as a common gene between the murine and human tolDC which was unrelated to TLR4 activation alone. (Table 2.8)

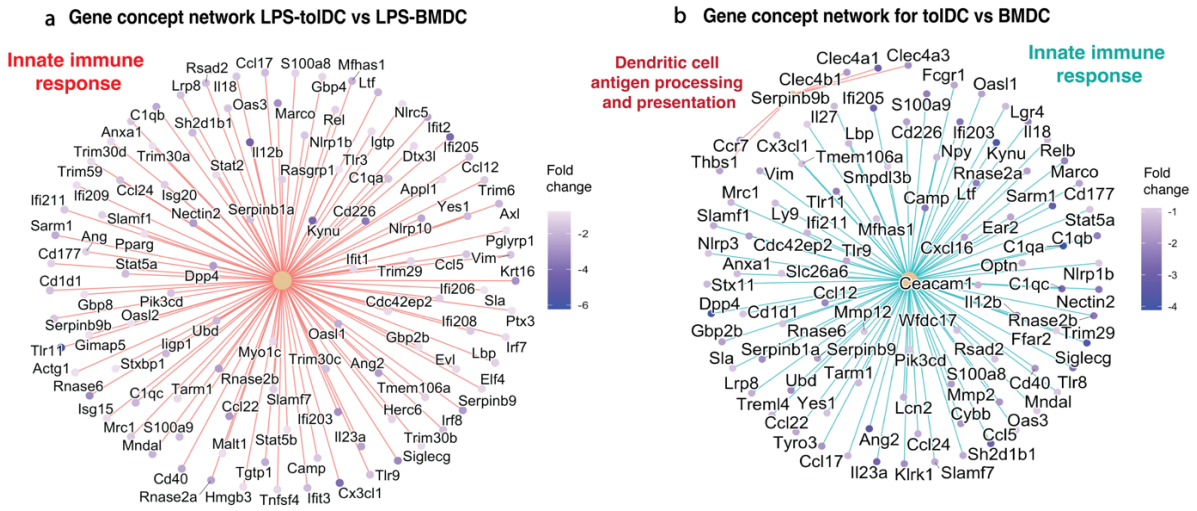

Figure 2.13: ***Effect of LPS exposure****. Gene concept networks for innate immune response showing downregulated genes (purple) for both a) LPS-tolDC vs LPS-BMDC and b) tolDC vs BMDC comparisons*

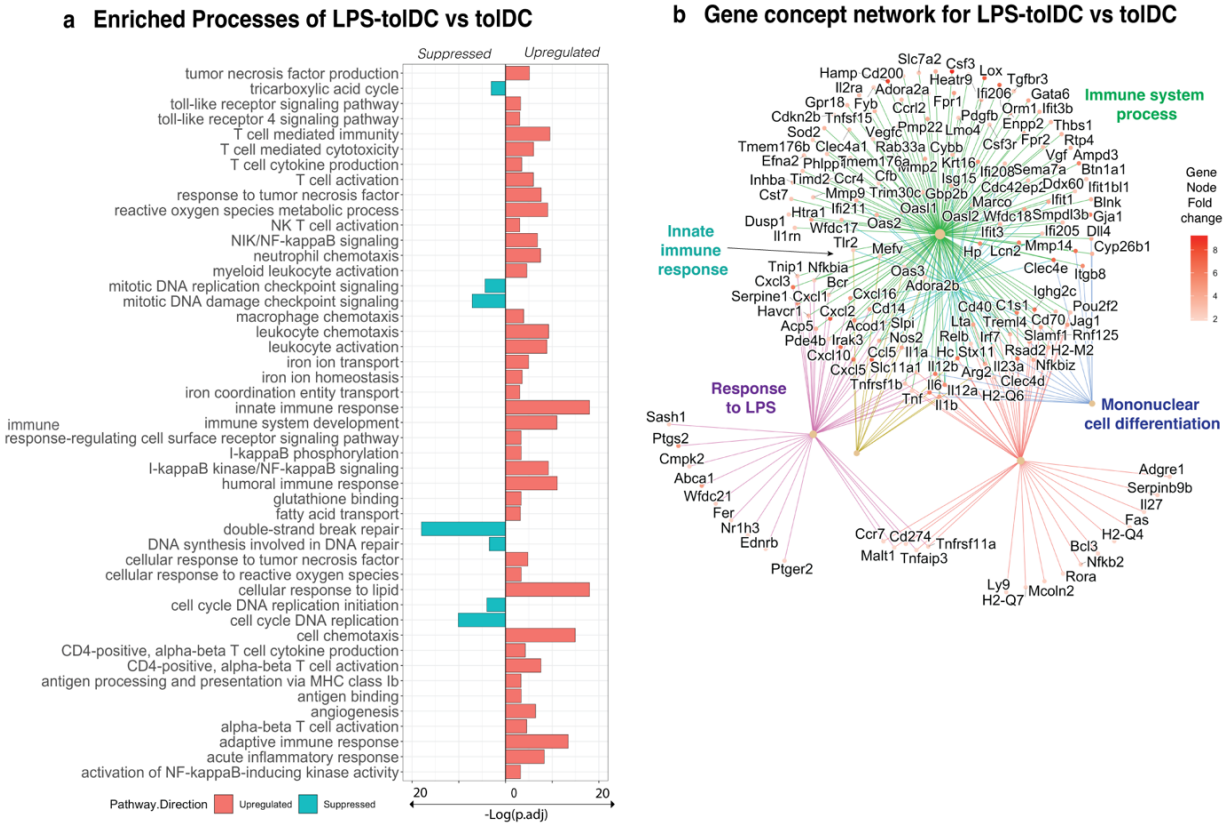

Figure 2.14: ***LPS effect on tolDC****. a) GSEA enrichment and b) gene concept network (upregulation of genes in red) of DEGs identified when LPS-tolDC was compared to tolDC alone, with relative upregulation of immune related pathways*

Table 2.8: ***Overlapping up-regulated genes*** *from our (LPS-tolDC vs tolDC) DEG vs meta-analysis AADC signature*

Gene symbol	Log_2FC of LPS-tolDC vs tolDC	Adj p value	Overlap with LPS-BMDC vs BMDC DEG
Birc3	1.20	3.70E-103	*Yes*
Btg3	0.80	0.041	*Yes*
Cd38	1.50	2.70E-94	*Yes*
Cd80	0.48	2.70E-20	*Yes*
Cd274	1.89	3.77E-26	*Yes*
Ccl5	7.31	1.02E-07	*Yes*
Cfb	7.11	7.72E-13	*Yes*
Cyp27b1	0.23	1.18E-10	*Yes*
Ebi3	1.11	1.9.E-144	*Yes*
Gch1	0.99	5.88E-12	*Yes*
Gramd1a	1.05	1.57E-78	*Yes*
Ifi27	0.67	1.93E-25	*No*
Ila5ra	1.00	2.86E-47	*Yes*
Il1b	4.36	1.21E-31	*Yes*
Il2ra	3.13	3.39E-24	*Yes*
Nfkb1	0.87	7.22E-65	*Yes*
Nfkb2	2.23	3.34E-24	*Yes*
Nub1	0.74	4.38E-58	*Yes*
Mcoln2	2.11	2.69E-22	*Yes*
Ptger4	0.84	3.38E-13	*Yes*
Rftn1	0.63	2.87E-18	*Yes*
Ripk2	0.21	0.001	*Yes*
Rfn19b	1.67	1.26E-20	*Yes*
Slamf7	1.72	1.00E-23	*Yes*
Tdrd7	0.80	1.46E-32	*Yes*
Tnfaip3	1.86	1.15E-23	*Yes*
Traf1	4.64	6.97E-27	*Yes*

2.4.7 Adoptive transfer of LPS-TolDC and Allo-TolDC protects against renal IRI

C56BL/6 mice undergoing renal IRI received either PBS (control), syngeneic (C57BL/6) or allogeneic (BALB/c) Allo-tolDC-based adoptive cell therapy. Mice which received LPS-tolDC or Allo-tolDC had lower renal injury following IRI based on lower serum creatinine, lower semi-quantitative injury scores based on H&E morphology and reduce cell death detected by TUNEL +ve staining. Timing of administration on the day prior or the day of injury did not appear influence outcomes. (Fig 2.15, *Supplementary table 2.16 and table 2.17*).

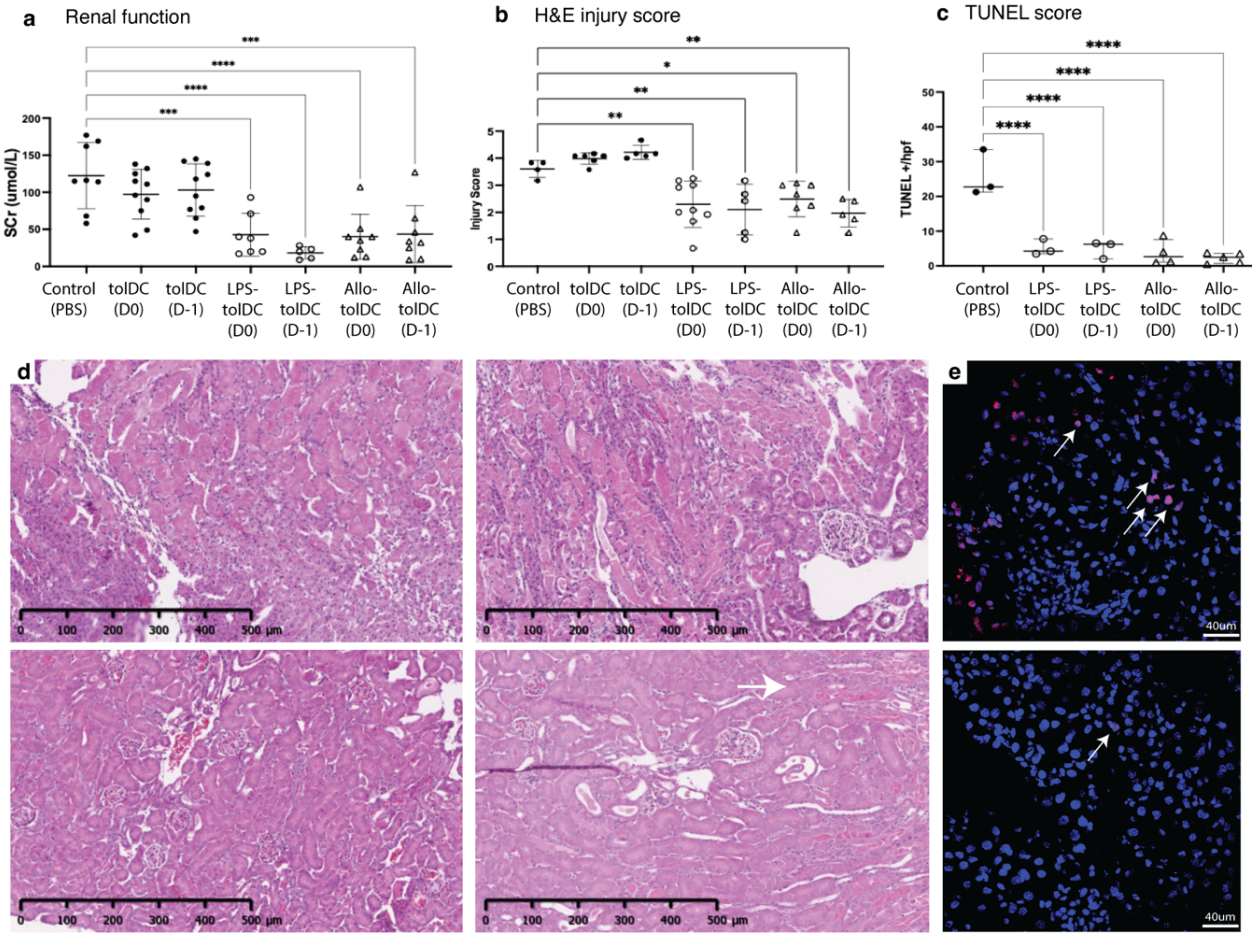

*Figure 2.15: **Adoptive transfer of tolDC protects against severe renal ischemia-reperfusion injury (IRI)**. **a)** C57BL6 derived tolDC and LPS-tolDC, and Allo-tolDC (tolDC from BALB/c) were enriched for live, CD11c+ cells by microbead magnetic columns prior to adoptive transfer into mice by the retro-orbital venous plexus. Either 1x10^6 cells in 150µL PBS, or PBS alone were administered at the time points for comparison (day prior (D-1) or day of surgery (D0)). Mice were recovered following 20 minutes of bilateral clamping of the renal pedicles with core temperature maintained between 35.6 – 36℃ to cause ischemia reperfusion injury. Samples collected 24-hours later demonstrate protection from severe acute kidney injury based on **b)** renal function (as a function of serum creatinine, µmol/L) and **c)** the semi-quantitative H&E kidney injury scores were all lower in LPS-tolDC or Allo-tolDC compared to control PBS. There was protection for mice treated with tolDC compared to controls. The degree of cell death quantified by d) TUNEL scores was also lower in LPS-tolDC and Allo-tolDC compared to controls. Representative images of renal tissue including **e)** haematoxylin & eosin stains (20x magnification) for control (top 2 panels), Allo-tolDC (bottom, left) and LPS-tolDC (bottom, right) treated mice, and **f)** TUNEL stains (40x magnification) for control (top) and LPS-tolDC (bottom) mice. Values represented as mean +/- SD and *P < 0.05, **P < 0.01, ***P < 0.001, ****P < 0.0001*

2.4.8 LPS-TolDC track to the injured kidney compared to unstimulated TolDCs

We next sought to determine if adoptively transferred cells could be found in the injured kidney, which would support a location-dependent cytoprotective effect. The intra-renal $CD45^+$ absolute cell count was similar between groups, however a greater percentage (and absolute number) of LPS-tolDC were found in the kidney post-IRI compared to unstimulated tolDC (Fig 2.16, *Supplementary table 2.18)*.

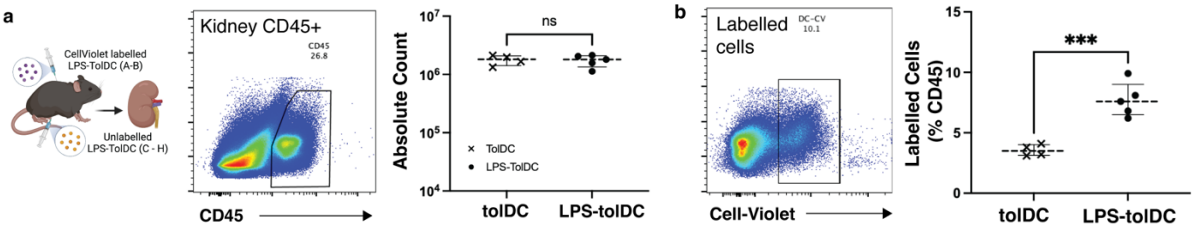

Figure 2.16: ***Intra renal cell tracking*** *in mice 24-hours post IRI. Kidney a) CD45+ cells and b) cell violet (tracer) gating and results shown.*

2.4.9 Myeloid subsets in kidney immune profiling following IRI

Inflammatory cell influx and perturbed immunological homeostasis is a hallmark of renal IRI and tolDC imparts a robust anti-inflammatory stimulus that mitigates inflammation through a by-stander effect.[49,50] We explored differences in immune populations following renal IRI with LPS-tolDC vs PBS. (Fig 2.17)

There was no significant difference in the absolute $CD45^+$, $CD11b^+$ or $CD3^+$ cell counts (Fig 2.18a, *Supplementary table 2.19*), or relative proportion of $Ly6G^+$ neutrophils and $CD3^-B220^-NK1.1^-Ly6G^-$ myeloid cells between control and treatment groups (Fig 2.18b). The $CD11b^+F4/80^+$ myeloid population displayed three distinct subsets, with similar $CD11b^{hi}F4/80^{lo}$, higher $CD11b^{hi}F4/80^{int}$ and lower $CD11b^{lo}F4/80^{hi}$ cells in the LPS-tolDC group (Figure 2.18c, *Supplementary table 2.20*).

These subsets demonstrated distinct co-stimulatory molecule profiles (Fig 2.18d-f). $CD11b^{hi}F4/80^{lo}$ and $CD11b^{lo}F4/80^{hi}$ subsets were $Ly6C^{lo}$ with similar CD40/CD86/PD-L1 expression. More the $CD11b^{hi}F4/80^{int}$ cells was seen in LPS-tolDC and likely represents recruited, activated monocyte-derived myeloid subset characterised by high Ly6C, CD40, CD80, CD86 and PD-L1 expression (Fig 2.18e).

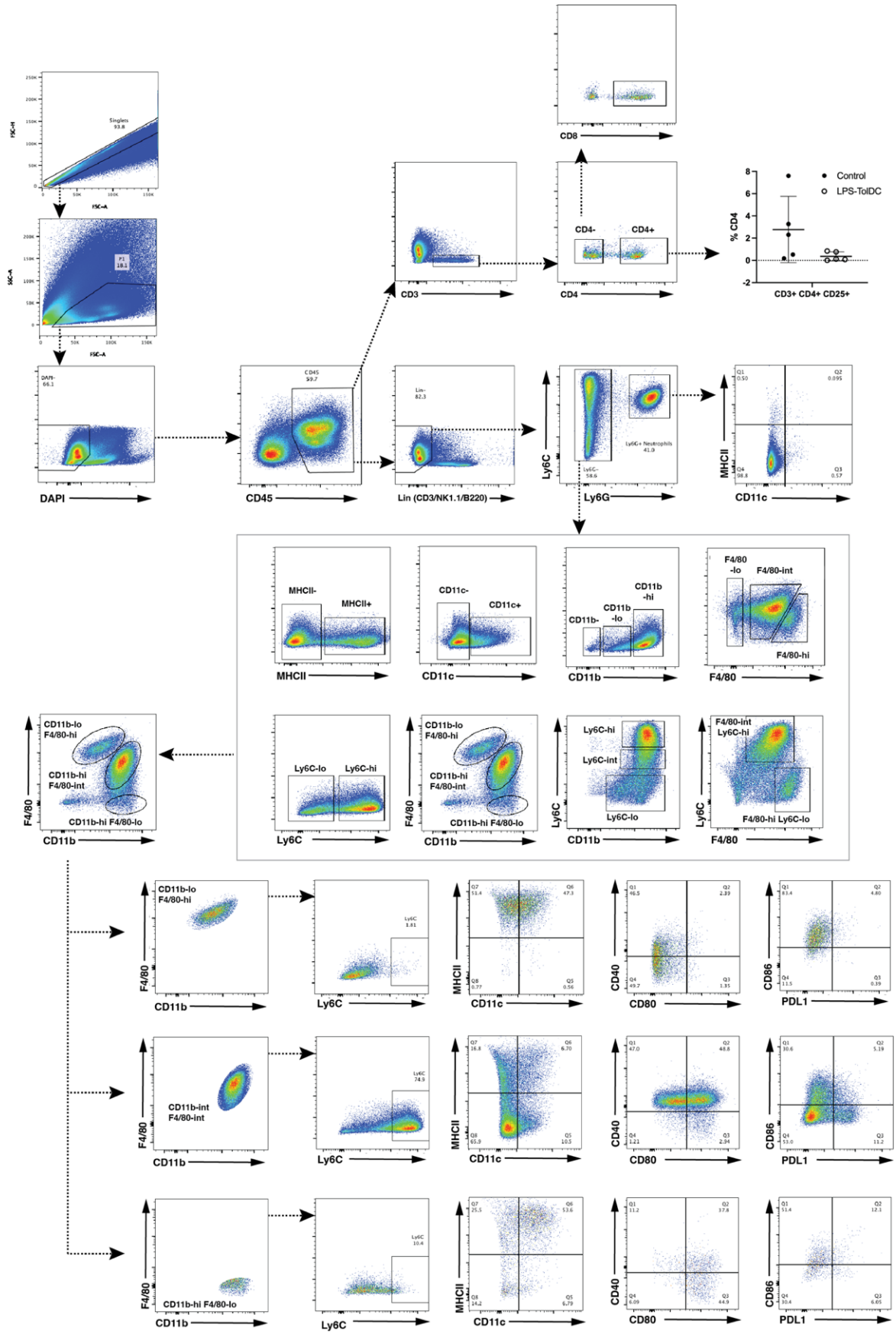

Figure 2.17: ***Overview of kidney gating strategy*** *applied for flow cytometry analysis of kidney homogenates post IRI*

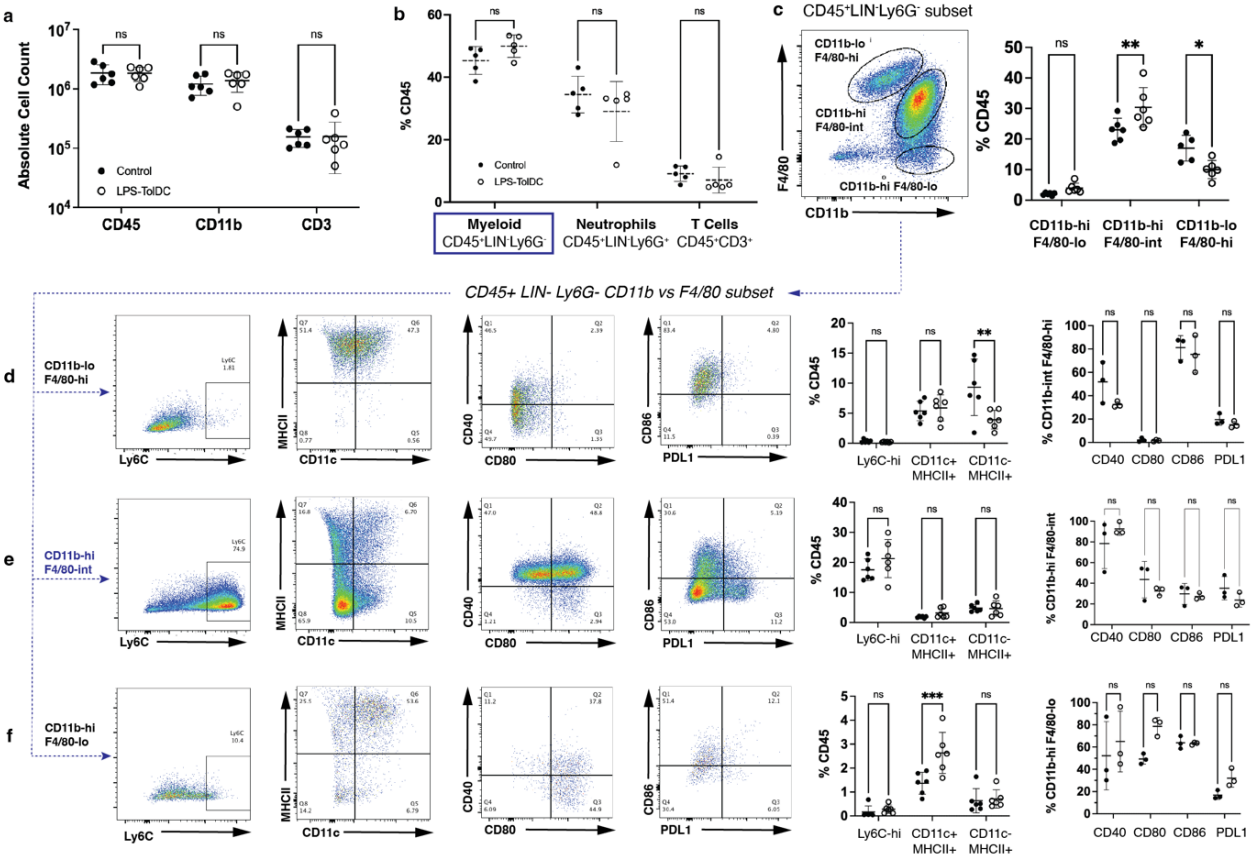

Figure 2.18: ***Flow analysis of renal immune cells of control vs LPS-tolDC treated mice****. Single cell suspension of kidneys 24-hours post IRI showed no statistical difference between control and LPS-tolDC treated mice with respect to* ***a)*** *the absolute CD45$^+$, CD11b$^+$ and CD3$^+$ cell counts or* ***b)*** *proportion of CD45% for CD45$^+$CD3$^+$ lymphocytes and CD45$^+$Lin$^-$Ly6G$^-$ myeloid and CD45$^+$Lin$^-$Ly6G$^+$ neutrophils.* ***c)*** *There were distinct subsets of CD45$^+$Lin$^-$Ly6G$^-$ cells when gated for CD11b vs F4/80, with relatively greater amounts of CD11^{hi}F4/80^{int} and less CD11b^{lo}F4/80^{hi} (%CD45) in LPS-tolDC treated mice. These CD11b vs F4/80 subsets were further characterised in* ***d-f)*** *based on Ly6C, CD11c, MHCII, CD40, CD80, CD86, PDL1 expression. Cells within the* ***d)*** *CD11b^{lo}F4/80^{hi} group had similar surface marker expression with the exception of lower MHCII+ expression if derived from LPS-tolDC mice.* ***e)*** *CD11^{hi}F4/80^{int} cells were similar in terms of high Ly6C, PDL1 and markers of activation whether derived from control or treatment groups. Lin: CD3/B220/NK1.1. Values represented as mean +/- SD and *P < 0.05, **P < 0.01, ***P < 0.001, ****P < 0.0001.*

2.4.10 TolDC therapy remains protective despite recipient myeloid cell depletion

The original dogma of tolDC treatment in transplantation assumed immunosuppression by direct action on T-cells *in vivo*, but this was debunked following evidence that Allo-tolDC are the antigenic source for recipient DC[22], and the latter compartment must remain functional for adequate antigen presentation. Although the timeframe for our adoptive transfer experiments was considerably shorter, we used liposomal clodronate to determine if recipient DC processing of apoptotic cells was responsible for renoprotection. Treatment with clodronate alone reduced injury from renal IRI in the absence of tolDC (Fig2.19a, *Supplementary table 2.21*), so the model was readjusted to provide a greater injury stimulus. Allo-tolDC provided renal protection despite clodronate, with a reduction in serum creatinine (Fig 2.19b) and reduced injury scores (Fig 2.19c-e), indicating that intact/live cells were likely mediating the renoprotective effect.

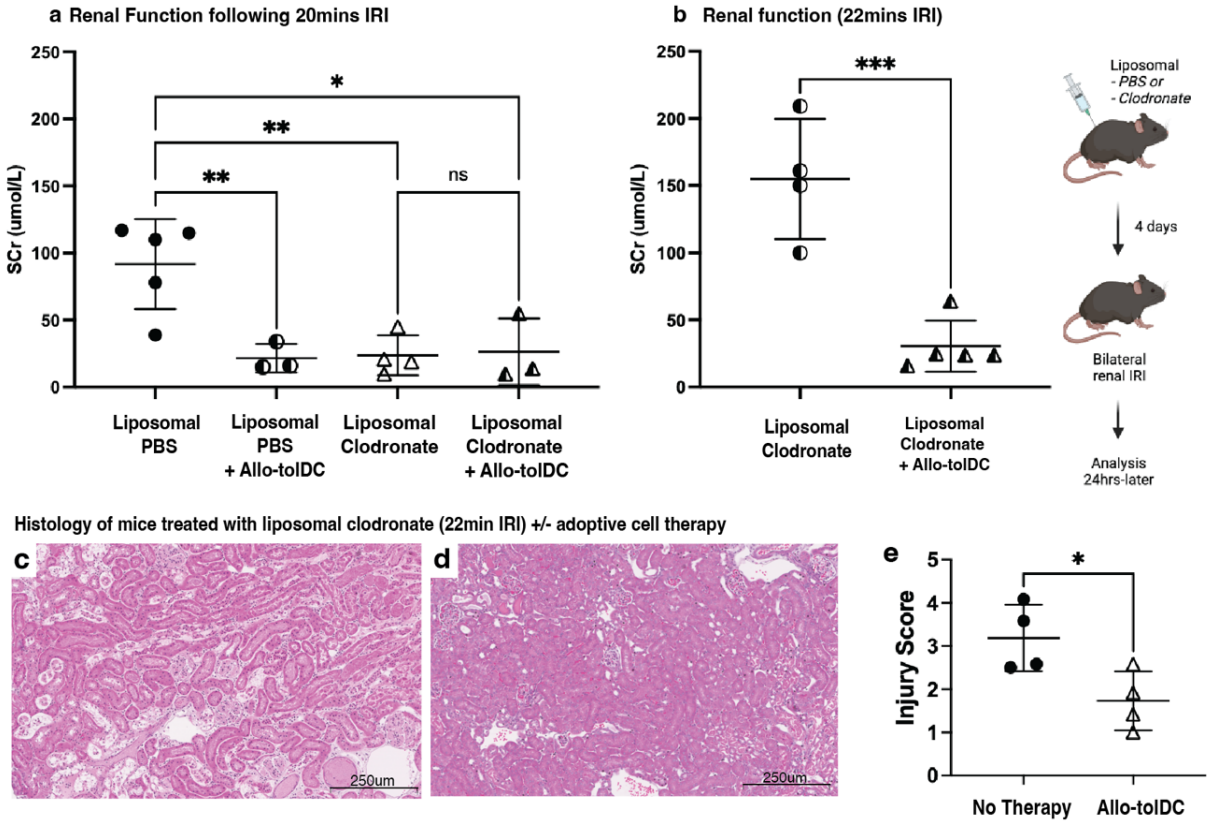

Figure 2.19: ***tolDCs retain their protective function in clodronate treated mice****. **a)** Mice treated with liposomal clodronate were protected against acute kidney injury (AKI) at baseline following 20 minutes of bilateral renal ischemia reperfusion injury (IRI), regardless of whether DCs were administered. **b)** Increasing the injury time to 22 minutes increased baseline injury with liposomal clodronate and revealed the addition of Allo-tolDC to these mice was still able to provide protection by lower serum creatinine levels. Representative renal H&E images at 20x magnification are shown in **c)** for liposomal clodronate and **d)** clodronate + Allo-tolDC and **e)** the injury scores were lower in the group with cell treatment, in keeping with serum creatinine results. Values represented as mean +/- SD and *P < 0.05, **P < 0.01, ***P < 0.001, ****P < 0.0001.*

2.4.11 Cell therapy reduced overall injury and inflammatory markers following renal IRI

RNA expression of pro-inflammatory cytokines TNFα, IL-1β, and IL-6 were markedly lower in LPS-tolDC and Allo-tolDC treated kidneys compared to controls. Similarly, the biomarker of tubular injury, kidney injury molecule-1 (Kim-1, also known as Havcr1) was lower in the LPS-tolDC and Allo-tolDC treated mice ($P < 0.001$) CCL2, SOD1 and iNOS were lower in treatment groups, but Cxcl2 and SOD3 were not significantly different between the groups. (Fig 2.20 and *Supplementary table 2.22*).

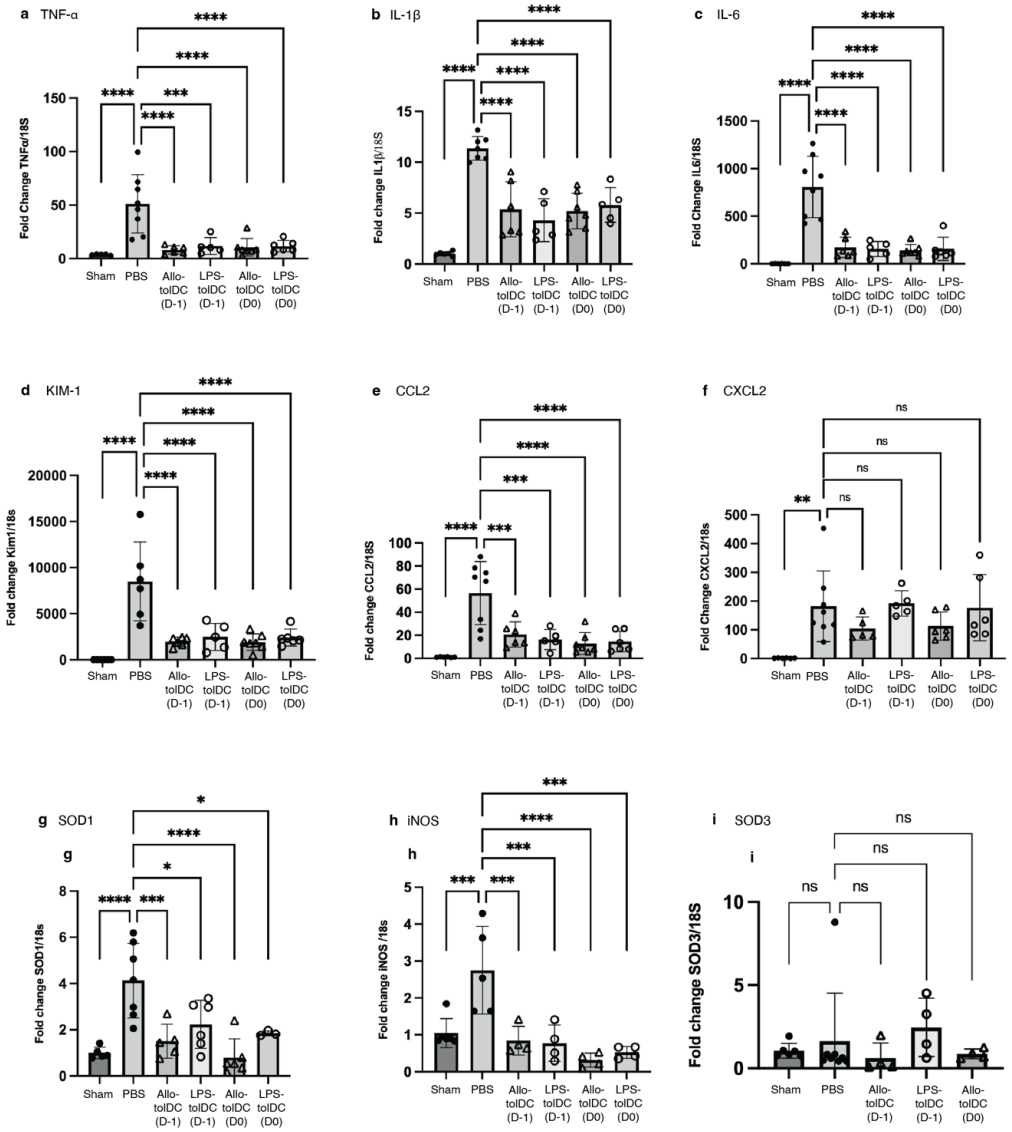

Figure 2.20: ***Kidney mRNA expression of pro-inflammatory markers*** *was lower in the treatment groups at 24-hours post injury. Fold change of the target gene with respect of 18S from kidney tissues of sham, control (PBS), LPS-tolDC and Allo-tolDC mice is shown for a) tumour necrosis factor (TNF-α), b) interleukin 1-beta (IL-1β), c) interleukin 6 (IL-6), d) kidney injury molecule (KIM-1, also known as TIM-1 and HAVCR-1), e) C-C Motif chemokine ligand 2 (CCL2, also known as MCP-1), f) C-X-C motif ligand 2 (CXCL2), g) superoxide dismutase 1 (SOD1), h) inducible nitric oxide synthase (iNOS,) i) superoxide dismutase 3 (SOD3). Values represented as mean +/- SD and *P < 0.05, **P < 0.01, ***P < 0.001, ****P < 0.0001.*

2.4.12 Spatial transcriptomic profiling of kidneys post IRI

Six murine kidneys were used to generate spatial transcriptomics data using 10x Visium, with 2 mice from each of the PBS, syngeneic tolDC and syngeneic LPS-tolDC used. There was similar distribution of total counts and unique genes for each of the 6 kidney samples and spots with < 100 transcript counts or < 200 unique genes were excluded from further analysis. Similar results were seen for percentage of mitochondrial and ribosomal genes and spots with > 30% mitochondrial genes were excluded to maximise analysis of viable cells (Fig 2.21). A total of 11,685 10x Visium spots for analysis remained after QC, filtering, normalisation, and batch correction, with 3840, 3330 and 5515 spots from the PBS, tolDC and LPS-tolDC treated kidneys respectively.

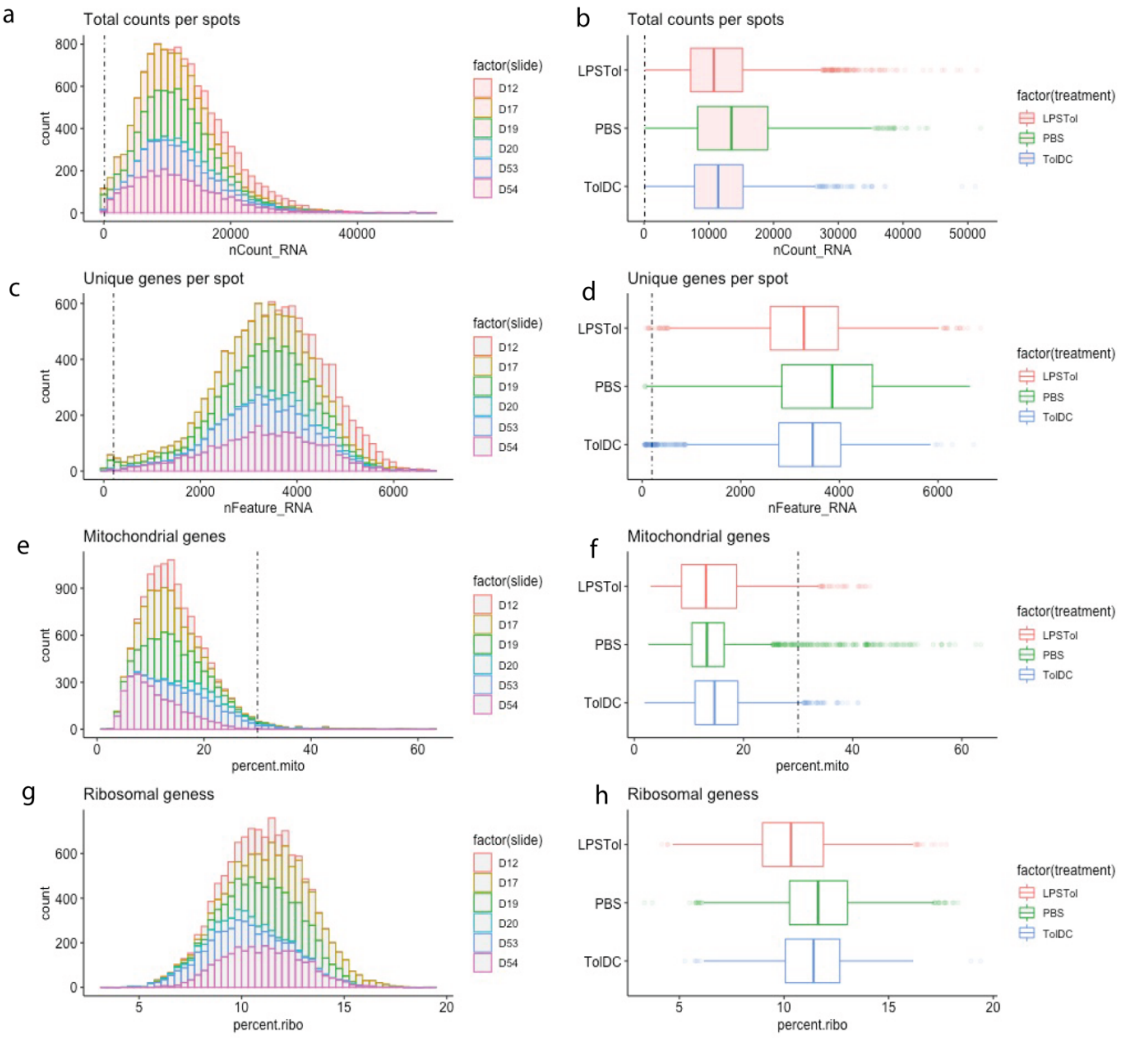

Figure 2.21: ***Basic quality control graphs of spatial transcriptomics data*** *before filtering (counts > 100, features > 200 and % mitochondrial genes < 30%) of a-b) total counts per spot, c-d) unique genes per spot (features), e-f) % mitochondrial genes and g-h) % ribosomal genes of spatial data acquired using 10x Visium for each slide and treatment group.*

2.4.12.1 Cell composition by deconvolution

Deconvolution to determine the relative cell composition of each 55µm spot in our kidneys (Fig 2.22a) was achieved using a public post unilateral IRI scRNA-seq dataset (GSE139506)[51]. For simplicity, principal and intercalated cells were combined into a 'collecting duct' subset with reasonable topic profile separation and marker gene overlap between cell types. (Fig 2.22b-c).

Pie charts of cell composition per spot are shown in Fig 2.22d. Other mice kidney datasets were explored, including, a non-injury (GSE107585)[52] set and a post-IRI snRNA-seq (GSE139107)[53] data set, but the suitability of these were limited by poor marker derivation when an AUC threshold of 0.8 was applied. Given these findings, scRNA-seq and/or snRNA-seq subsets were not combined computationally, nor were different time points for this particular analysis given our samples were all from the same post injury time point. Overall, the relative proportion of cell types per treatment group were similar between the treatment groups, with slightly more injured proximal tubular cells in tolDC treated kidneys (Fig 2.24a, Table 2.9).

Knowing that both PBS and tolDC treatment groups did not protect against severe IRI, differential expression was performed comparing LPS-tolDC vs PBS/tolDC treated kidneys and GSEA showed enrichment for spots with greater metabolic activity (lipid/fatty acid metabolic processes) and both oxidoreductase and monooxygenase activity, with relative suppression of cell death, cell cycle and angiogenesis. (Fig 2.23b). Both normal and injured proximal tubular cells, and loop of Henle/convoluted tubular cells were most likely to co-localise within a 55µm spot in all treatment groups, which is expected given the known structural relations of the nephron. (Fig 2.23c)

Table 2.9: Relative cell composition by treatment group following deconvolution of spatial data (% total)

Relative composition (%)	PBS	tolDC	LPSTol
Injured Proximal Tubule	19.16	23.90	19.16
Proximal Tubule	19.98	20.56	19.98
Mixed Identity	2.21	4.99	2.21
Loop of Henle/DCT	16.77	19.13	16.77
Collecting Duct	11.56	11.02	11.56
Stromal	11.76	7.95	11.76
Podocyte	1.39	1.05	1.39
Endothelial	7.93	3.80	7.93
Macrophage	7.69	7.08	7.69
T-cell	1.56	0.50	1.56

Regression-based deconvolution to GSE139506 reference set

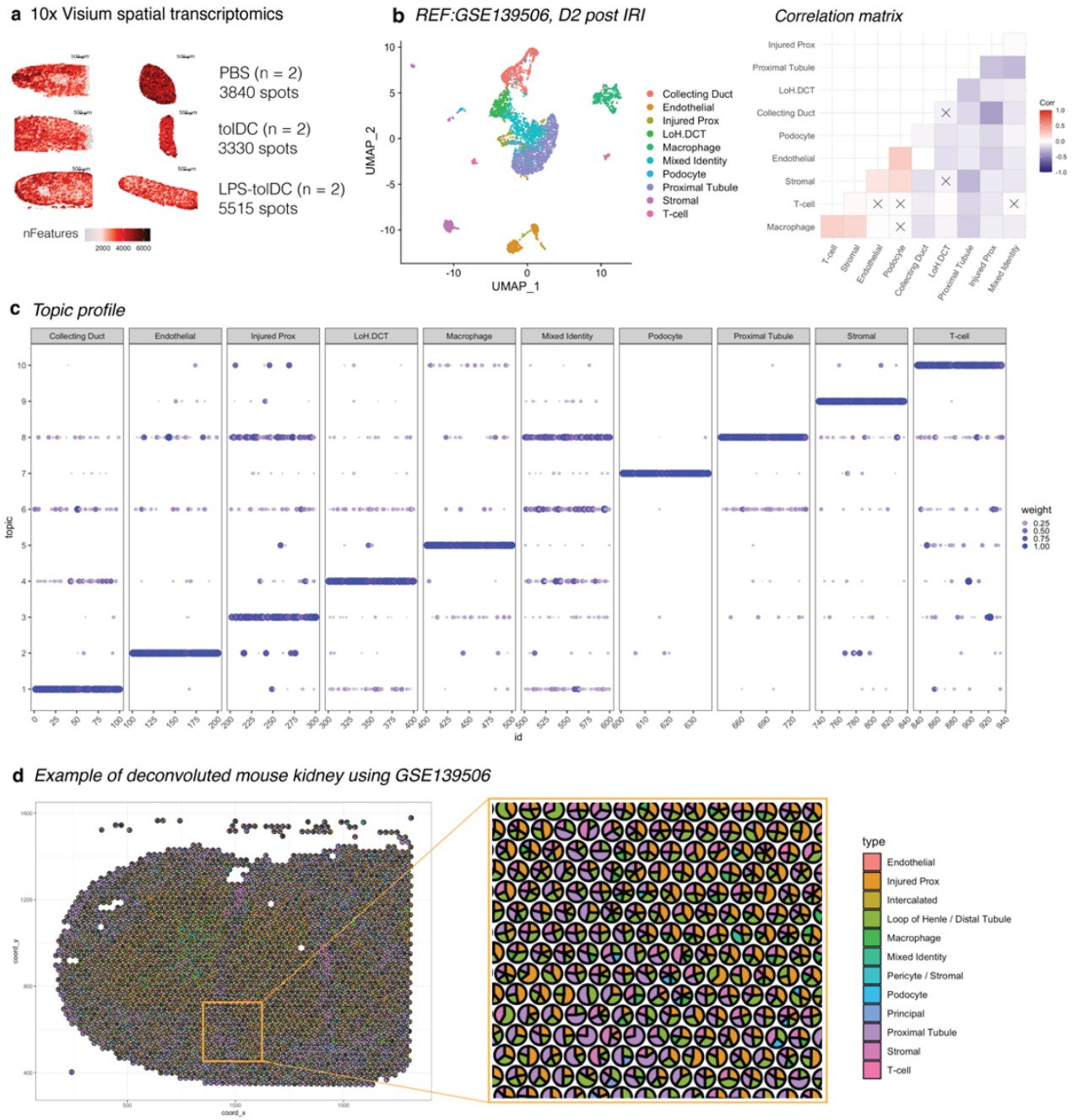

Figure 2.22: ***Spatial transcriptomics deconvolution*** *of a) 6 mice kidneys post QC/data filtering using b) the GSE139506 scRNAseq dataset, specifically day 2 post unilateral IRI. The correlation matrix shows spearmans correlation of cell types based on markers with AUC > 0.8 and c) topic profiles of marker genes per cell type. D) An example of the mouse kidney deconvolution results.*

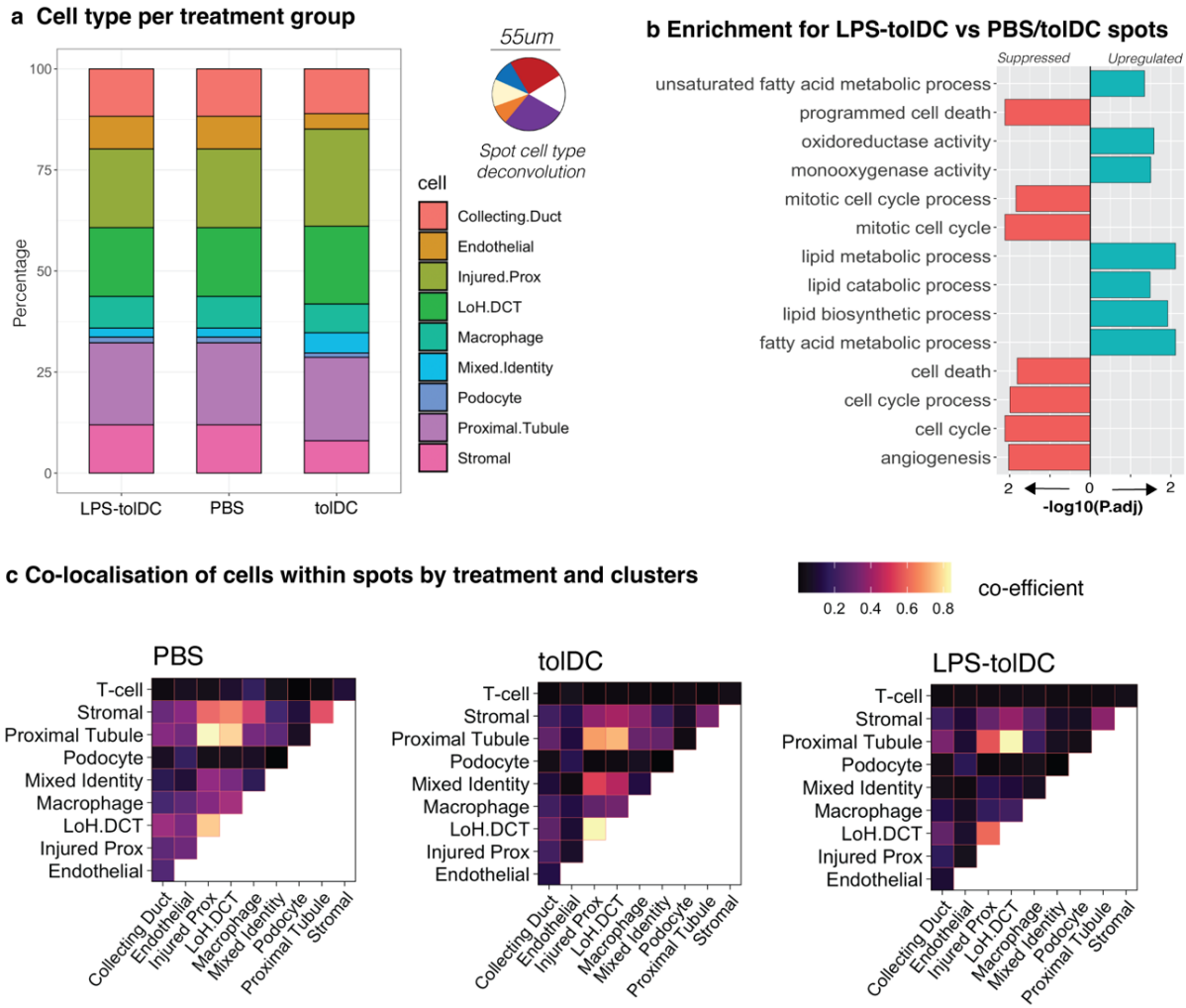

Figure 2.23: ***Deconvolution results*** *split based on treatment group, with a) relative cell types, b) GSEA enrichment of differentially expressed genes between LPS-tolDC and PBS/tolDC treated kidneys, and c) co-localisation of cell types per 55µm spot based on treatment group.*

2.4.12.2 Clusters defining transcriptomically similar spatial spots

Cell annotation was not performed, and this limited the ability to perform downstream analysis for ligand-receptor and cell-cell interaction. The assumption that the dominant cell can be labelled as the 'single' identity of the 55µm spot is a perilous assumption given the underlying cell type and cell number heterogeneity within the resolution of the current 10x Visium technology used in this project. Instead, unbiased clustering was performed to determine 'transcriptomically' similar spots, which the molecular signature of the cell mix in each location is used to group the 11,685 spots in our experiments.

Although there was some resemblance between the clustering distribution and cell-type deconvolution pattern (Fig 2.24), the resolution of clustering was set at 0.3, determined independently of these gross visual patterns based on k-means clustering and random matrix theory using the SC3 identify cell types but optimise computational time and stability of clustering consensus matrix (which estimates for the similarity between two cells/spots within each cluster)[54]. This approach revealed 10 transcriptomically similar clusters across the treatment groups and sections (Fig 2.25).

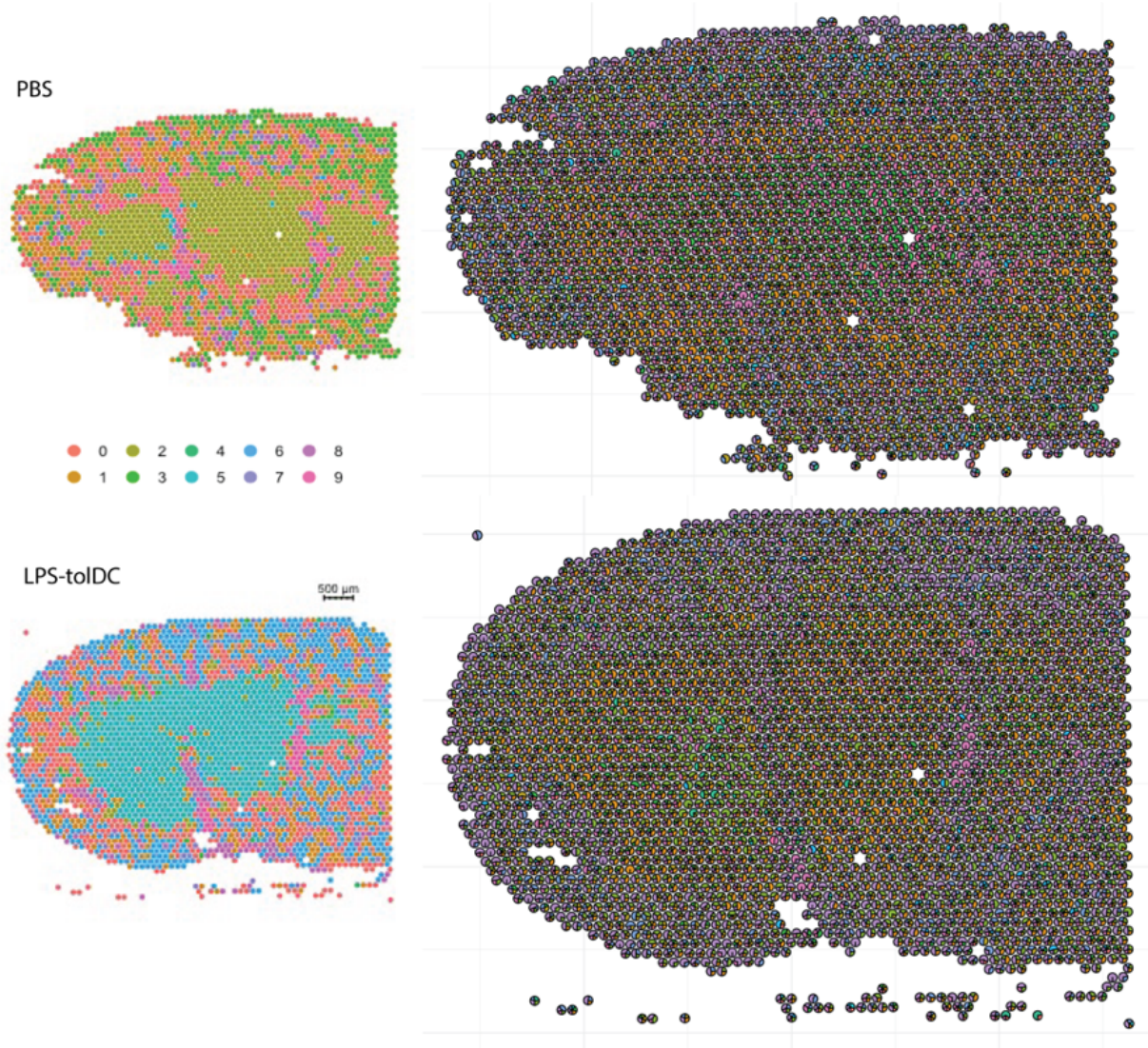

Figure 2.24: ***Representative kidney clustering and the corresponding deconvolution displays for PBS- (top) and LPS-tolDC treated kidneys (bottom) 24-hours post IRI***

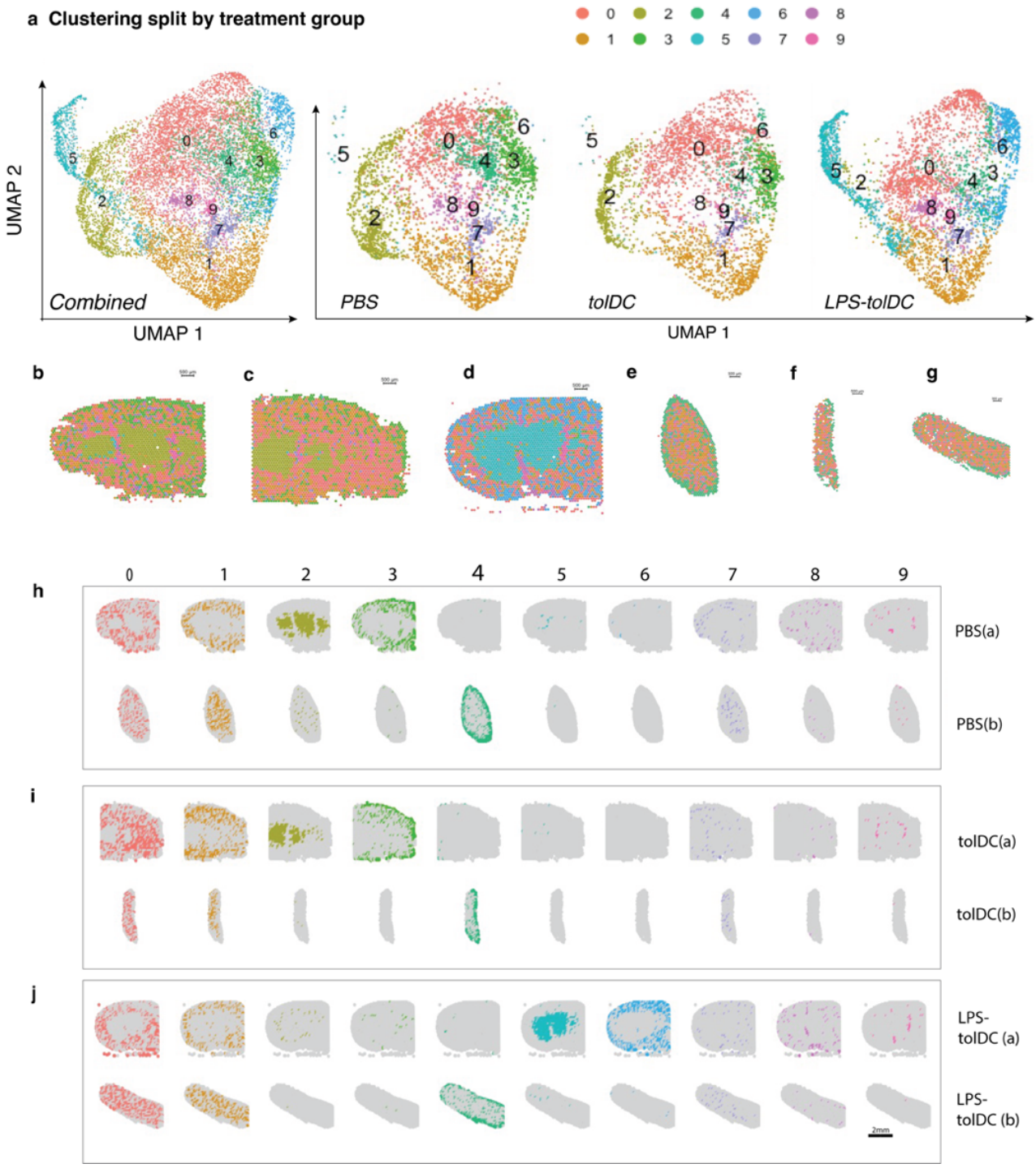

Figure 2.25: ***Clustering projected onto spatial plots****. Uniform manifold approximation and projection (UMAP) plots of 10 distinct clusters across a) all spots vs split by treatment group and mapped back to the histological location for b) PBS, c) tolDC, d) LPS-tolDC, e) PBS, f) tolDC and g) LPS-tolDC kidneys. These projections also displayed separately for each cluster in h) PBS, i) tolDC and j) LPS-tolDC groups.*

2.4.12.3 Clusters defining composition across treatment groups

Making sense of these 10 clusters, we assess their cell composition, distribution across treatment types and select pairwise clusters. Of interest were clusters 5 and 6, which were predominantly derived from LPS-tolDC spots and contrasted clusters 2 and 3 on a histological level and these contrasting clusters were also related in UMAP space, which is also a marker of how similar or related they are. Within clusters, the cell co-localisation mirrors findings with the combined treatment group distributions shown earlier. (Fig 2.26a). In terms of normal versus injured proximal tubular cell co-localisation, this was greater in cluster 3 (found in PBS/tolDC kidneys) versus cluster 6 (mainly LPS-tolDC kidney). Again, there was significant cell type heterogeneity within each cluster (Fig 2.26b, Table 2.10) and clusters 0, 3, 4 and 6 had > 50% of the spot composed of proximal tubular cells (sum of normal and injured), with normal outnumbering injured in clusters 3, 4 and 6.

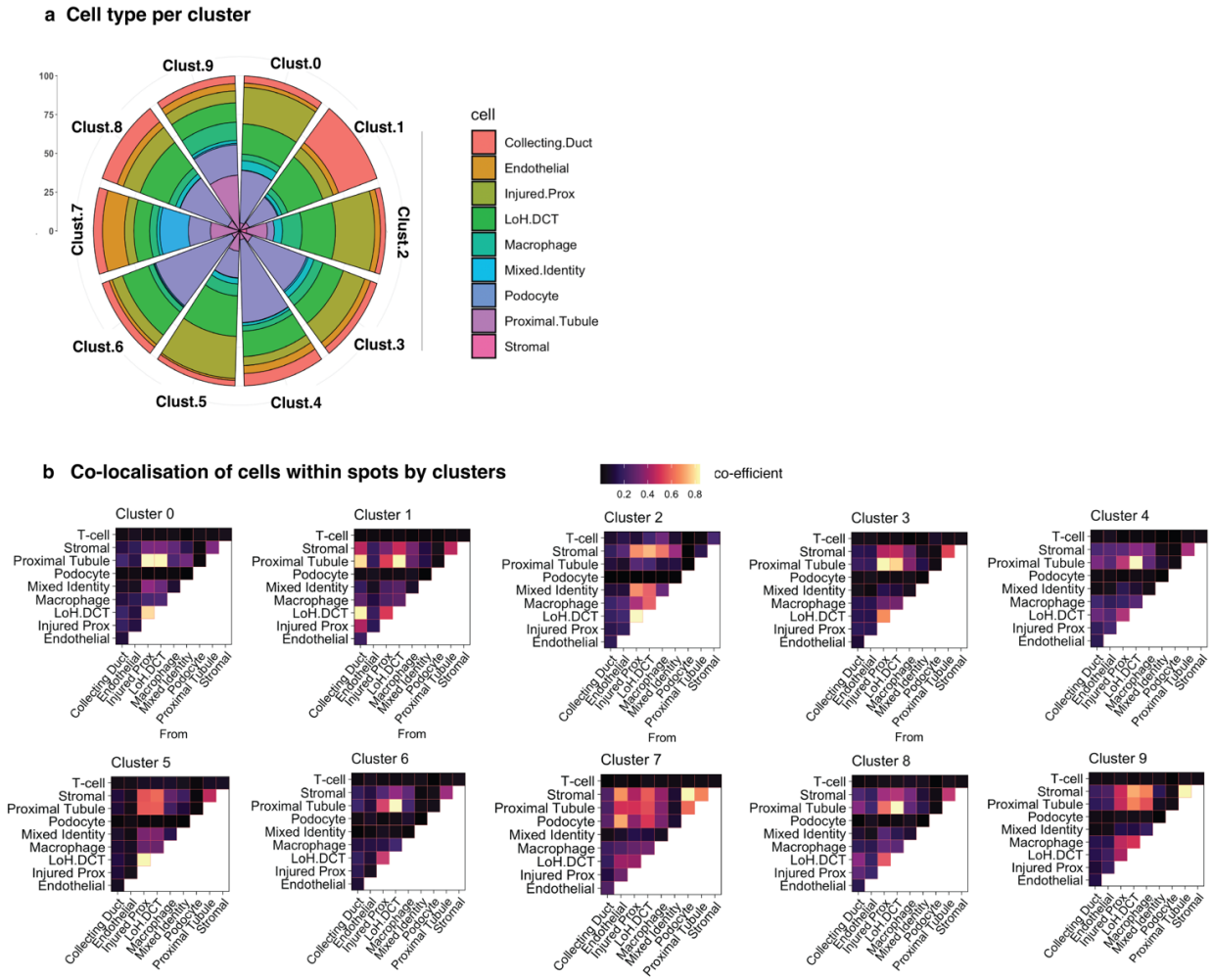

*Figure 2.26: **Spatial co-localisation** by a) cell types by deconvolution, and b) relative cell types for each of the 10 clusters*

Common kidney markers including *Slc5a2* (SGLT2), *Slc5a12* (SMCT2) and *Slc13a3* (NaDC3) denoting S1, S2 and S3 segments of the proximal tubule was concentrated in spots from clusters 0, 3, 4 and 6 and sparsely seen in spots from cluster 2 and 5. (Fig 2.27) *Slc13a3*, the marker of S3 segments was most concentrated in spots from cluster 6 on the UMAP projection, the same cluster with the highest proportion of normal proximal tubular cells. (Table 2.10).

Table 2.10: Relative cell composition by cluster based on deconvolution

Cluster	0	1	2	3	4	5	6	7	8	9
Proximal Tubule	30.3	17.4	3.8	35.0	46.9	14.3	49.1	12.8	30.9	16.4
Injured Proximal tubules	26.3	9.7	28.5	20.1	8.7	29.9	12.5	7.7	14.7	9.8
Mixed Identity	3.2	1.9	5.5	2.4	0.3	4.1	0.1	1.2	2.0	1.2
LoH/DCT	17.5	23.2	21.0	13.1	13.6	24.0	16.9	10.3	18.6	11.1
Collecting Duct	6.9	30.1	4.5	6.1	11.1	4.2	5.8	6.8	12.7	6.3
Endothelial	3.9	5.1	4.7	5.3	7.1	1.9	3.6	16.0	5.5	5.7
Podocyte	0.3	0.7	0.0	1.2	0.3	0.3	0.9	18.7	0.4	1.0
Stromal	6.1	7.2	14.3	8.8	6.8	11.8	6.0	20.3	8.6	35.2
Macrophage	5.3	4.5	13.7	7.2	5.1	8.1	4.4	5.8	5.7	12.7
T-cell	0.3	0.3	4.1	0.8	0.1	1.5	0.5	0.6	0.8	0.5

Regression-based deconvolution to GSE139506 reference set

Clusters 2 and 5 had a greater proportion of injured proximal tubular cells by deconvolution and also where the injury marker *Havcr1* (KIM1) was most concentrated. Despite the expression gradient, *Havcr1* was widely distributed, indicating the cell mix within each spot contained a proportion of injured tubular cells. Despite the limited immune cell types in our reference set, macrophage co-localisation with injured tubule and the loop of Henle/convoluted tubules was greater in cluster 2 (PBS/tolDC) compared to cluster 5 (LPS-tolDC). Spots with immune cells (macrophages/T-cells) from these clusters also had higher expression of *Lcn2* (a marker of injury and/or neutrophil infiltration), *IL-1β, IL-6* and *Ccl2*. (Fig 2.27)

Cluster 7 likely contained the majority of glomeruli in the sections given high percentage of endothelial and podocytes were matched with higher expression of *Nphs1* (nephrin) and *Nphs2* (podocin). Similarly, cluster 1 contained the majority of distal nephron segments, with high percentage of convoluted tubules and collecting ducts by deconvolution and high expression of *Slc12a1* (NKCC2), *Slc12a3* (NaCl co-transporter) and *Slc26a4* (pendrin) (Fig 2.27).

Similar cell distributions based on enrichment patterns were seen across the different sections using the Giotto package to perform parametric analysis of gene set enrichment (PAGE)[55-57]. This particular deconvolution result was not used for downstream analysis given both positive and negative enrichment scores complicate co-localisation interpretations. (Fig 2.28)

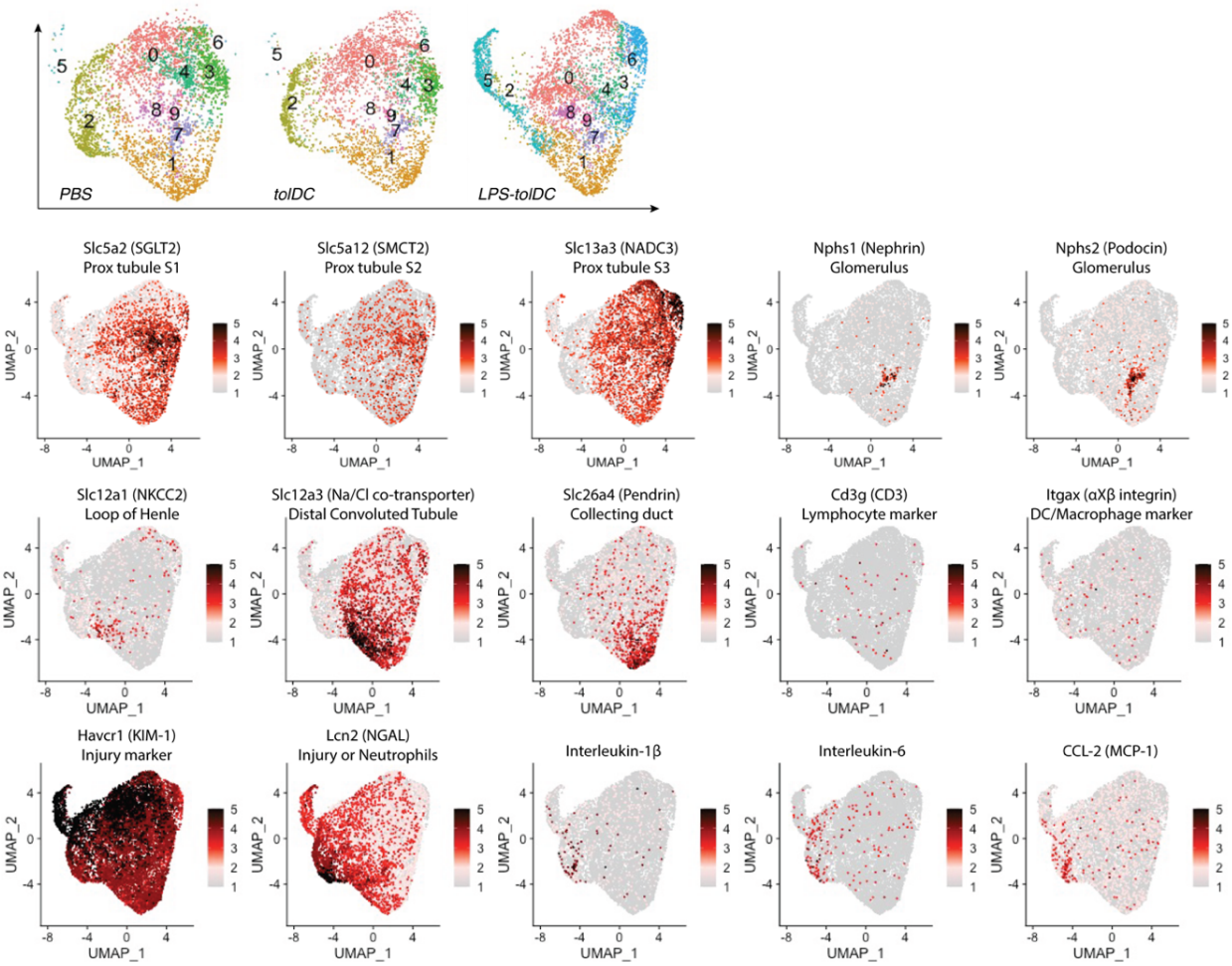

Figure 2.27: ***Marker distributions.*** *Clusters projected on UMAP space across treatment groups with targeted expression of select markers of different nephron segments and immune markers*

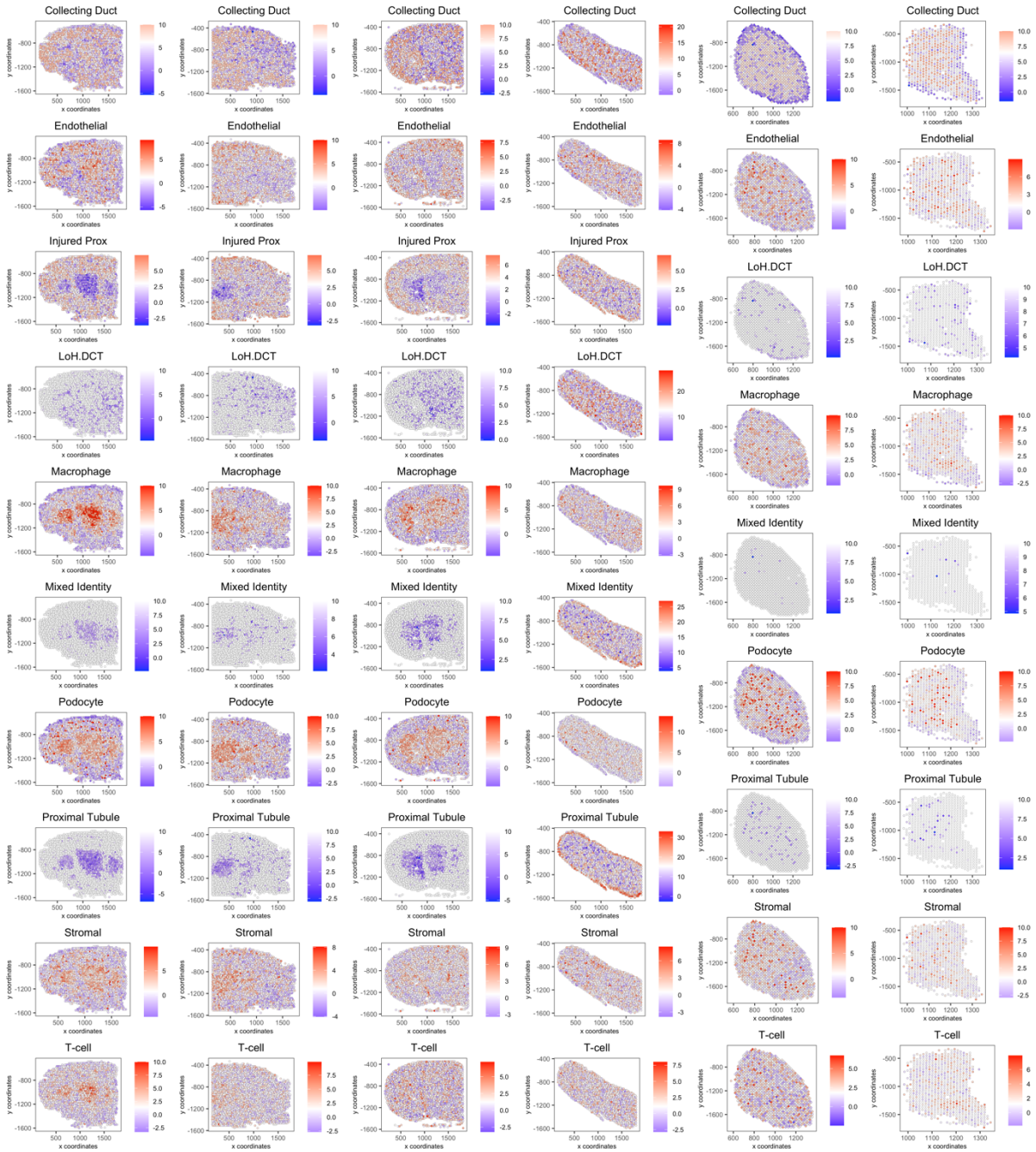

Figure 2.28: ***PAGE deconvolution*** *using the Giotto package and markers derived from GSE139506, showing relative enrichment scores for each cell type across tissue sections. Columns from left to right include PBS, tolDC, LPS-tolDC, PBS, tolDC and LPS-tolDC.*

2.4.12.4 GSEA pathways by spatial clusters across treatment groups

Spots from a specific cluster were compared to all remaining spots to generate 10 DEG lists for GSEA. Enriched pathways for immune, cell death and metabolic processes for each cluster are shown for LPS-tolDC versus PBS/tolDC (Fig 2.29) and aggregated spots across all sections (Fig 2.30). Cluster specific pathways were concordant with changes across treatment groups. Spots within cluster 2, was found on the inner portions of kidney sections from PBS and tolDC groups showed upregulation of immune pathways, cell death with relative suppression of pathways involved with metabolic and anti-oxidant processes. This corresponds to in vivo findings of more severe injury and cell death following IRI and deconvolution showing more injured proximal tubules and immune cells. Conversely, spots from LPS-tolDC contained within cluster 6 were enriched for mitochondrial processes for aerobic respiration, fatty acid metabolism and protective oxidoreductase pathways. Again, this corroborates with the renoprotective effects and greater proportion of 'normal' S3 proximal tubular cells identified by *Slc13a3* and deconvolution.

Figure 2.29: ***Enrichment across spatial clusters split by treatment group.*** *These were derived by GSEA enrichment of DEG of spots within a cluster versus the rest of the tissue and represented in stacked bar graphs for each relevant pathway.*

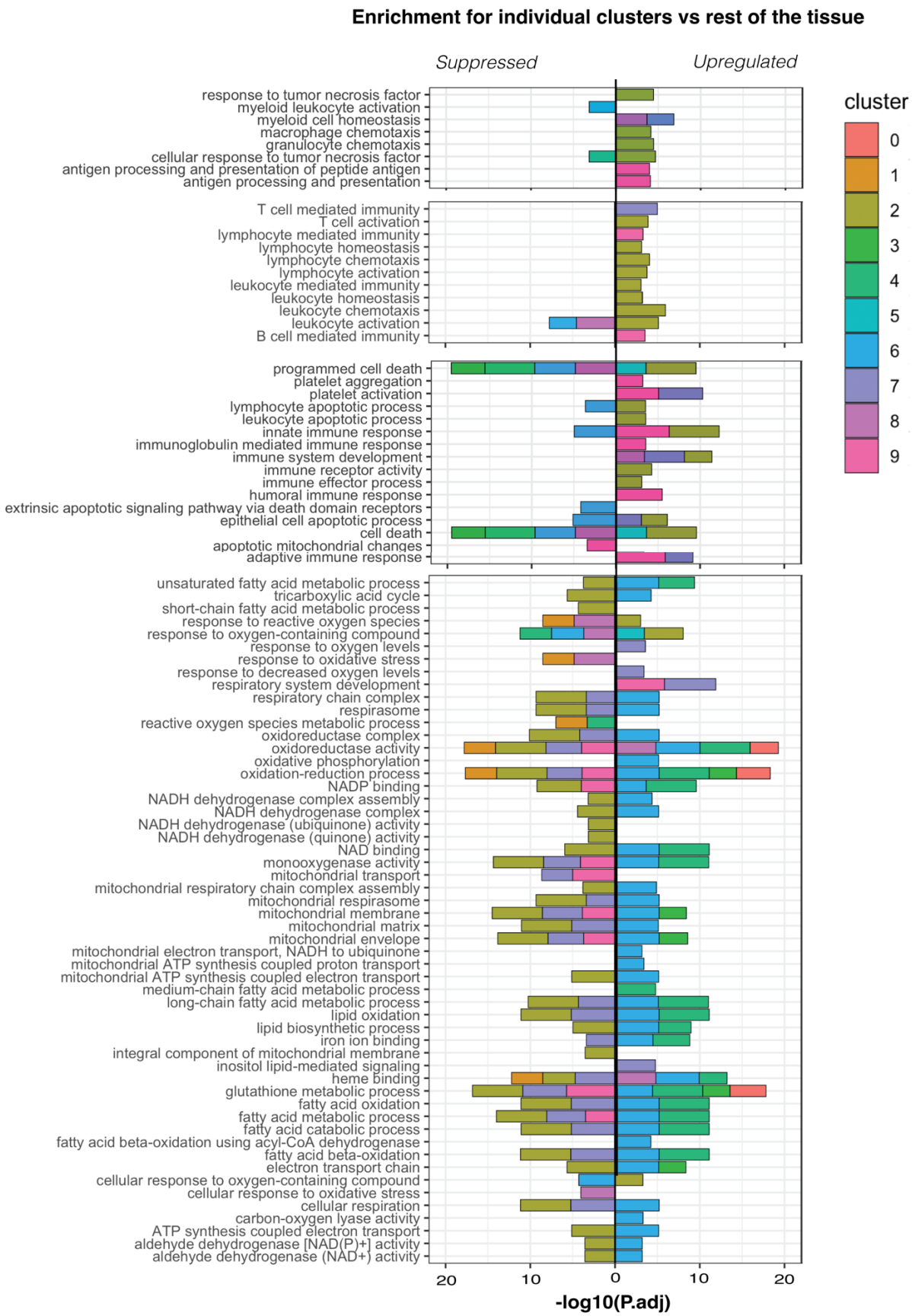

Figure 2.30: ***Enrichment across spatial clusters across all sections****. These were derived by GSEA enrichment of DEG of spots within a cluster versus the rest of the tissue and represented in stacked bar graphs for each relevant pathway.*

2.4.12.5 GSEA pathways by pairwise cluster comparison

Specific comparison of clusters 2 and 5 allows for assessment of spots on the inner areas of kidney sections from PBS or tolDC versus LPS-tolDC treatment, which contained the dominant proportion of injured tubular cells, loop of Henle/convoluted tubules and macrophages. Differential expression between cluster 2 vs cluster 5 (Fig 2.31a) showed downregulation of genes such as branched chain amino acid transaminase 1 (*Bcat1)*, arginase-2 (*Arg2*), glutathione-s-transferase *(Gstm1)* and ferritin heavy chain (*Fth1*) and upregulation of thrombospondin (*Thbs1*), lipocalin (*Lcn2*), clusterin (*Clu*) and connective tissue growth factor (*Ctgf*). Enrichment analysis showed upregulation of innate immune related pathways involved in neutrophil and macrophage chemotaxis, along with apoptosis related to DNA damage following IRI (Fig 2.31b), whereas cluster 5 was enriched for lipid metabolism and oxidoreductase related processes.

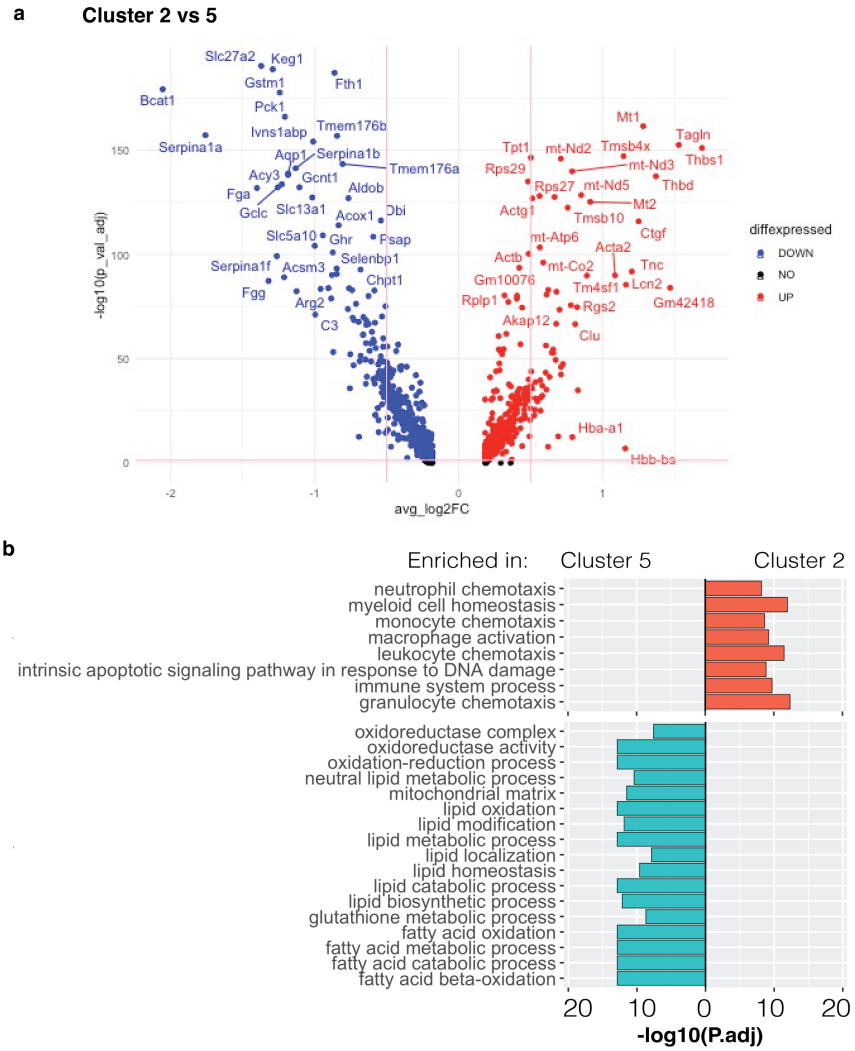

Figure 2.31: ***Pairwise comparison of cluster 2 and 5****. A) volcano plot of differential genes for cluster 2 vs cluster 5, and b) enriched pathways (by GSEA) for these differentially expressed genes.*

The region of interest identified from the earlier exploratory data analysis was spots derived from LPS-tolDC in cluster 6. The main comparison was cluster 3 vs 6, which were closely related on the UMAP plots but segregated by treatment group. The volcano plot (Fig 2.32a) shows differentially expressed genes, with relative greater expression of serine peptidase inhibitor Kazal type 1 (*Spink1*), the transmembrane protein Tmem176 (*Tmem176a, Tmem176b)*, *DNAse1* in spots derived from cluster 6, while cluster 3 had greater expression of galectin (*Lgals1, Lgals3*), *S100a6*, fibrinogen (*Fgb*) and cathepsin B (*Ctsb*). Overall, the pathways enriched mirror the favourable immune activation, cell death and metabolic activity profile from earlier analysis, whether cluster 6 was compared to cluster 0, 1 or 3 (mixed tissues) or to neighbours from the same LPS-tolDC section (Fig 2.32b and c).

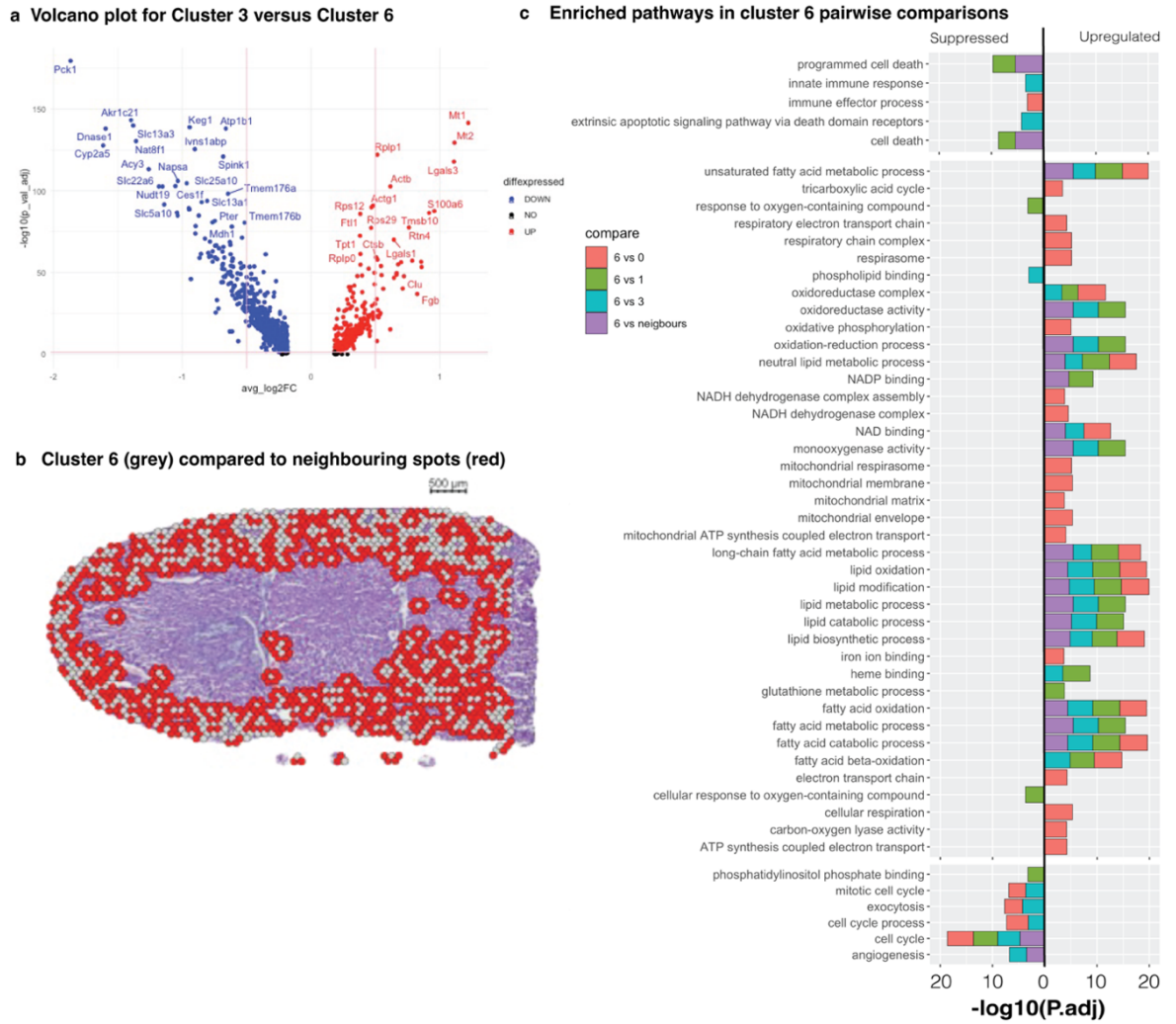

Figure 2.32: ***Comparison of cluster 6 versus cluster 3 and neighbouring spots****. A) volcano plot of differential genes for cluster 3 vs cluster 6, and b) plot of the spots for cluster 6 (grey) versus neighbouring (red) areas used for differential expression. c) pathways enriched for cluster 6 versus cluster 0, 1, 3 or neighbouring spots.*

2.4.12.6 GSEA pathways by proximal tubular cell dominant spots

Earlier results revealed that proximal tubule (PT), injured PT (iPT) and loop of Henle/distal convoluted tubule (LoH/DCT) cells were most likely to be co-localised in the same 55µm 10x Visium spots and the highest coefficient for macrophage co-localisation with these cells were found in cluster 2 or PBS/tolDC derived spots. To further focus on proximal tubular cells, a subset analysis of spots where >50% of the spot admixture was made up of a proximal tubular cell (PT+iPT > 50%) was performed, and coloured red if PT>iPT and yellow if PT<iPT. (Figure 2.33a). The relative distribution of spots where normal PT outnumber injured PT dominated the outer cortical regions, particularly for samples from LPS-tolDC. These spots where enriched for lipid and oxidoreductase activity in LPS-tolDC samples (Fig 2.33b). Fatty acid metabolism and monooxygenase activity were upregulated when macrophages co-localised with proximal tubule dominant spots, and epithelial cell apoptotic processes were suppressed in LPS-tolDC-derived spots compared to PBS or tolDC samples. (Fig 2.34c-d).

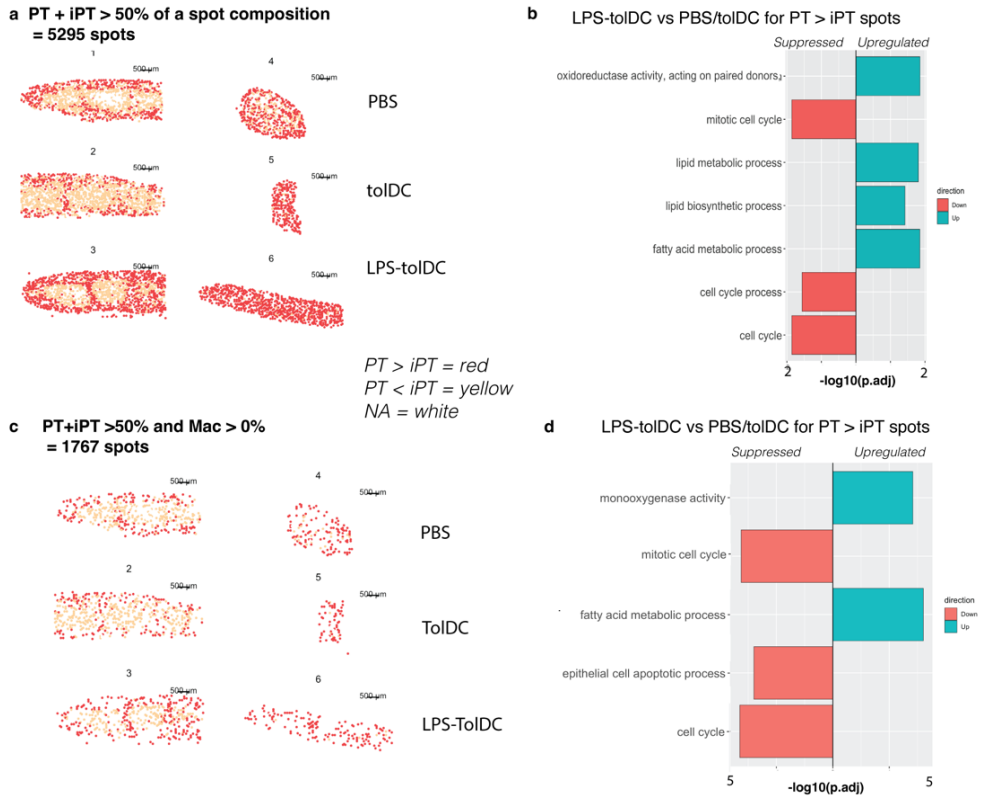

Figure 2.33: ***Sub-analysis of spots where proximal tubular (PT) cells (normal or injured) are dominant,*** *with threshold of combined percentage > 50% per spot. This threshold selected 5295 spots and the distribution is seen in* ***a)*** *where red indicates a greater proportion of normal PT than injured PT, and yellow indicates where injured PT dominated. A heatmap of co-localisation is shown, as is GSEA enrichment of LPS-tolDC vs PBS/tolDC-derived spots and the corresponding gene network map. Similarly,* ***b)*** *shows the sub-analysis of 1767 spots derived after the original PT + iPT > 50% was further selected for presence of macrophage cells identified within the spot – with distribution of PT vs iPT dominant spots, co-localisation heatmap, enrichment analysis and gene network map.*

2.4.12.7 Identification of cells utilising weighted kernel density estimation.

Nebulosa[44], a R-package was used to calculate weighted kernel density estimation to identify likelihood of co-expression of genes of interest. To demonstrate, spots from our spatial data which co-express of canonical injury markers including *Havcr1*, *Lcn2* and *Cryab* are shown in Fig 2.34. *Nebulosa* was originally developed overcome sparse data or low abundance transcripts to identify rare cells from single cell experiments[44] and this methodology was used in our attempts to identify LPS-tolDC in the spatial data.

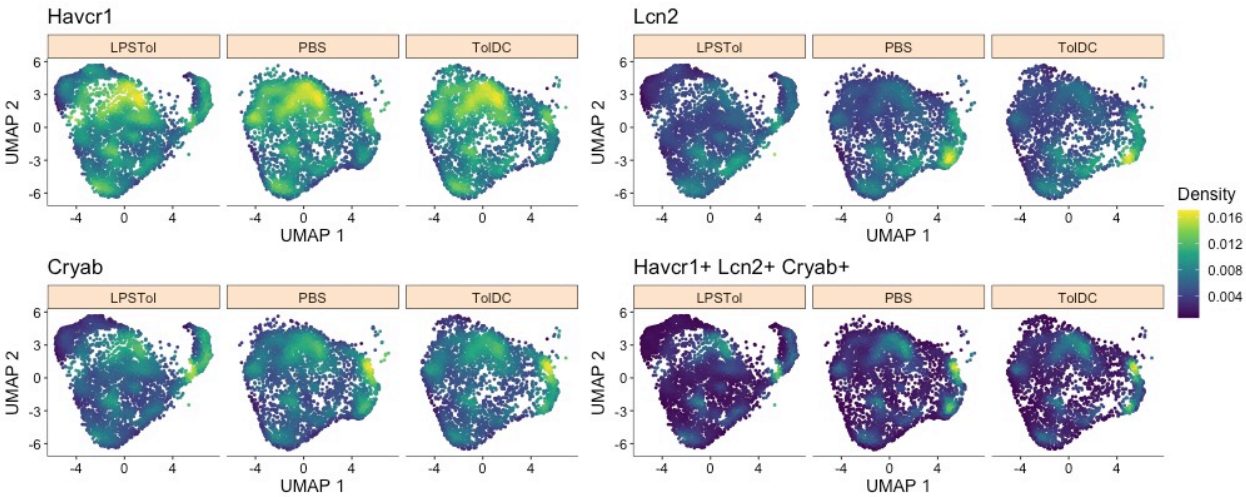

Figure 2.34: ***Nebulosa derived weighted density plots for Havcr1, Lcn2, Cryab and their co-localisation.***

The top 10 marker genes used to differentiate LPS-tolDC from tolDC and mature tolDC (LPS-BMDC) were identified based either LFC, smallest adjusted P-values, mixed metric (LFC multiplied by log (P value)) from earlier bulk RNA-seq results, or an *a priori* list of expected targets. (Table 2.11)

Given the inherent limitations of the cell admixture of each spot, LPS-tolDCs could not be reliably identified. There was extremely low probability based on the top 10 genes by LFC, the top P-value and mixed metric markers were not specific, with detection in the control PBS and tolDC groups. The use of use identified gene list based on a priori knowledge of high yield markers was able to detect a strong signal in the LPS-tolDC kidney, but this was not exclusive, with weak signals seen in the other treatment groups. Increasing marker genes did not significantly improve performance. (Fig 2.35).

Table 2.11: Top 10 marker genes for LPS-tolDC based on either LFC, p-value, mixed metric or a priori selection

By LFC		By P-value		By mixed metric		A priori	
Gpnmb	Tgm2	Cyp24a1	Adamts20	Msi1	Cdr2l	Cd274	Arg1
Acpp	Serpinb2	Msi1	Robo4	Nppc	Mmp13	Cyp24a1	Ifi27
Atp1a3	Cxcl3	Chga	Scara5	Loxl2	Hid1	Itgax	Dusp14
Arg1	Mmp13	Iqsec3	Drd4	Serpinb2	Pde10a	Tgfb1	Zfat
Rcbtb2	Stt3b	Cdr2l	Pde10a	Iqsec3	Adamts20	Ido2	Lamc3

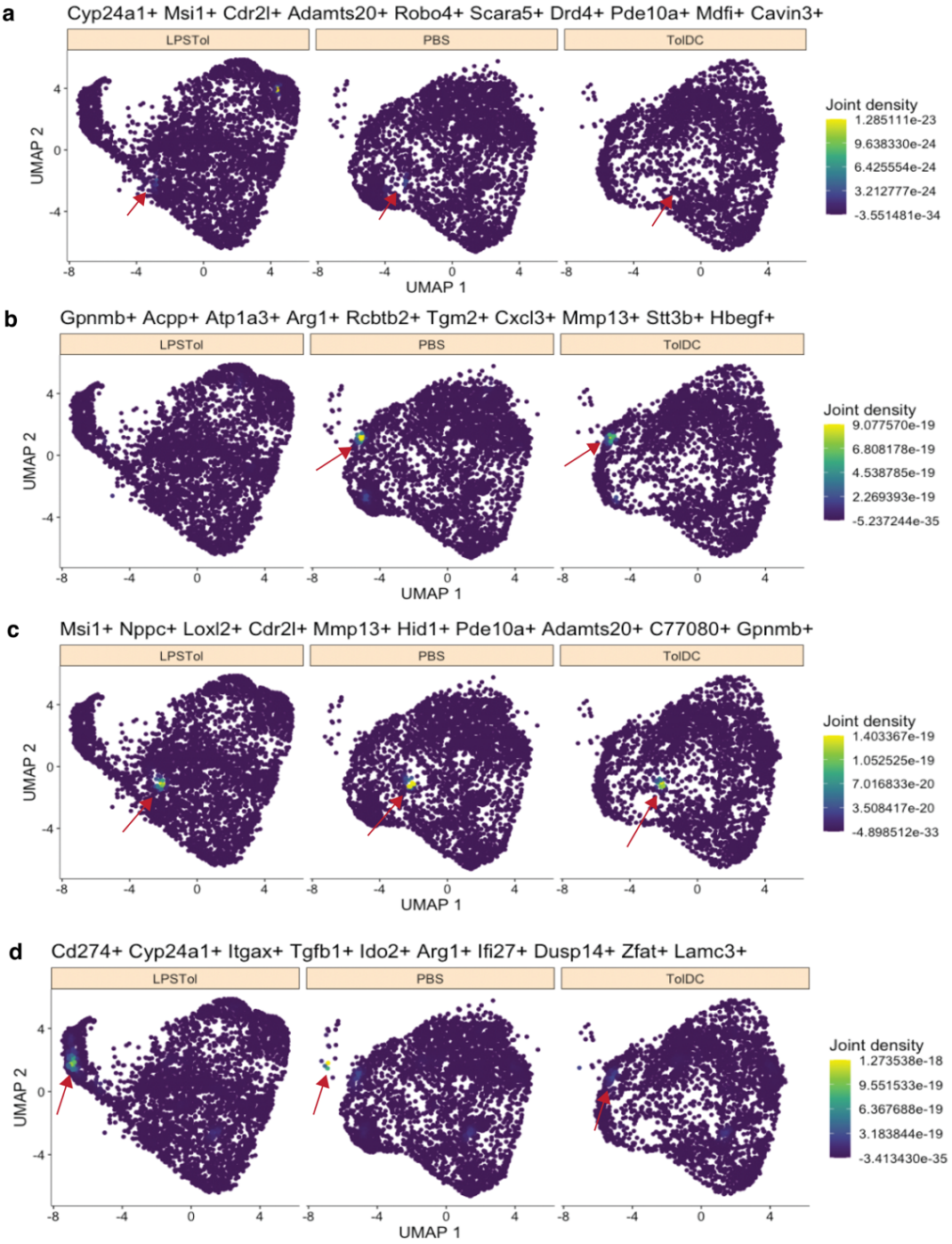

*Figure 2.35: **Nebulosa derived weighted density plots for LPS-tolDC markers** based on the top 10 genes by a) log-2 fold change (LFC), b) smallest p-value, c) mixed metric with LFC multiplied by log(p-value) and d) user defined list based on a priori knowledge. Red arrows indicate the highest density (and probability where cells of interest are found)*

2.5 Discussion

We showed that VitD3/IL-10-conditioned tolDC, despite the lack of antigen specificity can be leveraged to protect mice against developing severe AKI following IRI. Adoptive therapy of either (syngeneic) LPS-tolDC or Allo-tolDC limited AKI, RTEC damage and induction of pro-inflammatory cytokines. Potential contact-dependent mechanisms include increased PDL1 expression, induction of T-cell hypo-responsiveness and increased trafficking to the injured organ, and contact-independent mechanisms including changes in cytokine and transcriptomic profiles described above. The timing of LPS-tolDC or Allo-tolDC administration the day before or at time of injury did not influence their ability to protect against severe AKI, although we have yet to demonstrate protection by cellular therapy administered after the window of injury. Our in-depth characterisation adds considerable evidence to the therapeutic potential of tolDC for AKI and our VitD3 + IL-10 protocol is similar to that used in human clinical trials for liver (NCT03164265/NCT04208919)[58] and kidney (NCT03726307)[37] transplant tolerance. Other studies have shown tolDC conditioned with alternative agents (adenosine-2A receptor agonist[59], sphingosine-1-phosphate agonist[60,61] or rapamycin[62]) have also demonstrated renoprotection in murine models.

Syngeneic versus allogeneic tolDC

Ex-vivo tolDCs were resistant to TLR4-based activation[27,63] regardless of species background, evidenced by restricted MHCII, CD80, and CD86 expression, combined with elevated PDL1:CD86 ratio and IL-10 secretion. However, the PDL1:CD86 ratio was only ≥ 2 in the LPS-tolDC from C56BL7 mice, whereas both Allo-tolDC and Allo-LPS-tolDC from BALB/c mice exceeded this threshold. Furthermore, the absolute concentrations of IL-10 secreted by unstimulated tolDCs were greater for cells derived from BALB/c compared to C57BL6 mice. These two factors may explain why both Allo-tolDC and LPS-tolDC were both able provide renoprotection.

The tolDC molecular phenotype

These distinctions in biological DC phenotypes were supported by massively parallel sequencing and gene set enrichment analysis. This allowed for the assessment of over 10,000 genes of interest simultaneously between the different DC conditions compared to traditional qPCR methods. Differential expressed genes

between tolerogenic and non-tolerogenic conditions confirmed suppression of immune effector response and cell death pathways and DEGs upregulation of Cd274 (PDL1) and downregulation of Cd40, Cd80, Cd83 and Cd86, mirroring the above findings. Relative to unstimulated tolDC, LPS-tolDC had more activated immune pathways, but this degree of activation was still less compared to the non-tolerogenic condition (LPS-BMDC), thus supporting the notion of an 'alternatively-activated' DC (AADC) phenotype.[48,64]

IL-10 is a potent immunomodulatory cytokine[65-67], but this likely works in concert with other key candidates, such as TGF-β, arginases and indolamine-2,3-oxygenase to achieve the immunosuppressive effects seen with tolDCs[68]. This was supported by the conserved tolerogenic signature showing upregulated *TGF-β1*, *TGF-β3*, *Arg1, Trem2* and *Havcr2* for both tolDC and LPS-tolDC (thus, tolDC regardless of TLR-4 activation) were simultaneously compared to LPS-BMDC. Conversely, *Kmo, Kynu, Adgre5, Fabp5* and *Batf3* were downregulated in this conserved tolerogenic list. TGF-β has a pivotal role to maintain tolerance in various immune cells[69]. TGF-β can exert effects through SMAD-dependent mechanisms to induce peripheral CD4+CD25+Treg development[70], or SMAD-independent (through downstream MAPK) pathways to resist maturation in response to LPS induction[71]. TGF-β receptor 3 (*Tgfbr3, also known as bet-glycan*) acts as a co-receptor to promote high affinity binding and canonical TGF-β signalling and may augment autocrine IDO and arginase secretion to maintain tolerogenicity[68,72]. Arginase-1 metabolises L-arginine into urea and L-ornithine, thus limits diversion of arginine to produce reactive nitrogen species by inducible nitric oxide synthase (iNos). *Arg1* has well known roles on macrophage polarisation and myeloid cell tolerance[68,73,74].

Havcr2 (or Tim3) is upregulated in a negative-feedback fashion in response to TLR4 stimulation, and loss of function polymorphisms have been shown to result in immune hyperactivation states[75]. The innate immune receptor *Trem2* has previously been found in alternatively activated DCs and macrophages and can result in suppression of pro-inflammatory cytokines[76-78] but increase CCR7 expression, partial DC maturation and prolong DC survival[79]. The tolDC phenotype was further characterised by suppressed *Fabp5* expression, where *Fabp5* otherwise limits Foxp3+ Treg generation and promotes a pro-inflammatory phenotype in myeloid cells[80,81]. Lower *Batf3* and *Adgre5* (CD97) are beneficial to the tolerogenic phenotype,

as these are known to participate in cross-presentation and contact-dependent activation between DC-T-cell subsets[82-84].

Distinguishing LPS-tolDC and tolDC

In-vitro experiments confirmed that both tolDC and LPS-tolDC were able to induce T-cell hypo-responsiveness[19,36,85] and thus the failure of syngeneic, unstimulated tolDC to protect against AKI was surprising. In addition to the differences in PDL1:CD86 expression, cell tracking studies demonstrated LPS-tolDC were more able to track to the injured kidney compared to unstimulated tolDC and this may be important, as adoptively transferred DC have brief longevity and activity *in vivo* before converting into apoptotic bodies[86,87]. The difference in DC trafficking may be mediated through the higher expression of chemokine receptors *Ccr2, Ccr5, Ccr7* and *Cxcr2* in response to TLR4 stimulation when LPS-tolDC was compared to tolDC.

We showed that LPS-tolDC were able to limit RTEC inflammation, based on TNF-α, LCN-2 and KIM-1, in contact-independent co-culture experiments. This protection was provided by the anti-inflammatory effects of DCs, rather than autocrine RTEC production of IL-10, TGF-β, IDO1 or IDO2 mRNA. LPS-tolDC had greater expression of *Ido-1* compared to tolDC and this combined with downregulation of both *Kmo* and *Kynu* may render LPS-tolDC was more effective than tolDC in vivo. IDO converts tryptophan into L-kynurenine and its degradation is mediated by *Kmo* and *Kynu*. This combination can aid accumulation of kynurenine, which can act via aryl hydrocarbon receptors to limit T-cell activation, increase expression of other anti-inflammatory cytokines such as TGF-β, and avoid production of quinolinic or picolinic acid metabolites, which augment reactive oxygen stress[88-91].

In addition to *Ido1* and chemokine receptors, other genes which distinguished LPS-tolDC from tolDC included *Tnfaip3* (also known as A20) is a ubiquitin-editing protein which negatively regulates NF-κB[92-94]; and C-type Lectin receptors (*Clec4a, Clec4d, Clec4e*), which can sense danger associated molecular patterns released by injured or dying cells to moderate immune repsonses[95-97].

Examination of RNA-seq data also revealed *Dusp-14, Cxcl3* and *Sdc1* to be upregulated in LPS-tolDC compared to all other DC conditions. Elevated *Dusp14* (also known as MAP Kinase Phosphatase 6, *MKP6*) and members of the DUSP family are increasingly recognised to limit innate and adaptor immune function - including upregulating IL-10 while limiting IL-1, IL-12, TNF-α and IFN-γ[98-100] by dephosphorylation of MAPK to limit the TLR-Myd88 axis[101-103]. Hypofunctional *Dusp14* (human) polymorphisms are associated with higher transcription of Th1 immune-related genes[104] and an earlier rat IRI model showed protection against injury, apoptosis and oxidative stress with the administration of intra-peritoneal eriocitrin (eriodictyol glycoside), an enhancer of *Dusp-14*[105].

Cxcl3 is a strong neutrophil chemoattractant but high levels of *Cxcl3* transcripts are also known to drive human $CD14^+$ monocytes towards a myeloid derived suppressor cell phenotype and increase IL-10, TGF-β, PD-L1, IDO and Arg-1 production[106]. Furthermore, co-culture of *Cxcl3*-treated, monocyte-derived DCs with naïve T-cells result in higher IL-10 and lower IL-12 and IFN-γ expression[106]. Syndecan-1 (or CD-138, *Sdc-1*) is a heparin sulfate proteoglycan and its expression on epithelial and immune cells contribute to its migratory[107,108] and immunosuppressive roles[109]. *Sdc-1* is protective factor in renal IRI[110], promotes the clearance of CXC chemokines to facilitate the resolution of neutrophil inflammation[111,112] and controls renal CD4+ and CD8+ T-cell influx in a murine anti-GBM model[113]. We have highlighted some important genes relating to tolDC function, but this is not exhaustive and nor is it likely a single gene will control immunomodulatory activities in isolation. Enrichment helps to provide a framework to interpret gene expression data and biological pathways, but this is also limited by the current knowledge, genes of unknown function and criteria used to filter gene input for analysis.

Interactions with the immune infiltrate

The cytoprotective effects of LPS-tolDC was not mediated by changes in the inflammatory cell infiltrate in response to AKI. Although tolDC are known to inhibit immunity by promoting T cell anergy/apoptosis and induce regulatory $FoxP3^+$ regulatory T cells that produce IL-10 and TGF-β, we were unable to detect any changes in T cell populations within the renal parenchyma. The population of $Foxp3^+$ Tregs were not assessed given $CD3^+CD4^+CD25^+$ cells accounted for <0.1% of the total $CD45^+$ population, and this

mechanism is unlikely a key mechanism given the timeframe of acute protection, with only 24-48 hours from time of injury to post-IRI analysis. The question of whether peripheral or induced Tregs are important for tolDC mediated protection will be better addressed in future experiments using DEREG mice (diptheria toxin mediated Treg depletion). The mechanism of TolDC immunosuppression is both context-dependent and varies depending on the method of generation of TolDC. Unlike the alloimmune setting, where tolerance and prolongation of allograft function following tolDC infusion requires intact recipient DC function, the efficacy of tolDC in AKI was not critically dependent on recipient APC, as allo-tolDC retained renoprotective effects in clodronate treated mice. Experiments to quantify F4/80 or CD11c of the kidneys are in progress at time of submission.

Molecular changes in the kidney post injury

The evidence so far supports reduced cell death and inflammation with LPS-tolDC and Allo-tolDC treatment. This was supported by reduced pro-inflammatory cytokine mRNA expression by bulk kidney qPCR and suppressed acute immune pathways in LPS-tolDC versus PBS/tolDC from spatial analysis. Spatial transcriptomics overcomes the noise (and loss of signal) with the use of bulk kidney tissue, which has high heterogeneity of cell types and histological regions.

Introducing spatial or location information of transcriptomics increased the ability to detect subtle differences between control (PBS), ineffective tolDC treatment and renoprotective LPS-tolDC treatment. Spots from LPS-tolDC kidneys contained more ‘normal’ proximal tubular cells enriched for mitochondrial respiration and lipid/fatty acid metabolic pathways, which is the preferred energy source for tubular cells, suggesting more metabolically viable cells were found with this renoprotective therapy[114,115]. Despite the challenges with tissue sectioning, we were still able to establish reduced inflammatory and cell death molecular signatures and greater proportion of ‘injured’ tubular cells associated with LPS-tolDC compared to the other groups in the inner aspects of the kidney, which has greater susceptibility to ischemic injury.

In light of our flow cytometry data, we focused on macrophage and proximal tubular cell interaction by co-localisation. Spots composed of macrophages with ‘normal’ proximal tubules showed upregulated fatty acid

metabolism, monooxygenase activity and suppressed epithelial cell apoptotic process compared with spots where macrophages co-localised with injured proximal tubules. Injured proximal tubular cells also had greater metabolic viability in LPS-tolDC spots through upregulated fatty acid metabolism, lipid oxidation and oxidoreductase (including GPX4) processes compared to PBS and tolDC spots.

We were able to determine changes down to an approximate 55µm diameter, although the true resolution of this may be reduced somewhat due to lateral diffusion during sample preparation and cDNA acquision[116]. We focused the analysis on determining transcriptomically similar spots, while specific cell-cell level interactions were limited by this 55µm resolution - this issue will likely be addressed in future iterations of this technology. For deconvolution, a publicly available post-IRI scRNA-seq dataset from C57BL6 mice was used to minimise variations in biological model but correctness of mathematical modelling of the cell admixture will be limited by quality and model-equivalence of any public single cell reference used.

2.6 Conclusion and future directions

This study demonstrates the therapeutic potential of tolDC to reduce renal IRI and may be an option to reduce perioperative IRI under predictable clinical circumstances, such as cardiothoracic surgery, or with transplantation to reduce delayed graft function. We have shown that infusion at the time of injury can reduce inflammation and cellular injury, but it remains to be seen whether delayed administration following injury is able to dampen established injury and diminish maladaptive repair following AKI. Tolerogenic DC have been tested in pilot clinical trials for immunosuppression minimisation/transplant tolerance when administered a week prior to transplantation and monocyte-derived tolDC have been shown to retain maturation resistance when administered to healthy and patients with end-stage kidney disease[117]. Our tolerised cells received LPS, but monophosphoryl-Lipid-A (MPLA) is a non-toxic analogue which can engage with TLR-4 for human cell products. There is a need to investigate the risk of developing alloantigenicity (for Allo-tolDC), or whether donor-antigen-pulsed tolDC can provide protection in future studies. The utility of tolDC remains to be seen in other (non-ischemic) modalities of AKI, and further information regarding safety profile in terms of non-specific immunosuppression must be gathered if cell therapy is to be translated to clinical use.

2.7 Acknowledgements

We thank Dr Min Hu and Ms Elvira Jimenez-Vera for assistance and mentoring to perform flow cytometry, and Professor Philip O'Connell, Professor Stephen Alexander, Professor Gopi Rangan and Dr Brian Nankivell for their insightful perspectives during interim data analysis. Flow cytometry, genomic (for tolDC) and histology experiments were performed at the Westmead Scientific Platforms, which is supported by the Westmead Research Hub, the Westmead Institute for Medical Research, the Cancer Institute New South Wales, the National Health and Medical Research Council and the Ian Potter Foundation. We acknowledge the assistance from Dr Brian Gloss from the Westmead Research Hub for processing, QC and mapping of raw tolDC bulk RNA-seq data. Acquisition of raw spatial transcriptomics data was performed with the assistance of Mr Samuel Holland under the supervision of Prof Andrew Mallett and Dr Quan Nguyen at the Institute for Molecular Bioscience, University of Queensland.

2.8 Supplemental material

*Table 2.12: **Median fluorescence intensity** for **a)** C57BL6 and **b)** BALB/c derived DCs.*

a

C57BL6 cells	BMDC	LPS-BMDC	tolDC	LPS-tolDC
PDL1:CD86 ratio				
Mean ratio	1.418	1.546	1.842	5.089
Std dev	0.1928	0.1127	0.2043	0.3730
p-value	0.9519	ref	0.5249	<0.0001
p-value			ref	<0.0001
MHCII				
Mean MFI	631.3	715.0	548.7	495.3
Std dev	37.81	31.43	21.59	11.93
p-value	0. 0147	ref	0.0002	<0.0001
p-value			ref	0.1679
CD40				
Mean MFI	387.0	451.7	433.0	463.7
Std dev	18.52	10.69	35.79	10.41
p-value	0.0155	ref	0.63039	0.8351
p-value			ref	0.3694
CD80				
Mean MFI	753.3	1584	745.7	1257
Std dev	42.90	150.7	358.7	43.94
p-value	0.0034	ref	0.0032	0.2732
p-value			ref	0.0508
CD86				
Mean MFI	882.0	1228	861.0	787.3
Std dev	130.0	178.9	83.35	162.5
p-value	0.0708	ref	0.0543	0.0218
p-value			ref	0.5468
PDL1				
Mean MFI	1244	1886	1579	3906
Std dev	211.0	148.4	135.5	505.7
p-value	0.105	ref	0.655	0.0001
p-value			ref	<0.0001

b

BalbC cells	BMDC	LPS-BMDC	tolDC	LPS-tolDC
PDL1:CD86 ratio				
Mean ratio	1.112	1.200	2.421	4.066
Std dev	0.1792	0.1948	0.1441	0.4258
p-value	0.9908	ref	0.0017	<0.0001
p-value			ref	0.0002
MHCII				
Mean MFI	471.7	759.0	418.0	301.3
Std dev	108.2	194.0	53.78	68.97
p-value	0. 0719	ref	0.032	0.0062
p-value			ref	0.709
CD40				
Mean MFI	628.7	744.0	642.0	680.7
Std dev	117.2	46.57	87.48	91.24
p-value	0.4837	ref	0.5891	0.8791
p-value			ref	0.9769
CD80				
Mean MFI	683.7	1436	781.3	552.7
Std dev	74.66	678.5	166.4	76.26
p-value	0.1191	ref	0.1953	0.0607
p-value			ref	0.9091
CD86				
Mean MFI	233.0	311.7	282.7	283.3
Std dev	11.79	3.055	10.02	20.03
p-value	0.0003	ref	0.0915	0.1006
p-value			ref	>0.999
PDL1				
Mean MFI	529.7	629.7	1000	1531
Std dev	39.55	30.89	64.86	86.75
p-value	0.2656	ref	0.0003	0.0001
p-value			ref	<0.0001

*Table 2.13: **Cytokine expression** of DC conditions for IL-10 and IL-12p70*

Cytokine (pg/ml)		BMDC	LPS-BMDC	tolDC	LPS-tolDC
IL-10 (C56BL6)	Mean	16.86	93.95	123.7	111.4
	Std Dev	15.52	15.89	15.6	16.04
p-values vs BMDC		ref	0.002	0.0002	0.0005
p-values vs LPS-BMDC		-	ref	0.2632	0.7625
p-values vs tolDC		-	-	ref	0.9552
IL-10 (BalbC)	Mean	0	19.12	595	452.1
	Std Dev	0	10.28	52.14	74.58
p-values vs BMDC		ref	0.9971	<0.0001	<0.0001
p-values vs LPS-BMDC		-	ref	<0.0001	<0.0001
p-values vs tolDC		-	-	ref	0.0301
IL-12p70 (C57BL6)	Mean	0.9009	273.8	2.335	43.31
	Std Dev	0.7733	16.19	1.626	4.694
p-values vs BMDC		ref	<0.0001	>0.99	0.0017
p-values vs LPS-BMDC		-	ref	<0.0001	<0.0001
p-values vs tolDC		-	-	ref	0.0021
IL-12p70 (BalbC)	Mean	4.691	621.9	3.052	3.154
	Std Dev	0.7733	7.926	0.7733	1.242
p-values vs BMDC		ref	<0.0001	0.9976	0.9983
p-values vs LPS-BMDC		-	ref	<0.0001	<0.0001
p-values vs tolDC		-	-	ref	>0.99

*Table 2.14: **mRNA expression by co-cultured renal tubular epithelial cells** (RTEC) following LPS-exposure*

RT-qPCR	Time after LPS added		Baseline	2hr	4hr	6hr	24hr
Tumour necrosis factor-alpha (TNF-α)	Control (media)	Mean FC	1.00	26.02	13.99	3.91	2.74
		Std Dev		13.30	10.38	2.09	1.68
	LPS-tolDC	Mean FC	1.00	9.41	6.16	1.52	1.51
		Std Dev		6.93	5.26	0.38	0.34
		P – values vs 0hr		<0.0001	<0.0001	0.02	0.90
		P – values vs LPS-tolDC		0.00	0.00	0.46	1.00
Kidney injury molecule-1 (KIM-1, Havcr1)	Control	Mean FC	1.00	1.71	1.86	6.04	3.42
		Std Dev		0.08	0.61	1.34	1.51
	LPS-tolDC	Mean FC	1.00	1.03	2.30	3.90	1.50
		Std Dev		0.54	1.00	1.04	0.34
		P - values vs 0hr		0.95	0.95	0.79	<0.0001
		P - values vs LPS-tolDC		0.97	0.97	1.00	0.03
Lipocalin-2 (LCN-2)	Control	Mean FC	1.00	1.13	2.30	3.37	34.86
		Std Dev		0.15	0.66	0.65	22.70
	LPS-tolDC	Mean FC	1.00	0.82	1.09	1.30	3.93
		Std Dev		0.08	0.96	0.45	1.59
		P - values vs 0hr		>0.99	>0.99	>0.99	>0.99
		P - values vs LPS-tolDC		>0.99	>0.99	>0.99	>0.99
Interleukin-10 (IL-10)	Control	Mean FC	1.00	2.27	5.28	3.98	6.89
		Std Dev		1.35	1.93	2.19	1.78
	LPS-tolDC	Mean FC	1.00	4.31	3.30	2.70	8.08
		Std Dev		1.80	0.70	1.52	2.31
		P - values vs 0hr		0.96	0.96	0.01	0.15
		P - values vs LPS-tolDC		0.62	0.62	0.72	0.97
Transforming growth factor-β (TGF-β)	Control	Mean FC	1.00	1.40	2.01	2.44	1.83
		Std Dev		0.50	0.67	0.31	0.51
	LPS-tolDC	Mean FC	1.00	0.76	2.34	1.60	1.57
		Std Dev		0.18	1.77	0.68	0.64
		P - values vs 0hr		1.00	1.00	0.37	0.05
		P - values vs LPS-tolDC		0.94	0.94	1.00	0.62
Indoleamine-2 ,3-dioxygenase 1 (IDO-1)	Control	Mean FC	1.00	0.95	0.50	1.13	49.91
		Std Dev		0.42	0.24	0.42	19.38
	LPS-tolDC	Mean FC	1.00	0.55	0.71	1.69	2.75
		Std Dev		0.15	0.46	1.28	1.19
		P - values vs 0hr		>0.99	>0.99	>0.99	>0.99
		P - values vs LPS-tolDC		>0.99	>0.99	>0.99	>0.99

Indoleamine-2,3-dioxygenase 2 (IDO-2)	Control	Mean FC	1.00	1.34	1.35	1.08	2.04
		Std Dev		0.29	0.47	0.27	1.17
	LPS-tolDC	Mean FC	1.00	0.82	3.52	2.09	3.31
		Std Dev		0.37	1.54	0.42	2.18
		P - values vs 0hr		>0.99	>0.99	>0.99	>0.99
		P - values vs LPS-tolDC		1.00	1.00	0.12	0.87

Mean fold change (Mean FC) using 18S housekeeping genes and P values derived from one-way ANOVA

Table 2.15: ***Select list of immune related genes for LPS-tolDC*** *compared to other conditions.*

LFC	**LPS-tolDC vs tolDC**	**LPS-tolDC vs LPS-BMDC**	**LPS-tolDC vs BMDC**	LFC	**LPS-tolDC vs tolDC**	**LPS-tolDC vs LPS-BMDC**	**LPS-tolDC vs BMDC**
Arg1	-2.09667	1.976549	-1.07307	**Il11ra1**	0.319845	0.615778	0.281797
Arg2	3.253468	0.945835	3.776693	**Il12a**	5.153293	-0.49989	8.174076
Ccl12	-1.20387	-1.6824	-3.35729	**Il12b**	6.038782	-4.40924	3.304084
Ccl17	0.869039	-1.76436	-0.44145	**Il12rb1**	-0.86655	-0.63262	-0.33782
Ccl2	0.777039	1.295756	3.159349	**Il13ra1**	0.381808	0.235771	0.380526
Ccl22	1.699524	-2.84264	0.120871	**Il15ra**	0.997332	-1.24989	0.759189
Ccl24	-1.00171	-1.61567	-2.43157	**Il16**	-0.80926	1.0811	-0.63216
Ccl3	0.883949	-0.08235	1.388444	**Il17ra**	0.475846	-0.43051	-0.26361
Ccl4	0.080685	0.298145	0.842358	**Il1a**	4.083222	0.158433	5.510336
Ccl5	7.310175	-1.52527	4.21995	**Il1f9**	3.921249	-0.19619	3.328601
Ccl6	-0.66214	0.494104	-0.43154	**Il1r1**	0.538583	-0.27389	-1.19874
Ccl7	1.013848	2.045218	2.508771	**Il1rap**	0.391772	0.917001	0.832487
Ccl9	0.373023	0.690789	1.210622	**Il1rl2**	-0.1365	0.324336	-0.41626
Ccr2	-4.25522	-4.183	-8.68315	**Il21r**	-0.96005	1.225845	0.941482
Ccr4	3.091865	-1.88216	3.69387	**Il23a**	6.232995	-2.52401	3.352686
Ccr5	-1.56228	-1.75069	-3.58321	**Il27**	1.862236	-0.52438	0.979261
Ccrl2	2.950122	0.663071	4.147455	**Il27ra**	0.260326	1.342045	1.013055
Cd109	0.860948	2.105561	1.039456	**Il2ra**	3.131734	-1.33874	1.497666
Cd14	4.254058	-0.11193	4.311749	**Il2rb**	0.509473	1.054167	1.555929
Cd151	-0.30978	-0.4844	-0.61153	**Il2rg**	1.217845	0.689078	1.355969
Cd177	-0.89125	-1.15376	-2.52399	**Il31ra**	-1.32672	-0.4828	-0.34182
Cd180	-1.47746	-0.63154	-1.12366	**Il33**	0.781428	4.042477	5.282536
Cd1d1	1.362015	-1.64553	0.363935	**Il3ra**	0.889614	0.280511	1.253338
Cd200	2.388856	0.890437	2.768755	**Il4i1**	0.637245	-1.39064	0.425558
Cd200r1	-2.6753	0.255501	-2.36827	**Il4ra**	0.53788	0.457178	1.134218
Cd200r4	-2.42421	0.435824	-2.22663	**Il6**	6.172619	-0.72846	5.833814
Cd22	0.263418	1.319657	-0.65671	**Il6ra**	-0.81589	0.233061	0.177066
Cd226	-1.51034	-3.65962	-3.13629	**Il6st**	-0.73215	1.371917	1.973462
Cd244	0.274835	1.199536	1.601282	**Il7r**	0.555565	0.582119	1.067489
Cd247	1.758542	-0.84917	1.768529	**Nfkb1**	0.864066	-0.50974	0.799418
Cd24a	-1.68941	0.477645	-1.86979	**Nfkb2**	2.225631	-0.68571	1.427816
Cd28	-0.28587	5.563508	5.233684	**Nfkbib**	1.532381	-0.4266	1.070156
Cd2ap	-1.53768	-0.26908	-0.754	**Nfkbid**	-0.12642	-1.11724	-0.38109
Cd300a	-0.60325	1.308032	-0.61849	**Nfkbie**	1.865329	-0.8655	0.888297
Cd300c	-3.04182	-1.63016	-3.63117	**Nfkbil1**	0.356372	0.269935	0.621438
Cd300lb	-2.37264	1.244371	-1.70464	**Nfkbiz**	4.074504	-0.82656	4.143189
Cd300ld	-1.75146	2.687765	-0.14008	**Tgfb1**	-0.37207	0.722376	0.127624
Cd300lf	-1.17723	0.295884	-1.21381	**Tgfb2**	1.660008	-0.99451	0.876477
Cd302	1.735681	0.670423	1.116758	**Tgfb3**	-2.83785	6.613657	6.025008
Cd320	0.499306	0.354912	0.649395	**Tgfbi**	-0.47672	1.479348	0.581181
Cd33	1.5901	0.74805	0.943214	**Tgfbr2**	-0.84058	1.590422	0.265358
Cd34	-1.27435	1.481688	1.01553	**Tgfbr3**	2.573585	2.244869	2.540606
Cd36	-1.0477	-0.75114	-1.2373	**Tlr11**	-6.31607	-6.39833	-8.54699
Cd37	0.606601	1.237989	1.716224	**Tlr13**	-0.39969	1.118484	-0.71531
Cd38	1.493581	0.620906	1.137735	**Tlr2**	2.612965	0.351639	2.172397
Cd40	5.111989	-2.35435	3.221143	**Tlr4**	-0.90402	-0.22382	-1.29406

Cd52	-0.39939	0.84939	0.192901	**Tlr6**	0.756923	0.219094	0.83407
Cd53	0.473216	-0.54709	-0.13529	**Tlr7**	-0.24847	0.533498	-0.52461
Cd6	-2.28456	-0.80575	-2.31889	**Tlr9**	1.254828	-1.68691	-0.24937
Cd63	0.711756	0.448368	0.253058	**Tnf**	2.263949	-0.30507	3.092283
Cd68	0.583839	0.356308	0.667524	**Tnfaip1**	0.167402	-0.38076	0.144167
Cd72	1.855491	-0.86802	1.878253	**Tnfaip2**	1.114244	-0.31157	1.310507
Cd74	0.687567	-0.2491	0.673518	**Tnfaip3**	1.863345	0.320263	2.591937
Cd79b	0.858522	-0.85757	1.263182	**Tnfaip8**	0.345506	0.099522	0.349479
Cd80	0.476007	-1.28418	0.334481	**Tnfaip8l1**	-0.48053	-0.82551	-1.19827
Cd81	0.70824	-0.57711	0.289556	**Tnfaip8l2**	-0.43443	0.948932	0.306935
Cd82	1.03627	0.146741	1.114528	**Tnfaip8l3**	-4.78178	-1.57269	-4.19045
Cd83	1.197086	-2.61214	-1.36555	**Tnfrsf10b**	0.892513	-0.31934	1.0574
Cd84	-0.98901	0.892329	-0.88695	**Tnfrsf11a**	2.11007	-0.96582	0.907791
Cd86	0.444962	-2.69011	-0.82257	**Tnfrsf1a**	-0.21576	0.389238	0.325203
Cd9	-0.52012	0.301865	-0.65463	**Tnfrsf1b**	2.824154	0.375055	2.693143
Cd93	-1.50094	0.491892	-2.47585	**Tnfrsf21**	0.612022	0.52008	0.149051
Cxcl1	9.040715	0.601758	9.417942	**Tnfrsf22**	0.302311	1.742311	1.795871
Cxcl10	6.192707	-1.73903	4.558915	**Tnfrsf23**	0.520359	1.533683	1.410734
Cxcl16	4.70377	-0.26187	3.047288	**Tnfrsf26**	0.977304	1.525288	1.658149
Cxcl2	7.311417	0.965583	7.770714	**Tnfrsf4**	0.310738	-0.79512	-0.30326
Cxcl3	6.160446	1.791774	7.349578	**Tnfrsf8**	2.437934	0.7416	2.80395
Cxcl5	6.072586	0.44043	6.894228	**Tnfrsf9**	2.53655	0.127839	1.676944
Cxcl9	1.750885	-1.1062	0.685324	**Tnfsf10**	-1.95887	-1.27521	-2.36227
Cxcr2	-4.57896	-1.99869	-4.17705	**Tnfsf12**	-0.13511	0.856287	-0.16093
Cxcr4	-0.84732	-0.45993	-1.68927	**Tnfsf13**	-0.54041	0.781044	-0.54492
Cxcr5	1.992014	1.246426	4.202628	**Tnfsf13b**	0.715953	3.635555	3.839314
Gsdme	-0.41846	1.985026	1.128499	**Tnfsf14**	-0.67736	3.178998	2.693488
Il10ra	1.498481	-0.15602	1.235495	**Tnfsf9**	1.368414	-0.20251	2.913326
Il10rb	0.92446	-0.35589	0.505433	**Tnfsfm13**	-0.68829	1.00958	-0.66531

Table 2.16: ***Serum creatinine*** *and percentage weight change 24-hours post bilateral renal IRI*

IRI: 20min	**Creatinine (µmol//L)**				**% Weight change**		
	n	*Mean*	*Std Dev*	*P value*	*Mean %*	*Std Dev*	*P value*
Control/PBS	8	122.4	44.71	-	-11.79	3.088	-
tolDC (D0)	10	97.3	33.45	0.2817	-9.724	2.311	0.9096
tolDC (D-1)	10	103.1	35.19	0.4524	-11.15	1.662	0.9936
LPS-tolDC (D0)	7	42.71	29.02	0.0003	-8.829	2.523	0.1461
LPS-tolDC (D-1)	5	18.2	8.044	<0.0001	-8.937	2.5	0.1735
Allo-tolDC (D0)	8	40.13	30.32	0.0007	-9.324	1.196	0.1912
Allo-tolDC (D-1)	6	39.5	44.17	0.0011	-9.326	2.224	0.1705

P values derived from one-way ANOVA

Table 2.17:: ***Histological injury*** *and TUNEL scoring of mice kidney 24-hours post bilateral renal IRI*

IRI: 20min	**Histological Injury Score**				**TUNEL staining**			
	n	*Mean*	*Std Dev*	*P value*	*n*	*Mean*	*Std Dev*	*P value*
Control/PBS	4	3.60	0.31	-	3	25.83	6.68	-
tolDC (D0)	6	3.99	0.21	0.36	-	-	-	-
tolDC (D-1)	5	4.22	0.26	0.30	-	-	-	-
LPS-tolDC (D0)	9	2.30	0.86	0.01	3	5.17	2.27	<0.0001
LPS-tolDC (D-1)	5	2.10	0.93	0.01	3	4.92	2.53	<0.0001
Allo-tolDC (D0)	7	2.49	0.66	0.03	4	3.75	3.60	<0.0001
Allo-tolDC (D-1)	5	1.97	0.51	0.00	5	2.25	1.46	<0.0001

Histological score based on degree of tubular dilatation, cell necrosis, infarction and cast formation seen on haematoxylin and eosin staining. TUNEL scores based on number of positive cells per high power field. Both scored at 20x magnification. P values derived from one-way ANOVA

Table 2.18: Absolute and % of CD45 proportions from cell tracking studies

DCs in the kidney		**tolDC**	**LPS-tolDC**
Absolute $CD45^+$ count	*n*	4	5
	Mean	$1.772x10^6$	$1.73x10^6$
	Std Dev	$0.351x10^6$	$0.405x10^6$
	p-value	ref	0.8911
$Stain^+$ cell $\%CD45^+$	*Mean*	3.55	7.72
	Std Dev	0.4796	1.42
	p-value	ref	0.0009

Table 2.19: Absolute cell counts of kidney immune cells 24-hours post IRI

Absolute cell counts		**PBS (n = 6)**	**LPS-tolDC (n = 6)**	**P-value**
$CD45^+$	*Mean (Std Dev)*	1.840 (0.679) $x10^6$	1.823 (0.488) $x10^6$	0.998
$CD11b^+$	*Mean (Std Dev)*	1.209 (0.402) $x10^6$	1.370 (0.4050 $x10^6$	0.8955
$CD3^+$	*Mean (Std Dev)*	0.154 (0.051) $x10^6$	0.156 (0.119) $x10^6$	>0.99

Table 2.20: relative cell populations from kidneys 24-hours post renal IRI

Kidney Flow		**PBS**		**LPS-tolDC**		
% CD45+	N	Mean	Std Dev	Mean	Std Dev	p-value
Myeloid: CD3- NK- B220- Ly6G-	5	45.34	4.45	49.94	3.58	0.11
Ly6G+ Neutrophils	5	34.48	5.89	29.04	9.61	0.31
CD3+ T-cells	5	9.09	2.46	7.07	4.17	0.38
CD3+ CD4+ CD25+	5	2.77	2.98	0.07	0.06	0.18
CD11b-hi	6	26.02	2.81	37.73	5.33	0.00
CD11b-lo	6	14.65	4.46	10.06	2.34	0.05
CD11c+	5	13.14	1.67	18.92	3.61	0.01
CD11c-	5	31.16	4.70	31.30	4.17	0.96
F480-hi	6	17.32	4.85	11.72	3.05	0.04
F480-int	6	22.88	4.49	31.07	3.69	0.01
F480-lo	6	3.47	0.83	4.72	1.36	0.08
MHCII+	6	22.82	9.48	25.32	3.78	0.60
MHCII-	6	16.98	1.77	23.92	5.61	0.02
CD11b-hi Ly6C-hi	6	16.62	3.81	17.91	5.81	0.06
CD11b-hi Ly6C-int	6	4.38	0.76	10.01	1.72	0.36
F480-hi Ly6C-lo	6	15.77	5.67	12.50	3.24	0.66
F480-int Ly6C-hi	6	18.23	3.47	27.12	6.27	0.00
MHCII+ Ly6C+	6	6.22	1.53	7.57	3.59	0.25
MHCII+ Ly6C-lo	6	18.14	5.57	15.80	4.00	0.01
MHCII- Ly6C-hi	6	11.69	2.07	15.11	5.19	0.42
CD11b-hi F480-lo	6	2.04	0.45	3.98	1.59	0.42
CD11b Ly6c-lo	6	18.38	5.08	17.87	2.80	0.16
CD11b-hi F480-int	6	23.05	3.75	30.35	6.46	0.00
CD11b-lo F480-hi	6	15.02	6.19	10.02	2.97	0.03
CD11b-hi F480-lo	6	2.04	0.45	3.98	1.59	0.13
CD11b-hi F480-int Ly6C-hi	6	17.55	3.58	21.28	6.35	0.24
CD11b-hi F480-int MHCII+	6	6.61	1.37	7.77	3.93	0.51
CD11b-hi F480-int MHCII+ CD11c+	6	1.83	0.31	3.15	1.60	0.08
CD11b-hi F480-int MHCII+ CD11c-	6	4.50	0.80	4.63	2.54	0.91
CD11b-lo F480-hi Ly6C-hi	6	0.36	0.27	0.19	0.08	0.18
CD11b-lo F480-hi MHCII+	6	13.22	4.94	9.79	2.85	0.17
CD11b-lo F480-hi MHCII+ CD11c+	6	5.38	1.62	5.87	2.18	0.67
CD11b-lo F480-hi MHCII+ CD11c-	6	9.42	4.52	3.93	1.57	0.02
CD11b-hi F480-lo Ly6C-hi	6	0.17	0.25	0.28	0.17	0.37
CD11b-hi F480-lo MHCII+	6	2.00	0.47	3.35	1.16	0.02
CD11b-hi F480-lo MHC+ CD11c+	6	1.52	0.33	2.64	0.86	0.01
CD11b-hi F480-lo MHCII+ CD11c-	6	0.48	0.17	0.71	0.38	0.20
% Parent						
CD11b-lo F480-hi CD40+	3	9.09	2.46	7.07	4.17	0.38
CD11b-lo F480-hi CD80+	3	2.77	2.98	0.07	0.06	0.18

CD11b-lo F480-hi CD86+	3	26.02	2.81	37.73	5.33	0.00
CD11b-lo F480-hi PDL1+	3	14.65	4.46	10.06	2.34	0.05
CD11b-hi F480-int CD40+	3	13.14	1.67	18.92	3.61	0.01
CD11b-hi F480-int CD80+	3	31.16	4.70	31.30	4.17	0.96
CD11b-hi F480-int CD86+	3	17.32	4.85	11.72	3.05	0.04
CD11b-hi F480-int PDL1+	3	22.88	4.49	31.07	3.69	0.01
CD11b-hi F480-lo CD40+	3	3.47	0.83	4.72	1.36	0.08
CD11b-hi F480-lo CD80+	3	22.82	9.48	25.32	3.78	0.60
CD11b-hi F480-lo CD86+	3	16.98	1.77	23.92	5.61	0.02
CD11b-hi F480-lo PDL1+	3	16.62	3.81	17.91	5.81	0.06

P values derived from unpaired t-test

Table 2.21: serum creatinine for liposome PBS (L.PBS) or clodronate (L.Clod) treated mice 24-hours after renal IRI

Serum creatinine (μmol/L)	**N**	**Mean**	**Std Dev**	**P-value vs**		
				20min, L. PBS	20min, L.Clod	22min, L.Clod
20 minutes bilateral renal IRI						
L.PBS	5	91.8	33.48	*ref*		
L.PBS + AllotolDC	4	23.75	14.95	0.0115		
L.Clod	3	21.67	10.69	0.0176	*ref*	
L.Clod + AllotolDC	3	26.33	24.91	0.029	>0.9999	
22 minutes bilateral renal IRI						
L.Clod	4	155	44.73		<0.0001	*ref*
L.Clod + AllotolDC	5	30.6	19.02			<0.0001

P values derived from one-way ANOVA

Table 2.22: Kidney mRNA expression 24-hours following surgery

Kidney mRNA expression		**Sham**	**PBS/Control**	**AllotolDC (D-1)**	**LPS-tolDC (D-1)**	**AllotolDC (D0)**	**LPS-tolDC (D0)**
KIM1	*Mean*	1.90	8498.00	1976.00	2493.00	1923.00	2406.00
	Std Dev	1.89	4280.00	480.90	1469.00	888.80	914.40
	p-value	<0.0001	*ref*	<0.0001	<0.0001	<0.0001	<0.0001
CXCL2	*Mean*	1.15	182.00	104.30	191.80	113.00	177.00
	Std Dev	0.62	123.10	40.11	44.06	49.34	115.80
	p-value	0.00	*ref*	0.36	1.00	0.42	1.00
CCL2	*Mean*	1.05	56.59	20.79	16.27	12.88	14.54
	Std Dev	0.33	27.33	10.92	8.70	9.45	8.97
	p-value	<0.0001	*ref*	0.00	0.00	<0.0001	<0.0001
TNF-α	*Mean*	3.74	51.12	8.17	11.82	10.51	11.55
	Std Dev	0.53	27.31	3.85	7.85	8.33	5.40
	p-value	<0.0001	*ref*	<0.0001	0.00	<0.0001	<0.0001
IL1β	*Mean*	1.02	11.36	5.38	4.30	5.21	5.81
	Std Dev	0.20	1.17	2.73	2.10	1.75	1.71
	p-value	<0.0001	*ref*	<0.0001	<0.0001	<0.0001	<0.0001
IL6	*Mean*	1.09	806.60	171.80	154.50	141.50	156.50
	Std Dev	0.49	322.30	106.20	79.44	60.30	121.30
	p-value	<0.0001	*ref*	<0.0001	<0.0001	<0.0001	<0.0001
SOD1	*Mean*	1.00	4.13	1.50	2.23	0.80	1.85
	Std Dev	0.26	1.62	0.74	1.04	0.81	0.11
	p-value	<0.0001	*ref*	0.00	0.01	<0.0001	0.01
iNOS	*Mean*	1.05	2.75	0.84	0.77	0.31	0.53
	Std Dev	0.39	1.19	0.39	0.49	0.19	0.16
	p-value	0.00	*ref*	0.00	0.00	<0.0001	0.00
SOD3	*Mean*	1.06	1.63	0.63	2.46	0.87	2
	Std Dev	0.45	2.89	0.91	1.76	0.30	1.23
	p-value	0.95	*ref*	0.81	0.89	0.92	0.67

Mean fold change (Mean FC) using 18S housekeeping genes and P values derived from one-way ANOVA

Table 2.23: Software used for this manuscript

Software	Version	Company
R	V 4.0.3	R Core Team
R-studio	Ghost Orchid 2021.09.1	R Core Team
FlowJo	10.8.1	BD Bioscience
LegendPlex		BioLegend
Prism	Version 9	Graph Pad
Loupe Browser	Version 6	10x Genomics
Sydney University High Performance Computing Cluster		

Table 2.24:Reagent and equipment details

Item	Additional info	Company
UltraPure LPS-B5	# TLRL-B5LPS	InvivoGen
IL-10	# 210-10	Peperotech
Dead Cell Removal Kit	# 130-090-101	Miltenyi Biotec
CD11c beads	# 130-125-835	Miltenyi Biotec
IL-4	# 130-097-761	Miltenyi Biotec
GM-CSF	# 130-095-793	Miltenyi Biotec
Multi-tissue Dissociation Kit 2	# 130-110-203	Miltenyi Biotec
Transwell polyester inserts	0.4um pore, #CLS3450	Corning
IL-10 Instant ELISA kit	# BMS61	ThermoFischer
IL-12p70 mouse ELISA kit	# BMS6004	ThermoFischer
PMA	# P1585	Sigma Aldrich
Ionomycin	# 19657	Sigma Aldrich
1α,25-dihydroxyvitamin D3	# D1530	Sigma Aldrich
Epidermal growth factor	# E4127	Sigma Aldrich
PGE1	# P5515	Sigma Aldrich
Tri-iodothyronine	# T2877	Sigma Aldrich
Insulin	# I5500	Sigma Aldrich
Hydrocortisone	# H4001	Sigma Aldrich
Apotransferrin	# T1147	Sigma Aldrich
Liposomal Clodronate	# CP-005-005	Liposoma
Liposomal PBS	# CP-005-005	Liposoma
Red Cell Lysis Buffer	# 11814389001	ThermoFischer
RPMI 1640	# 21870076	Gibco
DMEM F/12	# 1130082	Gibco
FBS (heat-inactivated)	# 10099141	Gibco
Penicillin/streptomycin	# 10378016	Gibco
L-glutamine	# 25030081	Gibco
Sodium pyruvate	# 11360070	Gibco
Non-essential amino acid	# 11140076	Gibco
Bioline ISOLATE RNA II mini kit	# Bio-52073	Meridian Bioscience
SensiFast cDNA synthesis	# Bio-65054	Meridian Bioscience
SensiFast Probe no-ROX	# Bio-76005	Meridian Bioscience
β-mercaptoethanol	# 21985023	Gibco

2.9 References

1. Susantitaphong P, Cruz DN, Cerda J, et al. World Incidence of AKI: A Meta-Analysis. *Clinical Journal of the American Society of Nephrology*. 2013;8(9):1482. doi:10.2215/CJN.00710113
2. Chawla LS, Eggers PW, Star RA, Kimmel PL. Acute Kidney Injury and Chronic Kidney Disease as Interconnected Syndromes. *New England Journal of Medicine*. 2014/07/03 2014;371(1):58-66. doi:10.1056/NEJMra1214243
3. Griffin BR, You Z, Holmen J, et al. Incident infection following acute kidney injury with recovery to baseline creatinine: A propensity score matched analysis. *PloS one*. 2019;14(6):e0217935. doi:10.1371/journal.pone.0217935
4. Chawla LS, Amdur RL, Shaw AD, Faselis C, Palant CE, Kimmel PL. Association between AKI and Long-Term Renal and Cardiovascular Outcomes in United States Veterans. *Clinical Journal of the American Society of Nephrology*. 2014;9(3):448. doi:10.2215/CJN.02440213
5. Ikizler TA, Parikh CR, Himmelfarb J, et al. A prospective cohort study of acute kidney injury and kidney outcomes, cardiovascular events, and death. *Kidney International*. 2021;99(2):456-465. doi:10.1016/j.kint.2020.06.032
6. Sawhney S, Marks A, Fluck N, Levin A, Prescott G, Black C. Intermediate and Long-term Outcomes of Survivors of Acute Kidney Injury Episodes: A Large Population-Based Cohort Study. *Am J Kidney Dis*. Jan 2017;69(1):18-28. doi:10.1053/j.ajkd.2016.05.018
7. Gill J, Dong J, Rose C, Gill JS. The risk of allograft failure and the survival benefit of kidney transplantation are complicated by delayed graft function. *Kidney International*. 2016/06/01/ 2016;89(6):1331-1336. doi:https://doi.org/10.1016/j.kint.2016.01.028
8. Okusa MD, Davenport A. Reading between the (guide)lines--the KDIGO practice guideline on acute kidney injury in the individual patient. *Kidney Int*. Jan 2014;85(1):39-48. doi:10.1038/ki.2013.378
9. Summary of Recommendation Statements. *Kidney Int Suppl (2011)*. 2012/03/01/ 2012;2(1):8-12. doi:https://doi.org/10.1038/kisup.2012.7
10. Ostermann M, Zarbock A, Goldstein S, et al. Recommendations on Acute Kidney Injury Biomarkers From the Acute Disease Quality Initiative Consensus Conference: A Consensus Statement. *JAMA Network Open*. 2020;3(10):e2019209-e2019209. doi:10.1001/jamanetworkopen.2020.19209
11. Ronco C, Bellomo R, Kellum JA. Acute kidney injury. *The Lancet*. 2019/11/23/ 2019;394(10212):1949-1964. doi:https://doi.org/10.1016/S0140-6736(19)32563-2
12. Selby NM, Taal MW. Long-term outcomes after AKI—a major unmet clinical need. *Kidney International*. 2019;95(1):21-23. doi:10.1016/j.kint.2018.09.005
13. Doi K. How to sharpen a novel sword from AKI basic research. *Kidney International*. 2019;95(1):19-20. doi:10.1016/j.kint.2018.09.017
14. Li J, Rogers NM, Hawthorne WJ. Chapter 1 - Ischemia-reperfusion injury. In: Orlando G, Keshavjee S, eds. *Organ Repair and Regeneration*. Academic Press; 2021:1-42.
15. Dong X, Swaminathan S, Bachman LA, Croatt AJ, Nath KA, Griffin MD. Resident dendritic cells are the predominant TNF-secreting cell in early renal ischemia-reperfusion injury. *Kidney Int*. Apr 2007;71(7):619-28. doi:10.1038/sj.ki.5002132
16. Macconi D, Chiabrando C, Schiarea S, et al. Proteasomal processing of albumin by renal dendritic cells generates antigenic peptides. *J Am Soc Nephrol*. Jan 2009;20(1):123-30. doi:10.1681/asn.2007111233
17. Morelli AE, Thomson AW. Tolerogenic dendritic cells and the quest for transplant tolerance. Review Article. *Nature Reviews Immunology*. 07/13/online 2007;7:610. doi:10.1038/nri2132
18. Ezzelarab MB, Raich-Regue D, Lu L, et al. Renal Allograft Survival in Nonhuman Primates Infused With Donor Antigen-Pulsed Autologous Regulatory Dendritic Cells. *Am J Transplant*. Jun 2017;17(6):1476-1489. doi:10.1111/ajt.14182
19. Ezzelarab MB, Zahorchak AF, Lu L, et al. Regulatory dendritic cell infusion prolongs kidney allograft survival in nonhuman primates. *Am J Transplant*. Aug 2013;13(8):1989-2005. doi:10.1111/ajt.12310
20. Ezzelarab MB, Lu L, Shufesky WF, Morelli AE, Thomson AW. Donor-Derived Regulatory Dendritic Cell Infusion Maintains Donor-Reactive CD4(+)CTLA4(hi) T Cells in Non-Human Primate Renal Allograft Recipients Treated with CD28 Co-Stimulation Blockade. *Front Immunol*. 2018;9:250-250. doi:10.3389/fimmu.2018.00250
21. Fu F, Li Y, Qian S, et al. COSTIMULATORY MOLECULE-DEFICIENT DENDRITIC CELL PROGENITORS (MHC CLASS II+, CD80dim, CD86-) PROLONG CARDIAC ALLOGRAFT SURVIVAL IN NONIMMUNOSUPPRESSED RECIPIENTS12. *Transplantation*. 1996;62(5)
22. Divito SJ, Wang Z, Shufesky WJ, et al. Endogenous dendritic cells mediate the effects of intravenously injected therapeutic immunosuppressive dendritic cells in transplantation. *Blood*. Oct 14 2010;116(15):2694-705. doi:10.1182/blood-2009-10-251058
23. Bériou G, Pêche H, Guillonneau C, Merieau E, Cuturi MC. Donor-specific allograft tolerance by administration of recipient-derived immature dendritic cells and suboptimal immunosuppression. *Transplantation*. Apr 27 2005;79(8):969-72. doi:10.1097/01.tp.0000158277.50073.35
24. Turnquist HR, Raimondi G, Zahorchak AF, Fischer RT, Wang Z, Thomson AW. Rapamycin-conditioned dendritic cells are poor stimulators of allogeneic CD4+ T cells, but enrich for antigen-specific Foxp3+ T regulatory cells and promote organ transplant tolerance. *Journal of immunology (Baltimore, Md : 1950)*. Jun 1 2007;178(11):7018-31. doi:10.4049/jimmunol.178.11.7018
25. Taner T, Hackstein H, Wang Z, Morelli AE, Thomson AW. Rapamycin-Treated, Alloantigen-Pulsed Host Dendritic Cells Induce Ag-Specific T Cell Regulation and Prolong Graft Survival. https://doi.org/10.1046/j.1600-6143.2004.00673.x. *American Journal of Transplantation*. 2005/02/01 2005;5(2):228-236. doi:https://doi.org/10.1046/j.1600-6143.2004.00673.x
26. Sawitzki B, Harden PN, Reinke P, et al. Regulatory cell therapy in kidney transplantation (The ONE Study): a harmonised design and analysis of seven non-randomised, single-arm, phase 1/2A trials. *The Lancet*. 2020;395(10237):1627-1639. doi:10.1016/S0140-6736(20)30167-7
27. Marin E, Bouchet-Delbos L, Renoult O, et al. Human Tolerogenic Dendritic Cells Regulate Immune Responses through Lactate Synthesis. *Cell Metabolism*. 2019;30(6):1075-1090.e8. doi:10.1016/j.cmet.2019.11.011
28. Galea R, Nel HJ, Talekar M, et al. PD-L1– and calcitriol-dependent liposomal antigen-specific regulation of systemic inflammatory autoimmune disease. *JCI Insight*. 09/19/ 2019;4(18)doi:10.1172/jci.insight.126025
29. Flórez-Grau G, Zubizarreta I, Cabezón R, Villoslada P, Benitez-Ribas D. Tolerogenic Dendritic Cells as a Promising Antigen-Specific Therapy in the Treatment of Multiple Sclerosis and Neuromyelitis Optica From Preclinical to Clinical Trials. *Front Immunol*. 2018;9:1169-1169. doi:10.3389/fimmu.2018.01169
30. Thomas R. Dendritic cells and the promise of antigen-specific therapy in rheumatoid arthritis. *Arthritis Res Ther*. Feb 4 2013;15(1):204. doi:10.1186/ar4130
31. Giannoukakis N, Phillips B, Finegold D, Harnaha J, Trucco M. Phase I (safety) study of autologous tolerogenic dendritic cells in type 1 diabetic patients. *Diabetes Care*. Sep 2011;34(9):2026-32. doi:10.2337/dc11-0472

32. Jauregui-Amezaga A, Cabezón R, Ramírez-Morros A, et al. Intraperitoneal Administration of Autologous Tolerogenic Dendritic Cells for Refractory Crohn's Disease: A Phase I Study. *Journal of Crohn's and Colitis*. 2015;9(12):1071-1078. doi:10.1093/ecco-jcc/jjv144
33. Benham H, Nel HJ, Law SC, et al. Citrullinated peptide dendritic cell immunotherapy in HLA risk genotype–positive rheumatoid arthritis patients. *Science Translational Medicine*. 2015;7(290):290ra87. doi:10.1126/scitranslmed.aaa9301
34. Bell GM, Anderson AE, Diboll J, et al. Autologous tolerogenic dendritic cells for rheumatoid and inflammatory arthritis. *Annals of the Rheumatic Diseases*. 2017;76(1):227. doi:10.1136/annrheumdis-2015-208456
35. Li J, Thomson AW, Rogers NM. Myeloid and Mesenchymal Stem Cell Therapies for Solid Organ Transplant Tolerance. *Transplantation*. Dec 1 2021;105(12):e303-e321. doi:10.1097/tp.0000000000003765
36. Zahorchak AF, Kean LS, Tokita D, et al. Infusion of Stably Immature Monocyte-Derived Dendritic Cells Plus CTLA4Ig Modulates Alloimmune Reactivity in Rhesus Macaques. *Transplantation*. 2007;84(2)
37. Thomson AW, Metes DM, Ezzelarab MB, Raïch-Regué D. Regulatory dendritic cells for human organ transplantation. *Transplantation Reviews*. 2019/07/01/ 2019;33(3):130-136. doi:https://doi.org/10.1016/j.trre.2019.05.001
38. Suuring M, Moreau A. Regulatory Macrophages and Tolerogenic Dendritic Cells in Myeloid Regulatory Cell-Based Therapies. *International Journal of Molecular Sciences*. 2021;22(15)doi:10.3390/ijms22157970
39. Robinson MD, Oshlack A. A scaling normalization method for differential expression analysis of RNA-seq data. *Genome Biology*. 2010/03/02 2010;11(3):R25. doi:10.1186/gb-2010-11-3-r25
40. Lund SP, Nettleton D, McCarthy DJ, Smyth GK. Detecting differential expression in RNA-sequence data using quasi-likelihood with shrunken dispersion estimates. *Stat Appl Genet Mol Biol*. Oct 22 2012;11(5)doi:10.1515/1544-6115.1826
41. Chen Y, Lun AT, Smyth GK. From reads to genes to pathways: differential expression analysis of RNA-Seq experiments using Rsubread and the edgeR quasi-likelihood pipeline. *F1000Res*. 2016;5:1438. doi:10.12688/f1000research.8987.2
42. Rogers NM, Zhang ZJ, Wang J-J, Thomson AW, Isenberg JS. CD47 regulates renal tubular epithelial cell self-renewal and proliferation following renal ischemia reperfusion. *Kidney International*. 2016;90(2):334-347. doi:10.1016/j.kint.2016.03.034
43. Raghubar AM, Pham, D.T., Tan, X. et a. Spatially resolved transcriptomes of healthy mammalian kidneys illustrate the molecular complexity and interactions of functional nephron segments. *Front Med*. 2022;in press
44. Alquicira-Hernandez J, Powell JE. Nebulosa recovers single-cell gene expression signals by kernel density estimation. *Bioinformatics*. 2021;37(16):2485-2487. doi:10.1093/bioinformatics/btab003
45. Navarro-Barriuso J, Mansilla MJ, Naranjo-Gómez M, et al. Comparative transcriptomic profile of tolerogenic dendritic cells differentiated with vitamin D3, dexamethasone and rapamycin. *Sci Rep*. 2018/10/08 2018;8(1):14985. doi:10.1038/s41598-018-33248-7
46. Navarro-Barriuso J, Mansilla MJ, Quirant-Sánchez B, Teniente-Serra A, Ramo-Tello C, Martínez-Cáceres EM. Vitamin D3-Induced Tolerogenic Dendritic Cells Modulate the Transcriptomic Profile of T CD4+ Cells Towards a Functional Hyporesponsiveness. Original Research. *Front Immunol*. 2021-January-20 2021;11doi:10.3389/fimmu.2020.599623
47. Navarro-Barriuso J, Mansilla MJ, Quirant-Sánchez B, et al. MAP7 and MUCL1 Are Biomarkers of Vitamin D3-Induced Tolerogenic Dendritic Cells in Multiple Sclerosis Patients. Original Research. *Front Immunol*. 2019-June-19 2019;10doi:10.3389/fimmu.2019.01251
48. Robertson H, Li J, Kim HJ, et al. Transcriptomic Analysis Identifies A Tolerogenic Dendritic Cell Signature. Original Research. *Front Immunol*. 2021-October-20 2021;12doi:10.3389/fimmu.2021.733231
49. Unger WW, Laban S, Kleijwegt FS, van der Slik AR, Roep BO. Induction of Treg by monocyte-derived DC modulated by vitamin D3 or dexamethasone: differential role for PD-L1. *European journal of immunology*. Nov 2009;39(11):3147-59. doi:10.1002/eji.200839103
50. Nikolic T, Roep BO. Regulatory multitasking of tolerogenic dendritic cells - lessons taken from vitamin d3-treated tolerogenic dendritic cells. *Front Immunol*. 2013;4:113-113. doi:10.3389/fimmu.2013.00113
51. Rudman-Melnick V, Adam M, Potter A, et al. Single-Cell Profiling of AKI in a Murine Model Reveals Novel Transcriptional Signatures, Profibrotic Phenotype, and Epithelial-to-Stromal Crosstalk. *Journal of the American Society of Nephrology*. 2020;31(12):2793. doi:10.1681/ASN.2020010052
52. Park J, Shrestha R, Qiu C, et al. Single-cell transcriptomics of the mouse kidney reveals potential cellular targets of kidney disease. *Science*. May 18 2018;360(6390):758-763. doi:10.1126/science.aar2131
53. Kirita Y, Wu H, Uchimura K, Wilson PC, Humphreys BD. Cell profiling of mouse acute kidney injury reveals conserved cellular responses to injury. *Proc Natl Acad Sci U S A*. Jul 7 2020;117(27):15874-15883. doi:10.1073/pnas.2005477117
54. Kiselev VY, Kirschner K, Schaub MT, et al. SC3: consensus clustering of single-cell RNA-seq data. *Nat Methods*. 2017;14(5):483-486. doi:10.1038/nmeth.4236
55. Dixon EE, Wu H, Muto Y, Wilson PC, Humphreys BD. Spatially Resolved Transcriptomic Analysis of Acute Kidney Injury in a Female Murine Model. *Journal of the American Society of Nephrology*. 2022;33(2):279. doi:10.1681/ASN.2021081150
56. Dries R, Zhu Q, Dong R, et al. Giotto: a toolbox for integrative analysis and visualization of spatial expression data. *Genome Biology*. 2021/03/08 2021;22(1):78. doi:10.1186/s13059-021-02286-2
57. Kim S-Y, Volsky DJ. PAGE: Parametric Analysis of Gene Set Enrichment. *BMC Bioinformatics*. 2005/06/08 2005;6(1):144. doi:10.1186/1471-2105-6-144
58. Thomson AW, Humar A, Lakkis FG, Metes DM. Regulatory dendritic cells for promotion of liver transplant operational tolerance: Rationale for a clinical trial and accompanying mechanistic studies. *Human immunology*. May 2018;79(5):314-321. doi:10.1016/j.humimm.2017.10.017
59. Li L, Huang L, Ye H, et al. Dendritic cells tolerized with adenosine A_2AR agonist attenuate acute kidney injury. *J Clin Invest*. Nov 2012;122(11):3931-42. doi:10.1172/jci63170
60. Bajwa A, Huang L, Kurmaeva E, et al. Sphingosine 1-Phosphate Receptor 3–Deficient Dendritic Cells Modulate Splenic Responses to Ischemia-Reperfusion Injury. *Journal of the American Society of Nephrology*. 2016;27(4):1076. doi:10.1681/ASN.2015010095
61. Rousselle TV, Kuscu C, Kuscu C, et al. FTY720 Regulates Mitochondria Biogenesis in Dendritic Cells to Prevent Kidney Ischemic Reperfusion Injury. Original Research. *Front Immunol*. 2020-June-23 2020;11doi:10.3389/fimmu.2020.01278
62. Namwanje M, Bisunke B, Rousselle TV, et al. Rapamycin Alternatively Modifies Mitochondrial Dynamics in Dendritic Cells to Reduce Kidney Ischemic Reperfusion Injury. *Int J Mol Sci*. May 20 2021;22(10)doi:10.3390/ijms22105386
63. Anderson AE, Swan DJ, Sayers BL, et al. LPS activation is required for migratory activity and antigen presentation by tolerogenic dendritic cells. *J Leukoc Biol*. Feb 2009;85(2):243-50. doi:10.1189/jlb.0608374
64. Lan YY, Wang Z, Raimondi G, et al. "Alternatively activated" dendritic cells preferentially secrete IL-10, expand Foxp3+CD4+ T cells, and induce long-term organ allograft survival in combination with CTLA4-Ig. *Journal of immunology (Baltimore, Md : 1950)*. Nov 1 2006;177(9):5868-77. doi:10.4049/jimmunol.177.9.5868
65. Saraiva M, O'Garra A. The regulation of IL-10 production by immune cells. *Nature Reviews Immunology*. 2010/03/01 2010;10(3):170-181. doi:10.1038/nri2711

66. Ouyang W, O'Garra A. IL-10 Family Cytokines IL-10 and IL-22: from Basic Science to Clinical Translation. *Immunity*. 2019/04/16/ 2019;50(4):871-891. doi:https://doi.org/10.1016/j.immuni.2019.03.020
67. Sakai K, Nozaki Y, Murao Y, et al. Protective effect and mechanism of IL-10 on renal ischemia–reperfusion injury. *Laboratory Investigation*. 2019/05/01 2019;99(5):671-683. doi:10.1038/s41374-018-0162-0
68. Mondanelli G, Bianchi R, Pallotta MT, et al. A Relay Pathway between Arginine and Tryptophan Metabolism Confers Immunosuppressive Properties on Dendritic Cells. *Immunity*. 2017/02/21/ 2017;46(2):233-244. doi:https://doi.org/10.1016/j.immuni.2017.01.005
69. Esebanmen GE, Langridge WHR. The role of TGF-beta signaling in dendritic cell tolerance. *Immunologic Research*. 2017/10/01 2017;65(5):987-994. doi:10.1007/s12026-017-8944-9
70. Chen W, Jin W, Hardegen N, et al. Conversion of Peripheral CD4+CD25− Naive T Cells to CD4+CD25+ Regulatory T Cells by TGF-β Induction of Transcription Factor Foxp3. *Journal of Experimental Medicine*. 2003;198(12):1875-1886. doi:10.1084/jem.20030152
71. Mou HB, Lin MF, Huang H, Cai Z. Transforming Growth Factor-β1 Modulates Lipopolysaccharide-Induced Cytokine/Chemokine Production and Inhibits Nuclear Factor-κB, Extracellular Signal-Regulated Kinases and p38 Activation in Dendritic Cells in Mice. *Transplantation Proceedings*. 2011/06/01/ 2011;43(5):2049-2052. doi:https://doi.org/10.1016/j.transproceed.2011.02.054
72. Belladonna ML, Volpi C, Bianchi R, et al. Cutting Edge: Autocrine TGF-β Sustains Default Tolerogenesis by IDO-Competent Dendritic Cells. *The Journal of Immunology*. 2008;181(8):5194. doi:10.4049/jimmunol.181.8.5194
73. Murray PJ. Amino acid auxotrophy as a system of immunological control nodes. *Nature Immunology*. 2016/02/01 2016;17(2):132-139. doi:10.1038/ni.3323
74. Panfili E, Mondanelli G, Orabona C, et al. IL-35Ig-expressing dendritic cells induce tolerance via Arginase 1. *J Cell Mol Med*. May 2019;23(5):3757-3761. doi:10.1111/jcmm.14215
75. Wolf Y, Anderson AC, Kuchroo VK. TIM3 comes of age as an inhibitory receptor. *Nature Reviews Immunology*. 2020/03/01 2020;20(3):173-185. doi:10.1038/s41577-019-0224-6
76. Turnbull IR, Gilfillan S, Cella M, et al. Cutting Edge: TREM-2 Attenuates Macrophage Activation. *The Journal of Immunology*. 2006;177(6):3520. doi:10.4049/jimmunol.177.6.3520
77. Klesney-Tait J, Turnbull IR, Colonna M. The TREM receptor family and signal integration. *Nature Immunology*. 2006/12/01 2006;7(12):1266-1273. doi:10.1038/ni1411
78. Yao Y, Li H, Chen J, et al. TREM-2 serves as a negative immune regulator through Syk pathway in an IL-10 dependent manner in lung cancer. *Oncotarget*. May 17 2016;7(20):29620-34. doi:10.18632/oncotarget.8813
79. Bouchon A, Hernández-Munain C, Cella M, Colonna M. A DAP12-mediated pathway regulates expression of CC chemokine receptor 7 and maturation of human dendritic cells. *J Exp Med*. Oct 15 2001;194(8):1111-22. doi:10.1084/jem.194.8.1111
80. Moore SM, Holt VV, Malpass LR, Hines IN, Wheeler MD. Fatty acid-binding protein 5 limits the anti-inflammatory response in murine macrophages. *Molecular immunology*. Oct 2015;67(2 Pt B):265-75. doi:10.1016/j.molimm.2015.06.001
81. Xu B, Chen L, Zhan Y, et al. The Biological Functions and Regulatory Mechanisms of Fatty Acid Binding Protein 5 in Various Diseases. Review. *Frontiers in Cell and Developmental Biology*. 2022-April-04 2022;10doi:10.3389/fcell.2022.857919
82. Li Y, Liu X, Duan W, et al. Batf3-dependent CD8α⁺ Dendritic Cells Aggravates Atherosclerosis via Th1 Cell Induction and Enhanced CCL5 Expression in Plaque Macrophages. *eBioMedicine*. 2017;18:188-198. doi:10.1016/j.ebiom.2017.04.008
83. Hildner K, Edelson BT, Purtha WE, et al. Batf3 deficiency reveals a critical role for CD8alpha+ dendritic cells in cytotoxic T cell immunity. *Science*. Nov 14 2008;322(5904):1097-100. doi:10.1126/science.1164206
84. Liu D, Duan L, Rodda Lauren B, et al. CD97 promotes spleen dendritic cell homeostasis through the mechanosensing of red blood cells. *Science*. 375(6581):eabi5965. doi:10.1126/science.abi5965
85. Zahorchak AF, Macedo C, Hamm DE, Butterfield LH, Metes DM, Thomson AW. High PD-L1/CD86 MFI ratio and IL-10 secretion characterize human regulatory dendritic cells generated for clinical testing in organ transplantation. *Cell Immunol*. 2018;323:9-18. doi:10.1016/j.cellimm.2017.08.008
86. Domogalla MP, Rostan PV, Raker VK, Steinbrink K. Tolerance through Education: How Tolerogenic Dendritic Cells Shape Immunity. *Front Immunol*. 2017;8:1764-1764. doi:10.3389/fimmu.2017.01764
87. Chen M, Huang L, Shabier Z, Wang J. Regulation of the lifespan in dendritic cell subsets. *Molecular immunology*. 2007;44(10):2558-2565. doi:10.1016/j.molimm.2006.12.020
88. Smith SF, Hosgood SA, Nicholson ML. Ischemia-reperfusion injury in renal transplantation: 3 key signaling pathways in tubular epithelial cells. *Kidney International*. 2019;95(1):50-56. doi:10.1016/j.kint.2018.10.009
89. Mezrich JD, Fechner JH, Zhang X, Johnson BP, Burlingham WJ, Bradfield CA. An interaction between kynurenine and the aryl hydrocarbon receptor can generate regulatory T cells. *Journal of immunology (Baltimore, Md : 1950)*. Sep 15 2010;185(6):3190-8. doi:10.4049/jimmunol.0903670
90. Campesato LF, Budhu S, Tchaicha J, et al. Blockade of the AHR restricts a Treg-macrophage suppressive axis induced by L-Kynurenine. *Nature Communications*. 2020/08/11 2020;11(1):4011. doi:10.1038/s41467-020-17750-z
91. Chalise JP, Pallotta MT, Narendra SC, et al. IDO1 and TGF-β Mediate Protective Effects of IFN-α in Antigen-Induced Arthritis. *Journal of immunology (Baltimore, Md : 1950)*. Oct 15 2016;197(8):3142-3151. doi:10.4049/jimmunol.1502125
92. Lu X, Rudemiller NP, Wen Y, et al. A20 in Myeloid Cells Protects Against Hypertension by Inhibiting Dendritic Cell-Mediated T-Cell Activation. *Circulation Research*. 2019/12/06 2019;125(12):1055-1066. doi:10.1161/CIRCRESAHA.119.315343
93. Zammit NW, Siggs OM, Gray PE, et al. Denisovan, modern human and mouse TNFAIP3 alleles tune A20 phosphorylation and immunity. *Nat Immunol*. Oct 2019;20(10):1299-1310. doi:10.1038/s41590-019-0492-0
94. Ma A, Malynn BA. A20: linking a complex regulator of ubiquitylation to immunity and human disease. *Nature Reviews Immunology*. 2012/11/01 2012;12(11):774-785. doi:10.1038/nri3313
95. Cambi A, Figdor C. Necrosis: C-Type Lectins Sense Cell Death. *Current Biology*. 2009/05/12/ 2009;19(9):R375-R378. doi:https://doi.org/10.1016/j.cub.2009.03.032
96. Yamasaki S, Ishikawa E, Sakuma M, Hara H, Ogata K, Saito T. Mincle is an ITAM-coupled activating receptor that senses damaged cells. *Nature Immunology*. 2008/10/01 2008;9(10):1179-1188. doi:10.1038/ni.1651
97. Uto T, Fukaya T, Takagi H, et al. Clec4A4 is a regulatory receptor for dendritic cells that impairs inflammation and T-cell immunity. *Nature Communications*. 2016/04/12 2016;7(1):11273. doi:10.1038/ncomms11273
98. Marti F, Krause A, Post NH, et al. Negative-Feedback Regulation of CD28 Costimulation by a Novel Mitogen-Activated Protein Kinase Phosphatase, MKP6. *The Journal of Immunology*. 2001;166(1):197. doi:10.4049/jimmunol.166.1.197
99. Zheng H, Li Q, Chen R, et al. The Dual-specificity Phosphatase DUSP14 Negatively Regulates Tumor Necrosis Factor- and Interleukin-1-induced Nuclear Factor-κB Activation by Dephosphorylating the Protein Kinase TAK1*. *Journal of Biological Chemistry*. 2013/01/11/ 2013;288(2):819-825. doi:https://doi.org/10.1074/jbc.M112.412643

100. Yang C-Y, Li J-P, Chiu L-L, et al. Dual-Specificity Phosphatase 14 (DUSP14/MKP6) Negatively Regulates TCR Signaling by Inhibiting TAB1 Activation. *The Journal of Immunology*. 2014;192(4):1547. doi:10.4049/jimmunol.1300989
101. Lang R, Hammer M, Mages J. DUSP Meet Immunology: Dual Specificity MAPK Phosphatases in Control of the Inflammatory Response. *The Journal of Immunology*. 2006;177(11):7497. doi:10.4049/jimmunol.177.11.7497
102. Arthur JSC, Ley SC. Mitogen-activated protein kinases in innate immunity. *Nature Reviews Immunology*. 2013/09/01 2013;13(9):679-692. doi:10.1038/nri3495
103. Zheng H, Li Q, Chen R, et al. The Dual-specificity Phosphatase DUSP14 Negatively Regulates Tumor Necrosis Factor- and Interleukin-1-induced Nuclear Factor-κB Activation by Dephosphorylating the Protein Kinase TAK1 *. *Journal of Biological Chemistry*. 2013;288(2):819-825. doi:10.1074/jbc.M112.412643
104. Hijikata M, Matsushita I, Le Hang NT, et al. Influence of the polymorphism of the DUSP14 gene on the expression of immune-related genes and development of pulmonary tuberculosis. *Genes & Immunity*. 2016/06/01 2016;17(4):207-212. doi:10.1038/gene.2016.11
105. Xu J, Ma L, Fu P. Eriocitrin attenuates ischemia reperfusion-induced oxidative stress and inflammation in rats with acute kidney injury by regulating the dual-specificity phosphatase 14 (DUSP14)-mediated Nrf2 and nuclear factor-κB (NF-κB) pathways. *Ann Transl Med*. Feb 2021;9(4):350. doi:10.21037/atm-21-337
106. Chen H-W, Chen H-Y, Wang L-T, et al. Mesenchymal Stem Cells Tune the Development of Monocyte-Derived Dendritic Cells Toward a Myeloid-Derived Suppressive Phenotype through Growth-Regulated Oncogene Chemokines. *The Journal of Immunology*. 2013;190(10):5065. doi:10.4049/jimmunol.1202775
107. Averbeck M, Kuhn S, Bühligen J, Götte M, Simon JC, Polte T. Syndecan-1 regulates dendritic cell migration in cutaneous hypersensitivity to haptens. https://doi.org/10.1111/exd.13374. *Experimental Dermatology*. 2017/11/01 2017;26(11):1060-1067. doi:https://doi.org/10.1111/exd.13374
108. Angsana J, Chen J, Smith S, et al. Syndecan-1 Modulates the Motility and Resolution Responses of Macrophages. *Arteriosclerosis, Thrombosis, and Vascular Biology*. 2015/02/01 2015;35(2):332-340. doi:10.1161/ATVBAHA.114.304720
109. Kouwenberg M, Rops A, Bakker-van Bebber M, et al. Role of syndecan-1 in the interaction between dendritic cells and T cells. *PloS one*. 2020;15(7):e0230835. doi:10.1371/journal.pone.0230835
110. Celie JW, Katta KK, Adepu S, et al. Tubular epithelial syndecan-1 maintains renal function in murine ischemia/reperfusion and human transplantation. *Kidney Int*. Apr 2012;81(7):651-61. doi:10.1038/ki.2011.425
111. Hayashida K, Parks WC, Park PW. Syndecan-1 shedding facilitates the resolution of neutrophilic inflammation by removing sequestered CXC chemokines. *Blood*. Oct 1 2009;114(14):3033-43. doi:10.1182/blood-2009-02-204966
112. Zhang Y, Wang Z, Liu J, et al. Cell surface-anchored syndecan-1 ameliorates intestinal inflammation and neutrophil transmigration in ulcerative colitis. *J Cell Mol Med*. 2017;21(1):13-25. doi:10.1111/jcmm.12934
113. Rops AL, Götte M, Baselmans MH, et al. Syndecan-1 deficiency aggravates anti-glomerular basement membrane nephritis. *Kidney Int*. Nov 2007;72(10):1204-15. doi:10.1038/sj.ki.5002514
114. Doke T, Susztak K. The multifaceted role of kidney tubule mitochondrial dysfunction in kidney disease development. *Trends in Cell Biology*. doi:10.1016/j.tcb.2022.03.012
115. Lyu Z, Mao Z, Li Q, et al. PPARγ maintains the metabolic heterogeneity and homeostasis of renal tubules. *eBioMedicine*. 2018;38:178-190. doi:10.1016/j.ebiom.2018.10.072
116. Williams CG, Lee HJ, Asatsuma T, Vento-Tormo R, Haque A. An introduction to spatial transcriptomics for biomedical research. *Genome Medicine*. 2022/06/27 2022;14(1):68. doi:10.1186/s13073-022-01075-1
117. Bouchet-Delbos L, Even A, Varey E, et al. Preclinical Assessment of Autologous Tolerogenic Dendritic Cells From End-stage Renal Disease Patients. *Transplantation*. Apr 1 2021;105(4):832-841. doi:10.1097/tp.0000000000003315

3 Chapter 3

Gasdermin D mutation protects against Acute Kidney Injury

Overview

Hypothesis	▪ Gasdermin D (GSDMD) mutation can protect against acute kidney injury
Aims	▪ Ascertain if the single nucleotide polymorphism I105N in the GSDMD gene, and GSDMD inhibition using disulfiram can protect against severe renal IRI ▪ Determine if immune or renal GSDMD expression influences renal IRI severity
Main findings	▪ This chapter demonstrates the importance of pyroptosis in acute kidney injury and that this is mechanism is critically dependent on functional gasdermin D proteins. ▪ Mice with single nucleotide polymorphism mutation I105N in the gasdermin D gene were protected against severe acute kidney injury and we show localisation of this mutation to the kidney tissue determines the protective effects
Manuscript status	*Material from this chapter will be submitted to Kidney International* **Gasdermin D mutation protects against renal ischemia reperfusion injury** Jennifer S.Y. Li[1,2], MBBS, BE/BMedSci, FRACP Daniel N Meijles BSc, PhD Aadhar Moudgil BSc Sohel Julovi MBBS, PhD Katie Trinh MBBS, FRACP Stephen I. Alexander[3], MBBS, PhD Natasha M. Rogers[1,2,4] MBBS, FRACP, PhD *[1]Centre for Transplant and Renal Research, Westmead Institute for Medical Research, Australia* *[2]Sydney Medical School, Faculty of Health and Medicine, University of Sydney, Australia* *[3]Children's Medical Research Institute, Children's Hospital Westmead, Australia* *[4]Department of Renal Medicine, Westmead Hospital, Australia* ▪ The only deviation from the manuscript is **Section 3.8: Additional Material**.

3.1 Abstract

Pyroptosis, a pro-inflammatory form of cell death, is dependent on membrane pore formation governed by the assembly of cleaved Gasdermin D (GSDMD). In turn, this is regulated by the NOD-like receptor family pyrin 3 (NLRP3) inflammasome which senses danger signals following cellular damage. We hypothesized that these pathways are important in the pathophysiology of acute kidney injury (AKI). Mice with an isoleucine-to-asparagine mutation in the GSDMD (GSDMD$^{I105N/I105N}$) were protected from ischemia reperfusion injury (IRI), demonstrating lower serum creatinine, and limited histological injury, as well as decreased pro-inflammatory cytokine expression and oxidative stress. Chimeric mice, generated by whole body irradiation and infusion of syngeneic donor bone marrow, revealed renoprotection if parenchymal cells bore the *I105N* mutation. Pharmacological inhibition of GSDMD pore formation using disulfiram, but not blockade of NLRP3 inflammasome activation by MCC950, robustly protected against IRI. Manipulation of GSDMD is an attractive target to mitigate inflammation and cellular death following AKI.

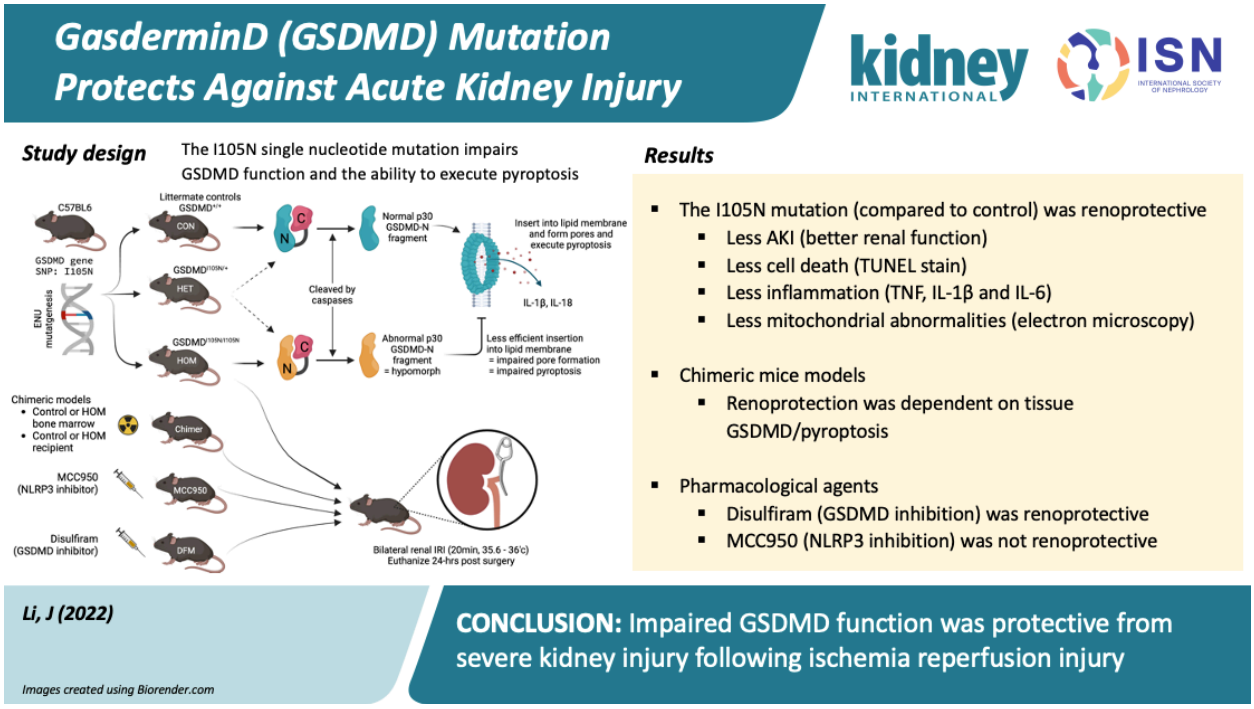

3.2 Introduction

Our understanding of cell death has expanded and now includes several forms of pro-inflammatory, regulated cell death pathways including pyroptosis, ferroptosis and necroptosis. We have focused on pyroptosis, programmed cell death which was first studied in context of cellular control of microbial infection but increasingly recognised as an important part of kidney disease pathophysiology[1-3]. Pyroptosis is initiated by inflammasome activation, caspase-1 cleavage, and insertion of gasdermin pores into the cell membrane resulting in the release of mature, pro-inflammatory cytokines. Inflammasomes are multimeric complexes comprised of an effector protein (pro-caspase 1 or pro-Casp1), an adaptor protein – apoptosis associated speck-like protein containing a caspase recruitment domain (ASC) and a receptor protein, either made up of nucleotide-binding oligomerisation domain (NOD) -like receptors (NLR), absent in melanoma 2 (AIM2)-like receptors (ALR) or pyrin. Of these, NLRP3 and AIM2 are of particular interest as they detect damage-associated molecular patterns (DAMPs)[4] released following sterile inflammation scenarios, such as ischemia reperfusion injury.

NLRP3 is found in both immune cells and both human and murine kidneys (including renal epithelial cells)[4-7] and previous studies have shown the absence[8-10] or inhibition of NLRP3 (with hydroxychloroquine[11] or MCC950[12]) can protect against ischemia reperfusion injury[5] (IRI) or cisplatin induced acute kidney injury (AKI). Gasdermin A to E isoforms share highly conserved domains[13-17] but gasdermin D (GSDMD) is the critical effector molecule for pyroptotic pore formation and release of mature, pro-inflammatory molecules[18,19]. GSDMD is cleaved by protease enzymes, caspase 1 (Casp-1) in the canonical inflammasome pathway, mouse caspase 11 (Casp-11) or human caspase 4/5 (Casp-4/5) by non-canonical pathways[19,20] into the GSDMD-N and GSDMD-C subunits[21]. Casp-1[22-25] and Casp-11[7,26-30] have both been shown as important contributors to the pathophysiology and severity of acute kidney injury.

GSDMD cleavage occurs most commonly at the D276 amino acid residue with Casp-1 and Casp-11[27,31], but also D275 (Casp-4/5)[19,32], D285 (Casp-11)[32], D 288 (Casp-11)[32] and D88 residues (caspase3)[33] to release the GSDMD-N from the auto-inhibitory GSDMD-C fragment. Active GSDMD-N terminal subunits oligomerise and insert as pores into the inner phospholipid cell membrane or cardiolipin on bacterial

surfaces[17], leading to cell death. The mechanism of GSDMD pore leading to cell death used to be considered a passive process, but this paradigm has shifted towards an active, secondary necrosis given the discovery of NINJI[34] and delayed pyroptosis through non-canonical mechanisms in the absence of Casp-1 and GSDMD[35]. GSDMD can also insert into cardiolipin found on the inner mitochondrial membrane and this has also been shown to augment release of reactive oxygen species[8] and caspase 3 mediated apoptosis[17,36,37]. GSDMD has been localised to innate immune cells[18,27,35,38-44] and organs and with respect to renal compartments, this includes tubular cells[7,11,12,29,45-47], podocytes[48] and glomerular endothelial cells[38].

Acute kidney injury models have also confirmed the absence of GSDMD protects against pyroptosis in AKI severity[7,47,49]. The ability of GSDMD-NT to execute pyroptosis is impaired if cellular calcium influx is disturbed[50], blockage of cysteine binding sites (GSDMD specific inhibition of Cys191/Cys193 by disulfiram[51] or necrosulfamide[52] inhibition of Cys191 and mixed lineage kinase domain-like (MLKL)), and hypomorphic mutations, such as the single nucleotide polymorphism *I105N* (isoleucine substituted by asparagine at amino acid residue 105 of the full length GSDMD protein, $GSDMD^{I105N/I105N}$) resulting in impaired GSDMD-NT pore formation, without altering cleavage or upstream inflammasome or caspase activity[26,27,53]. We hypothesise that disruption of the GSDMD-N function by either *I105N* mutation or disulfiram is critical to limiting pyroptosis and severity of AKI and characterise the inflammatory profile and ultrastructural changes following IRI in mice with limited GSDMD function.

3.3 Methods

3.3.1 Animals

Gasdermin D (GSDMD) mutants with the *I105N* (isoleucine-to-asparagine substitution) were derived from C57BL/6 mice following *N-ethyl-N-nitrosourea* (ENU) mutagenesis) and this mutation is known to impair caspase-1 and caspase-11 mediated GSDMD cleavage and reduce pyroptosis[18,20,26,54]. Mice were supplied by the Australian Phenomics Facility (APF, Australian National University) and housed in our animal facility (Westmead Institute for Medical Research) with access to standard chow and water *ad libitum* as approved by ethics committee (#4277, Western Sydney Local Health District). Studies were performed in accordance with the Australian code for the care and use of animals for scientific purposes developed by the National Health and Medical Research Council of Australia. Mice used in this study include: $GSDMD^{I105N/I105N}$ (homozygote, HOM), $GSDMD^{I105N/+}$ (heterozygote, HET) and littermate controls ($GSDMD^{+/+}$).

3.3.2 Bilateral renal ischemia reperfusion injury

Ten-to-twelve-week-old male mice were anaesthetised using isoflurane/oxygen titrated to effect, with body temperature maintained at 36°C for bilateral ischemia-reperfusion injury (IRI). A mid-line abdominal incision allowed access to occlude the renal pedicles using microaneurysm clamps for 20 minutes before releasing and abdominal closure with 5/0 monofilament. (Fig 3.1a) All mice were euthanised after 24-hours reperfusion, with collection of blood by cardiac puncture and kidney tissue either snap frozen, embedded in optimal cutting temperature (OCT) compound or fixed in 10% neutral-buffered formalin. (Fig 3.1)

3.3.3 Inhibition of pyroptosis with MCC950 or disulfiram

To test effects of pharmacological inhibition on AKI severity, mice were pre-treated with either MCC950, an inhibitor of NLRP3, or disulfiram, an inhibitor of GSDMD. C57BL/6 mice received intraperitoneal injections of 1) MCC950 (Sigma Aldrich, Burlington, MA, 10mg/kg in 0.2ml PBS) or 2) disulfiram (Sigma Aldrich, 25mg/kg) in 2 divided doses 12 h and 1 h prior to IRI (with ethanol as vehicle control). All mice were euthanised after 24-hours reperfusion.

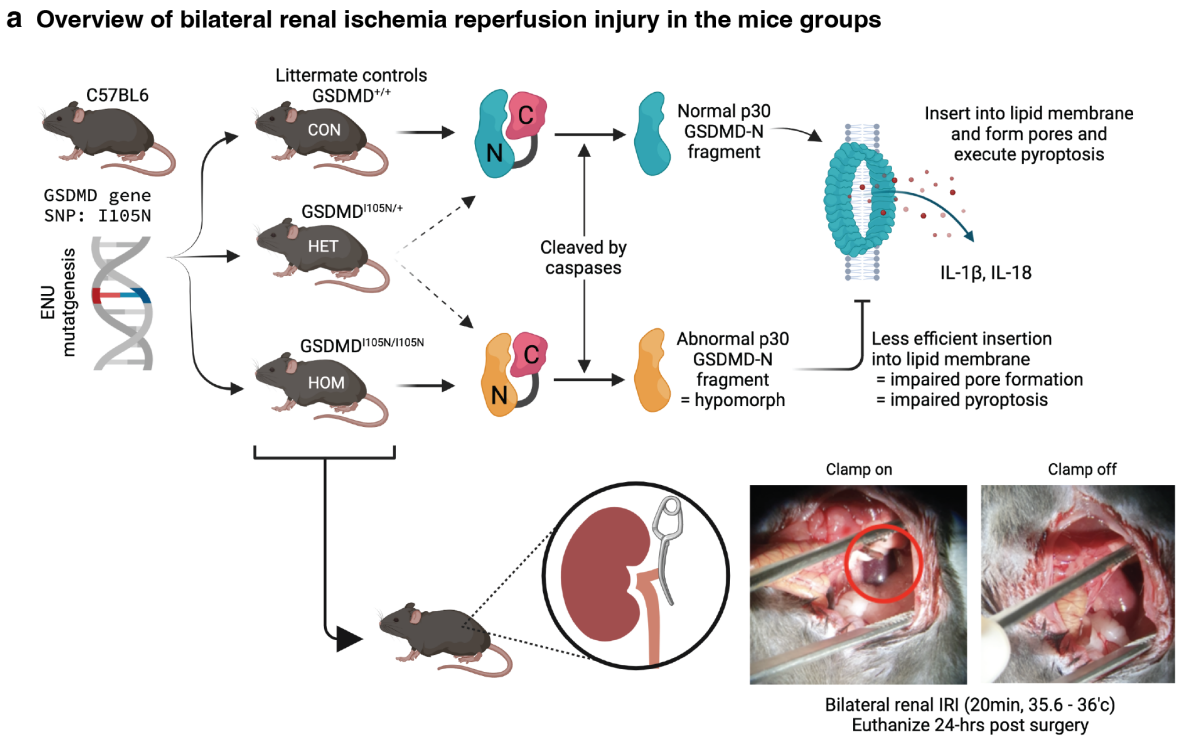

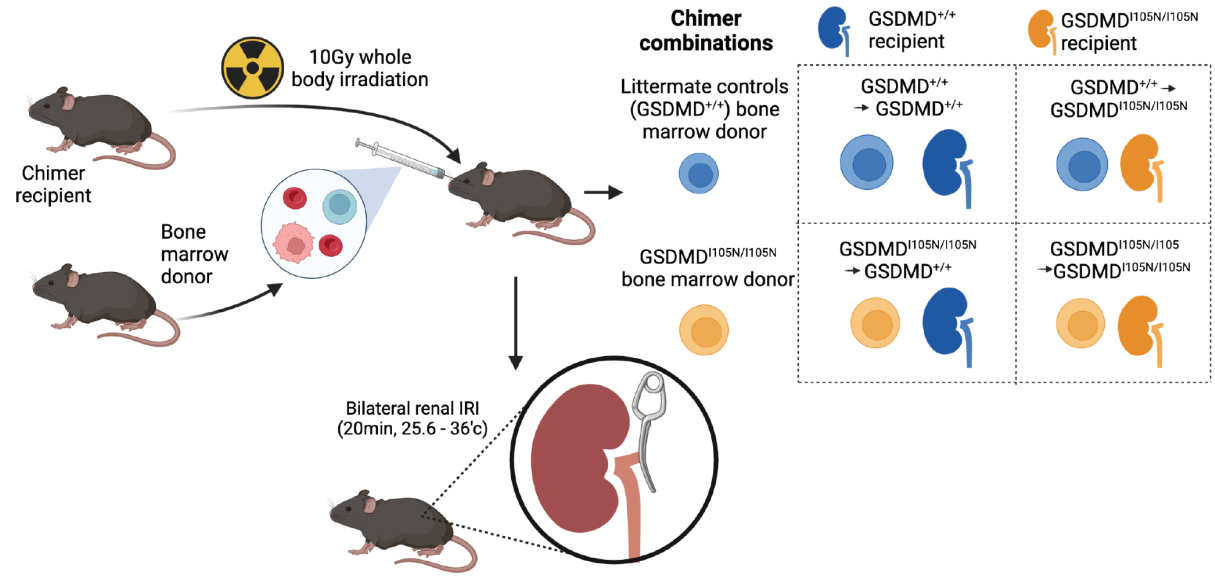

Figure 3.1: ***Overview of experimental groups*** *in a) bilateral renal ischemia reperfusion injury in mutant (HOM, GSDMD$^{I105N/I105N}$ and HET, GSDMD$^{I105N/+}$) versus littermate control (CON, GSDMD$^{+/+}$). Atraumatic, microvascular clamps were applied to both renal pedicles via a midline laparotomy approach. The core body temperature was monitored and maintained between 35.6 - 36℃ and microvascular clamps removed after 20 minutes, with visualisation of renal reperfusion before abdominal closure and analgesia. Mice were euthanised 24-hours later for analysis. This model was extended to include b) chimeric models where mice were exposed to a total 10 Gray whole-body irradiation, followed by infusion of fresh, bone marrow in a factorial design shown on the right. Mice were recovered in a clean environment with supplemental 0.2% neomycin water for 4 weeks before return to usual caging, chow and water for a further 4 weeks. Mice underwent the same 20-minute, bilateral IRI procedure 8 weeks after chimera induction.*

3.3.4 Chimeric mice models

Bone marrow was harvested from healthy, donor mice femurs using an aseptic technique from donor, aspirated using 22Gy syringe with sterile PBS and passed through a 70µm filter. These cells were spun down and resuspended in 150µl of PBS for use. To generate chimeric mice, male HOM or litter-mate control recipients were used. The mice groups used with the chimeric model includes (Fig 3.1b): $GSDMD^{+/+}$ bone marrow → $GSDMD^{+/+}$ recipient ($GSDMD^{+/+}$→$GSDMD^{+/+}$ or Con to Con); $GSDMD^{I105N/I105N}$ bone marrow → $GSDMD^{+/+}$ recipient ($GSDMD^{I105N/I105N}$→$GSDMD^{+/+}$ or HOM to Con); $GSDMD^{+/+}$ bone marrow → $GSDMD^{I105N/I105N}$ recipient ($GSDMD^{+/+}$→$GSDMD^{I105N/I105N}$ or Con to HOM); $GSDMD^{I105N/I105N}$ bone marrow $GSDMD^{I105N/I105N}$ recipient ($GSDMD^{I105N/I105N}$→$GSDMD^{I105N/I105N}$ or HOM to HOM). The recipient mouse was first exposed to a total of 10Gy, whole body irradiation over 2 sessions, 6 hours apart (X-RAD320 machine, Precision X-ray, Connecticut). Following irradiation, the freshly isolated, bone marrow cells were administered via a retro-orbital approach and chimers were monitored every 24 hours for the first week, then weekly for a total of 8 weeks to allow recovery and engraftment of cells. Chimeric mice were isolated in a clean room and provided hydration with 0.2% neomycin water for the first 4 weeks before returning to their usual animal housing facility. Following this period, chimeric mice underwent the same bilateral renal IRI procedure described above, with analysis performed 24-hours post-surgery. (Fig 3.1)

3.3.5 Serum analysis for renal function and cytokine levels

Serum was aliquoted for creatinine was measured using Atellica CH enzymatic creatinine assay (Siemens) by a centralised lab (Westmead ICPMR). Remaining serum was analysed for IL-1ß, IL-6, TNF-α using LegendPlex Mouse Inflammation Panel and their cloud-based analysis software (BioLegend, San Diego).

3.3.6 Histological staining, injury scoring and TUNEL staining

Kidneys embedded in paraffin were sectioned at 4µm and stained with haematoxylin and eosin (H&E) by standard methods[55]. Brightfield images were acquired using the NanoZoomer HT and images viewed using NDP.scan (Hamamatsu, Shizuoka, Japan). Sections were scored by two blinded, independent observers for features of injury in five randomly selected areas in corticomedullary area. Markers of acute tubular damage

(tubular dilatation, cell necrosis, infarction, and cast formation) were scored by semi-quantitative calculation of percentage of the corticomedullary junction involved: 0 (no features), 1-10%), 2 (11-25%), 3 (26-50%), 4 (51-75%) and 5 (>75%). Kidneys preserved in OCT were sectioned at 5μm thickness and stained with the TMR-red TUNEL in situ cell death detection kit (Roche, Basel, Switzerland). Images were acquired using the Olympus FV1000 confocal laser scanning microscope (Olympus) and images reviewed using FV-10-ASW (v4.2, Olympus). The number of TUNEL positive cells in a 20x field over 5 different regions were averaged.

3.3.7 RTEC and Kidney PCR

RNA was extracted from either tissue or cell lysate using Isolate II RNA Mini Kit (Bioline), quantified using a Nanodrop (BioTek, Winooski, VT), and reverse-transcribed using a SensiFAST cDNA synthesis kit (Bioline). cDNA was amplified in triplicate using the CFX384 real-time PCR machine (Bio-Rad) with SensiFAST No-ROX (Bioline) and targeted TaqMan primers (ThermoFisher, Waltham): TNF-α (Mm_00443258_m1), IL-1β (Mm_00434228_m1), IL-6 (Mm_00446190_m1), CCL2 (Mm_00441242_m1), CXCL2 (Mm_00436450_m1), RANTES (Mm_01302427_m1) and HPRT (Mm_01545399_m1). Data was analysed using the ΔΔCT method with expression normalised to the housekeeping gene, and littermate control ($GSDMD^{+/+}$), $GSDMD^{+/+}$ chimer mice, or PBS-treated animals were used as the referent control.

3.3.8 Macrophage and kidney samples for transmission electron microscopy

Bone marrow derived macrophages were derived from C57BL/6 mice. Bone marrow was aspirated under aseptic technique, passed through a 70μm filter before incubation for 3 minutes in red cell lysis buffer (eBioscience, Waltham, MA). Cells were resuspended at 1 – 1.5x10^5 cells/cm^2 in 6-well culture plates with glass coverslips (no.1 thickness, 0.13 – 0.16mm, Marenfield, Germany). Culture media was based with RPMI-1640 supplemented with 10% (v/v) heat-inactivated foetal calf serum, 1% (v/v) penicillin-streptomycin, 1% (v/v) L-glutamine, 1% (v/v) sodium pyruvate, 1% (v/v) non-essential amino acid, 10mM HEPES (4-(2-hydroxyethyl)-1-piperazineethanesulfonic acid (all Gibco, Waltham

MA) and 10ng/ml of mouse M-CSF (Miltenyi Biotec, Germany). Culture media was refreshed every 2nd day and 100ng/ml of LPS was added for 4-hours, followed by 10μM nigericin for 4-hours to induce pyroptosis. Media was removed and coverslips with adherent macrophages were washed with PBS and incubated with 2.5% glutaraldehyde (in 0.1M phosphate buffer) at room temperature for 2 hours.

Mouse kidney and macrophage culture samples were then processed by a centralised electron microscopy lab (Westmead Research Hub Electron Microscope Facility)). Cells were washed with 0.1M phosphate buffer, incubated in 2% osmium tetroxide (in 0.1M cacodylate buffer) for 2-hours, 2% uranyl acetate solution for 1-hour and then dehydrated through graded ethanol rinse series before final resin embedding. In addition to macrophage preparations, kidneys were also prepared for electron microscopy. Briefly, mice were euthanised 24-hours post bilateral renal IRI and 10ml of 2.5% glutaraldehyde perfusion was achieved by cardiac puncture for whole-organ fixation. Renal cortex specimens (approximately 1mm^3 pieces) were then fixed in 3.5% glutaraldehyde (in 0.1M phosphate buffer) for 2-hours. Cured resin blocks were sectioned at 90nm and a ultramicrotome (Leica UC6) and placed on copper grids for post staining with 2% uranyl acetate and lead citrate before image acquisition using the JEM-1400 Flash Electron Microscope (JOEL, Tokyo). Five different regions from each post-IRI kidney (n = 3 GSDMD$^{I105N/I105N}$ and n = 3 GSDMD$^{+/+}$) were selected and the mitochondrial number, perimeter, long-axis length and autophagic vesicles were measured using ImageJ (v1.53K, NIH, USA). The number of structurally abnormal mitochondria were also counted and expressed as the percentage of the total mitochondrial number from the same region of interest.

3.3.9 Statistical analysis

Data is represented as mean ± standard deviation unless otherwise stated. Data was analysed with t-test (parametric variables), Mann-Whitney U test (non-parametric variables) for means between two groups, or ANOVA between multiple groups using Prism (v9, GraphPad) unless otherwise stated. A $P < 0.05$ was deemed significant.

3.4 Results

3.4.1 GSDMD mutations prevent severe AKI in a dose dependent manner

GSDMD$^{I105N/I105N}$ mice were protected against severe acute kidney injury based on serum creatinine (SCr) measured 24-hours post IRI. (Fig 3.2a-b) The injury in littermate control GSDMD$^{+/+}$ (SCr 89.1±27.3μmol/L) was significantly higher than both GSDMD$^{I105N/+}$ and GSDMD$^{I105N/I105N}$ groups (SCr 48.1±16.9μmol/L (P < 0.001) and 15.7±6.8μmol/L (P < 0.0001) respectively). Homozygotes had greater protection than seen in GSDMD$^{I105N/+}$ mice (P = 0.01), indicating a dose-dependent relationship between the *I105N* mutation and protection from severity of AKI.

In keeping with the renal function, the degree of post-operative weight loss and cell death was lower in the mutant mice. The 24-hour weight change was -16.3±2.5% for controls, compared to -12.5±1.5% (P < 0.001) in GSDMD$^{I105N/+}$ and -10.5±1.4% (P < 0.0001) in GSDMD$^{I105N/I105N}$ mice. (Fig 1c) The semiquantitative injury score based on H&E images did not reach statistical significance between the 3 groups but cell death quantified by TUNEL staining was significant when GSDMD$^{I105N/I105N}$ mice (1.9±1.4 TUNEL+/hpf) were compared to controls (5.8±2.6 TUNEL+/hpf, P = 0.005). (Fig 3.2d-e, *supplementary table 3.1*)

3.4.2 GSDMD mutation limits inflammation and cell death

Kidney mRNA expression of pro-inflammatory targets, including TNF-α, IL-1β, IL-6, CCL2, CXCL2 and RANTES (CCL5) were significantly lower in both GSDMD$^{I105N/+}$ and GSDMD$^{I105N/I105N}$ mice compared to littermate controls. There was no significant difference in the pro-inflammatory profile between heterozygote versus homozygote mice. (Fig 3.3f-k, Table 3.1) Systemic cytokine expression was not reflective of the renal changes, as serum cytokine at the same time point did not reveal statistically significant differences between the groups for IL-1α, IL-1β, IL-6, TNF-α or MCP-1 (CCL2). (Fig 3.3g-i table 3.2). Analysis of oxidative stress showed decreased production of DPI- (but not SOD) related superoxide, or hydrogen peroxide (Fig 3.2o-q), suggesting a mitochondrial origin of the ROS moiety. *(supplementary table 3.2 & 3.3)*

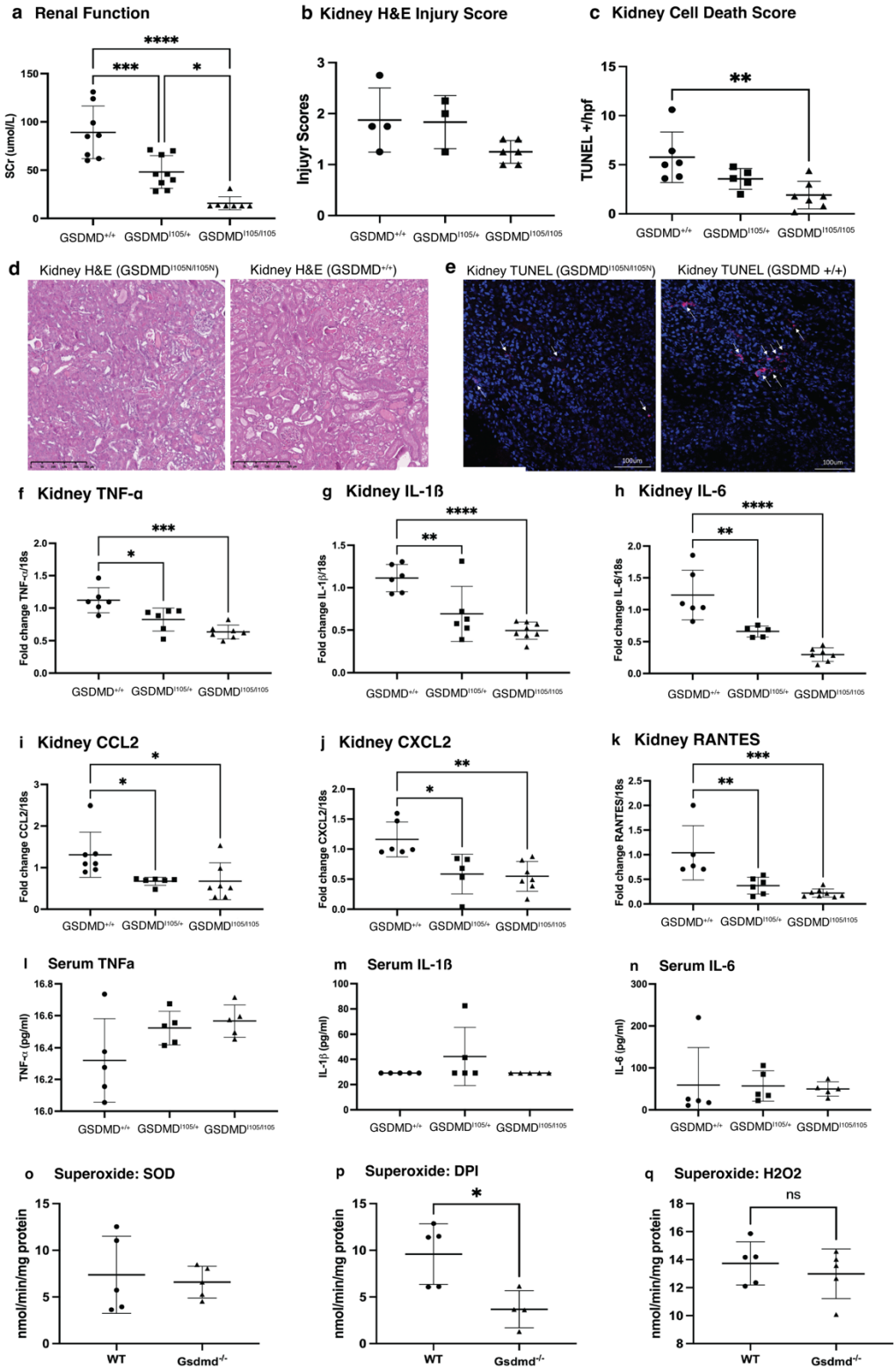

Figure 3.2: a) Renal function measured 24-hours post IRI demonstrate protection from severe kidney injury, with serum creatinine 89.1±27.3, 48.1±16.9 and 15.7±6.8µmol/L in controls, GSDMD$^{I105N/+}$ and GSDMD$^{I105N/I105N}$ respectively and b) the corresponding post-operative weight loss were -16.3±2.5, -12.5±1.5% and -10.5± 1.4%. c) The semi-quantitative injury score (with representative haematoxylin and eosin images) was not different between the control and mutant groups. d) TUNEL stain quantified cell death as 5.8±2.6 vs 3.6±1.1 and 1.9±1.4 TUNEL+ cells per high-power field (20x magnification) for controls versus GSDMD$^{I105N/+}$ and GSDMD$^{I105N/I105N}$, and only homozygote mice showed reduced cell death compared to controls.

3.4.3 GSDMD mutations were associated with less mitochondrial injury

Transmission electron microscopy was used to acquire images at 5000x magnification (high-powered field, hpf) were used to quantify mitochondrial characteristics in 15 regions across 3 kidneys from each group (control versus $GSDMD^{I105N/I105N}$ mice) 24-hours post injury. (Fig 3.5) There were fewer mitochondria per high power field (17.6±5.2 vs 21.3±6.4/hpf, $P = 0.03$) with greater proportion of these mitochondria with abnormal mitochondrial structure, such as swelling, abnormal cristae, disrupted membrane (23.48±16.36 vs 8.2±6.99%, $P = 0.0014$) in the control group compared to $GSDMD^{I105N/I105N}$ mice. (Fig 3.5a and e).

Representative images from control (Fig 4f and g) and HOM kidneys (Fig 4j and k) demonstrate clearly the increased abnormal mitochondrial ultrastructure between the groups. There was no significant difference in the autophagic vesicles (14.93±13.17 vs 13.91±7.09% of mitochondria), average mitochondrial area (0.63±0.23 vs 0.58±0.19μm^2), perimeter (3.23±0.8 vs 3.15±0.63μm), long axis length (1.18±0.31 vs 1.2±0.28μm) or ratio of area by long axis length (0.51±0.1 vs 0.46±0.06μm) for control versus $GSDMD^{I105N/I105N}$ kidneys respectively. (Fig 3.5c-e).

Pyroptotic bodies, previously described as an electron microscopic feature of pyroptosis with membrane extensions with blebbing by Chen et al[44] and Zhang et al[43], were difficult to detect in the kidney tubular environment with multiple mechanisms of cell deaths known post IRI. Pyroptotic bodies have not been described in non-immune cells so far and our sections taken at 24-hours post injury may not be the optimal time for detection. Screening the available ultra-sections, a lymphocyte with suggestive features of membrane extension and blebs was found in the glomerular region of a control kidney (Fig 3.5h) but this was not seen in monocytes/macrophages, or a neutrophil in the $GSDMD^{I105N/I105N}$ kidney (Fig 3.5l). Bone marrow derived macrophages, 4-hours post pyroptosis induction, were better able to show differences in pyroptotic body formation between control and $GSDMD^{I105N/I105N}$ mice (Fig 3.5i & m and *supplementary table 3.4*).

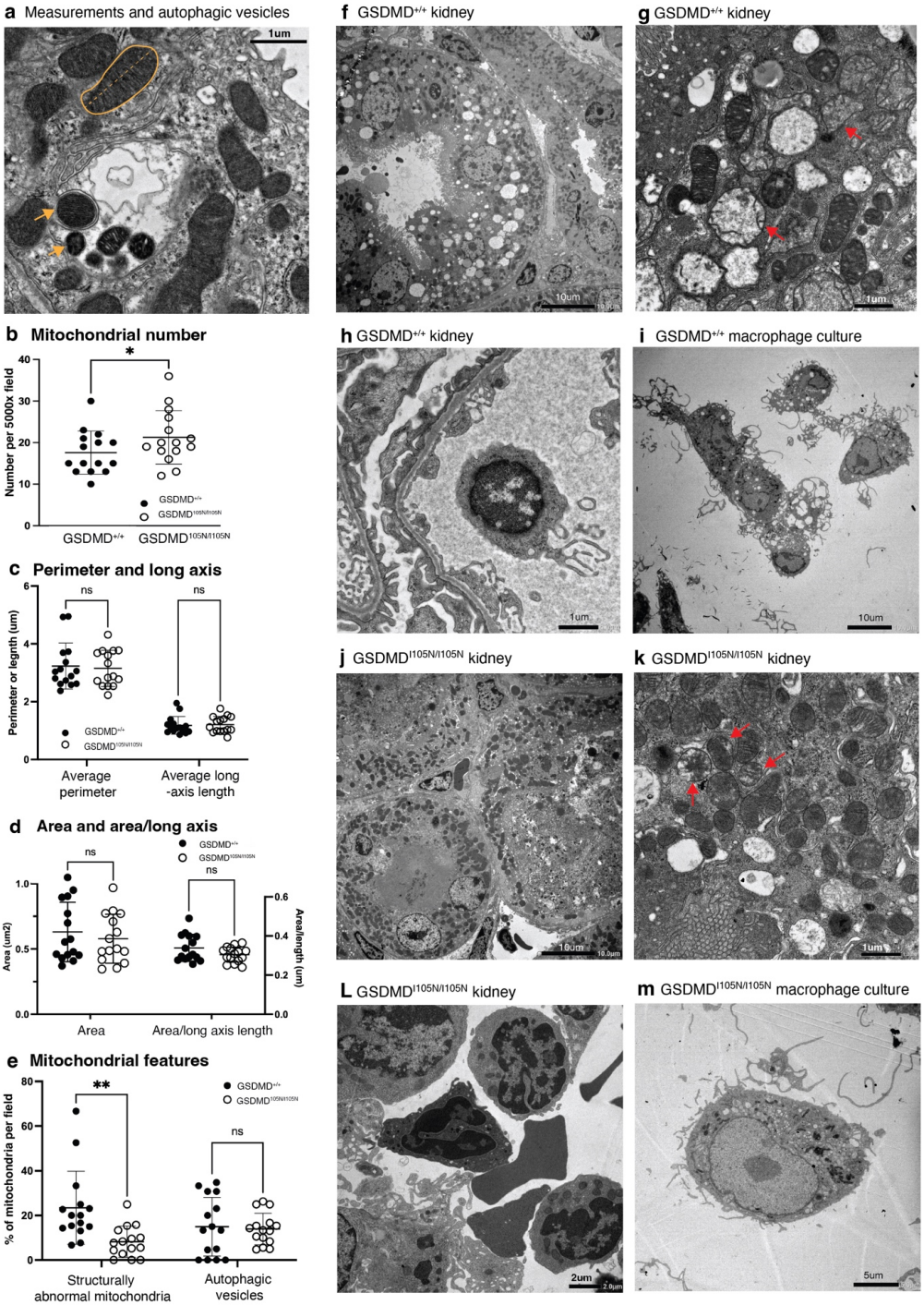

Figure 3.3: Transmission electron microscopy (TEM) images of kidneys 24-hour post ischemia reperfusion injury shown in a, d-h and j-l. a) Kidney tubular section from littermate control (GSDMD$^{+/+}$) demonstrates example of mitochondrial measurements for each high-power field (hpf, 5000x magnification). The yellow outline of the mitochondria used to calculate the perimeter and the enclosed area; yellow dotted line used to calculate the maximum long axis length of each mitochondrion; yellow arrows of example autophagic vesicles; and red arrows (g and k) were representative of structurally abnormal mitochondria. b) Homozygote mice had greater number of mitochondria (P = 0.03) but there was no significant difference between control versus GSDMD$^{I105N/I105N}$ homozygotes (P > 0.05) with respect to the average c) mitochondrial perimeter, long axis length, d) mitochondrial area or ratio of mitochondrial area to long axis length or e) autophagic vesicles. However, a greater proportion of structurally abnormal mitochondria were detected in the littermate controls compared to homozygotes (P = 0.0014). Representative low and high magnification images of post IRI kidneys of the controls are seen in f) and g), which revealed abundant swollen or disrupted mitochondria and h) was an image from the glomerular region with a passing with membrane extension and blebbing, suggestive of a pyroptotic body. i) Abundant membrane based pyroptotic bodies are visualised in a high-power image of a bone marrow derived macrophage 4-hours post lipopolysaccharide (LPS) and nigericin induction of pyroptosis. Similarly, j) and k) are high resolution images of GSDMD$^{I105N/I105N}$ kidneys with fewer structural mitochondrial abnormalities. l) shows neutrophils and monocytes/macrophages traversing the glomerular space and m) a macrophage derived from GSDMD$^{I105N/I105N}$ bone marrow 4-hours after pyroptosis induction – with fewer membrane protrusions and pyroptotic bodies compared to the wild-type derived macrophages.

3.4.4 Parenchymal rather than immune cell gasdermin D determines pyroptosis and AKI risk

Ischemia reperfusion injury in chimeric mice models revealed that renal parenchymal expression of the GSDMD mutation was critical to the protection from severe AKI. Recipient $GSDMD^{I105N/I105N}$ mice of bone marrow from either ($GSDMD^{+/+}$→$GSDMD^{I105N/I105N}$) or $GSDMD^{I105N/I105N}$ ($GSDMD^{I105N/I105N}$→$GSDMD^{I105N/I105N}$) donor mice had SCr 51.3±22.9 and 38±12.8μmol/L respectively (P=0.86). Recipient $GSDMD^{+/+}$ mice paired with $GSDMD^{+/+}$ ($GSDMD^{+/+}$→$GSDMD^{+/+}$) or $GSDMD^{I105N/I105N}$ ($GSDMD^{I105N/I105N}$→$GSDMD^{+/+}$) derived bone marrow had SCr of 114±19.7 and 132±69.5μmol/L (P = 0.86) respectively. Post-operative weight loss and semi-quantitative injury scores were similar between all groups. $GSDMD^{+/+}$ recipient chimers had worse serum creatinine and histological injury compared to any chimer with the $GSDMD^{I105N/I105N}$ recipient. (Fig 3.4 and *supplementary table 3.5)*.

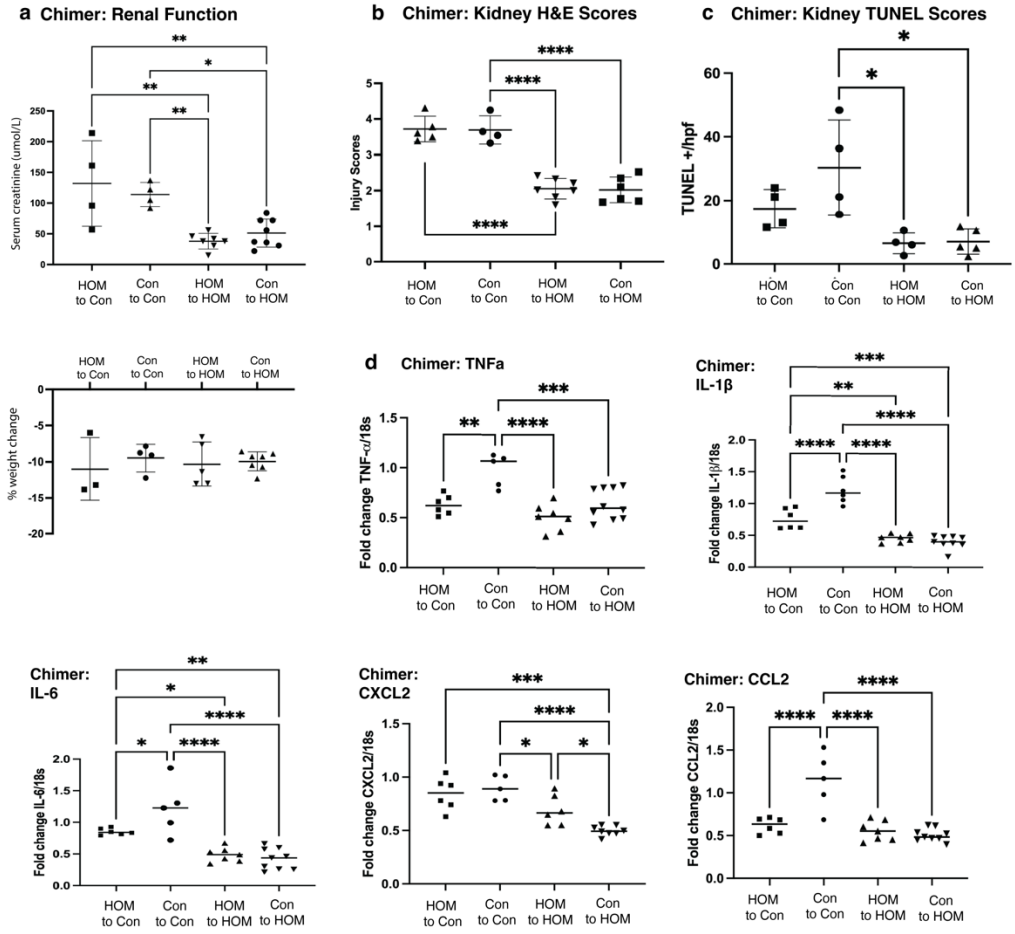

Figure 3.4: Chimeric mouse models with renoprotection in recipient HOM ($GSDMD^{I105N/I105N}$) mice, seen with a)serum creatinine and weight change 24-hrs post IRI, b) haematoxylin & eosin semi-quantitative injury score, c) TUNEL staining (each value is the average TUNEL+ cells at 20x for 5 fields over a kidney section), d) kidney mRNA expression of TNFα, IL-1β, IL-6, CCL2, CXCL2.

3.4.5 Disulfiram can limit AKI severity following IRI

Disulfiram, a known inhibitor of GSDMD, was able to protect mice from severe AKI compared to controls. Serum creatinine was 35.33±19.4 µmol/L in the disulfiram group, compared 145.6±30µmol/L in the control group which only received vehicle control (P = 0.004). In contrast, mice receiving MCC950 (total of 20mg/kg over 2 days prior) prior to surgery were not protected from IRI but had worse injury (serum creatinine 135±50.9 vs 113.5±28.33µmol/L in controls, P = 0.54). Disulfiram used at previously published doses (50mg/kg)[51] was toxic to mice (with 50% pre-AKI mortality), however 25mg/kg dosing provided protection against severe AKI, with decreased histological injury, and reduced pro-inflammatory cytokine production (Figure 3.5).

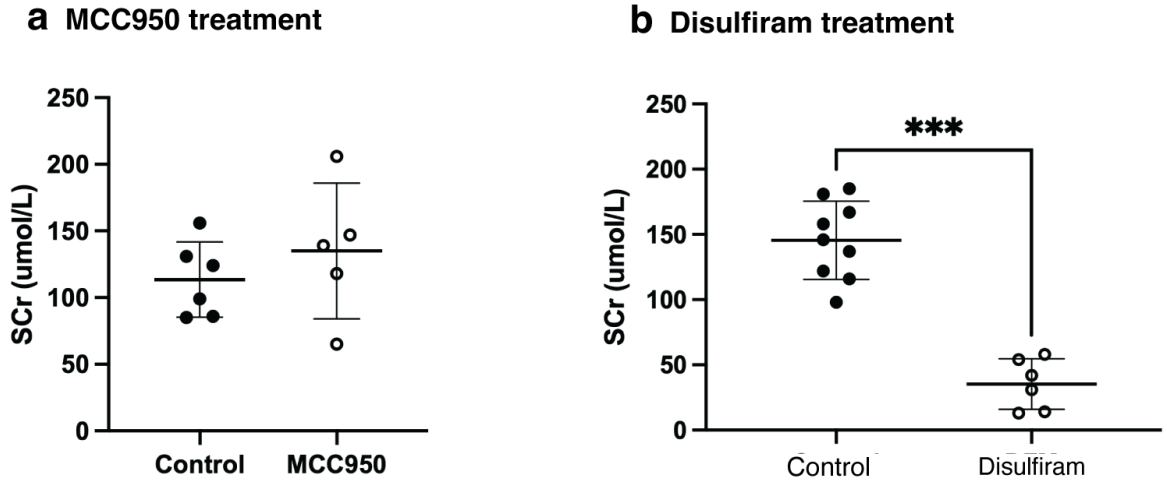

*Figure 3.5: serum creatinine 24-hrs post IRI for a) MCC 950 treated and b) disulfiram vs control groups. *** P<0.001.*

3.5 Discussion

Here, we demonstrate that disruption of GSDMD function and the ability to execute pyroptosis can limit AKI severity following IRI. GSDMD protein expression and cleavage is normal in our mice models but the ability to oligomerise and form GSDMD pores is impaired in mice with the *I105N* mutation[26,27,53]. Mice with homozygote mutation had lower serum creatinine, cell death, renal expression of pro-inflammatory TNF-α, RANTES and IL-6 mRNA and structurally abnormal mitochondria following IRI compared to control mice. Chimeric mice models showed that pyroptosis in renal parenchymal cells was critical to mediating cell death and injury following IRI. Homozygote mice receiving immune cells (with intact GSDMD function) from littermate controls were protected against severe renal injury, while control mice given bone marrow from

homozygote mice, with impaired pyroptosis in the immune cells still had severe injury following renal IRI. This is not surprising given the localised organ injury, with cellular stress and danger associated molecular pattern (DAMP) release can act on local renal tubular and interstitial cells to cause pyroptosis and cell death, rather than the damage being mediated by immune cells alone.

This differs from lack of renoprotection in GSDMD knock out mice, where clamps were applied for 50 minutes in the IRI model used to demonstrate elevated Casp-11 and GSDMD after ischemic injury.[7] We did not detect significant suppression of IL-1β expression homozygote mice. The GSDMD mutation is not expected to impair pro-IL-1β processing, but we are unsure of hypofunctional GSDMD-N signalling in the non-canonical inflammasome pathway, which can potentially drive Casp-1-dependent IL-1β processing.[20,56] Unfortunately, attempts to optimise the western blot to quantify cleaved IL-1β, Casp-1 and Casp-11 subunits were unsuccessful during this candidature, as outlined earlier. Serum cytokine analysis did not reveal differences in IL-1α, IL-1β, TNF-α or IL-6 between groups and highlights the potential discrepancy of peripheral blood cytokine levels compared to the local profile in the injured organ. Serum IFN-γ was significantly elevated in the heterozygote group - the reason for this remains unclear.

We show that RTEC mitochondria have similar number and overall dimensions based on area, perimeter, and area: long-axis ratio, but there were significantly more damaged or structurally abnormal mitochondria in the control compared to homozygote mice following IRI. GSDMD can insert into the inner mitochondrial membrane to augment apoptosis and may be another reason we saw reduced cell death. Recent evidence has shown that pyroptosis is not a passive cell death process like previously thought, but cooperates with functional NINJ1, which drives secondary necrosis following pyroptosis.[34] Future work is needed to delineate whether impaired pyroptosis impacts NINJ1 or secondary necrosis pathways.

Finally, administration of disulfiram, a known GSDMD inhibitor, was able to provide protection against severe kidney injury. It was surprising that mice which received MCC950 were not protected against severe injury, but more recent data suggest higher doses are required than first thought. Our mice received 2 doses of 10mg/kg based on earlier studies in hypertension models but studies published last year showed up to

50mg/kg was required to provide protection a rat model of kidney transplantation exposed to varying degrees of cold ischemia time[12]. Whether the protection with disulfiram was solely from inhibiting GSDMD pore formation and pyroptosis needs further investigation. The potential action of this drug on other cellular targets and pathways are possible, although whether these non-GSDMD targets offer any renoprotection is unknown. Future experiments to interrogate if disulfiram limits renal injury through GSDMD-specific mechanisms include direct visualization by fluorescent microscopy of membrane GSDMD pore formation, or release of IL-1β from renal tubular cells in vitro. The measurement of cell/kidney lysates IL-1β, IL-18 or caspases are not expected to be different if the inhibition is at the level of the GSDMD pore. The use of TUNEL stain and/or LDH release assay will also not be specific, given they do not differentiate between different forms of cell death."

3.6 Conclusions

Here, we show that both impaired GSDMD, either with the *I105N* mutation or following disulfiram in the renal parenchymal cells (rather than infiltrating immune cells), can limit severe AKI following IRI. This offers a potential target to limit AKI in various settings.

3.7 Additional material

Western blotting of kidney homogenates for caspase-1, caspase-11 and IL-1β were not successful during the period of this PhD, despite testing for the following factors: (1) Fresh instead of stored protein extraction and protein loading from 15 to 60 ug per well, (2) cell lysis using RIPA (#9806) or Chaps buffer (#9852) from cell signalling (New England), (3) wet transfer in ice for 20, 30, 60 or 90 mins at 200mA vs Trans-Blot Turbo Transfer system (Bio-Rad) or (4) different primary, anti-mouse antibodies at 1:50 to 1:1000 dilutions: Casp-1: #AG-20B-0042-C100 (Adipogen, San Diego); Casp-1: #SC-398715 (Santa Cruz Biotechnology, Santa Cruz); Casp-11: #NB120-10454SS (Novus Biologicals, Colorado); Casp-11: #AB180673 (Abcam, Cambridge); IL-1β: #AG-40b-0086-C010 (Adipogen). Due to covid restrictions, experimental work was limited during the candidature and ongoing or planned work to complete this manuscript includes analysis of samples obtained from disulfiram treated mice following IRI; and detection of GSDMD protein expression in kidney transplant patients with delayed graft function and/or rejection to confirm the importance of this pathway in clinical kidney injury. (Optimisation stage for immunohistochemistry)

3.8 Supplementary

Table 3.1: GSDMD mice 24-hours post IRI

Baseline	**GSDMD$^{+/+}$**	**GSDMD$^{I105N/+}$**	**GSDMD$^{I105N/I105N}$**
Serum creatinine (μmol/L)	89.1±27.3	48.1±16.9	15.7±6.8
Weight change %	-16.3±2.5	-12.5±1.5%	10.5±1.4%
H&E injury score	1.9±0.6	1.8±0.5	1.2±0.2
TUNEL scores/hpf	5.8±2.6	3.65 ±1.1	1.9±1.4
Comparison of serum creatinine (P values for row vs column)			
SCr vs GSDMD$^{+/+}$	-	< 0.001	< 0.0001
SCr vs GSDMD $^{I105N /+}$	-	-	0.01
% Weight vs GSDMD$^{+/+}$	-	< 0.001	< 0.001
H&E vs GSDMD$^{+/+}$	-	0.12	0.20
TUNEL vs GSDMD$^{+/+}$	-	0.15	0.005

Table 3.2: mRNA results (fold change to HPRT1)

Kidney mRNA	**GSDMD$^{+/+}$**	**GSDMD$^{I105/+}$**	*P value vs control*	**GSDMD$^{I105/I105N}$**	*P value vs control*	*P value vs GSDMD$^{I105/+}$*
TNF-α	1.12 ± 0.20	0.82 ± 0.18	*0.014*	0.63 ± 0.11	*0.0001*	*0.11*
IL-6	1.23 ± 0.40	0.66 ± 0.08	*0.004*	0.30 ± 0.11	*<0.0001*	*0.053*
IL-1β	1.14 ± 0.16	0.69 ± 0.32	*0.007*	0.49 ± 0.1	*<0.0001*	*0.21*
CCL2	1.16 ± 0.20	0.58 ± 0.33	*0.012*	0.55 ± 0.25	*0.004*	*0.97*
CXCL2	1.31 ± 0.55	0.67 ± 0.1	*0.037*	0.67 ± 0.44	*0.029*	*>0.99*
CCL5 (RANTES)	1.04 ± 0.55	0.37 ± 0.07	*0.005*	0.22 ± 0.08	*0.0005*	*0.62*

Table 3.3: GSDMD cytokines summary

Serum cytokine	**GSDMD$^{+/+}$**	**GSDMD$^{I105/+}$**	**GSDMD$^{I105/I105N}$**
IL-1α	7.3 ± 7.7	22.1 ± 25.4	6.1 ± 5.7
IL-1β	29.2 ± 0	42.3 ± 23.1	29.2 ± 0
IL-6	59.1 ± 90	57.0 ± 36.2	49.9 ± 16.9
IFN-γ	2.9 ± 0	16.8 ± 9.8	3.7 ± 1.7
TNF-α	16.3 ± 0.3	16.5 ± 0.1	16.6 ± 0.1
MCP-1	44.8 ± 13.2	106.5 ± 57.1	42.3 ± 29.8

Table 3.4: Mitochondrial features

Serum cytokine	**GSDMD$^{+/+}$**	**GSDMD$^{I105/I105N}$**	**P value**
Mitochondrial number	17.6 ± 5.18	21.27 ± 6.4	0.027
Average perimeter (μm)	3.23 ± 0.79	3.15 ± 0.63	0.89
Average length (μm)	1.18 ± 0.31	1.21 ± 0.28	0.99
Average area (μm^2)	0.63 ± 0.23	0.51 ± 0.1	0.61
Average area/length (μm)	0.51 ± 0.1	0.46 ± 0.06	0.61
Abn mitochondria %	23.48 ± 16.36	8.2 ± 6.99	0.001
Autophagic %	14.93 ± 13.17	13.91 ± 7.09	0.96

Table 3.5: Chimer summary for 24-hrs post IRI

Chimers	**GSDMD$^{I105N/I105N}$ →GSDMD$^{+/+}$**	**GSDMD$^{+/+}$ →GSDMD$^{+/+}$**	**GSDMD$^{I105N/I105N}$ →GSDMD$^{I105N/I105N}$**	**GSDMD$^{+/+}$ → GSDMD$^{I105N/I105N}$**
Serum creatinine (μmol/L)	132 ± 69.5	114 ± 19.7	38 ± 12.8	51.3 ± 22.9
Weight change %	-11±4.3	-9.5±1.9	-9.9±1.3	-10.3±3.0
H&E injury	3.7±0.4	2.0±0.4	2.1±0.3	3.7±0.4
TUNEL scores/hpf	30.4±14.9	17.5±6.1	6.5±3.3	7±4
P values for row vs column				
Serum creatinine				
GSDMD$^{+/+}$→GSDMD$^{+/+}$	0.86	-	-	-
GSDMD$^{I105N/I105N}$ →GSDMD$^{I105N/I105N}$	0.001	0.007	-	-
GSDMD$^{+/+}$ →GSDMD$^{I105N/I105N}$	0.004	0.026	0.86	-
% Weight change				
GSDMD$^{+/+}$→GSDMD$^{+/+}$	0.86	-	-	-
GSDMD$^{I105N/I105N}$→GSDMD$^{I105N/I105N}$	0.98	0.96	-	-
GSDMD$^{+/+}$→GSDMD$^{I105N/I105N}$	0.92	0.99	0.93	-
H&E score				
GSDMD$^{+/+}$→GSDMD$^{+/+}$	0.99	-	-	-
GSDMD$^{I105N/I105N}$→GSDMD$^{I105N/I105N}$	<0.0001	<0.001	-	-
GSDMD$^{+/+}$→GSDMD$^{I105N/I105N}$	<0.0001	<0.0001	0.99	-
TUNEL scores				
GSDMD$^{+/+}$→GSDMD$^{+/+}$	0.99	-	-	-
GSDMD$^{I105N/I105N}$→GSDMD$^{I105N/I105N}$	0.30	0.05	-	-
GSDMD$^{+/+}$→GSDMD$^{I105N/I105N}$	0.23	0.03	0.99	-

Chimer labelling: (donor of bone marrow) → (recipient, irradiated mouse)

3.9 References

1. Linkermann A, Chen G, Dong G, Kunzendorf U, Krautwald S, Dong Z. Regulated cell death in AKI. *Journal of the American Society of Nephrology : JASN*. 2014;25(12):2689-2701. doi:10.1681/ASN.2014030262
2. Krautwald S, Linkermann A. The fire within: pyroptosis in the kidney. *American Journal of Physiology-Renal Physiology*. 2014/01/15 2014;306(2):F168-F169. doi:10.1152/ajprenal.00552.2013
3. Hutton HL, Ooi JD, Holdsworth SR, Kitching AR. The NLRP3 inflammasome in kidney disease and autoimmunity. https://doi.org/10.1111/nep.12785. *Nephrology*. 2016/09/01 2016;21(9):736-744. doi:https://doi.org/10.1111/nep.12785
4. Komada T, Muruve DA. The role of inflammasomes in kidney disease. *Nature Reviews Nephrology*. 2019/08/01 2019;15(8):501-520. doi:10.1038/s41581-019-0158-z
5. Shigeoka AA, Mueller JL, Kambo A, et al. An inflammasome-independent role for epithelial-expressed Nlrp3 in renal ischemia-reperfusion injury. *Journal of immunology (Baltimore, Md : 1950)*. 2010;185(10):6277-6285. doi:10.4049/jimmunol.1002330
6. Wang J, Wen Y, Lv L-l, et al. Involvement of endoplasmic reticulum stress in angiotensin II-induced NLRP3 inflammasome activation in human renal proximal tubular cells in vitro. *Acta Pharmacologica Sinica*. 2015/07/01 2015;36(7):821-830. doi:10.1038/aps.2015.21
7. Miao N, Yin F, Xie H, et al. The cleavage of gasdermin D by caspase-11 promotes tubular epithelial cell pyroptosis and urinary IL-18 excretion in acute kidney injury. *Kidney International*. 2019;96(5):1105-1120. doi:10.1016/j.kint.2019.04.035
8. Wen Y, Liu Y-R, Tang T-T, et al. mROS-TXNIP axis activates NLRP3 inflammasome to mediate renal injury during ischemic AKI. *The International Journal of Biochemistry & Cell Biology*. 2018/05/01/ 2018;98:43-53. doi:https://doi.org/10.1016/j.biocel.2018.02.015
9. Kim H-J, Lee DW, Ravichandran K, et al. NLRP3 Inflammasome Knockout Mice Are Protected against Ischemic but Not Cisplatin-Induced Acute Kidney Injury. *Journal of Pharmacology and Experimental Therapeutics*. 2013;346(3):465. doi:10.1124/jpet.113.205732
10. Iyer SS, Pulskens WP, Sadler JJ, et al. Necrotic cells trigger a sterile inflammatory response through the Nlrp3 inflammasome. *Proc Natl Acad Sci U S A*. Dec 1 2009;106(48):20388-93. doi:10.1073/pnas.0908698106
11. Tang T-T, Lv L-L, Pan M-M, et al. Hydroxychloroquine attenuates renal ischemia/reperfusion injury by inhibiting cathepsin mediated NLRP3 inflammasome activation. *Cell Death & Disease*. 2018/03/02 2018;9(3):351. doi:10.1038/s41419-018-0378-3
12. Zou X-f, Gu J-h, Duan J-h, Hu Z-d, Cui Z-l. The NLRP3 inhibitor Mcc950 attenuates acute allograft damage in rat kidney transplants. *Transplant immunology*. 2020/08/01/ 2020;61:101293. doi:https://doi.org/10.1016/j.trim.2020.101293
13. Wang Y, Gao W, Shi X, et al. Chemotherapy drugs induce pyroptosis through caspase-3 cleavage of a gasdermin. *Nature*. Jul 6 2017;547(7661):99-103. doi:10.1038/nature22393
14. Xia W, Li Y, Wu M, et al. Gasdermin E deficiency attenuates acute kidney injury by inhibiting pyroptosis and inflammation. *Cell Death & Disease*. 2021/02/01 2021;12(2):139. doi:10.1038/s41419-021-03431-2
15. Wu M, Xia W, Jin Q, et al. Gasdermin E Deletion Attenuates Ureteral Obstruction- and 5/6 Nephrectomy-Induced Renal Fibrosis and Kidney Dysfunction. Original Research. *Frontiers in Cell and Developmental Biology*. 2021-October-21 2021;9doi:10.3389/fcell.2021.754134
16. Hindson J. Gasdermin B in IBD and epithelial barrier repair. *Nature Reviews Gastroenterology & Hepatology*. 2022/04/01 2022;19(4):216-216. doi:10.1038/s41575-022-00589-8
17. Liu X, Xia S, Zhang Z, Wu H, Lieberman J. Channelling inflammation: gasdermins in physiology and disease. *Nature Reviews Drug Discovery*. 2021/05/01 2021;20(5):384-405. doi:10.1038/s41573-021-00154-z
18. Evavold CL, Ruan J, Tan Y, Xia S, Wu H, Kagan JC. The Pore-Forming Protein Gasdermin D Regulates Interleukin-1 Secretion from Living Macrophages. *Immunity*. 2018/01/16/ 2018;48(1):35-44.e6. doi:https://doi.org/10.1016/j.immuni.2017.11.013
19. Shi J, Zhao Y, Wang K, et al. Cleavage of GSDMD by inflammatory caspases determines pyroptotic cell death. *Nature*. 2015/10/01 2015;526(7575):660-665. doi:10.1038/nature15514
20. Man SM, Kanneganti T-D. Gasdermin D: the long-awaited executioner of pyroptosis. *Cell Research*. 2015/11/01 2015;25(11):1183-1184. doi:10.1038/cr.2015.124
21. Liu Z, Wang C, Yang J, et al. Crystal Structures of the Full-Length Murine and Human Gasdermin D Reveal Mechanisms of Autoinhibition, Lipid Binding, and Oligomerization. *Immunity*. 2019/07/16/ 2019;51(1):43-49.e4. doi:https://doi.org/10.1016/j.immuni.2019.04.017
22. Jain S, Plenter R, Jeremy R, Nydam T, Gill RG, Jani A. The impact of Caspase-1 deletion on apoptosis and acute kidney injury in a murine transplant model. *Cell Signal*. Sep 2021;85:110039. doi:10.1016/j.cellsig.2021.110039
23. Chatterjee PK, Todorovic Z, Sivarajah A, et al. Differential effects of caspase inhibitors on the renal dysfunction and injury caused by ischemia-reperfusion of the rat kidney. *Eur J Pharmacol*. Oct 25 2004;503(1-3):173-83. doi:10.1016/j.ejphar.2004.09.025
24. Yang BIN, Jain S, Pawluczyk IZA, et al. Inflammation and caspase activation in long-term renal ischemia/reperfusion injury and immunosuppression in rats. *Kidney International*. 2005;68(5):2050-2067. doi:10.1111/j.1523-1755.2005.00662.x
25. Melnikov VY, Ecder T, Fantuzzi G, et al. Impaired IL-18 processing protects caspase-1–deficient mice from ischemic acute renal failure. *J Clin Invest*. 05/01/ 2001;107(9):1145-1152. doi:10.1172/JCI12089
26. Aglietti Robin A, Estevez A, Gupta A, et al. GsdmD p30 elicited by caspase-11 during pyroptosis forms pores in membranes. *Proceedings of the National Academy of Sciences*. 2016/07/12 2016;113(28):7858-7863. doi:10.1073/pnas.1607769113
27. Kayagaki N, Stowe IB, Lee BL, et al. Caspase-11 cleaves gasdermin D for non-canonical inflammasome signalling. *Nature*. 2015/10/01 2015;526(7575):666-671. doi:10.1038/nature15541
28. Nydam TL, Plenter R, Jain S, Lucia S, Jani A. Caspase Inhibition During Cold Storage Improves Graft Function and Histology in a Murine Kidney Transplant Model. *Transplantation*. 2018;102(9):1487-1495. doi:10.1097/tp.0000000000002218
29. Zhang Z, Shao X, Jiang N, et al. Caspase-11-mediated tubular epithelial pyroptosis underlies contrast-induced acute kidney injury. *Cell Death & Disease*. 2018/09/24 2018;9(10):983. doi:10.1038/s41419-018-1023-x
30. Yang J-R, Yao F-H, Zhang J-G, et al. Ischemia-reperfusion induces renal tubule pyroptosis via the CHOP-caspase-11 pathway. *American Journal of Physiology-Renal Physiology*. 2014/01/01 2013;306(1):F75-F84. doi:10.1152/ajprenal.00117.2013
31. Yang J, Liu Z, Wang C, et al. Mechanism of gasdermin D recognition by inflammatory caspases and their inhibition by a gasdermin D-derived peptide inhibitor. *Proceedings of the National Academy of Sciences*. 2018/06/26 2018;115(26):6792-6797. doi:10.1073/pnas.1800562115
32. Wang K, Sun Q, Zhong X, et al. Structural Mechanism for GSDMD Targeting by Autoprocessed Caspases in Pyroptosis. *Cell*. Mar 5 2020;180(5):941-955.e20. doi:10.1016/j.cell.2020.02.002

33. Bibo-Verdugo B, Snipas SJ, Kolt S, Poreba M, Salvesen GS. Extended subsite profiling of the pyroptosis effector protein gasdermin D reveals a region recognized by inflammatory caspase-11. *Journal of Biological Chemistry*. 2020;295(32):11292-11302. doi:10.1074/jbc.RA120.014259
34. Kayagaki N, Kornfeld OS, Lee BL, et al. NINJ1 mediates plasma membrane rupture during lytic cell death. *Nature*. 2021/03/01 2021;591(7848):131-136. doi:10.1038/s41586-021-03218-7
35. Schneider KS, Groß CJ, Dreier RF, et al. The Inflammasome Drives GSDMD-Independent Secondary Pyroptosis and IL-1 Release in the Absence of Caspase-1 Protease Activity. *Cell Reports*. 2017/12/26/ 2017;21(13):3846-3859. doi:https://doi.org/10.1016/j.celrep.2017.12.018
36. Ding J, Wang K, Liu W, et al. Pore-forming activity and structural autoinhibition of the gasdermin family. *Nature*. 2016/07/01 2016;535(7610):111-116. doi:10.1038/nature18590
37. Rogers C, Erkes DA, Nardone A, Aplin AE, Fernandes-Alnemri T, Alnemri ES. Gasdermin pores permeabilize mitochondria to augment caspase-3 activation during apoptosis and inflammasome activation. *Nature Communications*. 2019/04/11 2019;10(1):1689. doi:10.1038/s41467-019-09397-2
38. Chen H, Li Y, Wu J, et al. RIPK3 collaborates with GSDMD to drive tissue injury in lethal polymicrobial sepsis. *Cell Death & Differentiation*. 2020/09/01 2020;27(9):2568-2585. doi:10.1038/s41418-020-0524-1
39. Sollberger G, Choidas A, Burn GL, et al. Gasdermin D plays a vital role in the generation of neutrophil extracellular traps. *Science Immunology*. 2018;3(26):eaar6689. doi:10.1126/sciimmunol.aar6689
40. Chen KW, Monteleone M, Boucher D, et al. Noncanonical inflammasome signaling elicits gasdermin D–dependent neutrophil extracellular traps. *Science Immunology*. 2018;3(26):eaar6676. doi:10.1126/sciimmunol.aar6676
41. Ma C, Yang D, Wang B, et al. Gasdermin D in macrophages restrains colitis by controlling cGAS-mediated inflammation. *Science Advances*. 6(21):eaaz6717. doi:10.1126/sciadv.aaz6717
42. He W-t, Wan H, Hu L, et al. Gasdermin D is an executor of pyroptosis and required for interleukin-1β secretion. *Cell Research*. 2015/12/01 2015;25(12):1285-1298. doi:10.1038/cr.2015.139
43. Zhang Y, Chen X, Gueydan C, Han J. Plasma membrane changes during programmed cell deaths. *Cell Research*. 2018/01/01 2018;28(1):9-21. doi:10.1038/cr.2017.133
44. Chen X, He W-t, Hu L, et al. Pyroptosis is driven by non-selective gasdermin-D pore and its morphology is different from MLKL channel-mediated necroptosis. *Cell Research*. 2016/09/01 2016;26(9):1007-1020. doi:10.1038/cr.2016.100
45. Wang Y, Zhu X, Yuan S, et al. TLR4/NF-κB Signaling Induces GSDMD-Related Pyroptosis in Tubular Cells in Diabetic Kidney Disease. Original Research. *Frontiers in Endocrinology*. 2019-September-19 2019;10(603)doi:10.3389/fendo.2019.00603
46. Zou XF, Gu JH, Duan JH, Hu ZD, Cui ZL. The NLRP3 inhibitor Mcc950 attenuates acute allograft damage in rat kidney transplants. *Transplant immunology*. Aug 2020;61:101293. doi:10.1016/j.trim.2020.101293
47. Li Y, Xia W, Wu M, et al. Activation of GSDMD contributes to acute kidney injury induced by cisplatin. *Am J Physiol Renal Physiol*. Jan 1 2020;318(1):F96-f106. doi:10.1152/ajprenal.00351.2019
48. Cheng Q, Pan J, Zhou Z-l, et al. Caspase-11/4 and gasdermin D-mediated pyroptosis contributes to podocyte injury in mouse diabetic nephropathy. *Acta Pharmacologica Sinica*. 2021/06/01 2021;42(6):954-963. doi:10.1038/s41401-020-00525-z
49. Andreas Linkermann WT, Francesca Maremonti et al. Gasdermin D-deficient mice are hypersensitive to acute kidney injury. *PREPRINT (Version 1) available at Research Square [https://doiorg/1021203/rs3rs-1719338/v1]*. 2022;
50. Wang D, Zheng J, Hu Q, et al. Magnesium protects against sepsis by blocking gasdermin D N-terminal-induced pyroptosis. *Cell Death & Differentiation*. 2020/02/01 2020;27(2):466-481. doi:10.1038/s41418-019-0366-x
51. Hu JJ, Liu X, Xia S, et al. FDA-approved disulfiram inhibits pyroptosis by blocking gasdermin D pore formation. *Nature Immunology*. 2020/07/01 2020;21(7):736-745. doi:10.1038/s41590-020-0669-6
52. Rathkey Joseph K, Zhao J, Liu Z, et al. Chemical disruption of the pyroptotic pore-forming protein gasdermin D inhibits inflammatory cell death and sepsis. *Science Immunology*. 2018/08/24 2018;3(26):eaat2738. doi:10.1126/sciimmunol.aat2738
53. Liu Z, Wang C, Rathkey JK, et al. Structures of the Gasdermin D C-Terminal Domains Reveal Mechanisms of Autoinhibition. *Structure*. May 1 2018;26(5):778-784.e3. doi:10.1016/j.str.2018.03.002
54. Kayagaki N, Stowe IB, Lee BL, et al. Caspase-11 cleaves gasdermin D for non-canonical inflammasome signalling. *Nature*. Oct 29 2015;526(7575):666-71. doi:10.1038/nature15541
55. Rogers NM, Zhang ZJ, Wang J-J, Thomson AW, Isenberg JS. CD47 regulates renal tubular epithelial cell self-renewal and proliferation following renal ischemia reperfusion. *Kidney International*. 2016;90(2):334-347. doi:10.1016/j.kint.2016.03.034
56. Man SM, Karki R, Kanneganti T-D. Molecular mechanisms and functions of pyroptosis, inflammatory caspases and inflammasomes in infectious diseases. *Immunol Rev*. 2017;277(1):61-75. doi:10.1111/imr.12534

4 Chapter 4

Clinical and Transcriptomic Associations with Delayed Graft Function in the Australian Chronic Allograft Dysfunction Study (AUSCAD)

Overview

Hypothesis	▪ Patients with delayed graft function have distinct transcriptomic profiles which can guide intervention/treatment strategies
Aims	▪ Characterise the clinical characteristics and outcomes of patients enrolled in the single-centre AUSCAD study ▪ Perform differential gene and pathway analysis on bulk transcriptomic profiles of kidney biopsies comparing patients with and without DGF; and determine if these changes persist on protocol 1- and 3-month biopsies ▪ Determine if transcriptomic profiles of the pre-implant biopsy can guide selection of donor organs which would most benefit from intervention pre- or peri-transplantation. ▪ Determine the feasibility to quantify neutrophil infiltration and/or NETosis on FFPE kidney biopsies.
Main findings	▪ This chapter characterises the pro-inflammatory transcriptomic signatures in pre-implantation and protocol post-transplantation biopsies which differentiate delayed graft function from immediate graft function in patients after kidney or simultaneous kidney-pancreas transplantation. ▪ A proposed gene signature for DGF with severe outcomes is derived and will need external validation when possible. If validated, this signature(s) could help guide risk stratification and optimise treatment and resource utilisation.

4.1 Abstract

The AUSCAD cohort is a prospective study of kidney (KT) and kidney-pancreas transplant (SPK) patients recruited through Westmead Hospital with availability of paired clinical and 0-, 1- and 3- month blood and kidney transcriptomics data for analysis. Since 2012, a total of 266 patients have enrolled and 245 have data out to at least 12-months post transplantation. Focusing on prediction and outcomes following ischemia reperfusion injury (IRI) and donor-related acute kidney injury (AKI), the cohort was split into control (n=170), delayed graft function (DGF, n=53, 22%) and slow graft function (SGF, n=28, 11%) groups. The significant risk factors ($P<0.05$) for DGF were donor related factors (need for inotropes odds ratio (OR 6.14), donation after circulatory death (OR3.30) or deceased-donor allograft (OR 0.2 for living-donor allograft)), diabetic nephropathy in the recipient (OR 3.25) and transplantation before 2016 (OR 4.33). Clinical factors only had a modest ability to predict the incidence of DGF and this is not surprising with only 22% of variance explained on the first 5-PCA dimensions of clinical variables.

There were over 300 differentially expressed genes between DGF and controls on the pre-implantation biopsy when batch, organ type (SPK, live- or deceased- donor KT), DCD status, presence of pre-transplant DSA and graft number (1st transplant vs regraft) were accounted for. These transcripts were enriched for innate and adaptive (particularly humoral and B-cell related) pathways on the 0-month biopsy, with persistent humoral/B-cell upregulation on the 3-month biopsies even when controlled for biopsy proven acute rejection episodes. DGF was associated with increased risk of both early biopsy proven rejection and subclinical rejection and lower 3- and 12-month estimated (eGFR) and measured (mGFR) glomerular filtration rate. The relative risk of interstitial fibrosis and tubular atrophy (IFTA) scores ≥ 2 was 2.26 ($P=0.02$) and a 12-month mGFR ≤ 45 ml/min was 2.06 ($P=0.05$). Both 12-month IFTA and mGFR were associated with increased hazard ratios of death, regardless of DGF/SGF group. SGF was also associated with worse 12-month mGFR and transcriptomically had worse inflammation and injury compared to DGF on the implantation biopsy and persistently dysregulated humoral/B cell pathways on the 3-month biopsy. These suggest that transcripts can help identify patients at risk of SGF and DGF, although the gene list needs further optimisation and that SGF is not a benign entity and should not be ignored in future studies of acute peri-transplant events in clinical kidney transplantation.

4.2 Introduction

Delayed graft function (DGF) is a manifestation of severe acute kidney injury (AKI) which results from the culmination of renal insults sustained during the donor's terminal admission, factors related to organ retrieval and transplantation surgery, and ischemia reperfusion injury when blood flow is restored to the allograft[1,2]. Patients with DGF are burdened with worse graft and patient outcomes and there is an opportunity to improve clinical outcomes with targeted interventions to this form of severe AKI. To date, over 40 clinical studies of pharmacological to prevent DGF have not demonstrated convincing clinical utility[3,4] - although several are still in progress and there has been enthusiasm for machine perfusion technologies to help fill this void[5-7].

Some of the challenges that have hampered progress in this field include significant heterogeneity in the definition of DGF used by investigators[8], significant lead time required for translation of discovery research, and difficulties with trial recruitment in transplantation given relatively infrequent or low event rates for long term hard outcomes such as death, or death-censored graft loss[9,10]. To address DGF definitions, the FDA has limited DGF to needing dialysis post transplantation[11], which helps to unify prospective and retrospective studies moving forward. This definition only captures severe forms of AKI/IRI and clinically, this may be impacted by other factors which push the clinician to initiate dialysis, such as pre-transplant biochemical factors. Slow graft function, which itself does not have uniform definition is characterised by slow improvement in serum creatinine early post-transplantation, is also a form of AKI/IRI which has important clinical implications[12]. To address trial recruitment, economics and lag time to events, much focus has been invested in the area of biomarkers and surrogate endpoints[13-15] and this has been accompanied by increasing use of molecular profiling technologies in the quest to improve precision, discover new targets and/or determine potential causal effects of genetic variations[16-20].

In the attempt to improve patient enrichment for future clinical trials, pre-implantation transcriptomic data from the AUSCAD cohort was examined to determine their potential to improve prediction of DGF and long-term allograft function compared to clinical variables alone.

4.3 Methods

4.3.1 Study design and participants

The Australian Chronic Allograft Dysfunction Study (AUSCAD) is a prospective, single-centre, observational study recruiting patients at time of kidney or simultaneous kidney-pancreas transplantation at Westmead Hospital from 2012 onwards. The study was approved by the local Western Sydney Local Health District Human Research Ethics Committee. Serial blood, urine and kidney biopsies were obtained in addition to routine clinical care at time of transplantation and at protocolised follow up at 1-, 3- and 12-months post transplantation for biobanking to determine clinical and genomic factors which may be associated with rejection or allograft dysfunction.

Clinical data for this thesis was updated until 1st October 2020. Patients were eligible for enrolment into the study if they were aged 18 – 75 years, able to understand and provide written consent and receiving either a kidney transplant (KT), either from deceased or live-donor, or a simultaneous pancreas-kidney transplant (SPK). Exclusion criteria included if they were pre-sensitised or cross match positive; recipient of multiple organ transplants (excluding SPK); inability/unwilling to comply with the study protocol. (Fig 4.1)

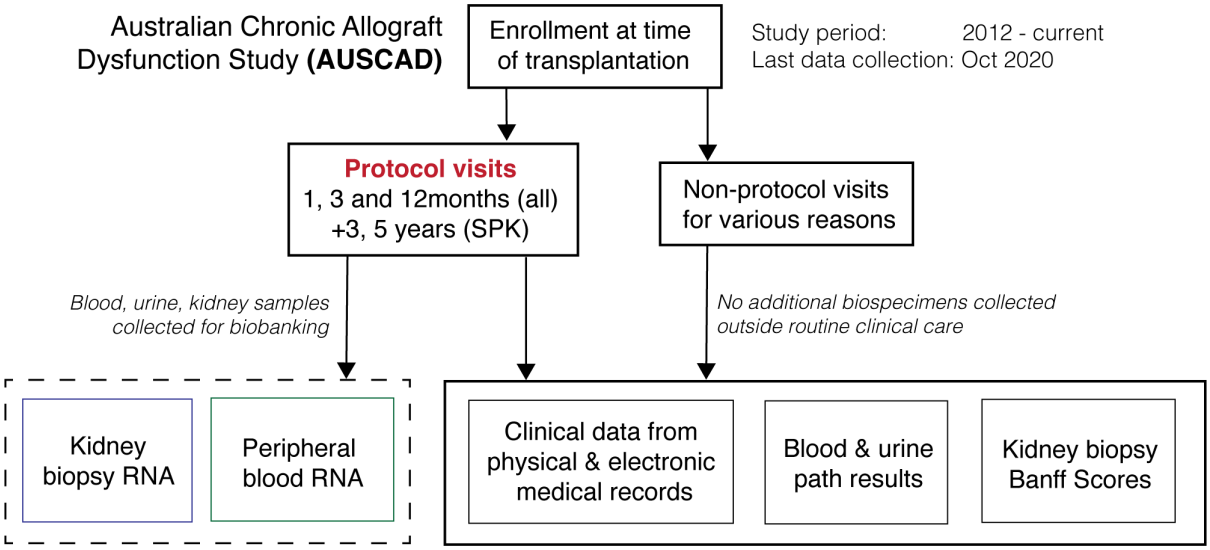

Figure 4.1: Overview of data and biospecimen collection for the Australian Chronic Allograft Dysfunction Study (AUSCAD).

4.3.2 Clinical data and statistical analysis

Of the enrolled subjects, only patients who had either been in the study for at least 12 months or had either died or lost their graft prior to this were included in the final cohort for analysis. Data collection was ceased for patients who either declined further participation in the study or were censored as lost to follow up if no clinical data was available on physical or electronic entries accessible through the Westmead Hospital medical records for 5 years after the last available records. The following section describes the donor, recipient pre-transplant and outcome data collected, and this can also be found in a supplementary digital file on https://github.com/jenli3/PhD2022.

Delayed graft function (DGF) was the study variable of interest, given it is a clinical manifestation of acute kidney injury early post transplantation which is captured in the clinical data. In light of the different definitions used in research, we aligned our definition with that used by the Food and Drug Authority (FDA), which defines DGF was any patient needing dialysis within the first 7 days post transplantation. Patients with a creatinine drop of ≤ 20% within the first 48-hours were categorised to have slow graft function (SGF) and the remaining patients who did not require dialysis in the first 7 days and > 20% drop the serum creatinine within the first 48 hours post transplantation were designated as controls. The following clinical variables were collected and include baseline, donor, perioperative and post-transplantation considerations and exploratory data analysis was performed using factorial analysis of mixed data (a generalised form of principal component analysis and multiple corresponding analysis) using the FactorMineR *R* package to normalise and derive eigenvalues and variances for each axis or dimension[21].

Baseline recipient characteristics included: age, gender, blood group, 1st transplant (or regraft), transplant type (kidney only or kidney-pancreas transplant), transplant year, pre-existing vascular comorbidities (ischemic heart disease, diabetes mellitus, hypertension, or dyslipidaemia), pre-emptive or on dialysis and their CMV and EBV IgG status at time of transplantation. The number of HLA mismatches and presence (or absence) of pre-existing donor specific antibodies (DSA) were recorded, along with induction immunosuppression. Patients were classified to require additional induction immunosuppression (including

anti-thymocyte globulin, rituximab, or plasma-exchange) if they received agents outside the standard induction protocol with basiliximab, tacrolimus, mycophenolate, and prednisolone.

Donor information collected included: donor type, age, gender, blood group, CMV and EBV IgG status and if deceased donor – the admission and terminal creatinine, inotrope and intubation requirements, ischemic times and KDPI if available. Donor types used in this section includes live and deceased donors. Deceased donors were further subdivided into donation after brain death (DBD) – donors meeting criteria for brain death but maintain intact circulatory and respiratory function prior to organ procurement; donation after cardiac death (DCD), where there was compromised cardiac function prior to organ retrieval; and expanded criteria donor (ECD), which encapsulates a donor who at time of death is aged over 60 years of age, or aged between 50-59 years but with either 2 of the following: cerebrovascular accident causing death, pre-existing hypertension, or terminal creatinine ≥132μmol/L[22].

Baseline recipient and donor characteristics of the cohort based on these DGF definitions was represented by the median & interquartile ranges displayed for continuous variables and median and percentage displayed for categorical variables. Chi-squared (or Fischer's exact test) for categorical variables and Mann-U Whitney or Kruskal-Wallis for variables depending on the number of groups to test for independence (if $P < 0.05$). Odds ratio of clinical risk factors for developing DGF were determined by backward, stepwise, multiple logistic regression of variables known to be important *a priori* and if univariate analysis determined $P \leq 0.3$. The confidence intervals for the C-statistic were derived by 999 bootstrapped replicates. The relative risks of DGF to 12-month outcomes renal function and IFTA scores were calculated.

Clinical, laboratory and histopathological data was recorded if available for all patients at immediate post-transplant period and protocol 1, 3, 12- month reviews for kidney transplant and additionally 3- and 5-year reviews for simultaneous kidney-pancreas transplant. Significant clinical events recorded during admissions or additional clinic visits outside these protocol visits were also recorded. Serum creatinine, eGFRs were recorded for pre-transplant, 0hr, 4hr, days 1, 2, 7, 14, 21 and months 1, 3 and 12 and then yearly post-transplant. Three- or 12-month measured GFR (by either technetium-99m diethylene triamine penta-acetic

acid (DTPA) or mercaptoacetyltriglycine (MAG3) scans) were recorded available. Trough tacrolimus levels at days 1 and 2, and week 1, 2, 3 and months 1, 3, 12 post-transplants were recorded.

Banff scores and reports extracted from electronic medical records for available biopsies. Acute, chronic, interstitial fibrosis and tubular atrophy ± inflammation (IFTA/iIFTA)[23] lesions were normalised by re-scoring, performed in a blinded fashion by an independent renal pathologist (M.S) according to the Banff 2018 reference[24] for available 3- and 12- month biopsies. Biopsy proven acute rejection (BPAR) included either T-cell mediated rejection (TCMR) and antibody mediated rejection (ABMR). Subclinical rejection was defined as *Banff-i* > 0 and *Banff-t* > 0 but not meeting acute TCMR or AMBR definitions **but** needing additional immunosuppression. IFTA, iIFTA, ci and ct scores were dichotomised as low if <2 and high if ≥ 2. Delta (Δ) biopsy scores were derived from the difference between current minus previous score (ie Δ 1-3m = 3-month Banff score minus 1-month Banff score), etc. Differences between DGF groups were again assessed using either Chi-squared (or Fischer's exact test) for categorical variables and Mann-U Whitney (if only 2-groups) or Kruskal-Wallis (more than 2-groups) for variables depending on the number of groups to test for independence (if $P < 0.05$). The relative risk was calculated for high IFTA or low mGFR depending on DGF group.

The primary outcomes assessed was the composite event of death, renal allograft loss or loss to follow up. Secondary outcomes included: graft survival (death-censored and non-censored), biopsy proven rejection (& subclinical rejection if additional immunosuppression given), 12-month renal function, chronic kidney biopsy scores and major post-transplant complication: infection, coronary, metabolic or malignancy events. Histopathological classification of renal biopsies was assessed by experienced pathologists as part of routine clinical care. Kaplan Meier survival curve with log-rank tests and cox regression (or proportional hazards regression) to estimate the hazard ratio using the survminer[25] package and time to event analysis with competing risks for DGF versus control was performed using the *cmprsk*[26] package.

Available clinical variables were tested in a penalised logistic regression model (using the least absolute shrinkage selection operator, LASSO method) to determine the ability to predict 12-month outcomes based

on the *a priori* list of important clinical parameters collected (described above) within this dataset using the *Caret*[27] package in R. The dataset was split 60:40 for clinical data (or 50:50 for the smaller RNAseq samples set) to a training and test dataset with ONE-HOT encoding to create dummy variables for conversion of categorical to continuous variables and missing variables were imputed using the k-Nearest neighbours' algorithm with 10-fold cross validation[28-31].

Data extraction of additional donor height, weight, ethnicity, and HCV status to retrospectively calculate the Kidney donor profile index (KDPI) and de-novo DSA parameters were not yet available for this cohort at time of analysis. The pre-implantation (0-month), 1-month and indication biopsies were not yet rescored by the time of this write up. Data analysis of the above groups were not propensity matched. All statistical analysis was performed using R (R studio) and figures were generated using R or BioRender.com.

4.3.3 RNAseq, data analysis

Kidney biopsy specimens were left in RNAlater (ThermoFischer) overnight at 4°C before removal from the RNAlater solution and stored at -80°C until RNA extraction. RNA was extracted using AllPrep DNA/RNA/microRNA and MiniElute clean up kits (Qiagen, Germany) and samples were then sent to Australian Genome Research Facility (AGRF), Melbourne, Australia. Sample QC and library preparation were performed in-house by AGRF, and the resultant libraries sequenced using the NovaSeq 6000 platform (Illumina) with 100bp, pair-end read length. Raw FASTQ files were trimmed, aligned (using the GRCh37-hg19 reference genome), and organised into a gene counts matrix for each sample by our bioinformatician Dr Brian Gloss (Westmead Institute for Medical Research) using the University of Sydney High Power Computing cluster. Downstream analysis was performed using R/R-studio (v4.1.2). *EdgeR/limma* packages[1-3] were used for differential expression analysis. Firstly, low counts (<10) were removed using the *filterByExpr* function and then normalised using *calcNormFactors*, using the trimmed mean of M-values (TMM) method[32]. Covariates in the design matrix included batch for all analysis, with specific clinical variables depending on the conditional analysis are described in the following sections. Differentially expressed genes (DEG) were determined by the generalised linear model function *glmQLFTest*[4]. This generates gene-wise dispersion coefficients to represent the variability of each gene between biological

conditions based on negative binomial modelling but using the quasi-likelihood (QL) method (utilising the F-test statistic) to minimise the higher false discovery rate (FDR) compared to standard likelihood ratio tests used otherwise[33,34]. The FDR threshold was set at 0.05 using the Benjamini-Hochberg method. Pathway enrichment analysis was then performed to help interpret the biological significance of DEG lists for specific conditional groups. Gene set enrichment analysis[8] (GSEA) leveraging the Gene Ontology (GO) database[9] was performed using *clusterProfiler*[10]. Again, the adjusted P <0.05, using the Benjamini-Hochberg method to correct for multiple hypothesis testing, was used as the minimum threshold for significance[11]. GSEA was chosen instead of over representation analysis as it leverages both magnitude and direction to determine genes at either the top or bottom ends of the input DEG gene vector are found in *a priori* defined gene sets are significantly different between two conditions.

4.3.4 Neutrophil quantification

Residual kidney biopsy tissue stored as formalin-fixed, paraffin-embedded (FFPE) blocks following routine histopathological assessment for rejection and Banff scoring were retrieved 0-, 1- and 3-month biopsies if available. These were then sectioned to obtained 3um thick samples, air-dried onto glass slides and stored at 4°c for further processing. Optimisation of neutrophil staining was performed on additional samples obtained from graft nephrectomy for chronic rejection (positive control) and minimal change disease (negative control). Neutrophil elastase was the only reliably reproduced stain using the mouse, anti-human neutrophil elastase (M0752, DAKO) polyclonal antibody following routine dewaxing using xylene, rehydration with decreasing concentrations of ethanol and antigen retrieval using Diva Decloaker (ph 6.2, Biocare) at 60°c for 90minutes. Secondary antibody staining was achieved through the use of goat, anti-mouse AF488 (ThermoFisher) and 7 – 10 images per sample were acquired at 60x magnification using the Olympus Confocal FV1000 machine (Westmead Research Hub, Westmead Institute for Medical Research). Images were then counted by two independent, blinded assessors for the number of neutrophils per high power field (hpf). Neutrophilic infiltration was determined as the average counts per hpf for each sample and compared for the specified groups with Kruskal Wallis rank sum test and Chi-squared tests.

4.4 RESULTS

4.4.1 Overall cohort characteristics

Two-hundred and fifty one of 266 patients enrolled were included in the AUSCAD cohort for analysis, with 179 kidney transplants (43 live- and 136 deceased-donor) and 72 simultaneous kidney-pancreas transplants. One-hundred and seventy (69%) patients and 118 patients (48%) had follow-up data up to 3- and 5- years post transplantation respectively during the defined study period. During follow up, a total of 33 primary composite events occurred – 22 patients died (17 of these with a functioning graft) and 14 patients lost their graft (3 of these were death censored graft loss).

Six of the 251 patients included had events before the 12-month time point, including 2 who died with a functioning graft, 1 died after soon after graft loss and 3 patients who survived but are back on dialysis after renal allograft loss. There were 52 recorded biopsy proven rejection events, with 28 occurring within the 1st month post transplantation and similarly, there were 62 recorded subclinical events, with 32 occurring within the first month.

Overall, there were 170 control patients, 53 DGF and 28 SGF patients and the number of DGF events stratified by definition/severity and donor criteria is shown in Table 4.1. DGF by any criteria were concentrated in the DCD group, with 38% needing dialysis within the 1st week compared to 17% from the DBD group. ($P < 0.001$). This pattern was maintained when stratified for DGF severity based on duration (greater or less than 7 days).

Table 4.1: DGF definition and severity stratified for donor criteria. Results shown as frequency (percent for each donor type).

Baseline	**DBD** N = 117	**DBD + ECD** N = 9	**DCD** N = 71	**DCD + ECD** N = 9	**LKD** N = 45
Delayed graft function	20	1	27	3	2
HD <= 7 days	13	1	17	2	0
HD > 7 days	7	0	10	1	1
Slow graft function	14	1	10	2	1
Cr drop < 20% (48hrs)	5	1	2	1	0
Cr drop < 10% (48hrs)	8	0	8	1	1

DGF.HD for DBD compared to DCD: P value < 0.001, Chi Square test

Donors meeting ECD criteria did not have significant impact on DGF rates, although this was likely related to the lower prevalence in the cohort. From these subgroups, there were 112, 34 and 89 RNAseq control samples of protocol biopsies collected at 0-, 1- and 3- months respectively. Similarly, there were 35, 13 and 31 available RNAseq samples of DGF based on dialysis criteria alone for these time points, but of the preimplantation biopsies, only 13 samples were available for DGF with 12-month IFTA scores and 19 for DGF with 12-month mGFR data. (Fig 4.2)

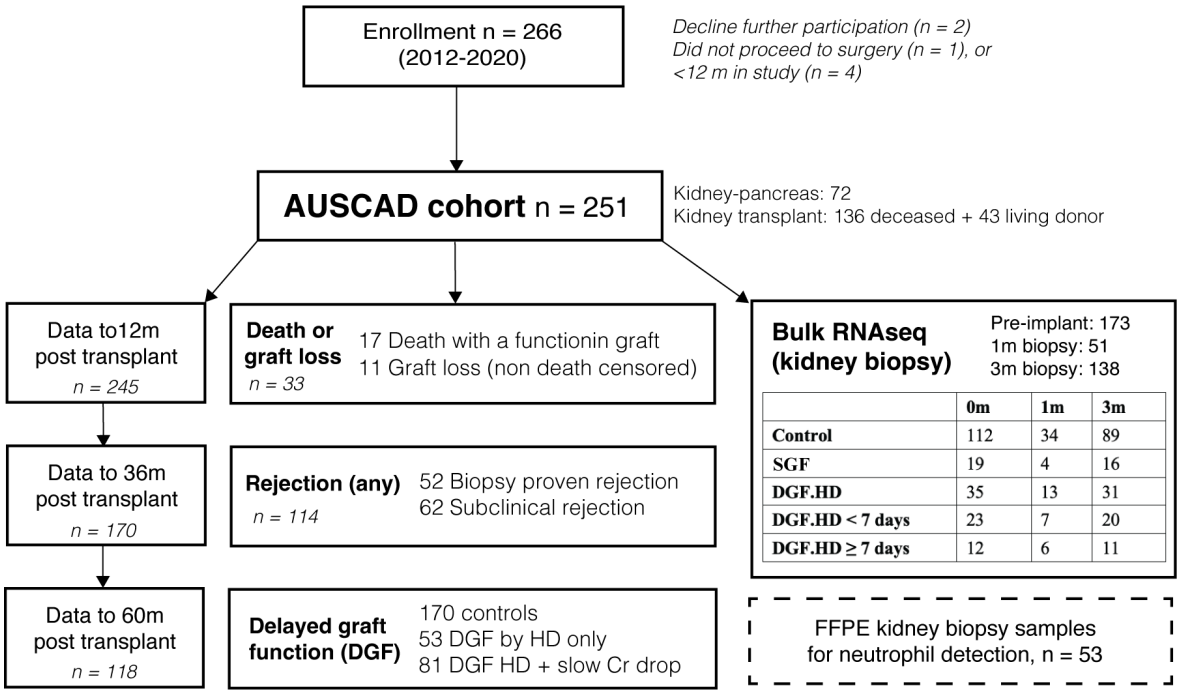

	0m	1m	3m
Control	112	34	89
SGF	19	4	16
DGF.HD	35	13	31
DGF.HD < 7 days	23	7	20
DGF.HD ≥ 7 days	12	6	11

Figure 4.2: Cohort details of n = 251 patients included for the final analysis in this manuscript with regards to clinical data, kidney bulk-RNA-seq samples and number of adequate formalin-fixed, paraffin-embedded (FFPE) samples (used in next section on neutrophil detection). (Slow graft function coded as DGF.Cr)

Exploratory data analysis to show significant relationships between 81 important continuous and categorical variables were assessed initially using factor analysis of mixed data (FAMD) (*FactoMineR*[21] package) for 245 patients with minimum 12 months of data. Factor analysis of clinical variables showed the most important ones to discriminate within the first 5 dimensions were renal function (eGFR), chronic biopsy scores (ci and ct0), organ type, donor criteria, cold ischemic time, DGF, rejection and BK virus associated nephropathy (BKVAN) (Supp Fig 4.17). These are all important and relevant clinical variables but could only account for 22% of the variability in the clinical dataset.

Considering factor plots (PCA plots) of all individuals (as dots) based on the a priori selected 81 important clinical variables, there was separation of the cohort based on transplant type (live-, deceased- donor kidney and simultaneous pancreas-kidney transplant), DGF criteria, donor inotrope requirements and cold ischemic time (particularly < 6 hours versus ≥ 6 hours) (Fig 4.3a). The separation based on these factors was reduced for DGF, donor inotropic support and cold ischemic time when only deceased-donor transplants were considered. (Fig 4.3b).

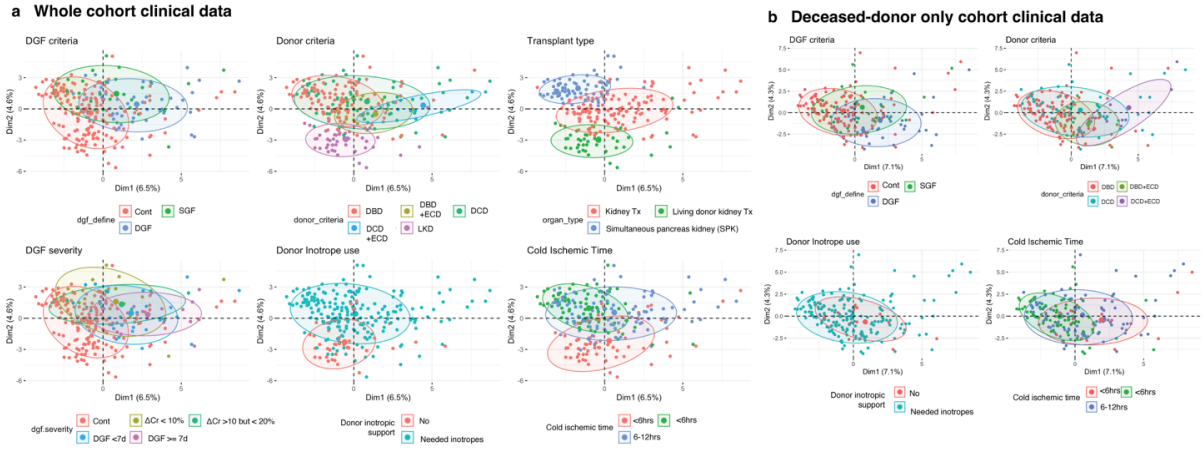

Figure 4.3:The first 2 dimensions of factor analysis of mixed data (FAMD) for clinical data shown for a) all patients in the cohort and b) patients who received deceased-donor organ only. These were then split into factors of function categories (contro; slow graft function, SGF; and delayed graft function, DGF), donor criteria (donor after brain death, DBD; donor after cirulatory death, DCD; extended-criteria donors, ECD; and living-donor kidney donor, LKD), transplant organ type, DGF severity, donor need for inotrope and cold ischemia time (split by every 6-hours).

This method scales both continuous and categorical variables to perform factor analysis of mixed data (mix of principal component analysis and multiple correspondence analysis) to determine associations between these variables in the dataset. This included DGF related variables (control subjects, slow creatinine change, or patients needing dialysis), donor variables (need for inotropes, donation criteria, sex, age, cold ischemic time), recipient variables (age at transplantation, sex, comorbidities including diabetes, hypertension and cardiac disease, transplant year for all transplants, deceased-donor only transplants), immunological variables (transplant type, HLA mismatches, pre-existing DSA, induction method, graft number and tacrolimus levels at day 2, 7, 14, 21 and months 1, 3 and 12) and outcome related variables (death, graft loss, biopsy proven rejection, subclinical rejection, eGFR at 1, 3 and 12 months and chronic biopsy scores (ci, ct, cg, cv, iIFTA), BKVAN, NODAT, post-transplant infections).

Baseline characteristics of control versus DGF or SGF are shown in table 4.2. Patients who received a living donor kidney transplant (pre-emptive) were less likely to develop DGF, an expected finding given the short ischemic times and allograft quality.

Table 4.2: Baseline recipient and donor characteristics for patients classified into control vs DGF

	All transplants					Deceased donor only		
Cohort n = 251	**Control** (n = 170)	**DGF** (n = 53)	p-value vs control	**SGF** (n = 28)	p-value vs control	**Control** (n = 131)	**DGF** (n = 50)	p-value vs control
Recipient age (yrs)	46 (38, 58)	53 (44, 59)	0.11	52 (44, 60)	0.11	46 (38, 57)	54 (44, 59)	0.049
Recipient sex (M)	109 (64%)	33 (62%)	0.8	16 (57%)	0.5	78 (62%)	31 (62%)	>0.9
Pre-emptive Tx	26 (15%)	0 (0%)	-	1 (3.6%)	0.14	11 (8.8%)	0 (0%)	-
Transplant type			<0.001		0.031			<0.001
Kidney	79 (46%)	43 (81%)		14 (50%)		79 (60%)	43 (86%)	
LKD	39 (23%)	3 (5.7%)		1 (3.6%)		-	-	
SPK	52 (31%)	7 (13%)		13 (46%)		52 (40%)	7 (14%)	
Co-morbidities								
IHD	25 (15%)	9 (17%)	0.8	23 (82%)	0.8	22 (18%)	8 (16%)	0.8
Diabetes (any)	73 (43%)	22 (42%)	0.8	18 (64%)	0.036	66 (53%)	20 (40%)	0.13
Hypertension	129 (76%)	43 (81%)	0.4	20 (71%)	0.6	90 (72%)	41 (82%)	0.2
Dyslipidaemia	24 (14%)	12 (23%)	0.2	6 (21%)	0.4	14 (11%)	11 (22%)	0.065
Renal disease			0.06		0.2			0.012
T1DM	53 (31%)	11 (21%)		14 (50%)		52 (42%)	10 (20%)	
T2DM	12 (7.1%)	10 (19%)		4 (14%)		8 (6.4%)	10 (20%)	
HTN	11 (6.5%)	1 (1.9%)		0		6 (4.8%)	1 (2.0%)	
GN	57 (34%)	21 (40%)		6 (21%)		36 (29%)	20 (40%)	
PCKD	17 (10%)	7 (13%)		1 (3.6%)		10 (8.0%)	6 (12%)	
Other	20 (12%)	3 (5.7%)		3 (11%)		13 (10%)	3 (6.0%)	
Re-graft	9 (5.0%)	7 (13%)	0.067			4 (3.2%)	6 (12%)	0.033
HLA mismatch			0.9		0.3			0.6
0	8 (4.7%)	4 (7.5%)		0 (0%)		2 (1.5%)	3 (6.0%)	
1	15 (8.8%)	6 (11%)		2 (7.1%)		10 (7.6%)	6 (12%)	
2	16 (9.4%)	6 (11%)		6 (21%)		13 (9.9%)	6 (12%)	
3	21 (12%)	4 (7.5%)		2 (7.1%)		17 (13%)	4 (8.0%)	
4	43 (25%)	14 (26%)		7 (25%)		31 (24%)	13 (26%)	
5	36 (21%)	9 (17%)		9 (32%)		29 (22%)	9 (18%)	
6	31 (18%)	10 (19%)		2 (7.1%)		29 (22%)	9 (18%)	
Pre-Tx DSA								
Class I	30 (18%)	15 (28%)	0.09	4 (14%)	0.8	24 (18%)	14 (28%)	0.2
Class II	28 (16%)	12 (23%)	0.3	8 (29%)	0.12	22 (17%)	11 (22%)	0.4
Standard induction	158 (93%)	46 (87%)	0.2	27 (96%)	0.9	7 (5.6%)	6 (12%)	0.2
Donor criteria			<0.001		0.021			0.003
DBD alone	83 (48%)	20 (38%)		14 (50%)		83 (66%)	20 (40%)	
DBD + ECD	7 (4.1%)	1 (1.9%)		1 (3.6%)		7 (5.6%)	1 (2.0%)	
DCD alone	34 (20%)	27 (51%)		10 (36%)		34 (26%)	27 (52%)	
DCD + ECD	4 (2.4%)	3 (5.7%)		2 (7.1%)		4 (3.2%)	3 (6.0%)	
LKD	43 (25%)	2 (3.8%)		1 (3.6%)		-	-	
Donor age	42 (32, 57)	43 (38, 58)	0.3	40 (26, 48)	0.088	43 (32, 57)	43 (38, 58)	0.4
Donor sex (male)	76 (47%)	31 (58%)	0.13	13 (46%)	>0.9	68 (54%)	31 (62%)	0.4
Donor inotrope use	137 (81%)	51 (96%)	0.006	25 (89%)	0.3	118 (94%)	48 (96%)	>0.9
Donor terminal creatinine	69 (58, 78)	70 (64, 94)	0.036	70 (58, 82)	0.5	69 (52, 84)	70 (63, 96)	0.073
Cold ischemic time (mins)	508 (293, 630)	511 (411, 676)	0.2	552 (512, 737)	0.018	556 (458, 676)	512 (412, 690)	0.3

Age at transplantation in years. SPK: simultaneous pancreas-kidney transplant, LKD: living-donor kidney transplant.
Pearson's Chi-squared test; Fisher's exact test; Wilcoxon rank sum test

Donor inotropic support before organ procurement ($P < 0.001$) or longer cold ischemic times ($P = 0.03$) were different between the control and DGF groups. However, when only deceased donor transplants were considered (living donor kidney transplant excluded), cold ischemic time was not significantly different between groups, although older donors were more likely to be found in the DGF cohort ($P = 0.049$). The distribution of donor criteria was different between the groups ($P < 0.001$), similar to earlier results. There was no significant difference between the control versus DGF with regards to HLA mismatch, pre-existing DSA, repeat transplantation, deviation from standard induction medication regimen or underlying renal diagnosis or vascular co-morbidities.

The risk of developing DGF was analysed with multiple logistic regression based on transplant type, induction regimen, re-graft, and pre-transplant DSA, transplant year, age at transplantation; *donor variables*: age, donation criteria, cold ischemic times; *recipient variables*: age, pre-emptive transplantation, and renal disease. The final model (C-statistic 0.808, CI 0.759-0.8839) identified independent risk factors for DGF to be diabetic nephropathy (from type II diabetes, OR 3.25, P = 0.045) and donor inotropic support (OR 6.14, p = 0.015), DCD criteria (OR 3.3, P = 0.001). Using 2016 to split our cohort, (enrolled between 2012 – 2020), transplantation pre-2016 had OR 4.33 (P = 0.002) of developing DGF. Transplant year split pre- and post- 2015 gave significant OR 3.09 (CI 1.4-7.28, p=0.007) and pre- and post-2016 was OR 4.33 (CI 1.77-11.68, p=0.002). Other years were tested but did not remain significant in the regression model and for the final table, 2016 was used to split the transplant cohort. The rates of DCD donors did not significantly increase, and this finding may either reflect the small cohort number, or an unexplained variable such as change to surgical technique or personnel at the centre, but this needs further analysis to validate.

Living donor kidneys are unlikely to suffer severe AKI needing dialysis and this was reflected with OR 0.2 (P = 0.034). Excluding living donors, the model showed that transplantation prior to 2016 (OR 5.03 (1.70-17.3), P = 0.006), donor inotropic use and DCD donor (OR 7.46 (2.66-23.54, P < 0.001) remained strong predictors of developing DGF. (Fig 4.4a) None of these variables were independent predictors of developing SGF.

a Table of significant variables in logistic regression

DGF		OR (univariable)	OR (multivariable)
Transplant year (pre-2016)		1.29 (0.67-2.57, p=0.447)	**4.33** (1.77-11.68, p=0.002)
Donor Inotrope Use		2.97 (0.74-19.95, p=0.173)	**6.14** (1.78-38.73, p=0.015)
Renal disease	GN	ref	ref
	HTN	0.25 (0.01-1.39, p=0.193)	0.23 (0.01-1.64, p=0.210)
	Other	0.41 (0.09-1.35, p=0.180)	0.32 (0.06-1.28, p=0.134)
	PCKD	1.12 (0.39-3.00, p=0.830)	1.26 (0.37-4.08, p=0.707)
	T1DM	0.56 (0.24-1.26, p=0.170)	0.49 (0.19-1.22, p=0.129)
	T2DM	2.26 (0.84-6.04, p=0.102)	**3.25** (1.03-10.60, p=0.045)
Donor criteria	DBD	ref	ref
	DBD + ECD	0.59 (0.03-3.61, p=0.634)	0.59 (0.03-3.61, p=0.634)
	DCD	3.30 (1.64-6.73, p=0.001)	**3.30** (1.64-6.73, p=0.001)
	DCD + ECD	3.11 (0.58-15.23, p=0.158)	3.11 (0.58-15.23, p=0.158)
	Living donor	0.20 (0.03-0.72, p=0.034)	**0.20** (0.03-0.72, p=0.034)

Odds ratio (OR) displayed with confidence intervals and P-values.

b DGF prediction by clinical variables

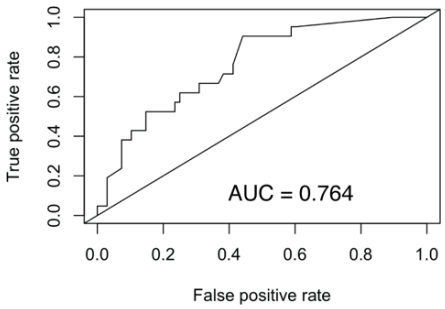

Figure 4.4: a) Table of independent risk factors for developing DGF by backwards, step-wise multivariable logistic regression. Only significant values shown, transplant type, induction regimen, 1st graft vs regraft, pre-transplant HLA mismatch and donor specific antibodies, recipient age/gender/underlying renal disease and donor age/gender/need for inotropes/cold-ischemic time/donor criteria and transplant era were not significantly associated with developing DGF. B) Pre-transplant clinical variables used in the logistic regression model had moderate predictive ability (AUC 0.764) for developing DGF using penalised logistic regression with kNN imputation and 10-fold cross validation after splitting the cohort into a 60:40 training: testing dataset.

Pre-transplant donor and recipient baseline clinical variables were used in a penalised logistic regression model analysis to determine the ability to identify DGF. The training model with 134 samples (31 with DGF) yielded RMSE 0.485 but only R^2 0.185 and was able to modestly predict the test set (89 samples, 22 DGF) with an area under the curve (AUC of 0.764). DCD, deceased-donor organ, cold ischemia time and diabetic nephropathy from type II diabetes were identified as the top 5 of the 40 predictors. (Fig 4.4b)

4.4.2 Post-transplant outcomes

DGF was associated with numerically higher percentage of graft loss but overall, death, non-censored graft loss or censored loss to follow up did not reach statistical significance comparing either DGF or SGF to controls for the whole cohort, or when only deceased-donor transplants were considered. DGF was associated with recurrent UTI (≥ 2 episode/year, *P*=0.03), BK viremia (P = 0.04) without BKVAN and incidence cardiovascular events (≤5years) for recipients of deceased-donor allografts (*P* = 0.05). There was no significant difference between the groups for other early surgical complications, infections, malignancy, or metabolic outcomes shown in (Table 4.3). DGF retained an independent association in multivariable regression, with OR 2.51 (1.2-5.15, P = 0.013) along with female gender (OR 4.54 (2.32, 9.23), P < 0.001) even when additional induction medications, subclinical or biopsy proven rejection (treated), tacrolimus levels, diabetes, NODAT, BK or CMV infections were included (C-statistic 0.781, CI 0.6932-0.9106).

DGF was not an independent risk factor for early cardiovascular events in a multivariable logistic regression model, when pre-existing ischemic heart disease and type 2 diabetes with diabetic nephropathy being the independent predictors. (C-statistic 0.747, CI 0.6585-0.862) considering DGF/SGF, pre-existing IHD, hypertension, diabetes, NODAT and biopsy proven rejection). The incidence of biopsy proven rejection (up to and including 1-month) and subclinical rejection (<1-month) was higher in the DGF cohort (Table 4.3). There was no significant difference in trough tacrolimus levels between the groups and rejection episodes after 1-month was similar between the groups.

DGF remained independently associated with early BPAR, with OR 3.65 (1.25-1.61, P=0.018) before 1-month and OR 7.67 (2.49-26.1, P=0.001) in a multivariable logistic regression model which included both donor and recipient age/gender, organ type, donor criteria, 1st or repeat graft, deviation from standard induction, HLA mismatch, pre-transplant DSA, subclinical rejection within the first 1-month and tacrolimus levels at day 2, day 7 and day 21 post-transplantation (C-statistic 0.7052, CI 0.703-0.88 for <1-month and C-statistic 0.658, CI 0.679-0.867 at 1-month). Similarly, DGF was independently associated with subclinical rejection (before 1-month, OR 5.58 (1.7-19.8), P = 0.006) with a similar model for BPAR, swapping the rejection type. The presence of class II pre-transplant DSA was also associated with subclinical rejection (OR 4.02 (1.29-12.9, P = 0.017) for the 0–1-month period (C-statistic 0.802, CI 0.764-0.915). Biopsy proven rejection was associated with poor outcomes (Fig 4.5). Patients who had suffered an episode of BPAR at any stage were at increased risk of non-censored graft loss, with cause-specific HR 5.4 (1.52-19.3, P=0.009).

The composite outcomes to into the death, graft loss and censored sub-categories allowed consideration of competing risk in time-to-event analysis are shown in Fig 4.6 and did not show any significant difference between DGF and controls in terms of composite outcomes or graft loss alone (P = 0.054 with cause-specific HR 3.19 (0.92-11.0, P = 0.067)) and this was unchanged for death censored graft loss (P=0.17). From earlier results, DGF is independently associated with early BPAR and sub-analysis of BPAR ≤1-month and BPAR ≤3-months versus controls yielded cause-specific HR 1.64 (0.35-7.62, P=0.5) and 4.71 (1.43-15.5, P=0.011) respectively for non-censored graft loss.

Table 4.3: Primary and major surgical, infectious, malignancy-related, metabolic and rejction outcomes of the cohort

	All Transplants					Deceased donor only		
	Control N =170	DGF N = 53	P value	SGF N = 28	P value	Control N = 131	DGF N = 50	P value
Primary composite	24 (14%)	13 (25%)	0.075	5 (18%)	0.6	19 (15%)	13 (26%)	0.07
Event types			0.12		0.6			0.13
Death	14 (8.3%)	5 (9.6%)		3 (11%)		11 (8.5%)	5 (10%)	
Graft loss[#]	5 (3.0%)	5 (9.6%)		1 (3.6%)		4 (3.1%)	5 (10%)	
Loss to follow up	3 (1.8%)	2 (3.8%)		1 (3.6%)		2 (1.6%)	2 (4.1%)	
Dialysis sessions	0	2.00 (1.50, 4.00)	-	-	-	0	2 (1.75, 4)	-
Dialysis days	0	5.0 (3.0, 11.0)	-	-	-	0	5.5 (3, 11)	-
duration < 7 days	0	2.00 (1.50, 4.00)	-	-	-	0	32 (64%)	-
duration ≥ 7 days	0	5.0 (3.0, 11.0)	-	-	-	0	18 (36%)	-
Surgical issues								
Return to theatre	20 (12%)	5 (9.4%)	0.6	7 (25%)	0.08	16 (12%)	5 (10%)	0.7
Transfusion	37 (22%)	16 (30%)	0.2	10 (36%)	0.11	32 (24%)	16 (32%)	0.4
Wound infection	24 (14%)	7 (13%)	0.9	4 (14%)	0.9	20 (15%)	7 (14%)	0.9
Infections								
CMV viremia	20 (12%)	7 (13%)	0.8	6 (21%)	0.2	15 (12%)	6 (12%)	>0.9
CMV disease	7 (4.2%)	3 (5.7%)	0.7	4 (14%)	0.06	5 (3.9%)	3 (6.0%)	>0.9
Resistant CMV	4 (2.4%)	1 (1.9%)	0.9	3 (11%)	0.063	3 (2.3%)	1 (2.0%)	>0.9
EBV infection	1 (0.6%)	1 (1.9%)	0.4	1 (3.6%)	0.3	1 (0.8%)	1 (2.0%)	0.5
BK viremia	50 (29%)	8 (15%)	0.04	10 (36%)	0.5	36 (27%)	8 (16%)	0.041
BKVAN	11 (6.5%)	3 (5.7%)	0.9	2 (7.1%)	0.9	7 (5.3%)	3 (6.0%)	>0.9
Invasive fungal	8 (4.7%)	7 (13%)	0.06	4 (14%)	0.07	6 (4.6%)	7 (14%)	0.14
Recurrent UTI	25 (15%)	16 (30%)	0.011	4 (14%)	0.9	18 (14%)	14 (28%)	0.03
Gastroenteritis	19 (11%)	12 (23%)	0.04	6 (21%)	0.13	15 (11%)	11 (22%)	0.086
Chest infection	35 (21%)	14 (26%)	0.4	5 (18%)	0.7	27 (21%)	14 (28%)	0.3
Malignancy								
PTLD	1	0	-	0	-	1 (0.8%)	0	-
Skin cancer	14(8.2%)	1 (1.9%)	0.14	4 (14%)	0.3	9 (6.9%)	0	-
Cardio/metabolic								
CV event < 5yrs	15 (8.8%)	9 (17%)	0.09	5 (18%)	0.2	10 (7.6%)	9 (18%)	0.05
NODAT	22 (13%)	9 (17%)	0.5	5 (18%)	0.6	15 (11%)	8 (16%)	0.4
Biopsy proven acute rejection (BPAR)								
0-1 month	13 (7.6%)	13 (25%)	0.011	2 (7.1%)	>0.9	10 (7.6%)	11 (22%)	0.007
1 month	12 (7.1%)	15 (28%)	0.001	2 (7.1%)	>0.9	10 (7.6%)	13 (26%)	<0.001
3 months	6 (3.5%)	1 (1.9%)	>0.9	1 (3.6%)	>0.9	4 (3.1%)	1 (2.0%)	>0.9
12 months	4 (2.4%)	0	-	0	>0.9	2 (1.5%)	0	-
Subclinical rejection								
0-1 month	16 (9.4%)	11 (21%)	0.027	5 (18%)	0.2	12 (9.2%)	11 (22%)	0.02
1 month	7 (4.1%)	1 (1.9%)	0.7	1 (3.6%)	>0.9	6 (4.6%)	1 (2.0%)	0.7
3 months	5 (2.9%)	3 (5.7%)	0.4	2 (7.1%)	>0.9	4 (3.1%)	3 (6.0%)	0.4
12 months	2 (1.2%)	1 (1.9%)	0.6	0	>0.9	2 (1.5%)	1 (2.0%)	>0.9
Tacrolimus trough (ng/ml)								
Day 2	17 (12, 22)	17 (12, 23)	0.5	19 (13, 28)	0.2	16 (12, 22)	17 (12, 23)	0.5
Month 1	9.60 (8.2, 10.7)	9.80 (7.8, 11.7)	0.5	10.2(8.5,12.5)	0.2	9.60 (8.4, 10.8)	9.58 (7.8, 11.5)	>0.9
Month 3	8.70 (6.8, 11.2)	8.40 (6.6, 11.2)	0.8	9.2 (7.9, 11.7)	0.025	9.00 (7.1, 11.2)	8.05 (6.6, 11.2)	0.7
Month 12	7.40 (6.3, 7.4)	7.40 (6.3, 8.3)	0.14	7.1(7.1,7.53)	0.3	7.40 (6.4, 7.6)	7.40 (6.3, 8.52)	0.3

Graft loss in this table is non censored, new onset diabetes after transplantation (NODAT), BK virus associated nephropathy (BKVAN)

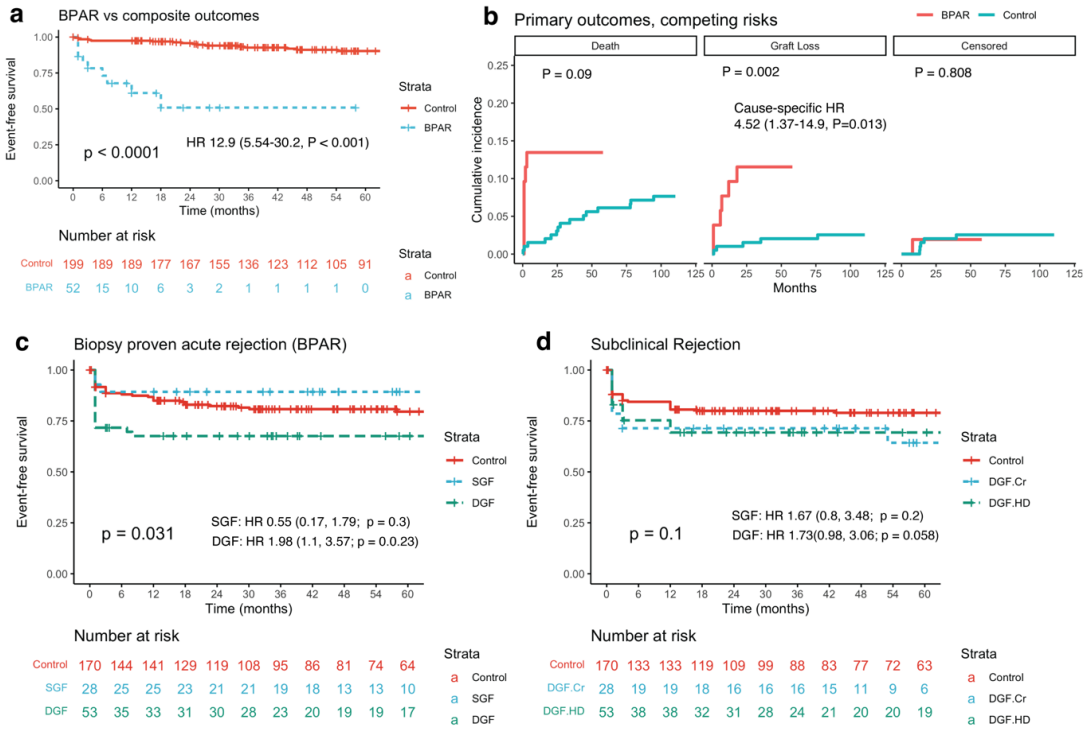

Figure 4.5:a) Kaplan Meier Survival curve for the primary composite outcome and b) time-to-event curve for each primary event for the cohort based on incidence(s) of biopsy proven rejection (BPAR) at any time in the study. There was a significant association between BPAR and non-censored graft loss, with cause-specific hazard ratio 4.52 (P= 0.013). c) Kaplan-Meier curves comparing control to DGF and SGF for BPAR, d) subclinical rejection free survival.

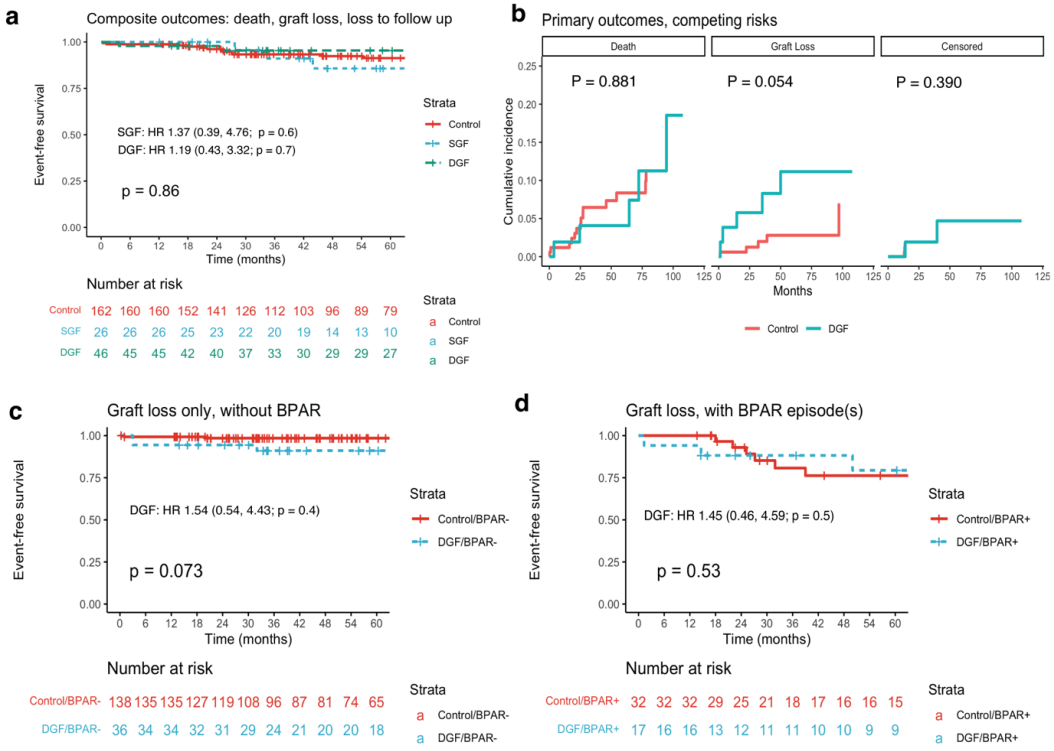

Figure 4.6: Kaplan-Meier survival curves comparing control to DGF (± SGF) for a) composite outcome of death, graft loss or censoring. b) time-to-event curves for competing risk analysis of the primary composite outcome, c) Kaplan-Meier curve for graft loss in subjects who never experienced an episode of biopsy proven rejection (BPAR), and d) those who had BPAR episode(s). P-values from log-rank tests and hazard ratio (HR) by cox-proportional model.

Renal function was worse in the DGF group compared to controls up to 12-months post-transplantation based on serum creatinine, eGFR and mGFR. (Table 4.4, Fig 4.6a). The delta eGFR (ΔeGFR) was -21 ml/min/1.73m^2 and delta mGFR (ΔmGFR) -8 ml/min in DGF versus control at 3-months but the difference at 12-months was minimal to modest (ΔeGFR -3ml/min/1.73m^2 and ΔmGFR 0ml/min) between the groups despite being statistically significant. The ΔmGFR was -8ml/min for SGF versus controls, despite no significant difference in earlier parameters. In keeping with these findings, both 3- and 12-month biopsy IFTA scores were less likely to be zero (unaffected) in the DGF compared to controls. (Table 4.4)

There was a trend to worse mGFR for DGF compared to controls when IFTA ≥2 (Fig 4.7 a,b), although this did not reach statistical significance for either 3-month (P = 0.7) or 12-month (P=0.14) samples. The alluvial plot in fig 4.7c displays the distribution of the cohort from DGF versus control (± subclinical rejection <1-month) to 12-month IFTA scores stratified by BPAR incidence. Compared to controls, the relative risk (RR) of a 12-month IFTA score ≥ 2 was 2.26 (1.48-4.46, P=0.019) and 2.27 (1.00-5.12, P=0.056) for DGF and SGF respectively. Similarly, the RR for having a 12-month mGFR < 45 ml/min was 2.06 (1.02-4.16, P=0.047) and 2.65 (1.25-5.63, P=0.015) for DGF and SGF versus control respectively. Further exploring the biopsy changes over the first 12-months, 58 patients in the cohort had the all 0-, 1-, 3- and 12-month biopsy scores available, within which there were 40 controls, 6 with SGF and 12 with DGF. The 0-month biopsy was used as the baseline and delta (Δ) Banff scores for i, t, ci and ct between 0-to-1 month (Δ 0-1), 1-to-3 months (Δ 1-3), and 3-to-12 months (Δ 3-12), are displayed as mean (± standard deviation) in figure 4.8. There was progressive increase in the ci score in subjects with acute BPAR with positive Δci scores over the first 12-months. (Fig 4.8a) DGF patients were likely to have positive Δci and Δct up in the first month, particularly DCD donor kidneys. (Fig4.8 a,b).Multivariate regression analysis considering SGF/DGF, 1-month eGFR, 3-month mGFR, subclinical rejection, BPAR, BKVAN, recipient and donor age and sex, transplant year (pre or post 2016), re-graft, deviation from standard induction regimen, HLA-mismatch, pre-transplant DSA and 3-month IFTA scores was performed to determine independent variables to predict 12-month mGFR. Only 1-month eGFR, 3-month mGFR and remained independently associated with 12-month mGFR, although the R^2 was only 0.44. (Table 4.5)

Table 4.4: Renal function and key kidney biopsy parameters of the cohort

	All transplants					Deceased donor only, DGF		
	Control N =170	DGF N = 53	p-value	SGF N = 28	P-value	Control N = 131	DGF N = 50	p-value
Serum creatinine (µmol/L)								
Pre-op	646 (520, 868)	765 (591, 900)	0.073	514 (441, 654)	0.003	702 (536, 912)	769 (594, 897)	0.3
Day 1	366 (261, 544)	700 (581, 851)	<0.001	474 (398, 578)	0.011	398 (280, 612)	702 (594, 858)	<0.001
Day 2	220 (140, 332)	720 (542, 866)	<0.001	476 (397, 612)	<0.001	261 (180, 400)	726 (544, 876)	<0.001
Month 1	108 (87, 132)	144 (121, 196)	<0.001	112 (96, 134)	0.2	104 (83, 131)	143 (120, 197)	<0.001
Month 3	106 (87, 124)	116 (97, 148)	0.008	110 (92, 138)	0.14	102 (84, 122)	115 (92, 150)	0.007
Month 12	112 (92, 126)	125 (104, 149)	0.024	112 (97, 138)	0.2	111 (90, 126)	124 (102, 156)	0.026
Month 24	118 (98, 138)	122 (104, 174)	0.2	113 (86, 134)	0.4	117 (94, 138)	122 (104, 172)	0.2
Month 36	111 (92, 138)	124 (102, 152)	0.14	120 (106, 142)	0.5	112 (92, 133)	125 (100, 152)	0.12
Month 48	117 (90, 149)	120 (99, 162)	0.5	122 (92, 156)	0.8	116 (90, 127)	122 (98, 163)	0.3
Month 60	104 (88, 129)	125 (108, 154)	0.019	122 (94, 131)	0.7	103 (86, 129)	128 (108, 154)	0.013
eGFR (ml/min/1.73m2)								
Month 1	60 (49, 77)	39 (28, 56)	<0.001	53 (47, 66)	0.13	64 (49, 78)	41 (27, 58)	<0.001
Month 3	62 (51, 78)	58 (38, 64)	0.002	57 (47, 69)	0.064	66 (53, 80)	58 (36, 67)	0.001
Month 12	59 (51, 76)	56 (38, 64)	0.026	56 (36, 72)	0.14	59 (52, 77)	57 (37, 65)	0.032
Month 24	54 (46, 73)	57 (31, 62)	0.2	63 (50, 76)	0.5	54 (48, 76)	57 (32, 65)	0.2
Month 36	60 (43, 71)	52 (38, 64)	0.2	50 (41, 65)	0.5	59 (46, 70)	52 (36, 62)	0.14
Month 48	59 (44, 76)	60 (35, 67)	0.2	56 (39, 76)	0.7	59 (46, 81)	60 (35, 67)	0.15
Month 60	64 (49, 77)	50 (42, 66)	0.11	57 (42, 74)	0.6	67 (50, 78)	50 (42, 66)	0.059
Measured GFR (ml/min)								
Month 3	64 (57, 73)	58 (42, 63)	<0.001	63 (45, 74)	0.2	64 (58, 73)	58 (43, 63)	<0.001
Month 12	61 (55, 75)	61 (46, 68)	0.039	53 (38, 62)	<0.001	61 (56, 73)	61 (46, 68)	0.041
Pre-implantation (0m) biopsy								
ci ≥ 2	1 (0.6%)	0	-	0	-	1 (0.8 %)	0	-
ct ≥ 2	1 (0.6%)	0	-	0	-	1 (0.8%)	0	-
1-month protocol biopsy								
ci ≥ 2	3 (1.8%)	6 (11%)	0.007	5 (23%)	0.002	3 (2.3%)	6 (12%)	0.014
ct ≥ 2	3 (1.8%)	6 (11%)	0.007	5 (23%)	0.002	3 (2.3%)	6 (12%)	0.014
3-months protocol biopsy (n = 185)								
	N = 127	**N =38**				**N = 99**	**N = 37**	
ci ≥ 2	12 (7.0%)	12 (23%)	0.001	3 (17%)	0.4	9 (6.9%)	11 (22%)	0.009
ct ≥ 2	10 (5.9%)	12 (23%)	0.001	3 (17%)	0.2	7 (5.3%)	11 (22%)	0.008
i-IFTA = 0	117 (68.8%)	32 (84%)	0.2	17 (89%)	0.7	91 (6.9%)	31 (62%)	0.2
IFTA = 0	94 (74%)	18 (47%)	0.002	12 (60%)	0.2	73 (74%)	17 (46%)	0.002
IFTA = 1	23 (18%)	9 (24%)	0.4	5 (25%)	0.5	18 (18%)	9 (24%)	0.4
IFTA = 2	6 (4.7%)	7 (18%)	0.12	2 (10%)	0.3	4 (4.0%)	7 (19%)	0.01
IFTA = 3	4 (3.1%)	4 (11%)	0.08	1 (5.0%)	0.5	4 (4.0%)	4 (11%)	0.2
12-months protocol biopsy (n = 162)								
	N = 108	**N = 38**				**N =76**	**N = 37**	
ci ≥ 2	20 (12%)	10 (19%)	0.2	6 (33%)	0.11	16 (12.2%)	9 (18%)	0.2
ct ≥ 2	20 (12%)	9 (17%)	0.3	6 (33%)	0.1	16 (12.2%)	8 (16%)	0.5
i-IFTA = 0	100 (58.8%)	28 (52.8%)	0.1	-	-	70 (53.4%)	27 (54%)	0.2
IFTA = 0	94 (74%)	18 (47%)	0.05	-	-	55 (72%)	18 (53%)	0.05
IFTA = 1	23 (18%)	9 (24%)	0.9	-	-	11 (14%)	5 (15%)	0.9
IFTA = 2	6 (4.7%)	7 (18%)	0.07	-	-	5 (6.6%)	7 (21%)	0.05
IFTA = 3	4 (3.1%)	4 (11%)	0.08	-	-	5 (6.6%)	4 (12%)	0.2

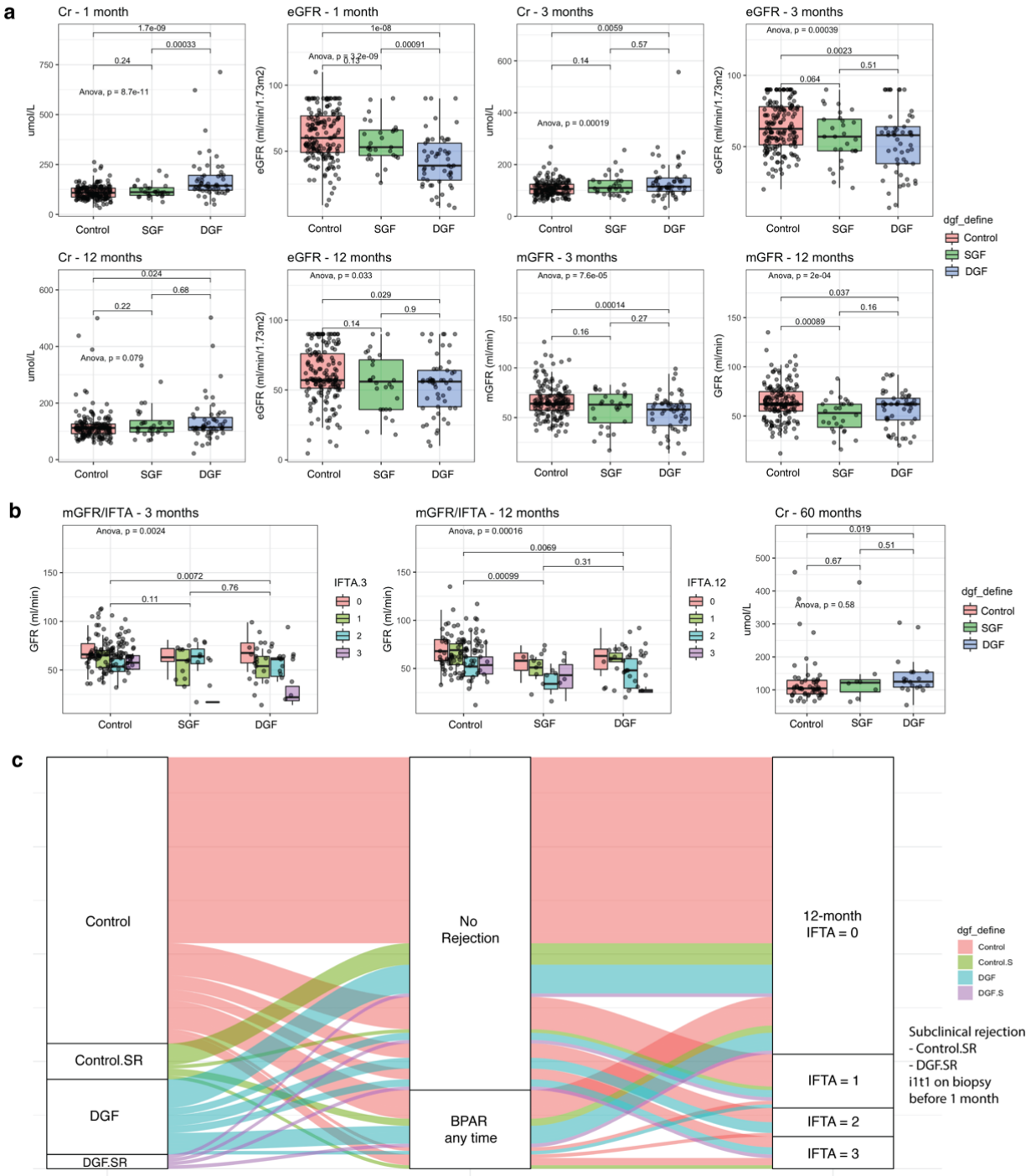

Figure 4.7: Renal function and IFTA scores in the study. A) shows the creatinine, eGFR and mGFR over the first 12-months, b) shows the mGFR stratified by IFTA status and the available creatinine values at 5-years (60-months). C) An alluvial diagram representative of the distribution of control and DGF patients (± subclinical rejection < 1-month) to BPAR and 12-month IFTA scores.

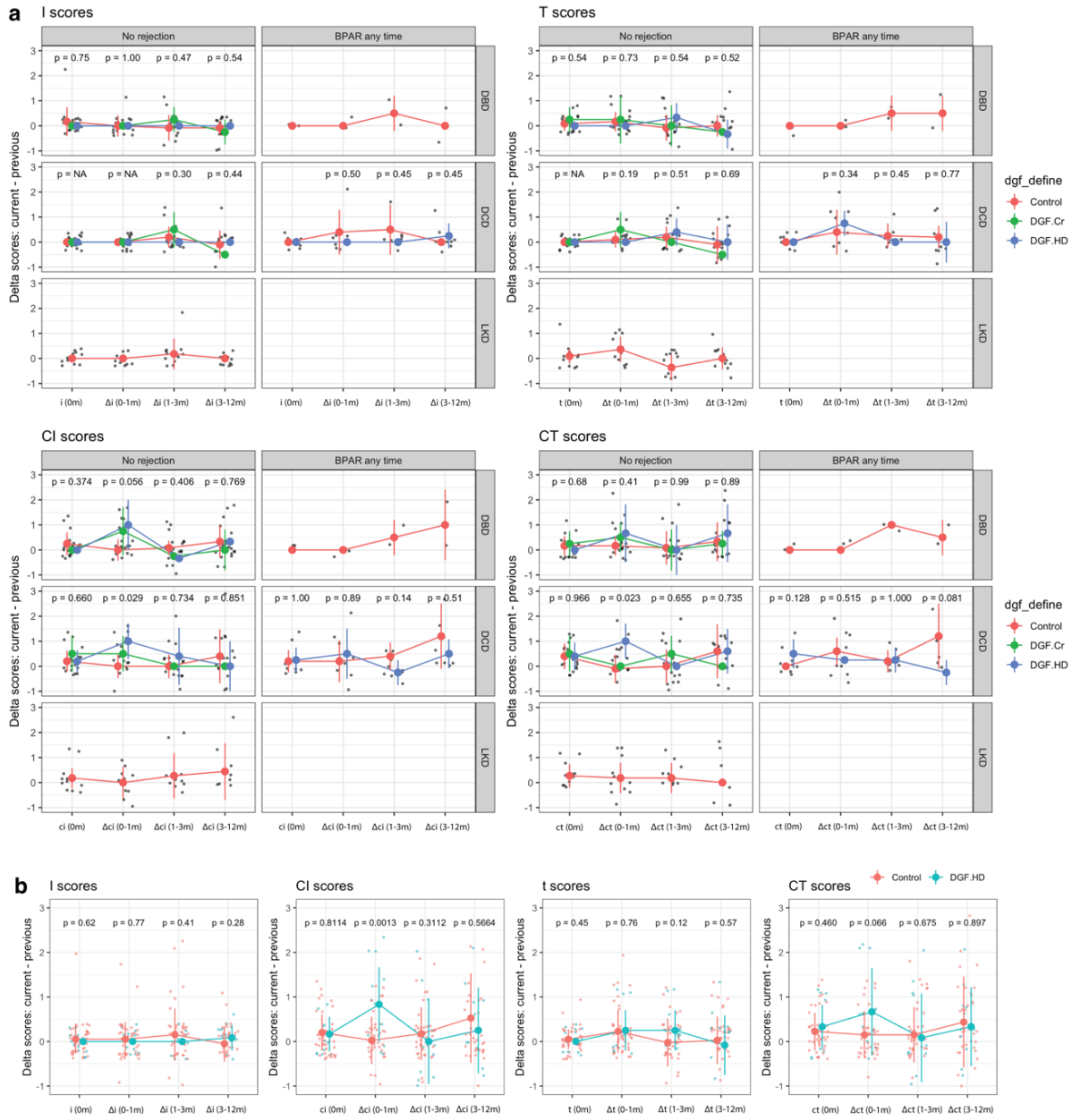

Figure 4.8: Progressive biopsy scores over 12-months. A) baseline i, t, ci and ct scores were followed by delta (Δ) scores for each subsequent biopsy for the 1-, 3- and 12-month protocol biopsies for DGF (and SGF) vs controls. b) shows the same information for DGF vs control only. Values displayed as mean ± standard deviation.

Table 4.5: Linear regression for associations with 12-month mGFR

$R^2 = 0.44$	**Coefficient (univariable)**	**Coefficient (multivariable)**
Measured GFR at 3 months	0.68 (0.58 to 0.78, p<0.001)	0.56 (0.44 to 0.68, p<0.001)
eGFR at 1 month	0.41 (0.31 to 0.51, p<0.001)	0.13 (0.02 to 0.24, p=0.016)
Early graft function: No DGF	ref	ref
Slow graft function (SGF)	-13.33 (-20.59 to -6.07, p<0.001)	-7.81 (-13.46 to -2.16, p=0.007)
Delayed graft function (DGF)	-7.81 (-13.40 to -2.21, p=0.006)	0.67 (-4.02 to 5.35, p=0.779)

Similar to earlier predictive analysis for DGF, available clinical variables were used to determine the ability to predict 12-month mGFR (low if < 45ml/min) and IFTA (high if ≥ 2) using transplant year, DGF status, regraft/induction regimen/HLA mismatch/pre-transplant DSA, donor and recipient age/gender, donor criteria/cold ischemic time/terminal creatinine/inotropic use, rejection (subclinical or BPAR), BK (viremia and nephropathy), 0-, 1- and 3-months creatinine/tacrolimus/ci/ct/iIFTA/IFTA results. The model split 50:50 for mGFR had 112 patients (20 with low mGFR) in the training set, with R^2 0.23 with 85 predictor variables, testing set with 111 patients (19 with low mGFR) and AUC 0.698. Similarly, for the IFTA model, the 50:50 split yielded 72 patients (13 with high IFTA) in the training dataset with 85 predictors, R^2 0.191 and 71 patients in the test set (13 with high IFTA) and AUC 0.603. The utility of clinical variables collected showed limited ability to predict the 12-month outcomes, although noted previously, de novo DSA results are not available and the number in groups were reduced due to availability of specific 12- IFTA results. (Fig 4.9)

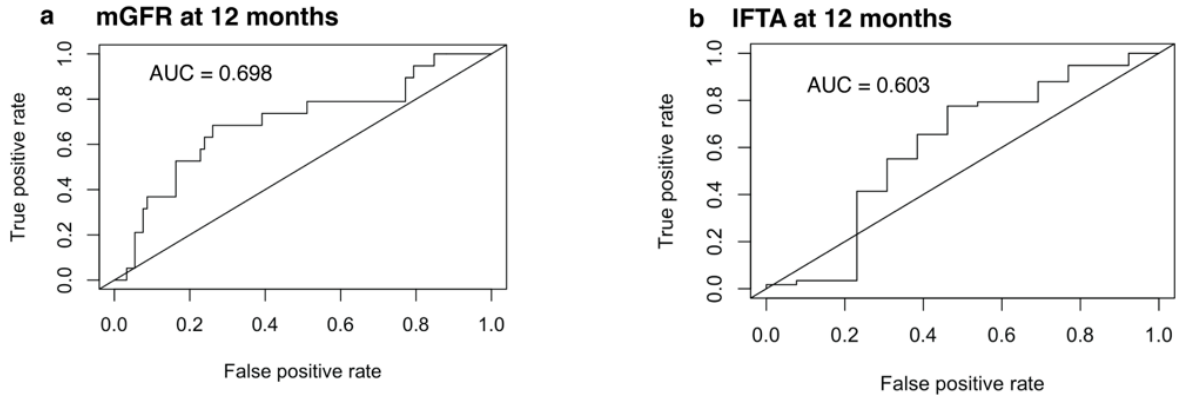

Figure 4.9: Receiver operator curves (ROC) for the prediction of a) 12-month mGFR (AUC 0.698) and b) 12-month IFTA (AUC 0.603) based on available clinical data.

Considering subgroups based on control, SGF, DGF status versus either IFTA (high IFTA ≥ 2) or mGFR (low mGFR < 45ml/min/1.73m^2), there were differences in the composite death/non-censored graft loss outcomes (P < 0.001) (Fig 4.10a, b). Separating this composite outcome into individual components for competing risk analysis, the main driver of these findings was increased risk of death associated with either 12-month IFTA ≥ 2 or mGFR < 45ml/min/1.73m2. Compared to controls with 12-month IFTA scores <2, the death-specific HR was 13.5 (2.2-81.8, P = 0.006) and 8.99 (1.8-44.6, P=0.007) for SGF and DGF with high-IFTA scores respectively. Similarly, compared to controls with 12-month mGFR ≥45 ml/min/1.73m^2, the death-specific HR was 6.7 (2.2-19.4, P<0.001), 6.9 (1.7-27.9, P=0.006) and 6.95 (1.7-27.8, P=0.006) for

patients with mGFR < 45ml/min in the control, SGF and DGF subgroups respectively. (Fig 4.10 c,d) These results are limited by the small numbers in the subgroups but indicates trends towards worse outcomes with poor allograft quality based on biochemical or histological quantifications.

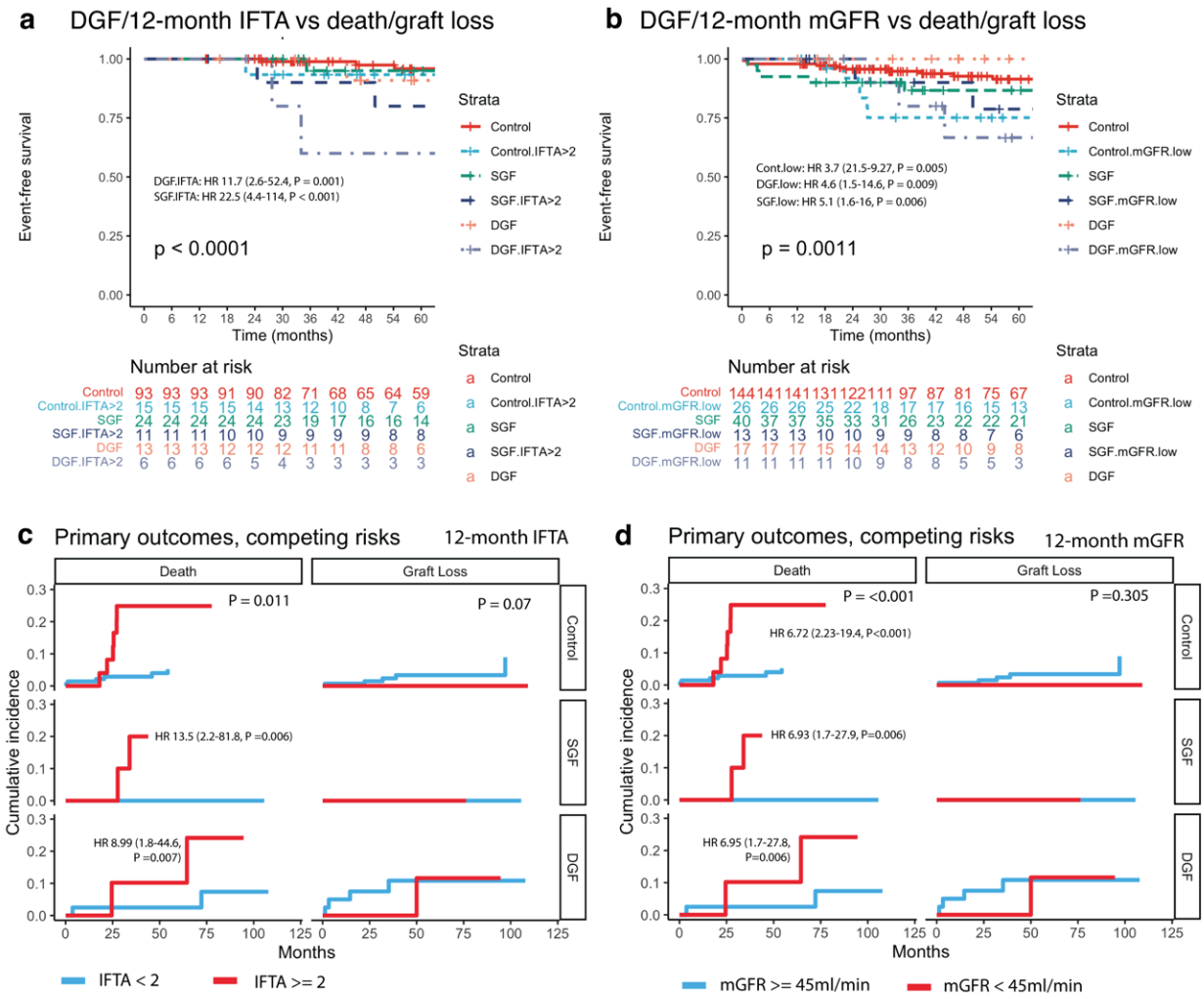

Figure 4.10: Death and graft loss outcomes. Kaplan Meier survival curves for death/non-censored graft loss for a) SGF/DGF split by 12-month IFTA (high if ≥2) and b) SGF/DGF split by 12-month mGFR (low if <45ml/min). Competing risk cox analysis revealed increased association with death for c) high IFTA and d) low mGFR. Cause-specific hazard ratio compared to controls with either IFTA<2 or mGFR ≥45 ml/min in the respective groups.

4.4.3 Transcriptomic analysis of kidney biopsies

4.4.3.1 DGF vs control with and without covariates

Thirty-six patients were identified to have DGF by dialysis criteria with available pre-implantation (0 month) kidney biopsy RNAseq data. In total, 1233 differentially expressed genes were identified after accounting for batch effects, with several acute phase reactant genes seen in the top 20 list (Fig 4.11a). These genes were enriched for neutrophil/leukocyte activation pathways and reactive oxygen species (Fig 4.11b).

a

Ensembl	LogFC	Fold Change	Symbol
ENSG00000125851	2.14	4.41	PCSK2
ENSG00000173432	1.95	3.88	SAA1
ENSG00000151365	1.77	3.41	THRSP
ENSG00000211653	1.75	3.37	IGLV1-40
ENSG00000171747	1.68	3.21	LGALS4
ENSG00000137473	1.65	3.13	TTC29
ENSG00000178602	1.56	2.95	OTOS
ENSG00000102837	1.56	2.95	OLFM4
ENSG00000166819	1.55	2.94	PLIN1
ENSG00000286042	1.55	2.93	LCAL1
ENSG00000175793	1.45	2.73	SFN
ENSG00000175315	1.44	2.71	CST6
ENSG00000128510	1.42	2.68	CPA4
ENSG00000170323	1.36	2.57	FABP4
ENSG00000095752	1.30	2.47	IL11
ENSG00000274736	1.30	2.46	CCL23
ENSG00000188257	1.27	2.40	PLA2G2A
ENSG00000139973	1.25	2.38	SYT16
ENSG00000211970	1.24	2.36	IGHV4-61
ENSG00000233913	1.20	2.31	RPL10P9

b

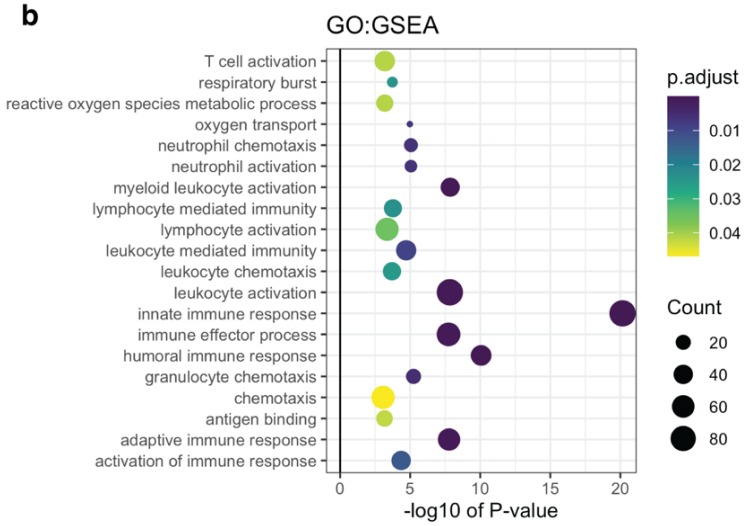

Figure 4.11: a) top 20 DGE for DGF.HD vs controls, and b) enriched pathways upregulated in DGF.HD in the 0-month biopsy

When organ type, to account for living versus deceased donor allografts, was included as a covariate in addition to batch in the model matrix to regress out these confounders, the reduction of the number of DGEs was most significant for 0-month (pre-implantation) biopsies (Table 4.6) and these 352 DGEs were enriched for various innate, adaptive inflammation and cell death pathways - in keeping with known systemic changes in the setting of brain death[35,36]. (Fig 4.12)

Table 4.6: Differential gene expression comparisons for 0-, 1- and 3- months kidney biopsies

Differential gene expression of kidney biopsies for DGF.HD vs Control		Control (n)	DGF (n)	Up-regulated genes	Down-regulated genes
Month 0	Correcting for batch effects only	117	36	534	699
Month 0	Correcting for batch & transplant organ type	117	36	103	249
Month 1	Correcting for batch effects only	34	13	108	124
Month 1	Correcting for batch &transplant organ type	34	13	101	32
Month 3	Correcting for batch effects only	90	32	433	374
Month 3	Correcting for batch &transplant organ type	90	32	236	398

Genes removed when accounting for deceased vs living donor transplantation

a

Ensembl	logFC	Fold Change	Symbol
ENSG00000173432	1.95	3.88	SAA1
ENSG00000286042	1.55	2.93	LCAL1
ENSG00000128510	1.42	2.68	CPA4
ENSG00000188257	1.27	2.40	PLA2G2A
ENSG00000211970	1.24	2.36	IGHV4-61
ENSG00000254166	1.20	2.30	PCAT2
ENSG00000197993	1.16	2.23	KEL
ENSG00000223609	1.13	2.18	HBD
ENSG00000144452	1.12	2.18	ABCA12
ENSG00000178752	1.08	2.11	ERFE
ENSG00000163221	1.07	2.11	S100A12
ENSG00000143546	1.06	2.08	S100A8
ENSG00000163220	1.02	2.03	S100A9
ENSG00000095970	0.99	1.98	TREM2
ENSG00000169385	0.98	1.97	RNASE2
ENSG00000019169	0.98	1.97	MARCO
ENSG00000160339	0.97	1.96	FCN2
ENSG00000189410	0.97	1.95	SH2D5
ENSG00000243264	0.97	1.95	IGKV2D-29
ENSG00000133317	0.94	1.92	LGALS12

b

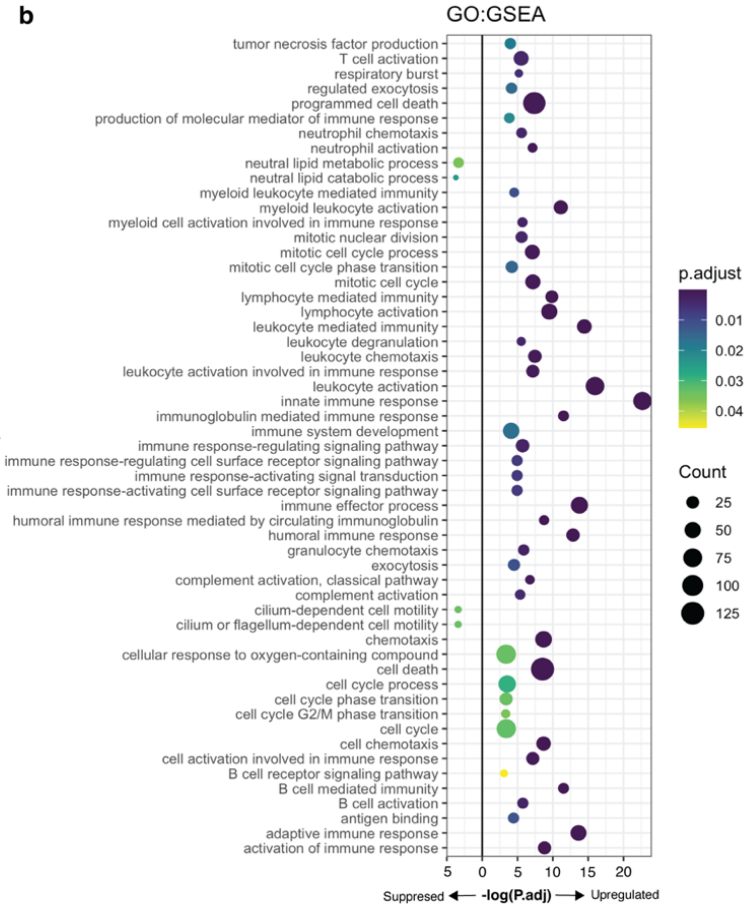

Figure 4.12: Effects of adding deceased vs living donor status as a covariate for modelling differential expression in the 0-month (pre-implant) biopsy. A) top 20 genes removed and b) enriched pathways of genes regressed out by deceased vs living donor.

Subsequent differential analysis performed between the groups outlined in table 4.7 accounted the following factors by considering them as covariates to when comparing DGF (or SGF) to controls.

- Batch (batch with sequencing at Australian Genome Research Facility (AGRF) was performed)
- Organ type (living donor versus deceased donor kidney-alone and kidney-pancreas transplantation),
- DCD donor status, presence of pre-transplant DSA and graft number (1st graft vs regraft)
- DCD donor status was removed as a covariate for DBD-only allografts for DGF vs Control
- DCD donor status was removed as a covariate for DCD-only allografts for DGF vs Control

Table 4.7: Number of available RNAseq samples & differential gene expression of pre-implantation (0-month) kidney biopsies

Conditions for 0-month	**Control (n)**	**DGF (n)**	***DGE Up***	***DGE Down***	***Top 10 up-regulated DGE***
DGF *vs* control *All patients*	117	36	103	249	PCSK2, SAA1, THRSP, IGLV1-40, LGALS4, TTC29, OTOS, OLFM4, PLIN1, LCAL1
DGF *vs* control *DBD allografts only*	64	17	112	106	IGHV3-15, IGLV6-57, LGALS4, OTOS, PCSK2, IGLV7-46, LTF, IGHV3-53, CXCL11, FUT9
DGF *vs* control *DCD allografts only*	15	15	110	147	AKR1B10, CRYBG2, IGLV1-40, IGLV3-25, IGLV2-11, B3GALT5, CNNM1, CXCL6, IGKV1-5, CILP
DGF *vs* control *Rejection free ≤ 3 months*	82	14	76	149	RPL10P9, RPL10P6, AKR1B10, THRSP, C2CD4A, IGHV1-24, IGHV1-69D, IGKV1-27, CPA4, OLFM4
DGF *vs* control *Any rejection ≤ 3 months*	35	22	59	99	LGALS4, LTF, ADCY8, TAGLN3, NAPSB, PCSK2, CCL23, TF, SMIM38, NEU4
DGF *vs* control *(Subclin <1m +ve, BPAR-ve)*	11	7	13	55	DDTL, CCL23, RPL13P12, ERAP2, PKHD1L1, MTRNR2L6, SPINK1, ANGPTL4, MEGF11, IL1RL1
DGF *vs* control *(BPAR +ve ≤ 3 months)*	10	11	60	87	LGALS4, SMIM38, EPO, ALOX15B, EMILIN3, EGFL6, HSPB9, TF, NAPSB, RN7SL1
DGF < 7 days *vs* control	117	24	107	155	ADIPOQ, LGALS4, THRSP, FABP4, TTC29, PCSK2, PNLDC1, IGHV7-4-1, RNU4-2, IGHV3-53
DGF ≥ 7 days *vs* control	117	12	149	497	IGLV1-40, PCSK2, SDS, RN7SKP23, C10orf99, MMP8, SLC25A47, IGHV4-61, OLFM4, FAM153B
DGF ≥7 days *vs* < 7 days	-	12 vs 24	159	377	IGLV1-40, MTCO3P13, SDS, C10orf99, SLC25A47, MYH1, RN7SKP23, MMP8, UMODL1-AS1, FAM153B
SGF *vs* control	117	20	140	117	IGLV3-10, IGHV1-3, IGHV7-4-1, IGHV5-51, SAA2, SAA1, IGLV3-21, IGHM, RTP3, MIR3142HG
DGF *vs* SGF	-	24 vs 19	78	187	RPL10P9, RPL13P12, GPBAR1, FBLL1, ASGR1, RPL10P6, DDIT4L, CRYBG2, OLFM4, HSD17B2
DGF < 7 days *vs* control *(Subclinical rejection +ve)*	11	4	56	39	IGLV1-36, TMC3, XIST, GATD3, IGKV1-6, IGKV3-11, RPS17P16, APOC3, TNFAIP6, PWP2
DGF ≥ 7 days *vs* control *(Subclinical rejection +ve)*	11	3	46	221	IGLV3-9, IGHV7-4-1, IGKV1-6, IGKV1-16, IGHV4-30-2, ERAP2, IGLV1-40, IGHV4-61, CCL23, ICOSLG
DGF/IFTA_12m ≥2 *vs* No DGF/IFTA_12m < 2	59	5	94	150	RPL10P9, COL6A5, IGLV1-40, LRRC3B, IGKV2-29, IGHV4-61, IGHV4-55, IGLV4-60, FUT9, RPL10P6
DGF/IFTA_12m <2 *vs*. No DGF/IFTA_12m < 2	59	8	126	123	RPL10P9, ACTG2, CIDEC, IGHV3-64D, ADIPOQ, IGLV4-60, SPRR2A, IGLV8-61, SIGLEC12, C2CD4A
No DGF/IFTA_12m ≥2 *vs*. No DGF/IFTA_12m < 2	5 vs 59	-	164	21	REG1A, GREM1, RPL10P9, IGHV1-3, REG3G, ACTG2, IGHV2-70, MEGF11, IGHV2-70D, PRKY
DGF/IFTA_12m ≥2 *vs*. DGF/IFTA_12m < 2	-	5 vs 8	94	107	COL6A5, LRRC3B, IGKV2-29, IGLV1-40, SCT, IGHV4-55, C3P1, FETUB, IGHV4-34, XIST
No DGF/mGFR <45 *vs* No DGF/mGFR ≥ 45	12 vs 87	-	625	134	SLC14A2, ACTG2, REG1A, GREM1, SCRG1, DES, ANGPT4, F2RL2, COL6A6, MYBPC2
DGF/mGFR <45 *vs* No DGF/mGFR ≥ 45	87	5	94	174	IGLV1-40, IGKV2-29, IGLV4-60, NMUR2, ADIPOQ, COL6A6, IGKV5-2, IGHV4-61, IGHV4-55, CALCB
DGF/mGFR < 45 *vs* DGF/mGFR ≥45	-	5 vs 14	118	102	MTCO3P13, IGLV1-40, LINC02172, COL6A5, C3P1, COL6A6, IGKV2-29, GPR22, IGHV4-55, IGKV5-2
DGF/mGFR ≥45 *vs* no DGF/mGFR ≥45	87	14	118	209	ADIPOQ, CIDEC, AKR1B15, PCSK2, THRSP, YWHAQP5, RPL10P9, TRARG1, IGLV1-36, FABP4

* Covariates: for batch, transplant organ type, DCD donor, regraft and pre-transplant DSA. Biopsy proven rejection (BPAR)

4.4.3.2 DGF vs control for DBD or DCD allografts

There was significant upregulation of innate and immune related pathways in DBD and DCD allografts prior to transplantation, reflecting the injury prior to or during organ procurement and/or during cold-storage transportation. (Fig 4.13) The degree of immune involvement was greater with the DCD allografts, especially the up-regulation of *IGHV*- and *IGLV*- related genes. These are important for immunoglobulin heavy and light chain production respectively and interesting to see prior to interaction with the recipients' immune system and may be donor specific antibodies or recipient lymphocytes. The top 20 up-regulated genes also included *CXCL11* in the DBD and *CXCL6* in the DBD cohort, both of which are potent chemokines for T-cells and granulocytes.

a

Ensembl	logFC	Fold Change	symbol
ENSG00000211943	2.37	5.17	IGHV3-15
ENSG00000211640	2.26	4.80	IGLV6-57
ENSG00000171747	2.06	4.16	LGALS4
ENSG00000178602	2.00	4.00	OTOS
ENSG00000125851	1.98	3.94	PCSK2
ENSG00000211649	1.94	3.84	IGLV7-46
ENSG00000012223	1.81	3.50	LTF
ENSG00000211967	1.71	3.27	IGHV3-53
ENSG00000169248	1.65	3.13	CXCL11
ENSG00000172461	1.57	2.96	FUT9
ENSG00000274576	1.56	2.96	IGHV2-70
ENSG00000239855	1.54	2.91	IGKV1-6
ENSG00000211666	1.49	2.80	IGLV2-14
ENSG00000188373	1.47	2.78	C10orf99
ENSG00000100985	1.43	2.70	MMP9
ENSG00000211662	1.43	2.69	IGLV3-21
ENSG00000135094	1.41	2.66	SDS
ENSG00000122025	1.40	2.63	FLT3
ENSG00000211651	1.38	2.60	IGLV1-44
ENSG00000085265	1.37	2.59	FCN1

b DBD only

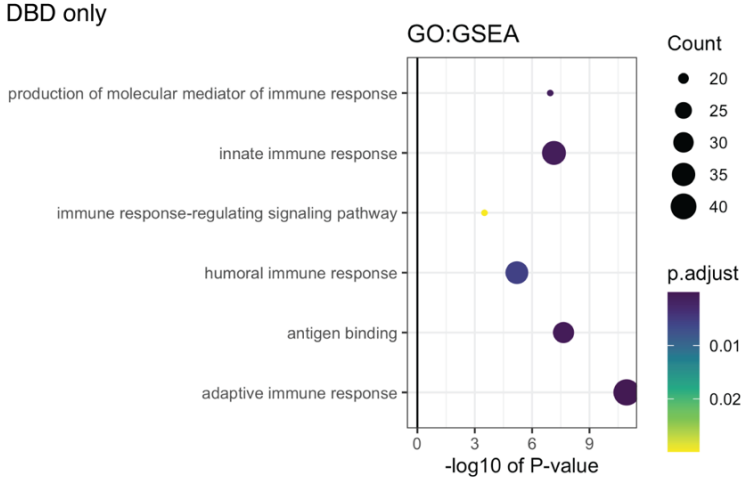

c

Ensembl	logFC	Fold Change	symbol
ENSG00000198074	2.72	6.59	AKR1B10
ENSG00000176092	2.51	5.70	CRYBG2
ENSG00000211653	2.47	5.52	IGLV1-40
ENSG00000211659	2.42	5.37	IGLV3-25
ENSG00000211668	2.36	5.13	IGLV2-11
ENSG00000183778	2.34	5.06	B3GALT5
ENSG00000119946	2.25	4.77	CNNM1
ENSG00000124875	2.24	4.71	CXCL6
ENSG00000243466	2.23	4.69	IGKV1-5
ENSG00000138615	2.20	4.61	CILP
ENSG00000211895	2.20	4.61	IGHA1
ENSG00000163817	2.14	4.42	SLC6A20
ENSG00000211598	2.14	4.39	IGKV4-1
ENSG00000223914	2.09	4.27	LINC02471
ENSG00000104722	2.09	4.26	NEFM
ENSG00000175793	1.99	3.96	SFN
ENSG00000163751	1.96	3.88	CPA3
ENSG00000278196	1.94	3.84	IGLV2-8
ENSG00000211938	1.94	3.84	IGHV3-7
ENSG00000106128	1.94	3.84	GHRHR

d DCD only

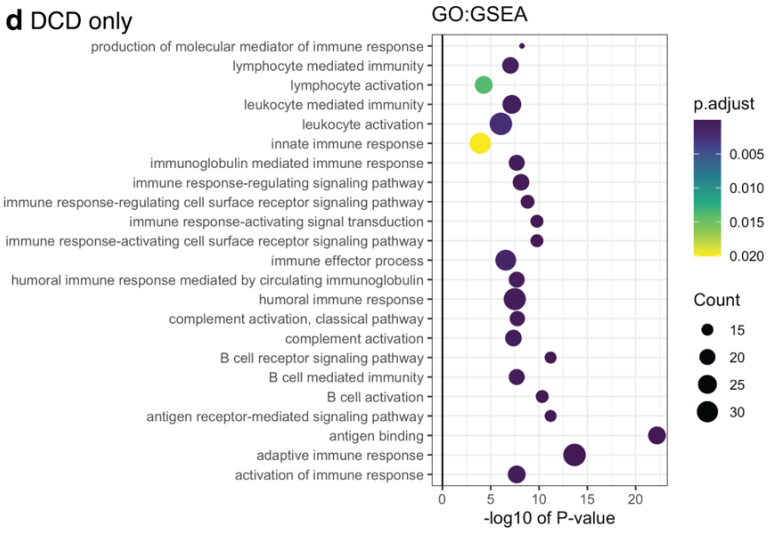

Figure 4.13: Differential expression of DGF vs control. A) The top 20 upregulated genes and b) enrichment analysis for DBD allografts; and similarly, c) top 20 upregulated genes and d) enrichment analysis for DCD allografts.

4.4.3.3 DGF vs control for 0- and 3-month biopsies in patients without BPAR

For patients who did not have any incident episodes of BPAR within the first month, differential expression analysis of the 0- and 3-month biopsy are shown in Fig 4.14. There were prominent immune related pathways in both, with granulocyte/neutrophil and CXCR chemokine related processes on the 0-month and persistent upregulation of lymphocyte and B-cell related pathways in DGF vs control.

Comparing DGF vs control on pre-implantation biopsy (0m) who did not have biopsy proven acute rejection

a

Ensembl	LogFC	Fold Change	Symbol
ENSG00000233913	3.58	12.00	RPL10P9
ENSG00000198074	2.45	5.47	AKR1B10
ENSG00000129204	2.31	4.97	USP6
ENSG00000151365	2.23	4.70	THRSP
ENSG00000188257	2.20	4.60	PLA2G2A
ENSG00000230076	2.15	4.43	RPL10P6
ENSG00000169248	1.84	3.57	CXCL11
ENSG00000198535	1.80	3.48	C2CD4A
ENSG00000102837	1.76	3.39	OLFM4
ENSG00000211640	1.76	3.38	IGLV6-57
ENSG00000211951	1.73	3.32	IGHV2-26
ENSG00000211943	1.73	3.31	IGHV3-15
ENSG00000146453	1.68	3.20	PNLDC1
ENSG00000173432	1.65	3.15	SAA1
ENSG00000166819	1.62	3.07	PLIN1
ENSG00000170323	1.58	2.98	FABP4
ENSG00000007908	1.57	2.97	SELE
ENSG00000128510	1.56	2.96	CPA4
ENSG00000099194	1.56	2.95	SCD
ENSG00000175592	1.55	2.93	FOSL1

b

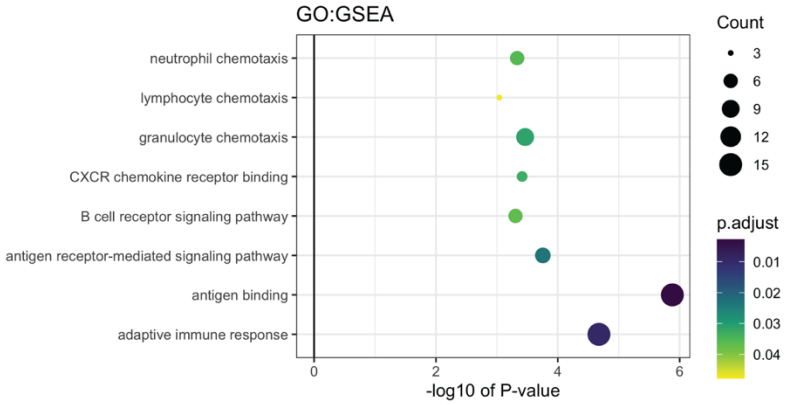

Comparing DGF vs control on 3-month biopsy in patients who did not have biopsy proven acute rejection

c

Ensembl	logFC	Fold Change	symbol
ENSG00000211659	3.805655	13.98351	IGLV3-25
ENSG00000138435	3.430353	10.78051	CHRNA1
ENSG00000211970	2.930128	7.621782	IGHV4-61
ENSG00000133055	2.817032	7.047111	MYBPH
ENSG00000122180	2.642531	6.244261	MYOG
ENSG00000196811	2.630589	6.192787	CHRNG
ENSG00000211899	2.310486	4.960501	IGHM
ENSG00000159251	2.287309	4.881449	ACTC1
ENSG00000105251	2.253501	4.768385	SHD
ENSG00000147256	2.19231	4.570367	ARHGAP36
ENSG00000135902	2.1703	4.50117	CHRND
ENSG00000211663	2.169738	4.499418	IGLV3-19
ENSG00000105664	2.164103	4.481877	COMP
ENSG00000149968	2.135918	4.395166	MMP3
ENSG00000148677	2.086466	4.247065	ANKRD1
ENSG00000169271	2.065607	4.1861	HSPB3
ENSG00000183873	2.035207	4.098816	SCN5A
ENSG00000211898	1.990334	3.973291	IGHD
ENSG00000241351	1.950419	3.864868	IGKV3-11
ENSG00000240382	1.843833	3.589625	IGKV1-17

d

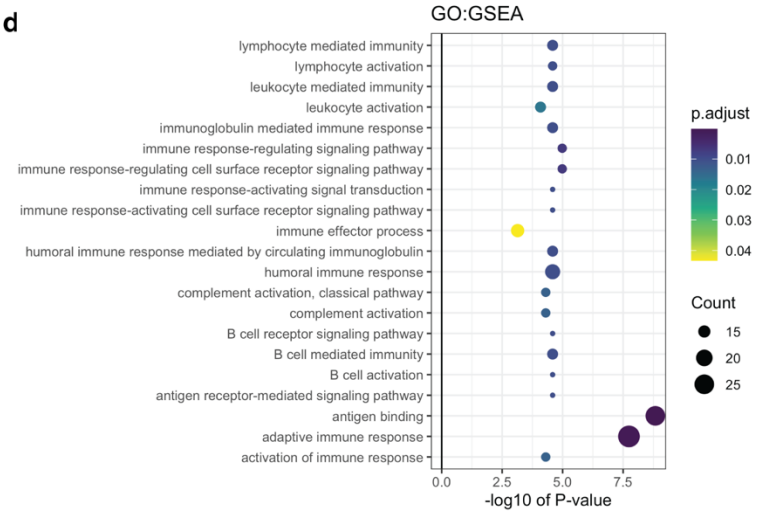

Figure 4.14: Differential expression of DGF vs control. A) The top 20 upregulated genes and b) enrichment analysis for the 0-month biopsy; and c) top 20 upregulated genes and d) enrichment analysis at 3-month biopsy for all patients without incidence BPAR in up to and including 3-months timepoint.

4.4.3.4 SGF vs control or DGF vs SGF at 0- and 3-month

Analysis of associations of SGF to important clinical parameters were limited by small cohort size, but there were detectable transcriptomic differences on pre-implantation biopsies. SGF had upregulation similar lymphocyte and B-cell related pathways as DGF vs controls, although the top 20 upregulated genes in the SGF group included *WNT7B*, *CST6* and *DDIT4L*, whereas immunoglobulin and collagen (*COL1*- and *COL3*-related genes) were prominent on the 3-month biopsy samples (15 SGF vs 80 controls with the exclusion of any patients with BPAR episodes). Contrary to expectation, enrichment analysis of the DGE derived from DGF vs SGF showed suppressed pathways, suggesting greater inflammatory response in SGF than DGF kidneys pre-implantation (Fig 4.15 d-e). The more intuitive interpretation is that SGF was associated with platelet activation, cell death and B cell signalling pathways compared to DGF. Analysis at the 3-month timepoint, again excluding any patients with BPAR episodes, allowed for differential expression analysis of 22 DGF vs 15 SGF biopsy samples, which revealed remarkable enrichment of immunoglobulin related genes in SGF (negative FC with the original DGF vs SGF reference). (Fig 4.15f).

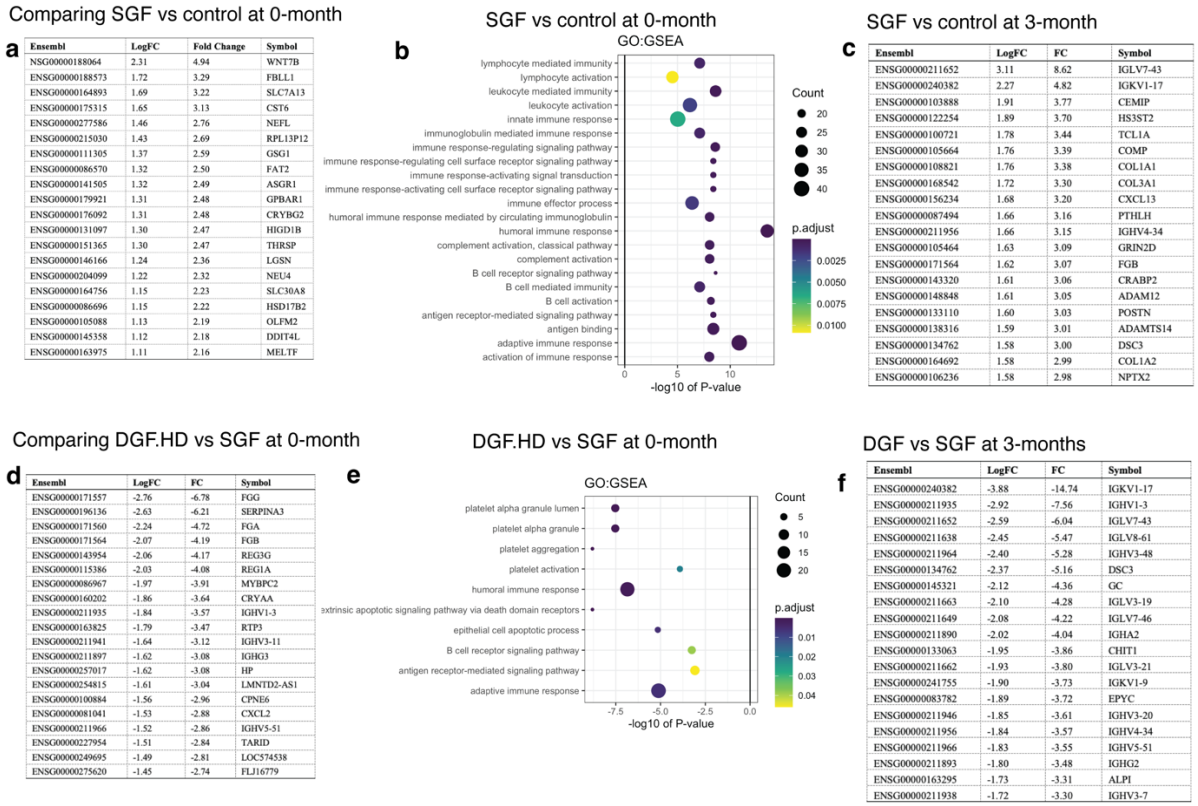

Figure 4.15: Differential expression of samples with slow graft function. A) top 20 upregulated genes, b) Enrichment analysis for SGF vs controls on 0-month biopsies and c) top 20 upregulated genes for SGF vs controls on 3-month biopsies (excluding individuals with BPAR). C) top 20 down-regulated genes, D) Enrichment analysis for DGF vs SGF on 0-month biopsies and c) top 20 down regulated genes for DGF vs SGF on 3-month biopsies (excluding individuals with BPAR).

4.4.3.5 Pre-implantation biopsy association to poor 12-months outcomes

To determine if there were genes on the pre-implantation biopsy which may be associated with poor 12-month outcomes, the following differential expression analysis was performed (excluding patients with subsequent episodes of BPAR or BKVAN): 72 pre-implantation biopsy samples for either DGF + IFTA ≥ 2 or DGF + IFTA ≤ 2 vs control (no DGF/12-month IFTA <2); 108 pre-implantation biopsy samples for DGF + mGFR ≤ 45 ml/min or DGF + mGFR ≥ 45 ml/min vs control (no DGF/12-month mGFR ≥45 ml/min); and DGF vs control; and mGFR ≤ 45 ml/min vs mGFR ≥ 45 ml/min alone. (Fig 4.16a).

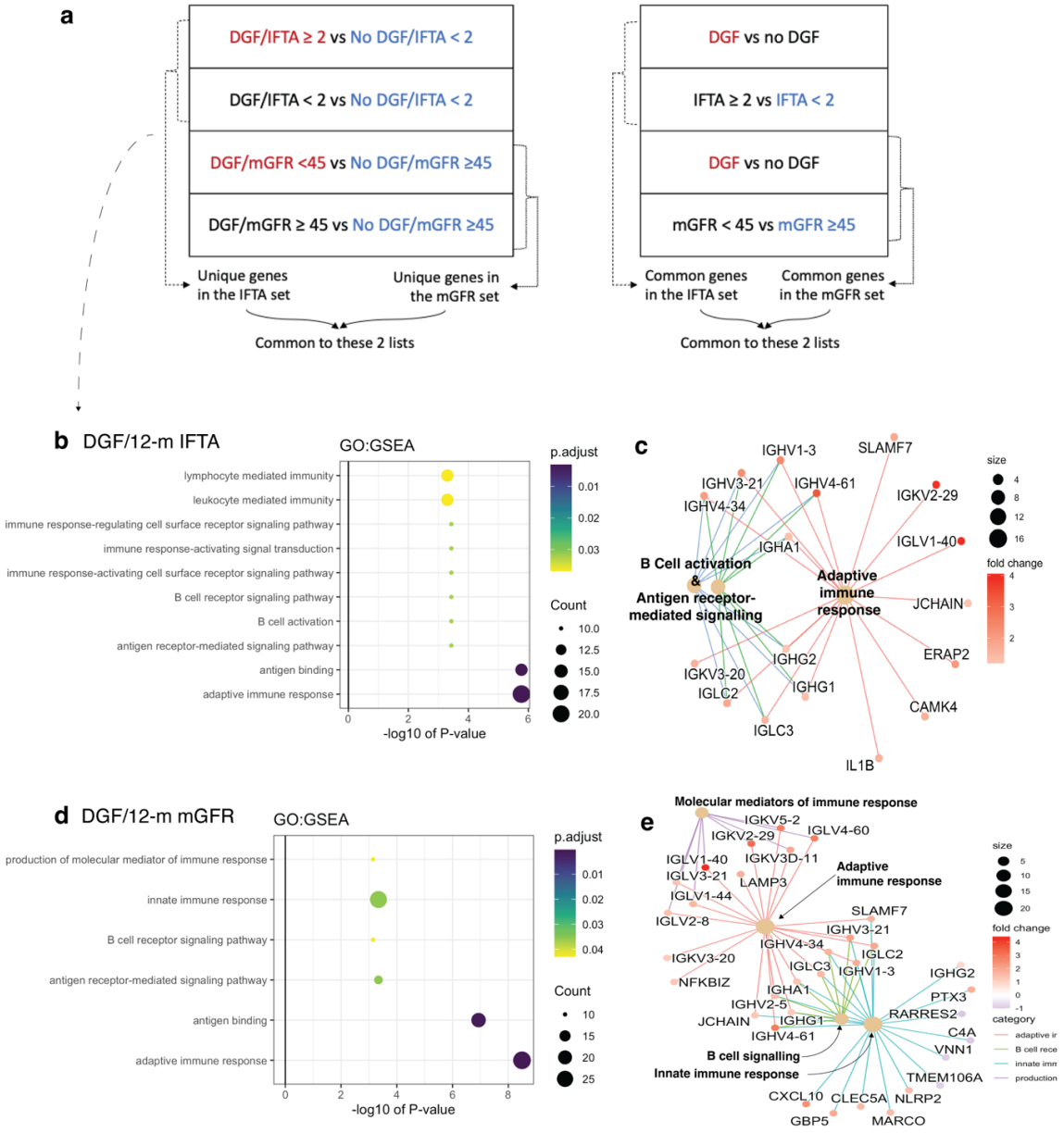

Figure 4.16: Pre-implantation transcript signatures associated with 12-month clinical outcomes a) differential expression analysis design; and enriched pathways and network plot for the b & c) unique DGF/IFTA gene set and d&e) unique DGF/mGFR gene set.

Enrichment analysis of the unique genes seen in DGF/IFTA>2 compared to controls (not overlapping with DGF who did not progress to high 12-month IFTA scores vs controls) was consistent with earlier findings of upregulated immune, particularly B-cell/immunoglobulin related pathways (Fig 4.16b,c). A similar theme of enriched B cell/adaptive immune pathways was seen in the unique gene set characterising DGF with progress to low 12-month mGFR. The DGF/mGFR set also revealed other innate immune pathway related genes including CXCL10, MARCO, NLRP2, PTX3 and CLEC5A. (Fig 4.16d,e). The list of common up- and down-regulated genes between the DGF/IFTA and DGF/mGFR comparisons is shown in Table 4.8. The list of differential genes for DGF vs no DGF and low versus high mGFR is shown in table 4.9, with only IGLV1-40, COL1A1, COL6A3 and FOSB, MT1X, XIRP2 as common up- and down-regulated genes.

Table 4.8: Common genes in DGF samples associated with 12-month IFTA ≥2 and mGFR < 45ml/min

Ensembl	logFC	symbol	Ensembl	logFC	symbol
ENSG00000211653	4.05	IGLV1-40	ENSG00000076258	-1.00	FMO4
ENSG00000253998	3.83	IGKV2-29	ENSG00000244731	-1.13	C4A
ENSG00000211970	3.31	IGHV4-61	ENSG00000149328	-1.14	GLB1L2
ENSG00000254395	3.07	IGHV4-55	ENSG00000204653	-1.15	ASPDH
ENSG00000172461	2.89	FUT9	ENSG00000187546	-1.24	AGMO
ENSG00000231475	2.80	IGHV4-30-2	ENSG00000116882	-1.25	HAO2
ENSG00000168824	2.55	NSG1	ENSG00000129988	-1.26	LBP
ENSG00000153404	2.51	PLEKHG4B	ENSG00000091986	-1.26	CCDC80
ENSG00000086696	2.40	HSD17B2	ENSG00000119147	-1.29	ECRG4
ENSG00000211935	2.40	IGHV1-3	ENSG00000167588	-1.30	GPD1
ENSG00000132911	2.37	NMUR2	ENSG00000121236	-1.32	TRIM6
ENSG00000211947	2.33	IGHV3-21	ENSG00000198417	-1.37	MT1F
ENSG00000140955	2.27	ADAD2	ENSG00000112299	-1.40	VNN1
ENSG00000134115	2.26	CNTN6	ENSG00000172955	-1.41	ADH6
ENSG00000206384	2.26	COL6A6	ENSG00000170099	-1.43	SERPINA6
ENSG00000232229	2.07	LINC00865	ENSG00000174348	-1.45	PODN
ENSG00000211956	2.01	IGHV4-34	ENSG00000116285	-1.55	ERRFI1
ENSG00000138755	1.99	CXCL9	ENSG00000257017	-1.56	HP
ENSG00000148848	1.94	ADAM12	ENSG00000205358	-1.59	MT1H
ENSG00000154451	1.90	GBP5	ENSG00000215277	-1.60	RNF212B
ENSG00000022556	1.90	NLRP2	ENSG00000204978	-1.65	ERICH4
ENSG00000211677	1.82	IGLC2	ENSG00000120645	-1.71	IQSEC3
ENSG00000026751	1.75	SLAMF7	ENSG00000002726	-1.76	AOC1
ENSG00000150594	1.72	ADRA2A	ENSG00000163631	-1.79	ALB
ENSG00000239951	1.64	IGKV3-20	ENSG00000125144	-1.79	MT1G
ENSG00000038427	1.58	VCAN	ENSG00000198848	-1.82	CES1
ENSG00000211679	1.51	IGLC3	ENSG00000173702	-1.88	MUC13
ENSG00000167995	1.44	BEST1	ENSG00000187193	-1.99	MT1X
ENSG00000159263	1.33	SIM2	ENSG00000091583	-2.01	APOH
ENSG00000211896	1.33	IGHG1	ENSG00000137868	-2.17	STRA6
ENSG00000090104	1.32	RGS1	ENSG00000134184	-2.61	GSTM1
ENSG00000211895	1.31	IGHA1	ENSG00000197614	-3.05	MFAP5
ENSG00000132465	1.20	JCHAIN	ENSG00000169218	-3.33	RSPO1
ENSG00000211893	1.19	IGHG2	ENSG00000180772	-3.69	AGTR2
ENSG00000176907	1.16	TCIM	ENSG00000101098	-3.92	RIMS4
ENSG00000130635	0.86	COL5A1	ENSG00000130595	-4.34	TNNT3
			ENSG00000171401	-6.14	KRT13

Table 4.9: Common genes of DGF and 12-month IFTA ≥2; DGF and mGFR < 45ml/min

DGF vs no DGF + high vs low IFTA			DGF vs no DGF + high vs low mGFR					
Ensembl	**logFC**	**symbol**	**Ensembl**	**logFC**	**symbol**	**Ensembl**	**logFC**	**symbol**
ENSG00000233913	2.01	RPL10P9	ENSG00000211653	0.98	IGLV1-40	ENSG00000186115	-0.50	CYP4F2
ENSG00000171747	1.78	LGALS4	ENSG00000206172	0.97	HBA1	ENSG00000170345	-0.50	FOS
ENSG00000211653	0.98	IGLV1-40	ENSG00000012223	0.84	LTF	ENSG00000100253	-0.51	MIOX
ENSG00000122025	0.99	FLT3	ENSG00000244734	0.75	HBB	ENSG00000162391	-0.53	FAM151A
ENSG00000142748	0.43	FCN3	ENSG00000137673	0.71	MMP7	ENSG00000119121	-0.54	TRPM6
ENSG00000108821	0.42	COL1A1	ENSG00000198535	0.69	C2CD4A	ENSG00000117322	-0.54	CR2
ENSG00000129824	0.36	RPS4Y1	ENSG00000124107	0.54	SLPI	ENSG00000179914	-0.58	ITLN1
ENSG00000131401	0.37	NAPSB	ENSG00000101443	0.51	WFDC2	ENSG00000175985	-0.65	PLEKHD1
ENSG00000163359	0.33	COL6A3	ENSG00000116183	0.44	PAPPA2	ENSG00000187193	-0.65	MT1X
ENSG00000125740	-1.54	FOSB	ENSG00000108821	0.42	COL1A1	ENSG00000197614	-0.66	MFAP5
ENSG00000196136	-1.45	SERPINA3	ENSG00000177575	0.41	CD163	ENSG00000146755	-0.69	TRIM50
ENSG00000187193	-0.65	MT1X	ENSG00000181019	0.41	NQO1	ENSG00000250529	-0.71	LINC02121
ENSG00000243064	-1.28	ABCC13	ENSG00000168542	0.38	COL3A1	ENSG00000101204	-0.74	CHRNA4
ENSG00000163092	-1.23	XIRP2	ENSG00000131401	0.37	NAPSB	ENSG00000120738	-0.76	EGR1
ENSG00000088836	-0.49	SLC4A11	ENSG00000115414	0.36	FN1	ENSG00000165181	-0.77	SHOC1
ENSG00000205364	-0.54	MT1M	ENSG00000163359	0.33	COL6A3	ENSG00000121454	-0.77	LHX4
ENSG00000248328	-0.44	MTCO3P28	ENSG00000198569	-0.35	SLC34A3	ENSG00000106483	-0.80	SFRP4
ENSG00000143632	-0.67	ACTA1	ENSG00000164303	-0.39	ENPP6	ENSG00000249201	-0.90	CTD-3080P12.3
			ENSG00000137204	-0.41	SLC22A7	ENSG00000163659	-0.92	TIPARP
			ENSG00000169715	-0.43	MT1E	ENSG00000229807	-0.96	XIST
			ENSG00000250799	-0.43	PRODH2	ENSG00000125414	-0.97	MYH2
			ENSG00000079557	-0.43	AFM	ENSG00000159248	-1.19	GJD2
			ENSG00000023171	-0.45	GRAMD1B	ENSG00000163092	-1.23	XIRP2
			ENSG00000125144	-0.45	MT1G	ENSG00000125740	-1.54	FOSB

These gene signatures were not leveraged to improve prediction modelling of DGF, and 12-month outcomes given the small cohort number with appropriate biopsy and clinical variables. Rather than internal validation, these data is better suited to use for external validation, ideally with 2- independent datasets which have pre-implantation biopsy RNAseq results, records of BPAR episodes, DCD status and 12-month IFTA and mGFR values. Furthermore, modelling will be improved with updating of KDPI and de-novo DSA results, which are being collected but not available at time of this analysis/submission.

4.4.4 Neutrophil quantification

The first 88 kidney bulk RNA-seq samples were analysed by CSL Ltd in a collaborative project. Their results demonstrated a strong neutrophil signature using the Ingenuity Pathway Analysis of the differentially expressed genes. Their analysis results remain confidential (not shown in this thesis) but the result was not validated in the subsequent batch of RNAseq samples. As demonstrated earlier, the granulocyte/neutrophil signature was upregulated in deceased vs living donor allografts, as well as seen in DGF patients who progress on to have low 12-month renal function.

The aim was to detect and quantify NETosis (or neutrophil extracellular traps) but unfortunately this was limited by access to FFPE samples, which require antigen retrieval and have a significant degree of autofluorescence. Of the NETosis related antibodies, anti-human MPO, CD66a, CD141, CD209, citrullinated H3 (Abcam, Cambridge) staining was unsuccessful. Only the polyclonal anti-human neutrophil elastase yielded reliable results (DAKO were unable to provide a monoclonal form of the neutrophil elastase antibody as a monoclonal form and thus, imaging mass cytometry to multiplex for NETosis and other immune cell targets were not attempted). The pilot project was modified to quantify neutrophil infiltration to the allograft. (Fig 4.17a-d).

Quantification of the number of neutrophils per high-power field across the 0-, 1- and 3- month time point revealed a greater number of neutrophils detected in the SGF samples compared to Control or DGF ($P = 0.017$ and $P = 0.0033$ respectively) on the available 0-month biopsies. There was no significant difference for neutrophil counts when controls were compared to DGF, nor for DBD/DCD/live-donor criteria allografts across the timepoints. (Fig 4.17e-f, *Supplementary Table 4.10*).

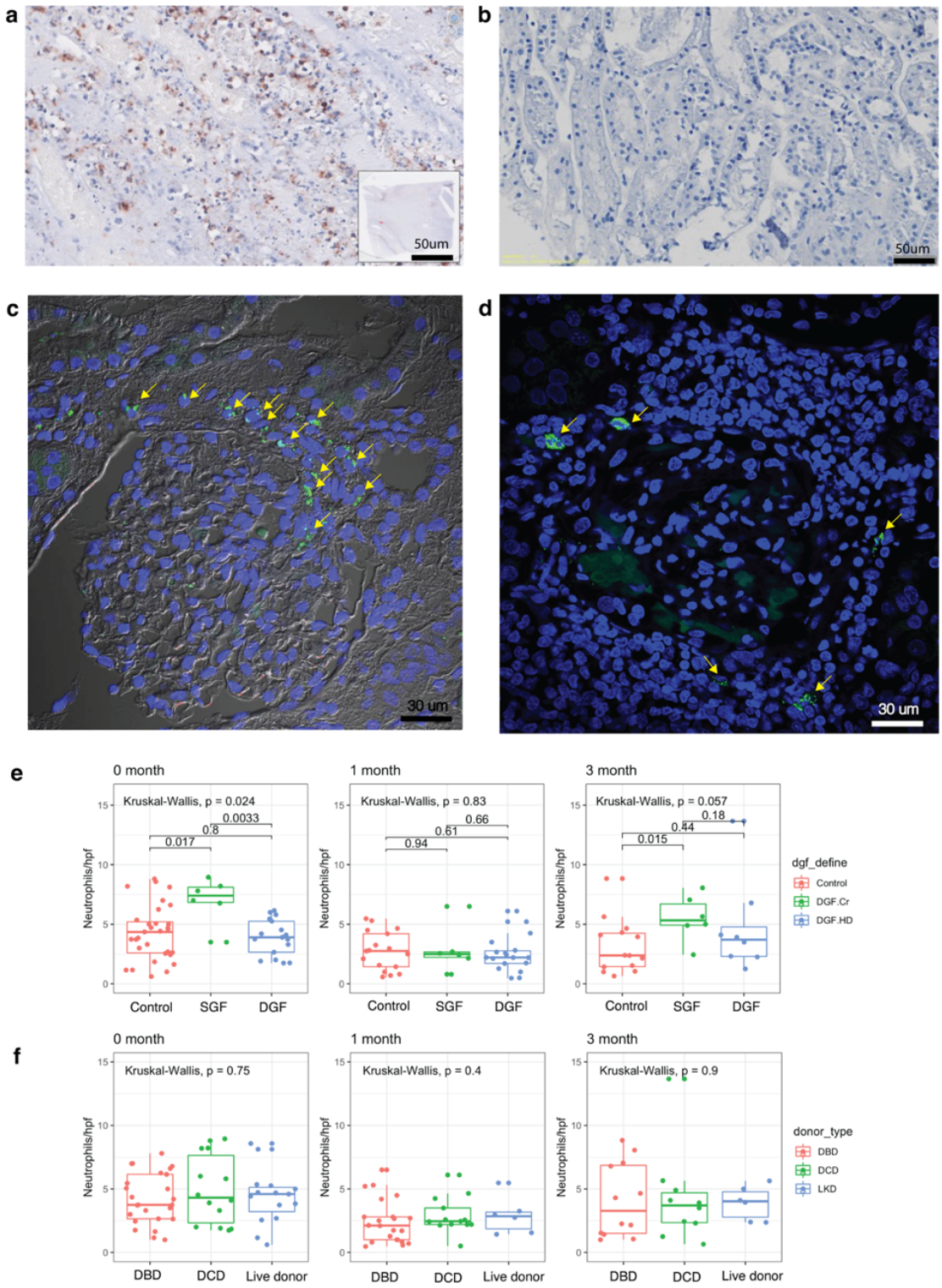

Figure 4.17: Neutrophil staining and quantification. Immunodetection with horse radish peroxidase to the primary neutrophil elastase antibody to a FFPE section following antigen retrieval for a) nephrectomy sample with chronic active rejection, and b) minimal change disease (negative control). Similarly, immunofluorescence to the primary neutrophil elastase antibody with secondary AF488 and DAPI staining for sample kidney biopsy sections c) with brightfield overlay and d) without overlay. The yellow arrows indicate example cells identified as neutrophils with strong, granular staining associated with a DAPI+ nucleus. Neutrophil counts per high power field for e) Control, SGF and DGF samples and f) DBD, DCD and living donor allografts for 0, 1 and 3-months.

4.5 Discussion

We show that pre-transplant clinical variables including inotrope requirement, DCD donor status and recipients with diabetic nephropathy (from type II DM) were risk factors for developing delayed graft function. Both DGF and SGF were associated with worse 3- and 12-month renal function. DGF and SGF as stand-alone variables, or in combination with 12-month IFTA ≥ 2 or mGFR < 45ml/min, were associated with increased mortality risk but not graft loss, whether death-censored or not. While DGF was linked with early BPAR (≤ 1-month), subsequent analysis demonstrated that DGF and early BPAR did not have a significant effect on graft loss, unlike the significant associations of graft loss with BPAR when episodes after 1-month were included. Theses analyses are limited by sample size in a contemporary single-centre prospective cohort study and noting < 50% have reached 5-years post-transplantation. This coupled with relatively low event rates[9] (~10% 5-year in this cohort) mirror some of the issues reported by earlier studies, which have shown conflicting results on the association of DGF with death and graft loss[12,37-42]. There were several interesting findings from the biopsy RNA-seq samples.

Firstly, there was strong representation of immunoglobulin-related transcripts comparing DGF to control for both DBD and DCD allografts. Despite the association of DGF with early rejection in our data and reported in the literature[43,44], the immunoglobulin-related the B-cell pathways were significantly enriched in both pre-implantation and 3-month biopsy samples even when subjects with incident BPAR were excluded, or when DGF with poor 12-month IFTA scores of mGFR values were compared to controls. This indicates B-cells have an important role in late phase renal IRI, maladaptive healing and rejection[45-47], similar to the findings of persistent B-cell signatures up to 12-months post transplantation[48] and is consistent with the known relationship between allograft quality and/or DGF with post-transplant graft function and histology[49,50]. The presence of B-cell activation on the pre-implantation biopsy, prior to reperfusion probably reflects earlier episodes of clinical or occult renal IRI during the donor's terminal admission episode, prior to confirmation of death, vascular clamping, and organ procurement. Furthermore, despite the acute upregulation of innate pathways post reperfusion, the 3-month biopsies of DGF patients also exhibited B-cell/immunoglobulin enrichment compared to controls – which indicates a group with maladaptive repair to target with earlier interventions.

Secondly, DGF was associated with significant enrichment of granulocyte/neutrophil migration pathways and innate immune response as a result of upregulation of chemokine related genes (CXCL6, CXCL10 and CXCL11), NLRP2 (involved in inflammasome signalling, previously identified in post-reperfusion DGF kidneys[51], although the ligands for this receptor are not well characterised like NLRP3) and MARCO (scavenger receptor on phagocytes) for example. Pre-implant biopsies were taken on the back table just prior to implantation/anastomosis and reperfusion during transplantation surgery. Post-perfusion biopsies were not available for this cohort and are not part of the surgical protocol at Westmead Hospital due to excessive bleeding risk associated with sampling post-reperfusion. It is likely that a post-perfusion biopsy would reveal an expanded set of genes and enriched pathways, and this limits inferences we can make for transplant related IRI. Indeed, innate inflammatory and cell death pathways were enriched in several post-reperfusion DGF samples compared to controls[51,52]. Whether post-reperfusion biopsies can better identify patients who will develop DGF and/or long-term sequelae is uncertain. Ultimately, the aim is to identify patients who would best benefit from early intervention (pre- or peri-transplantation).

Thirdly, SGF had similar enrichment of innate and adaptive immune responses compared to controls on the pre-implant biopsy, but counterintuitively displayed greater platelet, cell death and humoral pathway activation compared to DGF alone. The discrepancy of the DGF vs SGF results may be due to small sample size; differing post-biopsy surgical insults (such as warm ischemia times, fluctuations to MAP or perfusion pressures following anastomosis or wound closure, which are not recorded; or different temporal phase of IRI/acute kidney injury. The later may be possible if SGF allografts suffer IRI within the final few hours prior to donor expiration (such as DCD-related warm ischemia time) or absence of episodes of IRI/AKI earlier in the ICU course which could lead to compound injury. Neutrophil scoring seemed to be higher in the SGF group than controls or DGF alone for the available FFPE samples for staining, which is usually prominent early (<6 hours) post IRI.

The ability of clinical data to predict incident DGF or 12-month mGFR or IFTA results could be improved with the use of transcript markers from the pre-implantation biopsy, although the ideal candidate gene(s) needs further optimisation before clinical use. To do this, additional datasets with pre-implantation biopsy transcriptome samples are required to increase statistical power and perform external validation. Once

available, this could allow for testing prediction models with smaller gene numbers (based on cut-offs) or gene ratios (between select up- and down-regulated genes – such as using the on CPOP package by Mr Kevin Wang at the Department of Mathematics, University of Sydney and upgraded by Mr Harry Robertson as part of his current PhD candidature). An older study performed differential expression analysis on 92 pre-implantation kidney biopsies using Affymetrics data, comparing the cohort by factorial design of control vs DGF and high vs low eGFR (cut off 45ml/min/1.73m2) at 1-month post transplantation[53] and a more recent study of a 295 deceased-donor, kidney recipients (with DGF rates > 30%) showed improved predictive modelling of 24-month e-GFR outcomes by adding 13-gene panel to clinical data[54]. These studies were promising in their use of pre-implantation biopsy data, although they were based on microarray data, were dichotomised on eGFR values rather than mGFR or IFTA scores and lack granularity of BPAR or other clinically relevant events to be useful validation cohorts. Statistical analysis of the clinical data was restricted by the small cohort size, which limits the power and increases the risk of type II errors. The trade-off for the relatively small cohort is detail which is usually not captured in registry or linkage data – such as creatinine, tacrolimus at early time points, record of subclinical and biopsy-proven rejection with the change in immunosuppression at specific dates and records of the available protocol and indication biopsy scores. The clinical data in this cohort is complemented by availability of massively-parallel sequenced bulk-RNAseq data at 0-, 1- and 3- month time points. At time of writing, there were still more recent 0-, 1-, 3- and 12-month biopsies yet to be sequenced, which will increase the statistical power in the future.

4.6 Conclusions and future directions

Delayed and slow graft function represents early injury to the kidney allograft, which can increase the risk of rejection and poor long-term outcomes. Transcriptomic signatures were enriched for pathways in both innate and adaptive immune injury on the pre-implant biopsy and this up-regulation of adaptive (particularly B-cell) signature was persistent on the 3-month biopsies of DGF patients compared to controls, indicating long term maladaptive repair. These signatures may be used in addition to routine clinical factors to improve prediction of DGF and 12-month outcomes to guide therapy, or cohort enrichment in future transplant clinical studies. This will be particularly useful for selecting the right patients for cell therapies, such as tolerogenic DCs in future studies when the trial shifts to focus on deceased-donor transplant recipients.

4.7 Acknowledgements

The AUSCAD study was set up by Professor Philip O'Connell (principal PI) and recruitment/study coordination by Mrs Patricia Anderson. A/Prof Natasha Rogers and Dr Brian Nankivell for significant intellectual contribution during review and discussion of interim results. Clinical data collection set up by Dr Karen Keung and Dr Sebastian Hultin (donor details), Ms Haina Wang and Mr Paul Robertson assisted me at various stages to update and expand the dataset. Clinical specimen collection assessed by Dr Brian Nankivell, Prof Germaine Wong and A/Prof Natasha Rogers. Independent biopsy re-scoring by Dr Meena Shingde. Biobanking of specimens and flow assessment of samples performed primarily by Ms Elvira Jimenez and Dr Min Hu at the Westmead Institute for Medical Research and using Westmead Research Core Facilities. Dr Brian Gloss, Dr Ellis Patrick and Mr Harry Robertson were involved with initial bioinformatics and data cleaning of the RNAseq samples.

4.8 Supplementary material

Table 4.10: Neutrophil counts

Time point	N	Control	SGF	DGF	P-value
0 month	54	4.35 (2.59, 5.20)	7.40 (6.83, 8.11)	3.90 (2.65, 5.25)	0.024
1 month	41	2.75 (1.43, 4.20)	2.49 (2.21, 2.66)	2.21 (1.71, 2.77)	0.8
3 month	28	2.38 (1.44, 4.25)	5.32 (4.93, 6.70)	3.70 (2.30, 4.78)	0.057
Time point	N	**DBD- kidney**	**DCD- kidney**	**Live-donor kidney**	**P-value**
0 month	54	3.75 (2.65, 6.15)	4.31 (2.33, 7.64)	4.60 (3.21, 5.12)	0.8
1 month	41	2.11 (1.00, 2.80)	2.45 (2.20, 3.50)	2.85 (1.85, 3.17)	0.4
3 month	28	3.28 (1.50, 6.85)	3.70 (2.34, 4.70)	4.02 (2.78, 4.78)	>0.9

* Kruskall Wallace rank sum test

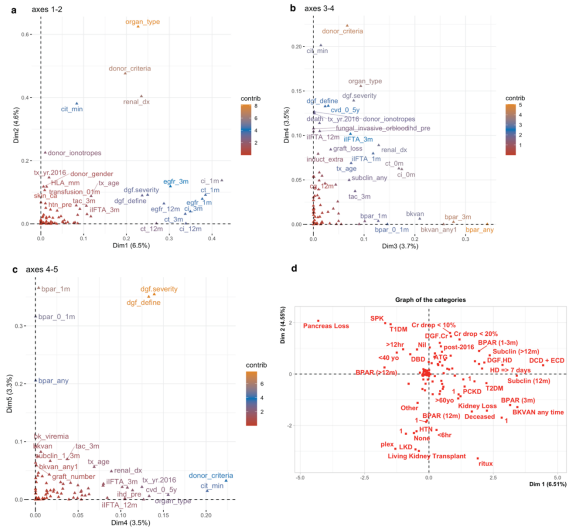

Figure 4.18: Factor analysis of mixed variables was used for exploratory data analysis of important clinical variables to produce the factor (PCA) plots a-c) along the first 5 dimensions; and d) variable plot for categorical variables in the first 2 dimensions for the 245 patients in the AUSCAD cohort with at least 12 months data.

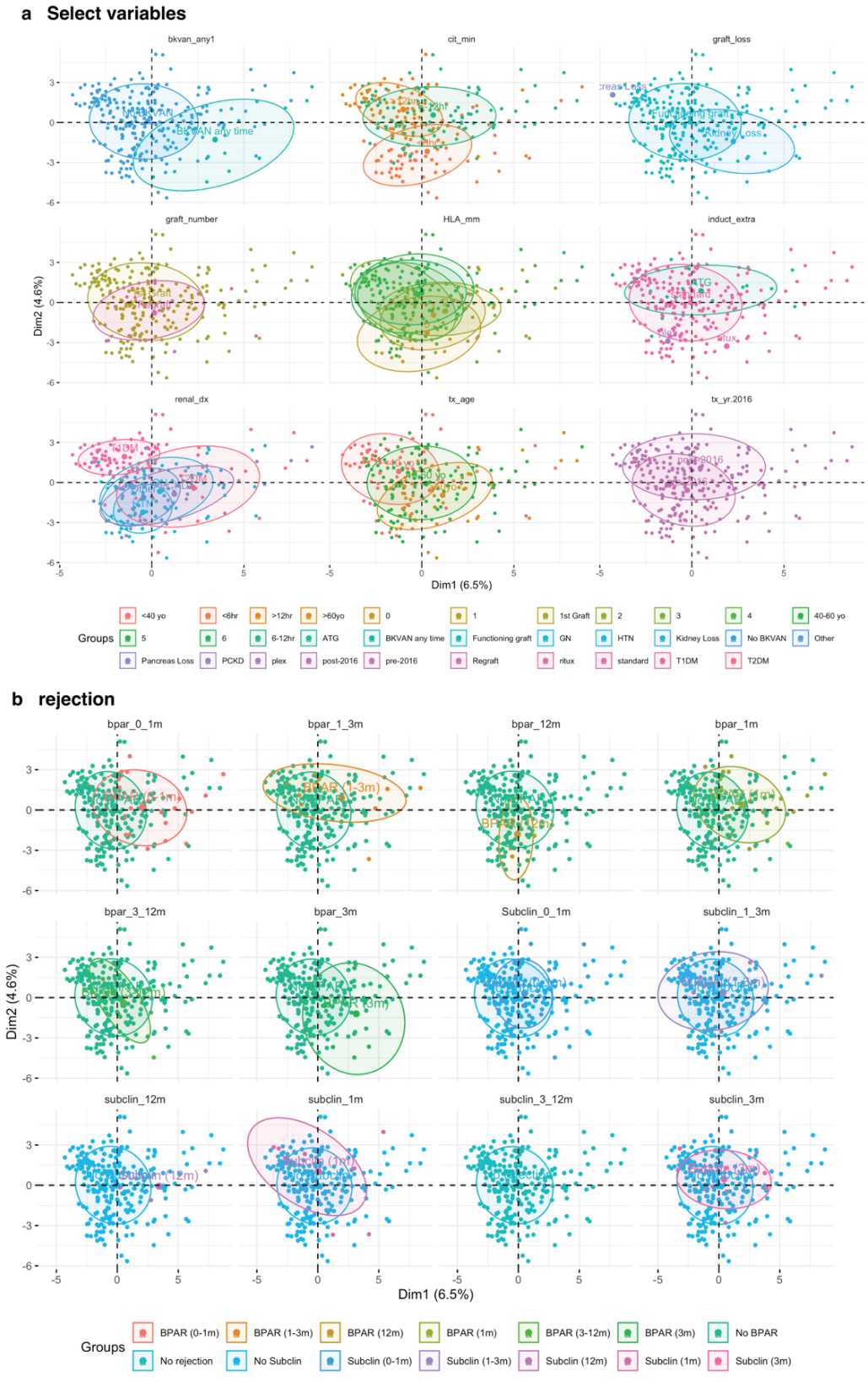

Figure 4.19: Exploratory data analysis of select pre-transplant and rejection variables

4.9 References

1. Perico N, Cattaneo D, Sayegh MH, Remuzzi G. Delayed graft function in kidney transplantation. *The Lancet*. 2004/11/13/ 2004;364(9447):1814-1827. doi:https://doi.org/10.1016/S0140-6736(04)17406-0
2. Mannon RB. Delayed Graft Function: The AKI of Kidney Transplantation. *Nephron*. 2018;140(2):94-98. doi:10.1159/000491558
3. Lim MA, Bloom RD. Medical Therapies to Reduce Delayed Graft Function and Improve Long-Term Graft Survival. *Clinical Journal of the American Society of Nephrology*. 2020;15(1):13. doi:10.2215/CJN.13961119
4. Li J, Rogers NM, Hawthorne WJ. Chapter 1 - Ischemia-reperfusion injury. In: Orlando G, Keshavjee S, eds. *Organ Repair and Regeneration*. Academic Press; 2021:1-42.
5. Tingle SJ, Figueiredo RS, Moir JAG, Goodfellow M, Talbot D, Wilson CH. Machine perfusion preservation versus static cold storage for deceased donor kidney transplantation. *Cochrane Database of Systematic Reviews*. 2019;(3)doi:10.1002/14651858.CD011671.pub2
6. Samoylova ML, Nash A, Kuchibhatla M, Barbas AS, Brennan TV. Machine perfusion of donor kidneys may reduce graft rejection. *Clin Transplant*. Oct 2019;33(10):e13716. doi:10.1111/ctr.13716
7. Hosgood SA, Brown RJ, Nicholson ML. Advances in Kidney Preservation Techniques and Their Application in Clinical Practice. *Transplantation*. 2021;105(11)
8. Siedlecki A, Irish W, Brennan DC. Delayed Graft Function in the Kidney Transplant. *American Journal of Transplantation*. 09/19 2011;11(11):2279-2296. doi:10.1111/j.1600-6143.2011.03754.x
9. O'Connell PJ, Kuypers DR, Mannon RB, et al. Clinical Trials for Immunosuppression in Transplantation: The Case for Reform and Change in Direction. *Transplantation*. 2017;101(7):1527-1534. doi:10.1097/tp.0000000000001648
10. Li J, O'Connell PJ. The Fragility Index: The P-Value by Another Name? *Transplantation*. 2022;106(2)
11. (FDA) FaDA. Delayed Graft Function in Kidney Transplantation: Developing Drugs for Prevention Guidance for Industry. *Guidance for Industry*. 2019;
12. Lim WH, McDonald SP, Russ GR, et al. Association Between Delayed Graft Function and Graft Loss in Donation After Cardiac Death Kidney Transplants—A Paired Kidney Registry Analysis. *Transplantation*. 2017;101(6):1139-1143. doi:10.1097/tp.0000000000001323
13. Naesens M, Anglicheau D. Precision Transplant Medicine: Biomarkers to the Rescue. *Journal of the American Society of Nephrology*. 2018;29(1):24. doi:10.1681/ASN.2017010004
14. Naesens M, Budde K, Hilbrands L, et al. Surrogate Endpoints for Late Kidney Transplantation Failure. Consensus Report. *Transplant International*. 2022-May-20 2022;35doi:10.3389/ti.2022.10136
15. Mannon RB, Morris RE, Abecassis M, et al. Use of biomarkers to improve immunosuppressive drug development and outcomes in renal organ transplantation: A meeting report. *American Journal of Transplantation*. 2020/06/01 2020;20(6):1495-1502. doi:10.1111/ajt.15833
16. Van Loon E, Lamarthée B, de Loor H, et al. Biological pathways and comparison with biopsy signals and cellular origin of peripheral blood transcriptomic profiles during kidney allograft pathology. *Kidney International*. doi:10.1016/j.kint.2022.03.026
17. O'Connell PJ, Zhang W, Menon MC, et al. Biopsy transcriptome expression profiling to identify kidney transplants at risk of chronic injury: a multicentre, prospective study. *Lancet*. Sep 3 2016;388(10048):983-93. doi:10.1016/s0140-6736(16)30826-1
18. Zhang W, Yi Z, Wei C, et al. Pretransplant transcriptomic signature in peripheral blood predicts early acute rejection. *JCI Insight*. 06/06/ 2019;4(11)doi:10.1172/jci.insight.127543
19. Davies NM, Holmes MV, Davey Smith G. Reading Mendelian randomisation studies: a guide, glossary, and checklist for clinicians. *BMJ*. 2018;362:k601. doi:10.1136/bmj.k601
20. Jameson JL, Longo DL. Precision Medicine — Personalized, Problematic, and Promising. *New England Journal of Medicine*. 2015;372(23):2229-2234. doi:10.1056/NEJMsb1503104
21. Lê S, Josse J, Husson F. FactoMineR: An R Package for Multivariate Analysis. *Journal of Statistical Software*. 03/18 2008;25(1):1 - 18. doi:10.18637/jss.v025.i01
22. Rao PS, Ojo A. The Alphabet Soup of Kidney Transplantation: SCD, DCD, ECD—Fundamentals for the Practicing Nephrologist. *Clinical Journal of the American Society of Nephrology*. 2009;4(11):1827. doi:10.2215/CJN.02270409
23. Nankivell BJ, Shingde M, Keung KL, et al. The causes, significance and consequences of inflammatory fibrosis in kidney transplantation: The Banff i-IFTA lesion. https://doi.org/10.1111/ajt.14609. *American Journal of Transplantation*. 2018/02/01 2018;18(2):364-376. doi:https://doi.org/10.1111/ajt.14609
24. Roufosse C, Simmonds N, Clahsen-van Groningen M, et al. A 2018 Reference Guide to the Banff Classification of Renal Allograft Pathology. *Transplantation*. 2018;102(11)
25. survminer: Survival Analysis and Visualization. *https://rpkgsdatanoviacom/survminer/indexhtml*.
26. Kawaguchi ES, Shen J, Li G, Suchard MA. A Fast and Scalable Implementation Method for Competing Risks Data with the R Package fastcmprsk. *R J*. 2020;12:163.
27. Kuhn M. Building Predictive Models in R Using the caret Package. *Journal of Statistical Software*. 11/10 2008;28(5):1 - 26. doi:10.18637/jss.v028.i05
28. Au EH, Francis A, Bernier-Jean A, Teixeira-Pinto A. Prediction modeling—part 1: regression modeling. *Kidney International*. 2020;97(5):877-884. doi:10.1016/j.kint.2020.02.007
29. Shah JS, Rai SN, DeFilippis AP, Hill BG, Bhatnagar A, Brock GN. Distribution based nearest neighbor imputation for truncated high dimensional data with applications to pre-clinical and clinical metabolomics studies. *BMC Bioinformatics*. Feb 20 2017;18(1):114. doi:10.1186/s12859-017-1547-6
30. Poldrack RA, Huckins G, Varoquaux G. Establishment of Best Practices for Evidence for Prediction: A Review. *JAMA Psychiatry*. May 1 2020;77(5):534-540. doi:10.1001/jamapsychiatry.2019.3671
31. Pavlou M, Ambler G, Seaman SR, et al. How to develop a more accurate risk prediction model when there are few events. *Bmj*. Aug 11 2015;351:h3868. doi:10.1136/bmj.h3868
32. Robinson MD, Oshlack A. A scaling normalization method for differential expression analysis of RNA-seq data. *Genome Biology*. 2010/03/02 2010;11(3):R25. doi:10.1186/gb-2010-11-3-r25
33. Lund SP, Nettleton D, McCarthy DJ, Smyth GK. Detecting differential expression in RNA-sequence data using quasi-likelihood with shrunken dispersion estimates. *Stat Appl Genet Mol Biol*. Oct 22 2012;11(5)doi:10.1515/1544-6115.1826
34. Chen Y, Lun AT, Smyth GK. From reads to genes to pathways: differential expression analysis of RNA-Seq experiments using Rsubread and the edgeR quasi-likelihood pipeline. *F1000Res*. 2016;5:1438. doi:10.12688/f1000research.8987.2

35. Pratschke J, Wilhelm MJ, Kusaka M, et al. BRAIN DEATH AND ITS INFLUENCE ON DONOR ORGAN QUALITY AND OUTCOME AFTER TRANSPLANTATION1. *Transplantation*. 1999;67(3):343-348.
36. van Der Hoeven JAB, Molema G, Ter Horst GJ, et al. Relationship between duration of brain death and hemodynamic (in)stability on progressive dysfunction and increased immunologic activation of donor kidneys. *Kidney International*. 2003;64(5):1874-1882. doi:10.1046/j.1523-1755.2003.00272.x
37. Lim WH, Johnson DW, Teixeira-Pinto A, Wong G. Association Between Duration of Delayed Graft Function, Acute Rejection, and Allograft Outcome After Deceased Donor Kidney Transplantation. *Transplantation*. 2019;103(2):412-419. doi:10.1097/tp.0000000000002275
38. Zens TJ, Danobeitia JS, Leverson G, et al. The impact of kidney donor profile index on delayed graft function and transplant outcomes: A single-center analysis. *Clin Transplant*. Mar 2018;32(3):e13190. doi:10.1111/ctr.13190
39. Lee J, Song SH, Lee JY, et al. The recovery status from delayed graft function can predict long-term outcome after deceased donor kidney transplantation. *Sci Rep*. 2017/10/20 2017;7(1):13725. doi:10.1038/s41598-017-14154-w
40. Gill J, Dong J, Rose C, Gill JS. The risk of allograft failure and the survival benefit of kidney transplantation are complicated by delayed graft function. *Kidney International*. 2016/06/01/ 2016;89(6):1331-1336. doi:https://doi.org/10.1016/j.kint.2016.01.028
41. Troppmann C, Gillingham KJ, Benedetti E, et al. DELAYED GRAFT FUNCTION, ACUTE REJECTION, AND OUTCOME AFTER CADAVER RENAL TRANSPLANTATION: A Multivariate Analysis. *Transplantation*. 1995;59(7)
42. Wang CJ, Wetmore JB, Crary GS, Kasiske BL. The Donor Kidney Biopsy and Its Implications in Predicting Graft Outcomes: A Systematic Review. https://doi.org/10.1111/ajt.13213. *American Journal of Transplantation*. 2015/07/01 2015;15(7):1903-1914. doi:https://doi.org/10.1111/ajt.13213
43. Nankivell BJ, Shingde M, P'Ng CH. The Pathological and Clinical Diversity of Acute Vascular Rejection in Kidney Transplantation. *Transplantation*. 2022;106(8)
44. Fuquay R, Renner B, Kulik L, et al. Renal Ischemia-Reperfusion Injury Amplifies the Humoral Immune Response. *Journal of the American Society of Nephrology*. 2013;24(7):1063. doi:10.1681/ASN.2012060560
45. Jang HR, Gandolfo MT, Ko GJ, Satpute SR, Racusen L, Rabb H. B cells limit repair after ischemic acute kidney injury. *J Am Soc Nephrol*. Apr 2010;21(4):654-65. doi:10.1681/ASN.2009020182
46. Burne-Taney MJ, Ascon DB, Daniels F, Racusen L, Baldwin W, Rabb H. B Cell Deficiency Confers Protection from Renal Ischemia Reperfusion Injury. *The Journal of Immunology*. 2003;171(6):3210. doi:10.4049/jimmunol.171.6.3210
47. Pineda S, Sigdel TK, Liberto JM, Vincenti F, Sirota M, Sarwal MM. Characterizing pre-transplant and post-transplant kidney rejection risk by B cell immune repertoire sequencing. *Nat Commun*. Apr 23 2019;10(1):1906. doi:10.1038/s41467-019-09930-3
48. Cippà PE, Liu J, Sun B, Kumar S, Naesens M, McMahon AP. A late B lymphocyte action in dysfunctional tissue repair following kidney injury and transplantation. *Nature Communications*. 2019/03/11 2019;10(1):1157. doi:10.1038/s41467-019-09092-2
49. Kuypers DR, Chapman JR, O'Connell PJ, Allen RD, Nankivell BJ. Predictors of renal transplant histology at three months. *Transplantation*. May 15 1999;67(9):1222-30. doi:10.1097/00007890-199905150-00005
50. Nankivell BJ, Agrawal N, Sharma A, et al. The clinical and pathological significance of borderline T cell–mediated rejection. https://doi.org/10.1111/ajt.15197. *American Journal of Transplantation*. 2019/05/01 2019;19(5):1452-1463. doi:https://doi.org/10.1111/ajt.15197
51. McGuinness D, Mohammed S, Monaghan L, et al. A molecular signature for delayed graft function. *Aging Cell*. Oct 2018;17(5):e12825. doi:10.1111/acel.12825
52. Mueller TF, Reeve J, Jhangri GS, et al. The transcriptome of the implant biopsy identifies donor kidneys at increased risk of delayed graft function. *Am J Transplant*. Jan 2008;8(1):78-85. doi:10.1111/j.1600-6143.2007.02032.x
53. Mas VR, Scian MJ, Archer KJ, et al. Pretransplant Transcriptome Profiles Identify among Kidneys with Delayed Graft Function Those with Poorer Quality and Outcome. *Molecular Medicine*. 2011/11/01 2011;17(11):1311-1322. doi:10.2119/molmed.2011.00159
54. Archer KJ, Bardhi E, Maluf DG, et al. Pretransplant kidney transcriptome captures intrinsic donor organ quality and predicts 24-month outcomes. https://doi.org/10.1111/ajt.17127. *American Journal of Transplantation*. 2022/06/22 2022;n/a(n/a)doi:https://doi.org/10.1111/ajt.17127

THE UNIVERSITY OF SYDNEY

The Westmead Institute FOR MEDICAL RESEARCH

5 Chapter 5

Final conclusions & future directions

The central theme for this PhD was to improve therapy options for patients with acute kidney injury. In Chapters 2 and 3, we showed that tolerogenic dendritic cell therapy and disruption of pyroptosis (with the GSDMD mutation or pharmacological inhibition with disulfiram) can limit the severity of acute renal ischemia reperfusion injury. The renoprotective effects of these interventions improved biochemical, histological, and molecular parameters associated with AKI.

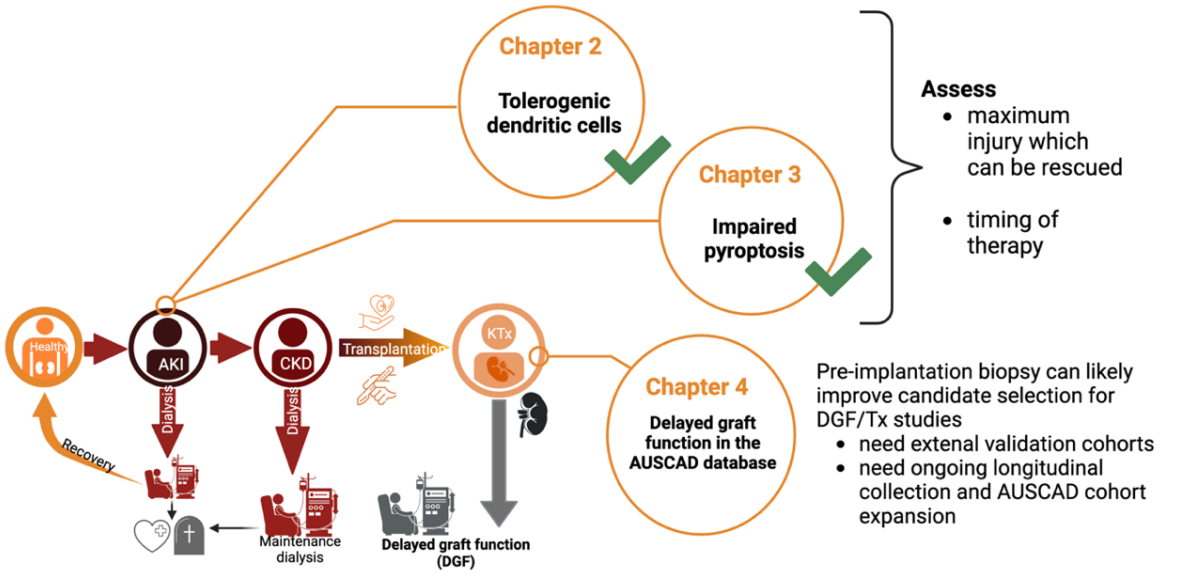

Image created using biorender.com

The utility of these interventions following IRI is yet to be demonstrated and will be explored following submission of this thesis. We plan to assess the optimal therapeutic window, minimal dosing requirements and the degree of renal insult for which these interventions cannot overcome and do not provide favourable risk/benefit considerations. These questions will be followed by significant challenges in trial design and patient selection to gather meaningful and robust evidence to support or refute these treatment options in humans (as highlighted in Chapter 1). One strategy is an enrichment strategy to select patients at high risk of severe AKI with poor short and/or long-term outcomes (we are trying to prevent) to be included. To do this, highly granular clinical meta-data and transcriptomics collected in the AUSCAD study were leveraged to see if an optimised, pre-implantation transcript signature could be used to predict transplant recipients who were likely to suffer from slow or delayed graft function, and/or delayed graft function with poor 12-month outcomes. Validation of these results, ideally with at least 2 independent external cohorts could be a valuable enrichment strategy for future transplant clinical trials.

That’s it.

Thanks for reading.